SYNTHESIS OF CARBAZOLE DENDRIMERS AS HOST MATERIALS FOR ORGANIC LIGHT EMITTING DIODES

ZAINAL ABIDIN BIN HASAN

FACULTY OF SCIENCE
UNIVERSITY OF MALAYA
KUALA LUMPUR

2017

SYNTHESIS OF CARBAZOLE DENDRIMERS AS HOST MATERIALS FOR ORGANIC LIGHT EMITTING DIODES

ZAINAL ABIDIN BIN HASAN

THESIS SUBMITTED IN FULFILMENT OF THE REQUIREMENTS FOR THE DEGREE OF DOCTOR OF PHILOSOPHY

FACULTY OF SCIENCE
UNIVERSITY OF MALAYA
KUALA LUMPUR

2017

UNIVERSITY OF MALAYA

ORIGINAL LITERARY WORK DECLARATION

Name of Candidate: Zainal Abidin bin Hasan (I.C/Passport No:)

Registration/Matric No: SHC120057

Name of Degree: Doctor of Philosophy

Title of Project Paper/Research Report/Dissertation/Thesis ("this Work"): SYNTHESIS OF CARBAZOLE DENDRIMERS AS HOST MATERIALS FOR ORGANIC LIGHT EMITTING DIODES

Field of Study: Organic Chemistry

I do solemnly and sincerely declare that:

(1) I am the sole author/writer of this Work;
(2) This Work is original;
(3) Any use of any work in which copyright exists was done by way of fair dealing and for permitted purposes and any excerpt or extract from, or reference to or reproduction of any copyright work has been disclosed expressly and sufficiently and the title of the Work and its authorship have been acknowledged in this Work;
(4) I do not have any actual knowledge nor do I ought reasonably to know that the making of this work constitutes an infringement of any copyright work;
(5) I hereby assign all and every rights in the copyright to this Work to the University of Malaya ("UM"), who henceforth shall be owner of the copyright in this Work and that any reproduction or use in any form or by any means whatsoever is prohibited without the written consent of UM having been first had and obtained;
(6) I am fully aware that if in the course of making this Work I have infringed any copyright whether intentionally or otherwise, I may be subject to legal action or any other action as may be determined by UM.

Candidate's Signature Date:

Subscribed and solemnly declared before,

Witness's Signature Date:

Name:

Designation:

ABSTRACT

Four new types of carbazole dendrimers were successfully synthesized namely 1, 4-bis (3, 6-bis (3, 6-ditert-pentyl-carbazol-9-yl)carbazol-9-yl)benzene (**13**), 1, 3-bis (3, 6-bis (3, 6-ditert-pentyl-carbazol-9-yl)carbazol-9-yl)benzene (**14**), 4, 4'-bis (3, 6-bis (3, 6-ditert-pentyl-carbazol-9-yl)carbazol-9-yl)biphenyl (**15**), and 4, 4'-bis (3, 6-bis (3, 6-ditert-pentyl-carbazol-9-yl)carbazol-9-yl)-2,2'-dimethylbiphenyl (**16**) in six steps. Synthetic route involves Ullmann reaction process as a key reaction to obtain the final products. The dendrimers were isolated in moderate yield between 40-65 % after purification by column chromatography and recrystallization. These dendrimers were fully characterized by NMR, MALDI-TOF mass spectroscopy and CHN analysis. The pure dendrimers were further studied for their optical properties by UV-Vis, fluorescence and low-temperature phosphorescence. The thermal properties of the dendrimers have been study by TGA and DSC analysis. Their electrochemical properties were measured by cyclic voltammetry (CV) to determine their HOMO and LUMO energy levels. All of the dendrimers showed good thermal stability, high triplet energy and appropriate HOMO and LUMO energy levels to serve as host materials for OLEDs. Compound **16** was found to be the best choice to be used as host material for blue, green and red OLEDs because of its high triplet energy (E_T = 2.82 eV) along with high glass transition temperature (T_g = 270 °C), high thermal decomposition stability (T_d = 470 °C) and suitable HOMO level (E_{HOMO} = -5.24 eV). Compound **16** was used as a host material in the fabrication of single-layer, double-layer and multi-layer devices for blue, green and red OLEDs by a solution-process method. An increment in device efficiency was observed from single layer to double layer devices and further increment can be observed for multilayer devices. The morphology of the thin films was analysed by atomic force microscopy (AFM), which revealed that fluorinated alcohol can form a good thin film with low surface roughness compared to

normal alcohol. Fluorinated alcohol has been used to increase the electron injection property of the devices and enable fabrication of electron transport layer through wet process.

ABSTRAK

Empat jenis dendrimer baru berasaskan karbazola telah berjaya disintesis iaitu 1, 4-bis [3, 6-bis (3, 6-ditert-pentyl-carbazol-9-yl) carbazol-9-yl] benzena (**13**), 1, 3 -bis [3, 6-bis (3, 6-ditert-pentyl-carbazol-9-yl) carbazol-9-yl] benzena (**14**), 4, 4'-bis [3, 6-bis (3, 6 -ditert-pentyl-carbazol-9-yl) carbazol-9-yl] bifenil (**15**) dan 4, 4'-bis [3, 6-bis (3, 6-ditert-pentyl-carbazol-9-yl) carbazol -9-yl] -2,2'-dimethylbifenil (**16**) melalui enam langkah laluan sintetik. Tindak balas proses Ullmann adalah tindak balas utama untuk mendapatkan produk akhir. Dendrimer-dendrimer ini telah diasingkan dalam hasil sederhana antara 40-65 % selepas proses penulenan dengan kaedah kolum kromatografi dan penghabluran semula. Kesemua dendrimer dicirikan sepenuhnya oleh NMR, MALDI-TOF spektroskopi jisim dan analisis CHN. Kesemua dendrimer tulen telah dikaji sifat-sifat optik mereka dengan UV-Vis, pendarfluor dan pendarfosfor suhu rendah. Sifat haba dendrimer-dendrimer ini telah dikaji melalui analisis TGA dan DSC. Sifat elektrokimia mereka diukur menggunakan voltammetri berkitar (CV) untuk mendapatkan tahap tenaga HOMO dan LUMO mereka. Semua dendrimers menunjukkan kestabilan haba yang baik, tenaga triplet yang tinggi dan tenaga HOMO dan LUMO di tahap yang sesuai untuk digunakan sebagai hos untuk OLED. Sebatian **16** dipilih sebagai calon yang terbaik untuk digunakan sebagai hos untuk OLED biru, hijau dan merah kerana tenaga tripletnya yang tinggi (E_T = 2.82 eV), suhu peralihan kaca yang tinggi (T_g = 270 ° C), kestabilan haba penguraian yang tingi (T_d = 470 ° C) dan tahap HOMO sesuai (E_{HOMO} = -5,24 eV). Sebatian **16** telah digunakan sebagai hos untuk peranti lapisan tunggal, dua lapisan dan peranti pelbagai lapis untuk OLED biru, hijau dan merah dengan kaedah proses larutan. Kenaikan dalam kecekapan peranti dapat diperhatikan dari lapisan tunggal kepada peranti dua lapisan dan kenaikan lanjut boleh diperhatikan untuk peranti berbilang lapisan. Morfologi filem nipis telah dianalisis dengan kaedah mikroskopi daya atomik (AFM) yang mendedahkan bahawa alkohol berfluorin boleh menghasilkan filem nipis yang lebih

baik dengan kekasaran permukaan rendah berbanding penggunaan alkohol normal. Alkohol berfluorin telah digunakan untuk meningkatkan keberkesanan suntikan elektron didalam peranti dan memungkinkan pembuatan lapisan pengangkutan elektron melalui proses larutan.

ACKNOWLEDGEMENTS

Firstly, I would like to express my sincere gratitude to my advisor Prof. Dr Azhar Ariffin and Dr. Woon Kai Lin for their continuous support of my PhD study and related research, for their patience, motivation, and immense knowledge sharing. Their guidance helped me along the research journey and writing of this thesis. I could not have imagined having a better advisor and mentor for my PhD study.

My sincere thanks also go to Prof Dr. Wan Jeffry and Chemistry Department staff members who provided me opportunity to access the laboratory and research facilities. Without they precious support it would not be possible to conduct this research.

I thank my fellow lab mates from Chemistry Department; Nurul Nadiah, Ong Bee Kian and Kumayl for their kind support and help in finishing this project. Special thanks also go to LDMRC research group from Physic Department for the stimulating discussions, working together and for all the fun we have had in the last couple of years. Special thank for my friend Wong Wah Seng for the guidance and help in device fabrication process.

Last but not the least, I would like to thank my parents and my family members for supporting me spiritually throughout this project and thesis writing process. Finally, I must thank my wife, Nurul Ain for providing me with everlasting support and continuous encouragement throughout my years of study and the process of research and writing this thesis. Not to forget, my little princess, Zara Rania and Zara Raisha that give me strength and motivation to finish this project. This accomplishment would not have been possible without them.

Thank you.

TABLE OF CONTENTS

LIST OF FIGURES

LIST OF SCHEMES

LIST OF TABLES

LIST OF SYMBOLS AND ABBREVIATIONS

^{13}C NMR	13-Carbon nuclear magnetic resonance
^{1}H NMR	Proton nuclear magnetic resonance
AFM	Atomic Force Microscopy
BHJ	Bulk heterojunction
Br	Bromine
Calcd	Calculated
$CDCl_3$	Deuterated trichloromethane
CH_3COOH	Ethanoic acid
CHN analysis	Carbon Hydrogen Nitrogen combustion analysis
Cl	Chlorine
CsF	Cesium Fluoride
Cu	Copper
$Cu(OAc)_2.3H_20$	Copper (II) acetate trihydrate
Cu_2O	Copper (I) oxide
CV	Cyclic Voltammetry
DI	Deionized
DMAc	*N, N'*-dimethylacetamide
DMAP	4-Dimethylaminopyridine
DMSO	Dimethyl sulfoxide
DSC	Differential Scanning Calorimetry
EML	Emissive/emission layer
EQE	External Quantum Efficiency
ET	Triplet Energy
ETM	Electron Transport Materials
FIrpic	Iridium (III)-bis[4,6-(difluorophenyl)pyridine-N,C2'] picolinate
FIrpic	Bis[2-(4,6-difluorophenyl)pyridinato-C2,N](picolinato)iridium(III)
H_2O	Water
Hex-Ir(phq)3	Tris[2-(4-n-hexylphenyl)quinoline)]iridium(III)
HOMO	Highest Occupied Molecular Orbital

HTL	Hole Transport Layer
HTM	Hole Transport Materials
Hz	Hertz
I	Iodine
Ir	Iridium
IR	Infra-red
Ir(mppy)3	Tris[2-(p-tolyl)pyridine]iridium (III)
ITO	Indium tin oxide
J	J coupling
K_2CO_3	Potassium carbonate
KI	Potassium iodide
KIO_3	Potassium iodate
KOH	Potassium hydroxide
LCD	Liquid Crystal Display
L_E	Luminous efficiency
LiOAc	Lithium acetate
LUMO	Lowest Unoccupied Molecular Orbital
m	Meta
MHz	Megahertz
N_2	Nitrogen
NIS	*N*-iodosuccinimide
o	Ortho
OFETs	Organic field-effect transistors
OLEDs	Organic light emitting diodes
OPPI	4-Octyloxydiphenylidonium hexa-fluoroantimonate
OXD-7	1,3-bis[2-(4-tert-butylphenyl)-1,3,4-oxadiazo-5-yl]benzene
p	Para
$Pd(OAc)_2$	Palladium (II) acetate
PEDOT	Poly(3,4-ethylenedioxythiophene)
PEDOT: PSS	Poly(3,4-ethylenedioxythiophene): polystyrene sulfonate
PhOLEDs	Phosphorescent organic light emitting diodes
PL	Photoluminescence

Ppm	Parts per million
Rh	Rhodium
RMM	Relative molecular weight
SPPO13	2,7-bis(diphenylphosphoryl)-9,9′-spirobi[fluorene]
T_d	Thermal decomposition temperature
T_g	Glass transition temperature
TGA	Thermogravimetric analysis
THF	Tetrahydrofuran
TLC	Thin Layer Chromatography
TMS	Tetramethylsilane
UV/Vis	Ultra-violet/Visible
UVSs	Ultraviolet sensors
w/v	Weight/volume
X-F6-TAPC	*N*,*N*'-(4,4'-(Cyclohexane-1,1-diyl)bis(4,1-phenylene))bis(*N*-(4-(6-(2-ethyloxetan-2-yloxy)hexyl)phenyl)-3,4,5-trifluoroaniline)

CHAPTER 1: OVERVIEW

1.1 Overview

Organic Light-Emitting Diodes (OLEDs) have attracted much attention in academic (Yeh et al., 2005) and industrial fields (Fyfe, 2009) as flat panel displays (Forrest, 2004) and solid-state lighting (Sasabe et al., 2013; Service, 2005; Sun et al., 2006; Zhang et al., 2012a). OLED technology has several advantages compared to previous generation technology (e.g. LCD or LED) such as they are exceptionally thin (White et al., 2013), flexible (Gustafsson et al., 1992; Kim et al., 2011; Nakajima et al., 2014; Noda et al., 2011; Wang et al., 2011; Zhou et al., 2014), variable in shapes (Bi et al., 2014), colours (Cheng et al., 2014; Fan et al., 2013; Liu et al., 2013a; Mingxiao et al., 2013; Zhang et al., 2013), sizes (Shin et al., 2015), and some even crystal clear images (Lee et al., 2015; Lifka et al., 2011; Masuyama et al., 2015; Park et al., 2012a; Park et al., 2014; Park et al., 2010; Takayuki et al., 2013). OLEDs are brighter and do not need a backlight, so they consume less energy and produce a higher contrast than LCDs. This will prolong the battery lifetime of our daily electronic devices, such as smartphones, tablets, and laptops. Furthermore, OLEDs exhibit response time up to 200 times faster than those of LCDs. These characteristics are important in the projection of realistic motion pictures. In solid state lighting, OLEDs will substitute our existing technology (fluorescence lamp, etc.) because OLEDs are self-illuminating, eco-friendly and power saving (Levermore et al., 2012; Yamae et al., 2013; Yu et al., 2012). Apart from that, there are some disadvantages, where OLED displays may not last as long as LCDs because the degradation of the organic molecules meant that early versions of OLEDs tended to wear out faster than conventional LCDs or LED displays (Scholz et al., 2015). Another disadvantage of OLEDs is that organic molecules in OLEDs are very sensitive to water and oxygen. But this problem can be solved by purification and encapsulation (Ghosh et al., 2005; Kim et al., 2013; Ueno et al., 2013; Yong-Qiang et al., 2014).

In order to maximize the device efficiency for solution processable phosphorescent OLEDs (PhOLEDs), suitable organic host materials are needed. The materials need to be amorphous, exhibit a high glass transition temperature (T_g) and be thermally stable at high temperature, exhibit suitable HOMO and LUMO levels and appropriate triplet energy (Tokito, 2004). Phosphorescent emitters are usually doped into a host to diminish self-aggregation quenching and triplet-triplet annihilation. It is crucial that the triplet energy of the host material should be higher than that of the phosphorescent emitter to prevent energy back transfer and to confine the electro-generated triplet excitons on the dopant molecules (Yang et al., 2013).

The design and synthesis of organic materials for the application as host materials in electronic device are very important aspects in the development of efficient OLEDs (Agarwal et al., 2011; Ameen et al., 2016; Zhang et al., 2015). In order to overcome earlier problems using small organic molecules and polymers, a new class of materials was introduced, i.e., dendrimers (Hwang et al., 2008; Li et al., 2009; Lo et al., 2007). Dendrimers are superior in terms of their physical properties compared to small molecules and polymers because of their high molecular weight nature and high purity level that can reach up to 99.9 % (Morgan et al., 2014). Dendrimers from carbazoles and the derivatives can be used to achieve an efficient and solution processable host materials for OLEDs (Albrecht et al., 2015; Ban et al., 2015).

Present-day technology for fabrication of OLEDs display is vacuum deposition technique. This fabrication technology is expensive and inefficient use of materials because of difficulty to control deposition of mixture materials with a fixed ratio. One way to reduce the cost and loss of materials during the fabrication process is solution process technique. One of the advantages of using solution process is the ability to reduce materials usage because materials can be directly applied to the target area through slot-

die method. This technology is more suitable in mass production line as in large panel OLED lighting while inkjet printing can be used for OLED displays.

In term of efficiency, blue phosphorescence organic light-emitting diodes (PhOLEDs) is still lagging behind compared to red and green PhOLEDs due to the lack of solution processable high triplet energy host materials. One way to overcome this problem is to use organic dendrimers based on carbazole as the host materials. This kind of structure has the benefit in term of high thermal stability and amorphous because of the highly-twisted structure along with high molecular weight (Jiang et al., 2012b; Li et al., 2013; Yang et al., 2013). Furthermore, carbazole dendrimers tend to retain high triplet energy of the carbazole component (Wang et al., 2014). Unlike small molecules, carbazole dendrimers will not crystallize during spin-coating. It is important to get a smooth surface without pinholes to ensure high efficiency of PhOLEDs. All of these carbazole dendrimer characteristics will benefit us in achieving our goal to produce blue host materials that have suitable properties for long life-time solution-processable PhOLEDs.

1.2 Objectives of Study

1. To synthesis carbazole-based host materials for solution processable OLEDs.
2. To purify the compounds and to characterize their optical properties using UV/Vis, fluorescence, and phosphorescence spectroscopy.
3. To investigate their thermal stability in terms of thermal decomposition temperature (T_d) and glass transition temperature (T_g).
4. To determine their HOMO and LUMO levels by cyclic voltammetry.
5. To design, fabricate and characterize solution processed single, double and multilayer devices as red, green and blue PhOLEDs.

1.3 Organization of the thesis

This thesis consists of six chapters. Chapter 1 covers the overview of the thesis, problem statement, objectives of study and organization of the thesis.

Chapter 2 is the literature review for the synthesis of carbazole derivatives, carbazole as host materials for OLEDs, carbazole dendrimers as host materials for PhOLEDs, history of OLEDs, host materials for PhOLEDs, type of host materials, type and device structure of OLEDs, photoluminescence, and generation of light in OLEDs.

Chapter 3 describes the synthesis and physical characterization of OLEDs materials including photophysical, thermal, and electrochemical properties of the materials synthesized.

In Chapter 4, it discusses the results of device fabrication of OLED devices based on compound **16** as the host materials for red, green and blue PhOLEDs devices.

The experimental section comprises in Chapter 5.

Chapter 6 summarizes the work done and also future work.

CHAPTER 2: LITERATURE REVIEW

2.1 Introduction

Carbazole is an aromatic heterocyclic organic compound that consists of a five-membered nitrogen-containing ring sandwiched between two phenyl rings as shown in Figure 2.1. Carbazole derivatives are an important class of heterocycles known for their photophysical and biological activity such as antimicrobial, antitumor and antioxidative agents (Bashir et al., 2015; Bouaziz et al., 2015; Głuszyńska, 2015; Gu et al., 2014; Hieda et al., 2014; Maria Stefania et al., 2015; Ochung' et al., 2015). Recently, carbazole derivatives have been used widely in organic devices including photovoltaic solar cells (Kamaladin et al., 2015; Sathiyan et al., 2016; Xie et al., 2012) and organic light emitting diodes (OLEDs) (Chen et al., 2015; Moonsin et al., 2013; Sudyoadsuk et al., 2014; Xie et al., 2015; Zhang et al., 2015). Carbazole can be obtained from coal tar (Graebe, 1872) but the difficulty of removing impurities renders the synthetic preparation of carbazole the best option to produce pure carbazole in a large quantity.

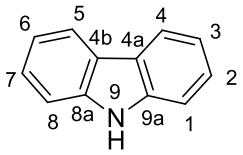

Figure 2.1: Structure and numbering of 9H-carbazole

In natural plants, many carbazole alkaloids have been isolated. In 2012, Yang et al. (2012) have isolated carbazole alkaloids from stems of *Glycosmis pentaphylla* namely 4-(7-hydroxy-3-methoxy-6-methyl-9H-carbazol-4-yl)but-3-en-2-one (A), and two new dimeric carbazole alkaloids, bisglybomine B (B) and biscarbalexine A (C), together with seven known alkaloids (Figure 2.2).

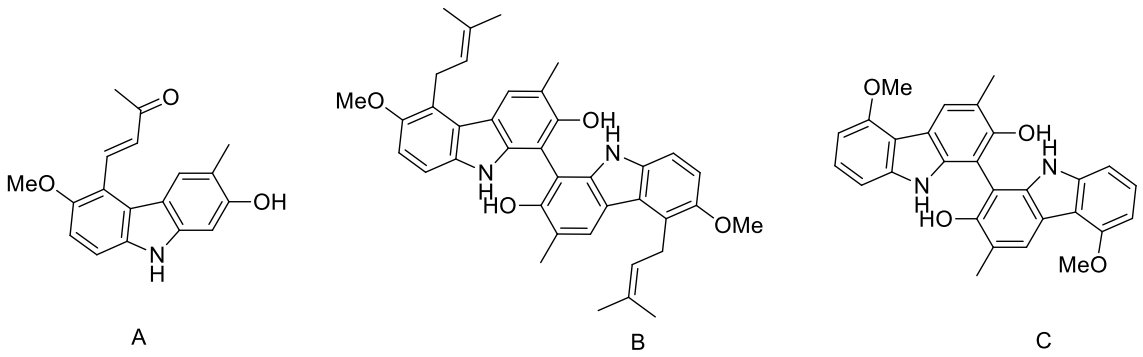

Figure 2.2: Molecular structure of alkaloids A, B, C

Maneerat et al. (2013) isolated the carbazole alkaloids, clausenawallines G-K along with another 12 known alkaloids from twigs *of Clausena wallichii* (Figure 2.3).

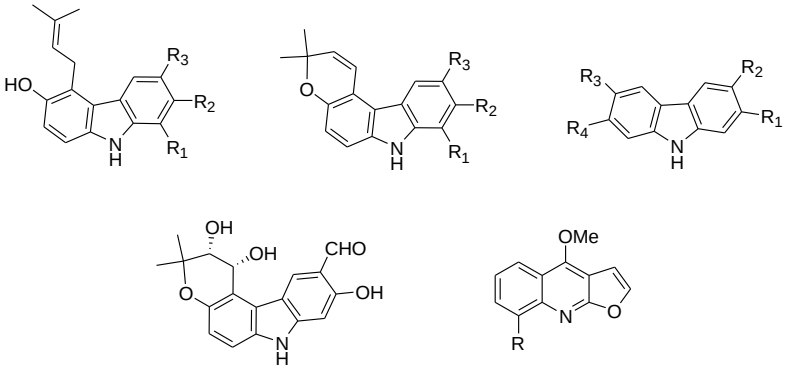

Figure 2.3: Some of the alkaloids from *C. wallichii twigs*

Other examples of carbazole alkaloids were isolated from *Murraya euchrestifolia* (Rutacea) by Ito et al. (2012). 13 carbazoles have been isolated so far and some of them show significant effects in the induction of apoptosis in HL-60 cells. They could be possible candidates as a cancer chemopreventive agents (Figure 2.4).

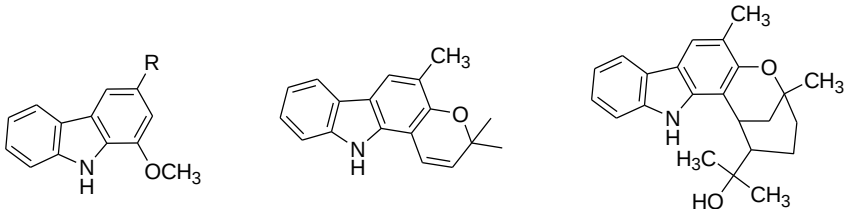

Figure 2.4: Some of the alkaloid isolated from *Murraya euchrestifolia*

In the field of organic electronics, carbazole-based materials have been widely used as organic semiconductors in electronic devices. Carbazole oligomeric semiconductors for use in organic field-effect transistors (OFETs) have been reported by Drolet et al. (2005). The structure of CPC, RCPCR, CCC, and RCCR are shown in Figure 2.5.

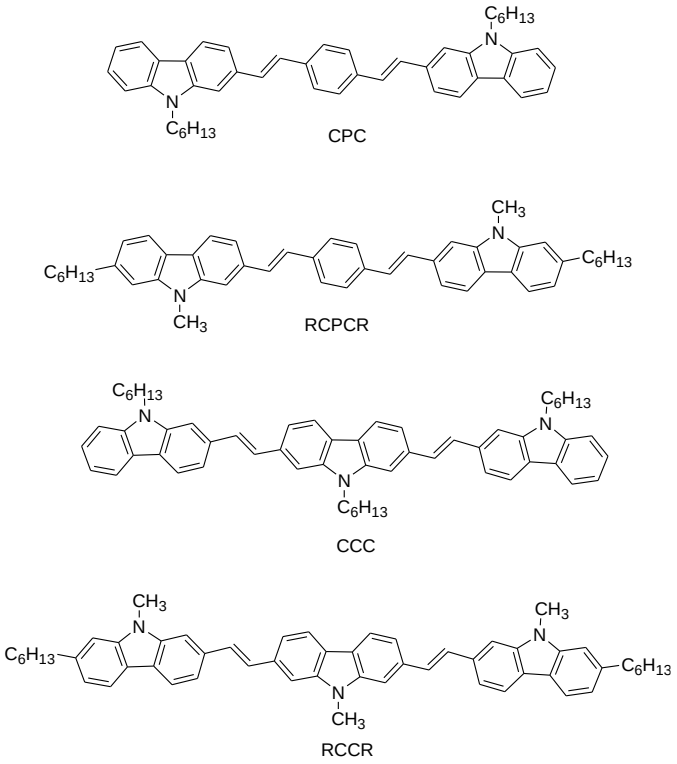

Figure 2.5: Molecular structure of 2,7-carbazolene-vinylene-based oligomers

In the organic bulk heterojunction (BHJ) solar cells, carbazole-based materials have been reported to be used as sensitizer molecules. Choi et al. (2011) reported the synthesis of HMBI for solution-processed BHJ (Figure 2.6).

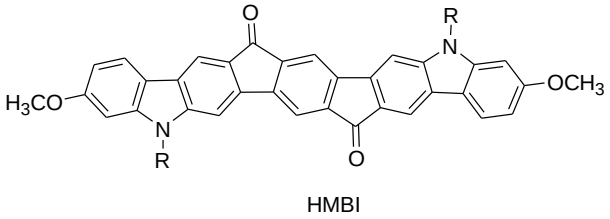

Figure 2.6: Molecular structure of HMBI

Carbazole-based semiconductors for use in organic ultraviolet sensors (UVSs) have also been synthesized by Zhang et al. (2012b). The triphenylbenzene-containing carbazole derivative (PCP) was reported to exhibit a wide band gap, good hole mobility, and excellent thermal stability to be used as UVSs (Figure 2.7).

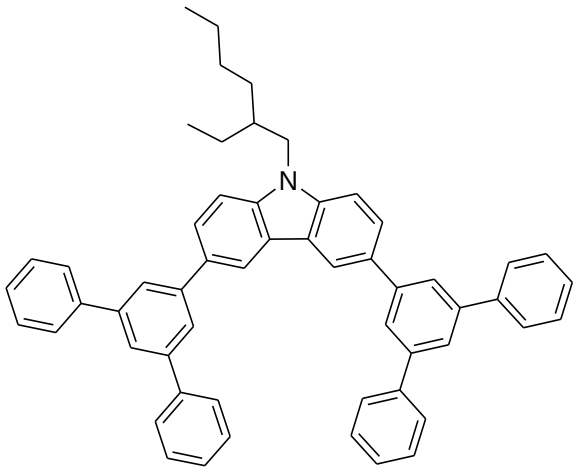

PCP

Figure 2.7: Molecular structure of PCP

2.2 Synthesis of carbazole and substituted carbazoles

Because of the importance of carbazole and its derivatives, there have been an enormous collection of synthetic strategies reported in the literature. In early times, carbazole synthesis relies on nitrene insertion, Fisher indolization, Pummerer cyclization, Diels-Alder reaction, etc. In recent times, transition metal-mediated C-C and C-N bond formation, cyclotrimerization, benzannulation, Suzuki-Miyara coupling, ring-closing metathesis, etc., have played an important role in the formation of carbazole derivatives (Roy et al., 2012).

Two examples of the classic synthesis of carbazole and it derivative involve the Borsche-Drechsel cyclization and Grabe-Ullmann reaction. In the Borsche–Drechsel cyclization reaction (Borsche, 1908; Drechsel, 1888), phenylhydrazine is condensed with

cyclohexanone to form the corresponding imine and then the reaction proceeds to a hydrochloric acid catalyzed rearrangement and ring-closing reaction to form the tetrahydrocarbazole as shown in Scheme 2.1.

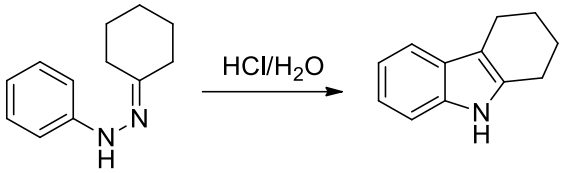

Scheme 2.1: Borsche-Drechsel synthesis of tetrahydrocarbazole

In the Graebe-Ullmann method (Graebe et al., 1896), *o*-aminodiphenylamine was treated with nitrous acid to give 1-phenyl-1,2,3-benzotriazole which upon heating loses two nitrogen atoms to give carbazole as shown in Scheme 2.2.

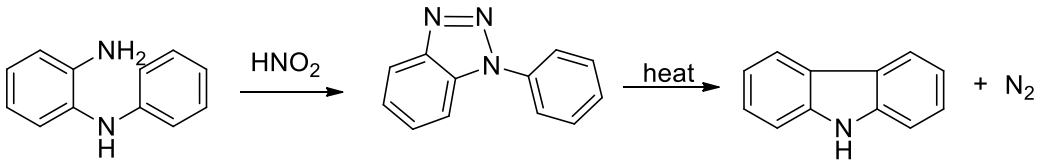

Scheme 2.2: Graebe-Ullmann synthesis of carbazole

Many methods have been developed in the modern age in order to increase the yield of the desired carbazole products in a more cost-effective manner. In this literature review, we will only discuss some important examples of the synthesis of carbazole derivatives from the last 10 years and above.

Antiostatin A_1, a potent antioxidant that contains carbazole moiety was synthesized by Alayrac et al. (2009). The synthesis of A_1 involves a palladium-catalysed arylamidation and a chemo- and regioselective rhodium-catalysed cross alkyne cyclotrimerisation reaction as the key step. *O*-iodoaniline was used as the starting material

that undergoes a tosylation reaction with ethynyl(phenyl)iodonium triflate. Then, three effective transition metal-catalysed reaction; a Sonogashira reaction, a rhodium-catalysed reaction and a palladium-catalysed reaction was used to formed antiostatin A_1 (Scheme 2.3).

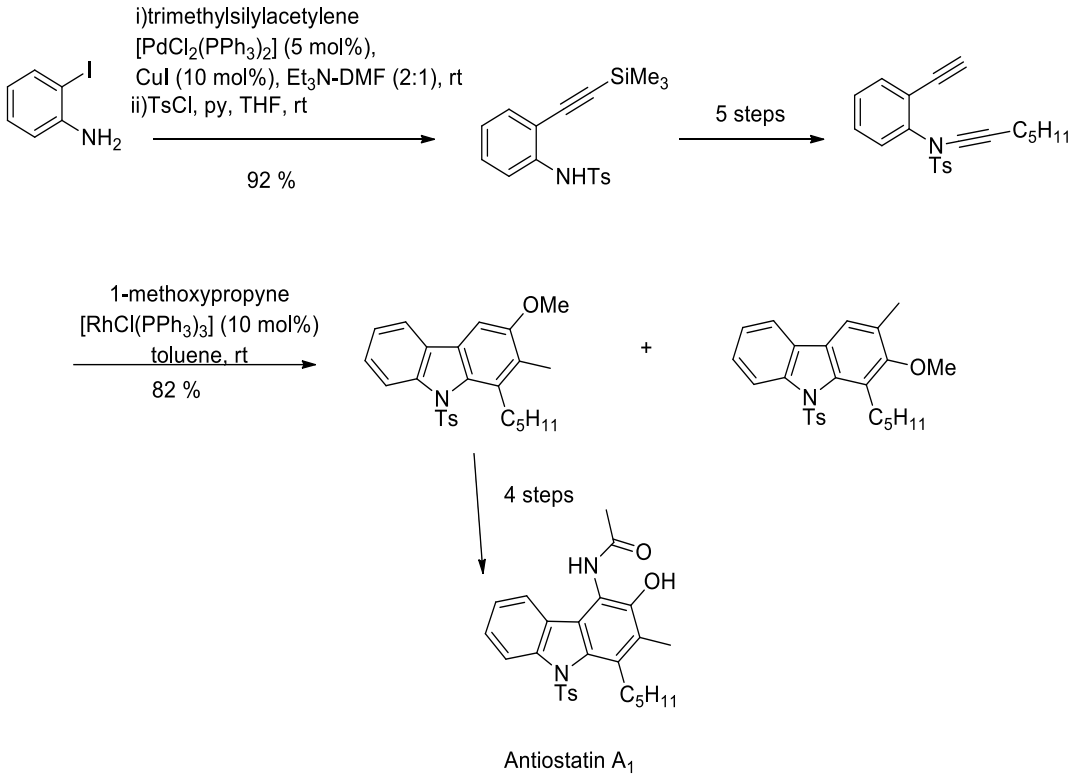

Scheme 2.3: Total synthesis of antiostatin A_1

Yamashita et al. (2009) reported the selective synthesis of 1,2,3,4-tetrasubstituted carbazoles using palladium-catalyzed oxidative cycloadditions of indoles with alkynes in the presence of $Pd(OAc)_2$ as a catalyst, $Cu(OAc)_2.3H_2O$ as oxidant and LiOAc as addictive. No reaction occurred when Ir or Rh derivatives were used as the catalysts.1-Methylindole-3-carboxylic acid underwent an oxidative coupling with the alkyne to yield 1,2,3,4-tetraphenyl-9-methylcarbazole (Scheme 2.4).

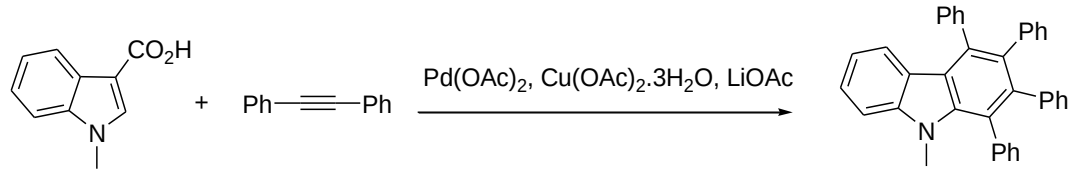

Scheme 2.4: Pd-catalyzed oxidative coupling of 1-methylindole-3-carboxylic acid with alkynes

Fischer indolization was employed as the key step in carbazole synthesis by Park et al. (2009) in the reaction of Cbz-protected aryl hydrazides with cyclohexanone to produce tetrahydrocarbazoles. Subsequent oxidative aromatization of D with DDQ in benzene afforded the corresponding *N*-Cbz-carbazoles (Scheme 2.5).

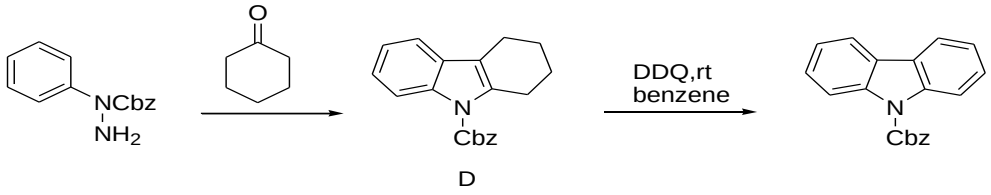

Scheme 2.5: Fischer indolization of bishydrazides

Ramesh et al. (2009) synthesized di-, tri-, and tetra- substituted carbazole analogs based on Hauser annulations (Hauser et al., 1978) which involve a one-pot operation of three reaction sequences of Michael addition, Dieckmann condensation, and sulfoxide elimination. In this reaction, bromomethylindole (E) was converted into sulfoxide (F) which was then treated with different Michael acceptors in the presence of t-BuOK resulting in the formation of carbazole analogs G (Scheme 2.6).

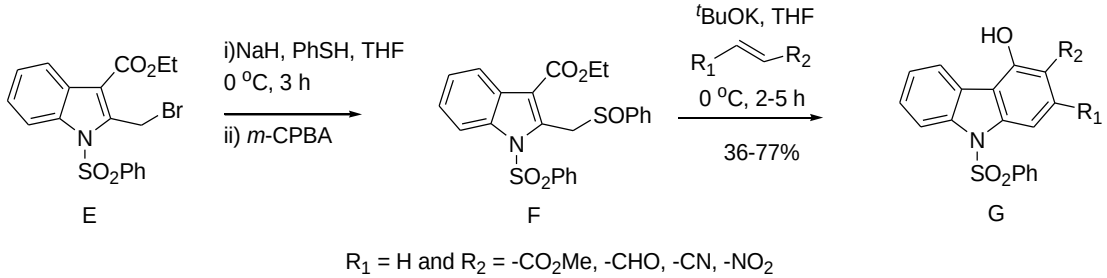

Scheme 2.6: Synthesis of trisubstituted carbazoles from indole intermediate

In the OLEDs field studies, many materials have been synthesized based on carbazole derivatives. In 2011, study from You et al. (2011), reported the synthesis of P1 in which Suzuki Coupling was a key as shown in Scheme 2.7. 1,3,6,8-Tetrabromopyrene (H) was obtained by bromination of pyrene using molecular bromine. An Ullmann reaction was used in the synthesis of 9-(4-bromophenyl)-carbazole (I) using carbazole and 1,4-dibromobenzene as the starting materials. Element I reacted with *n*-BuLi in THF followed by the addition of triisopropyl borate and then a hydrolysis process to give 4-(9H-carbazol-9-yl)phenylboronic acid (J). P1 was obtained via a Suzuki coupling reaction between H and J in the presence of *tetrakis*(triphenylphosphine) palladium and K_2CO_3 in toluene.

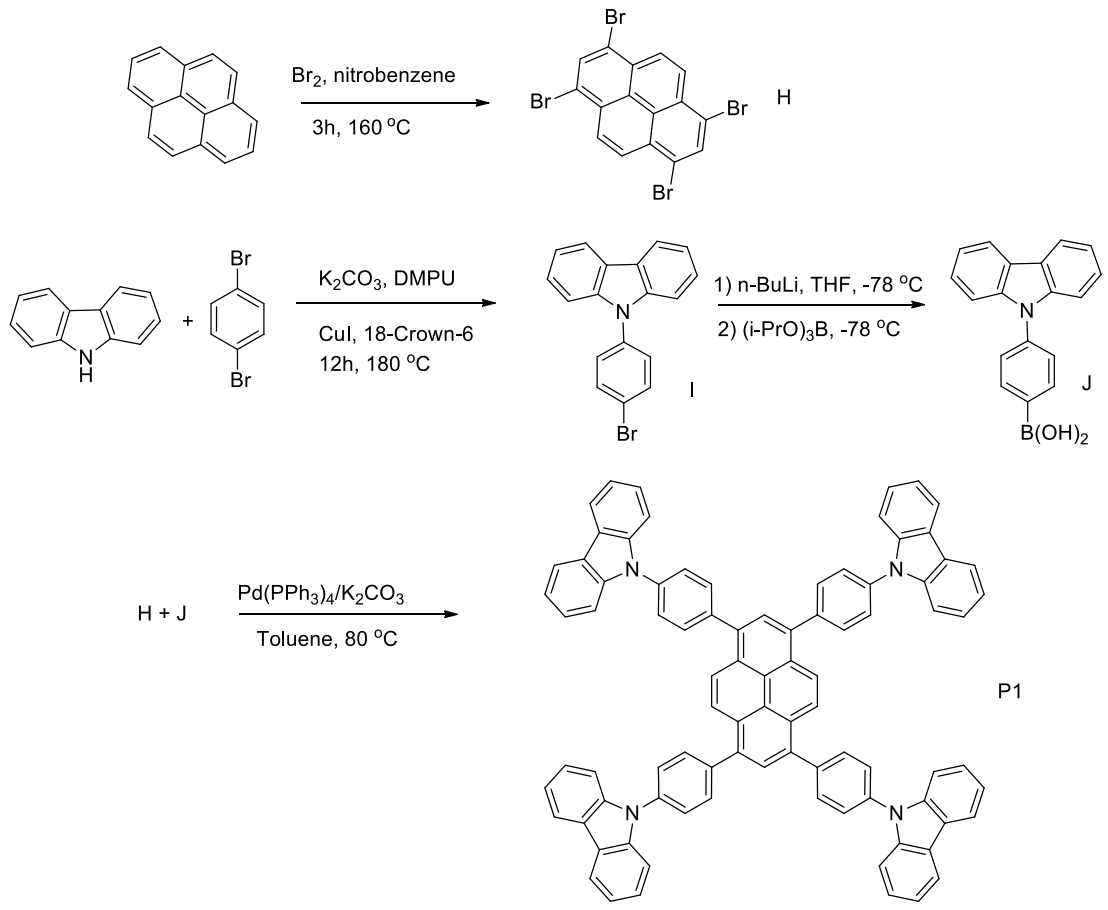

Scheme 2.7: Synthesis route of P1

There are many more reports on the synthesis of carbazole derivatives such as those by Cho et al. (2011), Youn et al. (2011), Yuan et al. (2016), and few others.

2.3 Carbazole as host materials for PhOLEDs

In the area of organic electronics especially OLEDs, carbazoles have been used widely as one of the main components in the synthesis of host materials for OLED devices. Many literatures have reported the use of carbazole derivatives as their main backbone (Grigalevicius et al., 2008; Lee et al., 2012; Romero et al., 1996; Tsai et al., 2006; van Dijken et al., 2004; Zhao et al., 2011). Carbazole derivatives have been one of the popular host materials for OLEDs due to their high triplet energy and good hole-transporting ability. Carbazole has been reported to have triplet energy as high as 3.0 electron volt (eV) (Birks, 1970). This energy possesses by carbazole being often used as building block for host materials. For blue emitting phosphors, host materials with higher triplet energies more than 2.80 eV are necessary to prevent energy back transfer from emitter guest to host (Yook et al., 2012).

One commonly used host for phosphorescent emitters is 4,4'-bis(9-carbazolyl)-biphenyl (CBP) (Figure 2.7) with a triplet energy of 2.56 eV (Adachi et al., 2001). CBP is used as an efficient host material for green and red phosphorescent organic light-emitting diodes (PhOLEDs), but not an efficient host for blue PhOLEDs because of its relatively low triplet energy compared to popularly used blue emitter, iridium (III) bis(4,6-(difluorophenyl)pyridine-*N*,$C^{2'}$) picolinate (FIrpic, 2.65 eV) (Holmes et al., 2003). In order to increase the triplet energy of CBP, scientists have developed a series of structurally modified CBP-derivatives.

By introducing methyl groups at 2- and 2'-positions of the core biphenyl in CBP, 4,4'-bis(9-carbazolyl)-2,2'-dimethylbiphenyl (CDBP) (Figure 2.7) with higher triplet

energy of 3.0 eV was produced (Tokito et al., 2003). It shows that by incorporation of the steric group or non-conjugated linkage between the two carbazole moieties plays a key role in achieving high triplet energy.

One more common example of modified CBP is 1,3-bis(*N*-carbazolyl)benzene (mCP) (Figure 2.8) with triplet energy of 2.9 eV (Holmes et al., 2003). The mCP was synthesized by replacing the core biphenyl group by single benzene group that attached to carbazoles at *meta*-position instead of *para*-position in 1,4-bis(*N*-carbazolyl)benzene (CCP). It is obvious that modifying the structure in PhOLED host is a critical principle to achieve high triplet energy.

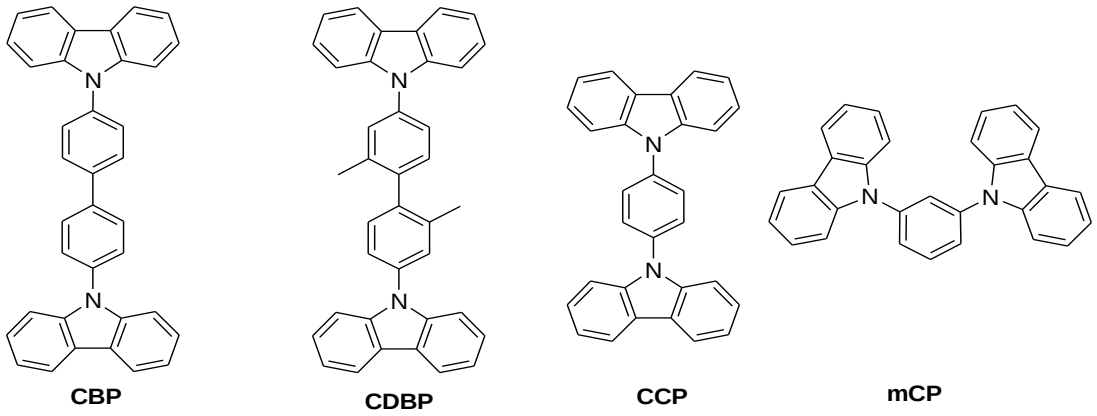

Figure 2.8: Molecular structure of CBP, CDBP, CCP and mCP

Even though CDBP and mCP showed appropriate triplet energies and suitable to be blue host materials for PhOLEDs, problems still remain in terms of relatively low thermal and morphological stability due to their low molecular weight (Shirota, 2000). Low molecular weight organic compound generally tends to crystallize above room temperature and usually exist as crystals below their melting points. Crystalline compounds are not favorable in solution-processed PhOLEDs and OLEDs.

Amorphous host materials were then introduced to overcome these problems. Amorphous molecular materials or molecular glasses are preferable because they are in

thermodynamically non-equilibrium state and hence may exhibit glass transition phenomena usually associated with amorphous polymers. In contrast to single crystals and liquid crystals, which show anisotropic properties, amorphous materials exhibit isotropic properties as well as homogenous properties due to the absence of grain boundaries. They often form a uniform and transparent amorphous thin films by solution-processed methods (Shirota, 2000).

2.4 Carbazole dendrimers as host materials for PhOLED

To overcome the problem of crystallization in small molecules, dendrimer materials for solution-processing were designed to suppress crystallization by introducing alkyl chains, by adopting an asymmetric molecular structure and by introducing bulky side groups to increase their molecular weight.

Dendrimers are now regarded as the third class of materials in application for OLEDs and PhOLEDs. Dendrimers also called dendritic macromolecules or branched macromolecules. A typical dendrimer usually consists of three components (Li & Liu, 2009):

(1) Core: located in the geometrical center or focus and usually determines the most important function of the dendrimer.
(2) Surrounding dendrons: contain branching points and the branching level defines the dendrimer generation.
(3) Surface groups: covalently grafted onto the periphery of the dendrons to tune solubility and processability of the dendrimer.

Dendritic type materials represent an alternative to small molecule and polymeric host materials, since they maintain small molecular characteristics, which are usually easy to purify, exhibit a well-defined structure, and improved morphological behavior making

it remains non-crystallizable during spin coating. Because of their high molecular weight, dendrimers show amorphous characteristics with high thermal glass transition temperature. Dendrimers also have good solubility and appropriate viscosity in common organic solvents making them suitable for solution processing.

Many dendrimers based on carbazole derivatives have been reported, including Cz-TCP, by Jiang et al. (2012a). Cz-TCP has an excellent thermal and morphological stability due to its twisted and non-planar molecular structure (Figure 2.9). Cz-TCP also possesses a high triplet energy at 2.86 eV, which makes it a suitable as host material for blue phosphorescent dopants. Additionally, the attachment of bulky alkyl groups (*tert*-butyl) ensures the solubility of the dendrimers in common solvents. Fabrication of blue PhOLEDs using Cz-TCP as the host materials doped with the guest of iridium (III) bis[4,6-(di-fluoropenyl)-pyridinato-N,C’] (Flrpic) shows a high performance with luminescence efficiency (LE) value of 25.7 cd A^{-1} and the external quantum efficiency (EQE) of 13.0 %. While using deep blue phosphorescent emitter of iridium (III) tris[3,5-difluoro-4-cyanophenyl)pyridinato-N,C’] (FCNIrpic), the deep-blue-emitting devices shows a value of LE of 10.9 cd A^{-1} and EQE of 6.4 %. The efficiencies of these devices are outstanding compared with the values exhibited by other works related to solution-processed blue PhOLEDs.

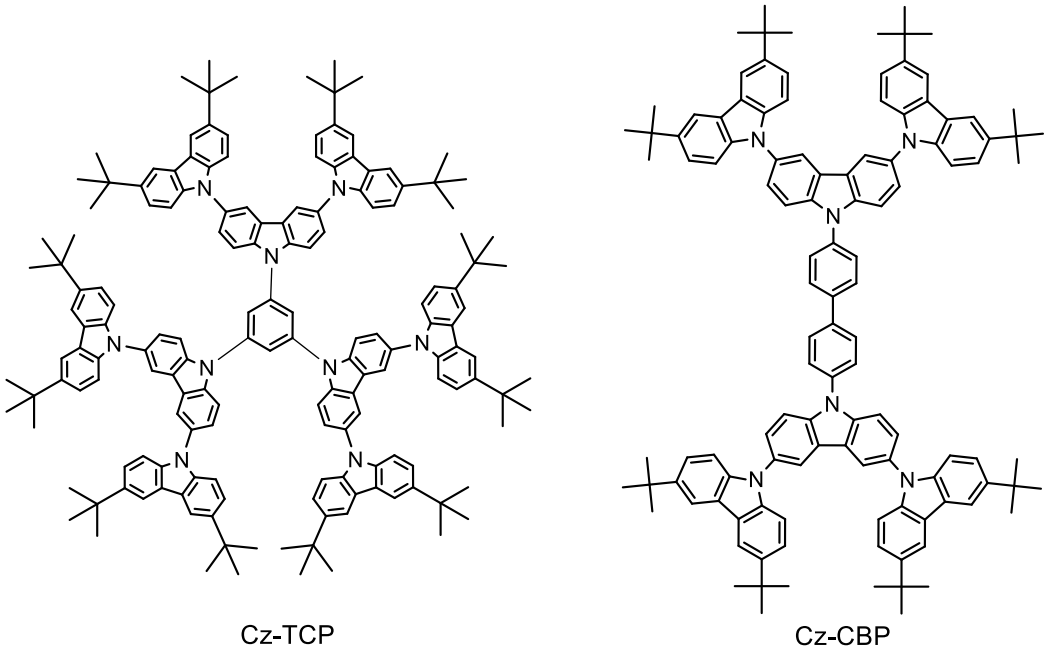

Figure 2.9: Molecular structure of Cz-TCP and Cz-CBP

Another example is Cz-CBP (Figure 2.9) synthesized by Yang et al. (2013). Cz-CBP exhibit a high thermal stability due to its high thermal decomposition temperature (T_d) of 475 °C which is about 100 °C above the CBP. Cz-CBP also has much higher glass transition temperature (T_g) which is 287 °C compared to CBP (T_g = 62 °C). This showed that this dendritic structure can greatly enhance thermal stability Cz-CBP which facilitates the formation of amorphous film through solution processing. The triplet energy of Cz-CBP was determined to be 2.68 eV which is sufficiently high to serve as host for FIrpic (2.62 eV). Single layer device was fabricated using Cz-CBP as host for FIrpic showed the maximum luminance efficiencies of 5.8 cd A^{-1} and maximum quantum efficiencies of 2.8 %. If compared to CBP based device, the efficiency of Cz-CBP based device was almost 3 times higher. HOMO energy of Cz-CBP was estimated to be -5.30 eV. Compared with CBP (HOMO = -5.51 eV), it is believed that the holes are easily injected from PEDOT: PSS to the emitting layer that contributes to the high efficiency of Cz-CBP.

Cz-CCP and Cz-mCP (Figure 2.10) are another examples of dendritic molecules that have been modified from CCP and mCP (Jiang et al., 2012b). It has been reported that Cz-CCP and Cz-mCP exhibit high triplet energy (2.85 eV), excellent film-forming ability, high glass-transition temperatures (242-248 °C), high T_d (415-443°C) and appropriate HOMO energy levels. The surface of dendrimers doped with 10 wt % FIrpic are free of pinholes and are quite smooth, with the root-mean-square (rms) values less than 0.2 nm, while the films prepared from mCP doped with FIrpic exhibit more aggregation, or phase segregation, with the rms values more than 1.0 nm. The HOMO energy levels of Cz-CCP and Cz-mCP were estimated to be -5.33 eV and -5.35 eV, respectively. These energy levels have been well tuned to approach the work function of PEDOT (-5.20 eV), which allows in a low barrier of hole injection. The single layer device using Cz-CCP and Cz-mCP as host for FIrpic showed maximum luminance efficiencies of 9.6 and 10.8 cd A^{-1} respectively.

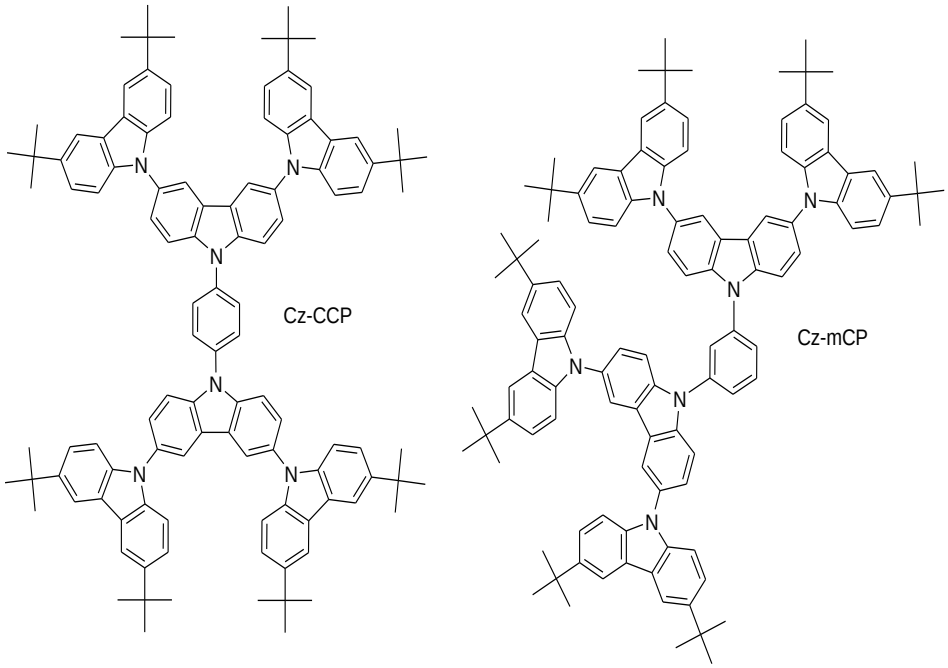

Figure 2.10: Molecular structure of Cz-CCP and Cz-mCP

Study from Li et al. (2013) reported the synthesize of third generation dendritic structure of G3 (Figure 2.11). G3 was reported to have triplet energy of 2.61 eV which is slightly lower than triplet energies of CBP at 2.67 eV. This dendritic molecule has shown high thermal stability with T_d at 500 °C. G3 also have excellent T_g of 376 °C. This amorphous nature is believed to arise from their three-dimensional molecular conformation due to the existence of twisted biphenyl core and the bulky carbazole dendrons. The high T_d and T_g of G3 ensure the suitability for this compound to have a stable amorphous thin film by solution process for OLEDs fabrication. If compared to the second-generation dendritic structure based on CBP, the third-generation structure shows a decrease in triplet energy that is lower than FIrpic which result in G3 not suitable as blue host materials.

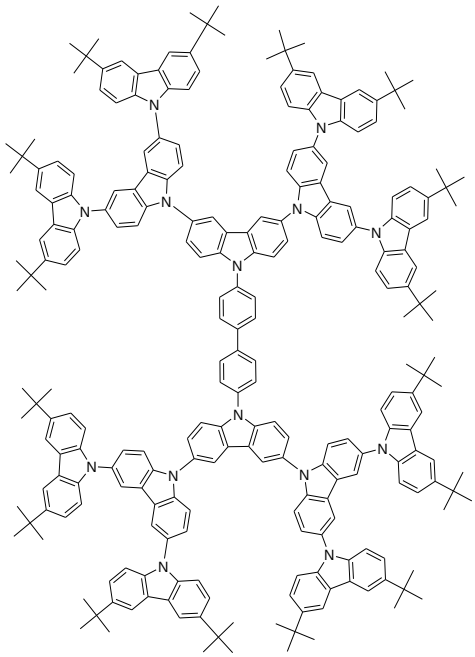

Figure 2.11: Molecular structure of G3

In 2014, Wang et al. (2014) reported the synthesis of first, second and third generation of dendrimers based on modified CDBP namely G1MP, G2MP, and G3MP (Figure 2.12) through Ullmann reaction. (Note: this paper has been published after we start our project in 2012). G2MP and G3MP have high T_d of 510 °C and 515 °C

respectively. Compared to G1MP (T_d =395 °C), G2MP and G3MP show enhancement about 115-120 °C which arises from the high molecular weight and bulky carbazole dendrons. The T_g value for higher generation dendrimers of G2MP and G3MP also increased to 297 °C and 368 °C respectively. These excellent morphological properties, ensures G2MP and G3MP to form a good film for solution process PhOLEDs. The triplet energy showed a decrease in value from 2.98 eV, 2.89 eV and 2.85 eV for G1MP, G2MP, and G3MP respectively but is sufficient enough to serve as host materials for common blue emitter for OLEDs. G1MP-G3MP show higher triplet energy than dendrimers with a biphenyl core which indicates that the presence of the two methyl group plays important role in maintaining high triplet energy. G3MP also have an appropriate HOMO level (-5.30 eV) which suitable for a wide color range of phosphors. G3MP as host materials also showed high-performance deep-blue, blue, green and red PhOLEDs with significant efficiencies of 18.2, 28.2, 54.0 and 12.7 cd A^{-1}, respectively.

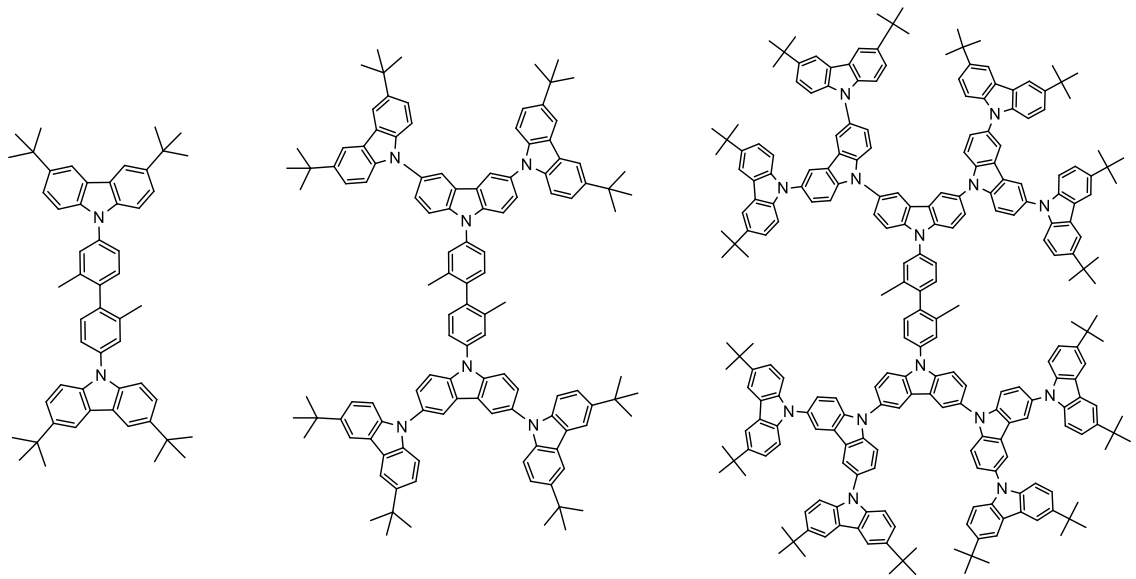

Figure 2.12: Molecular structure of G1MP, G2MP and G3MP

From above examples, it can be concluded that carbazole dendrimers will benefit in term of thermal stability, good film formation during solution spin coating process,

increase bandgap and appropriate HOMO energy levels while maintaining high triplet energy. All the properties mentioned above makes carbazole dendrimers as the suitable candidate as host materials for solution process OLEDs.

2.5 History of OLEDs

The first electroluminescence (EL) in organic materials was observed by Helfrich and Schneider from anthracene in National Research Council, Canada in 1965 (Helfrich et al., 1965). However, no practical application of this technology was seen to be possible due to its extremely high operation voltage. In 1979, Tang and Van Slyke from Kodak generated light by passing current through conjugated materials in a bilayer OLED, that lead to first efficient low-voltage organic EL (Tang et al., 1987). An organic heterostructure was used and this is the most significant step towards the practical applications of OLEDs technology. Since then, OLED technology has made significant progress in the field of diode. In 1988, Chihaya Adachi and Tetsuo Tsutsai (Adachi et al., 1988) developed a commercially multi-layered OLED by introducing an heterostructured OLED. In 1990, Jeremy Borough (Burroughes et al., 1990) from Cambridge University along with Richard Friend and Donal Bradley reported the first polymer-based LEDs (PLEDs) and this technology had huge contribution in lowering the manufacturing cost. In 1997, the first commercial passive matrix OLEDs (PMOLEDs) displays have been developed at Pioneer by Teruo Tohma that lead to full-color displays. In 1998, first Phosphorescent OLEDs (PhOLEDs) was developed by Mark E. Thompson and Stephen R. Forrest (Baldo et al., 1998) that make great improvement in OLEDs efficiency compared to fluorescent LEDs. In 2007, Samsung Mobile Display developed the first commercial active matrix organic LED (AMOLED) display.

2.6 Host materials for OLEDs

To achieve high-efficiency OLEDs device, designing and development of effective host materials is extremely important. In the search for novel host materials for phosphorescent OLEDs, several requirements have to be considered:

(i) The hosts should possess higher triplet energy than those of the dopant emitters to prevent reverse energy transfer from the guest back to the host, as well as confine triplet excitons in the emissive layer.

(ii) The highest occupied molecular orbitals (HOMOs) and the lowest unoccupied molecular orbitals (LUMOs) of host materials should match with those of neighboring active layers to reduce the hole and electron injection barrier, thus lowering the device driving voltages.

(iii) The hosts are expected to have good and balanced charge carrier transport properties for the hole–electron recombination process and confinement of the exciton formation zone in the emissive layer.

(iv) The host materials should have good thermal and morphological stability, which could reduce the possibility of phase separation upon heating, thus prolonging the device operational lifetime. Generally, a bulky and sterically hindered molecular configuration is preferable to enhance the glass transition temperature (T_g) and form morphologically stable and uniform amorphous films. This kind of materials would permit the formation of uniform films without pinholes.

2.7 Type of host materials

There are many types of host materials for OLEDs including polymer (Ananthakrishnan et al., 2014; Dumur, 2015; Lengvinaite et al., 2010; Trattnig et al., 2011; van Dijken et al., 2004), small molecules, (Duan et al., 2010; Duan et al., 2011; Kim et al., 2008; Lee et al., 2014b; Oda et al., 2013) and dendrimers (Albrecht et al., 2009; Hwang et al., 2008; Lo & Burn, 2007; Xiong et al., 2007; Zhang et al., 2004b). Small molecule host materials are commonly used because of high purity, chemical stability, high triplet energy and good lifetime. Small molecules can achieve as high as 99.9 % purity level when purified by sublimation process, which cannot be applied to polymer materials. The impurity of host materials will shorten the lifetime of PhOLEDs and long lifetime can be achieved by using highly purified small molecules as host materials. In term of chemical stability, small molecules host materials are highly stable because of the aromatic characteristic of their backbone structure. Almost all small molecules host materials are made up from the combination of aromatic units with high bonding energy that will benefit the chemical stability of the host materials. Because of its shorter conjugation length compared to polymer host materials, it is easy to obtain high triplet energy with small molecule host materials. The triplet energy of small molecules can be easily modified in the range of 2.0 eV to 3.0 eV by manipulation of conjugation length.

Host materials for OLEDs can be classified into hole transport materials (HTM) and electron transport materials (ETM). Generally, the molecular structure of HTM usually contains electron-donating moieties such as triarylamine, diphenylamine, carbazole and etc. In contrast to HTM, ETM normally contain electron withdrawing group in their molecular structure.HTM and ETM play a critical role in determining the quantum efficiency of OLEDs.

Among properties that HTM for OLEDs should possess are (Tao et al., 2011):

i) good hole mobility, a high glass transition temperature (T_g) to form thermally and morphologically stable thin films

ii) an appropriate HOMO level to ensure low energy barrier for hole injection from the anode and then into the emissive layer

iii) a suitable LUMO level to block electron injection from EML to the HTL

iv) a high triplet energy to confine triplet excitons in the EML

High triplet energy unit with good hole transport properties should be used in order to achieve high triplet energy and high hole mobility. Many core structure of HTM have been used including carbazole (Grigalevicius et al., 2008; Romero et al., 1996), diphenylamine (Cho et al., 2005; Koene et al., 1998), ditolylamine (Lee et al., 2014a; Yoo et al., 2015) and indole (Park et al., 2012b; Shimizu et al., 2012). Commonly used HTM are represent in Figure 2.13.

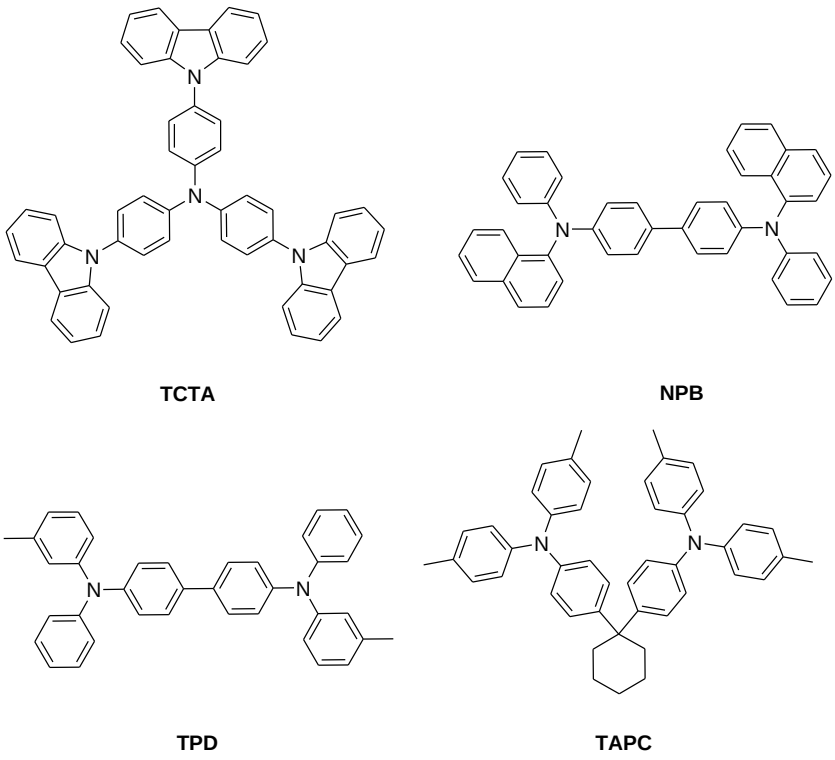

Figure 2.13: Commonly used HTM for OLEDs

2.8 Type and device structure of OLEDs

2.8.1 Components of OLEDs

Generally, OLED devices consist of the following component:

Substrate: commonly used substrate is glass, clear plastic and metal foil. Need to be transparent and conductive with high work function.

Anode: transparent electrode to inject hole into organic layers. Must have low roughness and high work function. The anode component usually used is indium tin oxide (ITO)

Hole injection layer (HIL): Materials with high mobility, electron blocking capacity and high glass transition temperature such as PEDOT: PSS

Hole transport layer (HTL): Transporting holes and blocking electron to prevent electron from reaching the opposite electrode without recombining with holes.

Emissive layer (EML): A layer between HTL and ETL. Materials can be organic molecules or polymers with high efficiency, lifetime and color purity.

Electron transport layer (ETL): Materials need to have a good electron transporting and hole blocking properties.

Cathode: low work function metal or metal alloy. The cathode injects electrons into the emitting layers. (barium, calcium, aluminum)

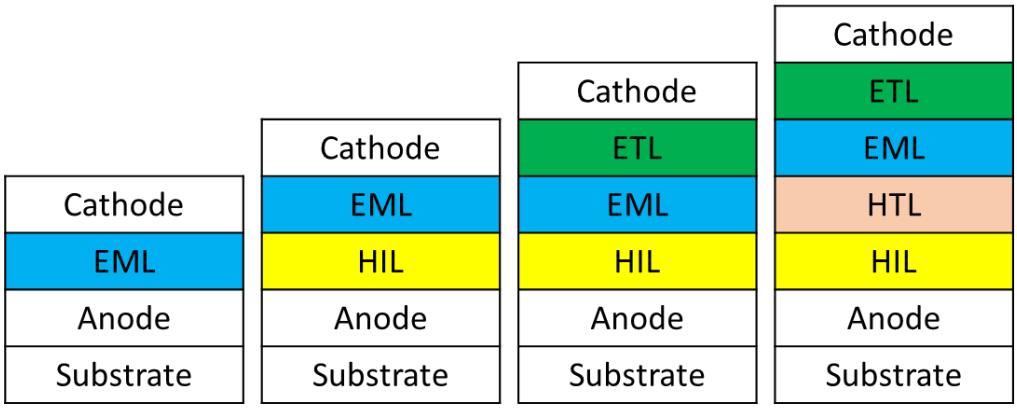

Figure 2.14: Different types of OLEDs structure (from left) simple single-layer OLEDs, common single-layer OLEDs, two-layers OLEDs, multilayer OLEDs

2.8.2 Simple single-layer OLEDs

In a simple single-layer OLED (Figure 2.14), the organic host material is sandwiched between two electrodes (anode and cathode) and deposited on a substrate. To achieve an efficient OLED with this single layer configuration, the organic material in EML need to have high luminescence quantum yield and should be able to facilitate injection and transport of electrons and holes. The demand for multifunctional capabilities from a single organic material can be very difficult to meet by nearly all current materials (Kulkarni et al., 2004) .This simplest structure gave very poor brightness, efficiency and demand high driving voltage (Burroughes et al., 1990; Helfrich & Schneider, 1965; Tang & VanSlyke, 1987; Vincett et al., 1982).

2.8.3 Common single-layer OLEDs

While in a common single-layer OLED (Figure 2.14), a hole injection layer (HIL) is introduced before deposition of an emissive layer (EML). Electrons are injected from the cathode in the conduction band (LUMO) of the organic compound, and holes are injected from the anode in the valence band (HOMO) of the organic compound. The hole–

electron pair recombination that takes place at the interface between the two layers will result in electroluminescence.

2.8.4 Two-layer OLEDs

In a two-layer OLED (Figure 2.14) an emitting layer (EML) is positioned between the hole injection layer (HIL) and the electron transporting layer (ETL). The emitting layer is primarily the site where hole-electron recombination occurred and thus for electroluminescence. This device structure is useful for emissive materials that do not possess high carrier transport properties.

2.8.5 Multilayer OLEDs

A multilayer OLED involved introduction of hole transport layer (HTL) (Figure 2.14). Multilayer device structure eliminates the charge carrier leakage as well as exciton quenching, as excited states are generally quenched at the interface of the organic layer and the metal. Multilayer OLEDs consist of different layers namely substrate, anode, hole injection layer (HIL), hole transport layer (HTL), emissive layer (EML), electron transporting layer (ETL) and cathode (Thejo Kalyani et al., 2012). The vacuum deposition process is effective to fabricate a multilayer device structure because each organic layer can be easily stacked without any damage to the underlying organic layer. But the multilayer structure is difficult to be formed by a solution process due to intermixing of organic materials during the wet coating process. Therefore, a simple device structure with only two organic layers, a hole injection layer, and an emitting layer was initially used to fabricate solution processed OLEDs (Yook et al., 2014).

2.9 Photoluminescence

Photoluminescence can be referred to the emission of light from a substance, and occurs from electronic excited states. Photoluminescence can be classified into two main categories; fluorescence and phosphorescence depending on the nature of the excited state. For easy understanding, Joblonski energy diagram is commonly used to describe the fluorescence and phosphorescence phenomena (see Figure 2.15). The singlet ground, first, and second electronic states are depicted by S_0, S_1, and S_2, respectively. Fluorophores can exist in a number of vibrational energy level, depicted by 0, 1, 2, etc. at each of these electronic energy level.

When a fluorophore absorbed light energy or electromagnetic radiation, electrons will be raised from ground state to a higher vibrational level of either S_1 or S_2. In few rare circumstances, molecules in condensed phases rapidly relax to the lowest vibrational level of S_1. The process is known as internal conversion and occurs within 10^{-12} s or less. In excited singlet state (S_1 or S_2) orbital, electron is paired (by opposite spin) to the second electron in the ground state (S_0). Consequently, relaxation of electron occurred where electron in S_1 orbital returned to S_0 very rapidly to produce emission of light. The emission rates of fluorescence are typically at 10^8 s^{-1}, so that fluorescence lifetime is very short, for about 10 ns (10×10^{-9} s).

Phosphorescence is a phenomenon where relaxation of molecules from T_1 to the singlet ground state that produces emission of light. The process of electrons transfer from S_1 to T_1 is called intersystem crossing. Spin conversion occurred, where electron in the T_1 have the same spin orientation to the one in singlet ground state (not paired). Transition from T_1 to the singlet ground state is forbidden and resulted in slower emission rate (10^3 to 10^0 s^{-1}), so that phosphorescence lifetime is much longer within millisecond to second range.

When electrons move from the excited state to the ground state, they will lose their vibrational energy. Consequently, the emission spectrum is always shifted to a longer wavelength than the excitation spectrum. This phenomenon is known as Stoke Shift. Phosphorescence spectrum will be shifted to a longer wavelength (lower energy) compared to fluorescence spectrum. The emission intensity peak is usually lower than the excitation peak, and the emission curve is the mirror image of the excitation curve, but shifted to a longer wavelength ("Introduction to Fluorescence," 2006).

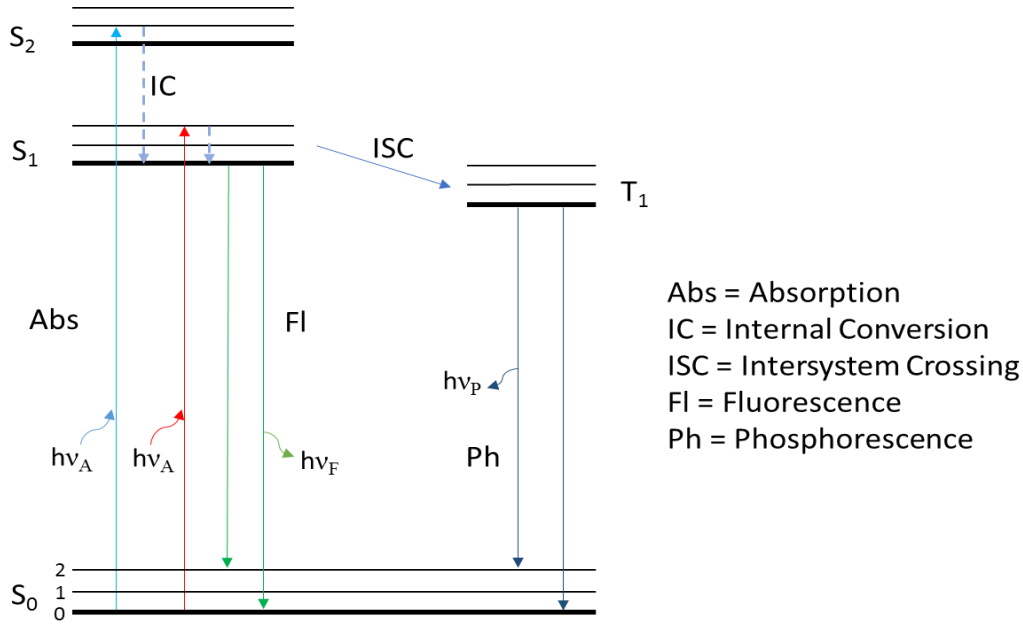

Figure 2.15: A simplify Joblonski diagram

2.10 How OLEDs generate light?

OLEDs emit light in similar way LED does and the process is known as electroluminescence. This involves the fluorescent or phosphorescent emission from an organic emitter. OLEDs are double charge injection devices, which require the simultaneous supply of both holes and electrons to the emissive layer (Kulkarni et al., 2004). The process starts with the application of a voltage (potential difference), from a battery or a power supply, across the anode and cathode. An electrical current will flow from cathode to anode through the organic layers (emitting layer). The cathode loses

electrons while anode gains them. At the boundary between the emissive and conductive layers, electrons and holes will combine to produce energy in the form of a photon and OLED will emit light. The color of the light is determined by the type of organic compound in the emissive layer. Meanwhile the intensity and brightness depends on the current density. Scheme 2.8 represent the generation of light in OLED devices.

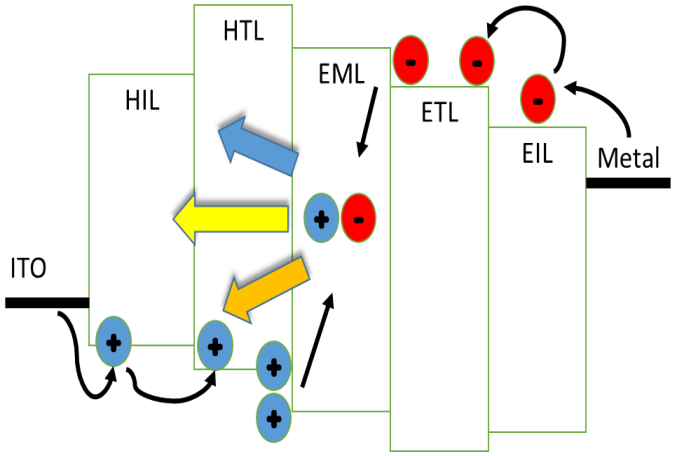

HIL: Hole Injection Layer

HTL: Hole Transport Layer

EML: Emissive Layer

ETL: Electron Transport Layer

EIL: Electron Injection Layer

Scheme 2.8: Generation of light in OLED devices

CHAPTER 3: SYNTHESIS, CHARACTERIZATION, AND PHYSICAL PROPERTIES

3.1 Overview of Ullmann Reaction

Originally, Ullmann reaction is a coupling reaction between two aryl halides and copper as reagent or catalyst to form C-C bond. It was first reported over a hundred years ago by Ullmann in 1901 (Ullmann et al., 1901).

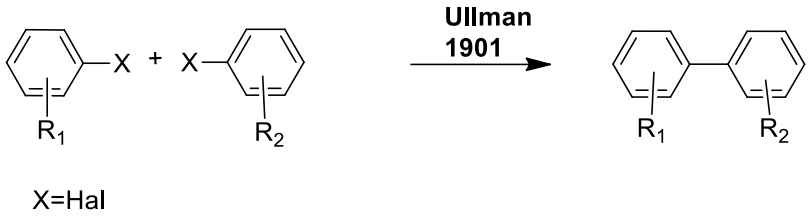

It was then employed by chemists to generate a C(aryl)-N, C(aryl)-S, C(aryl)-O bond formation and this kind of reaction was known as Ullmann Condensation Reaction. This involves a reaction between an aryl halide with a phenol, an aniline, or a thiophenol, respectively, mediated by a copper species (Ullmann, 1903).

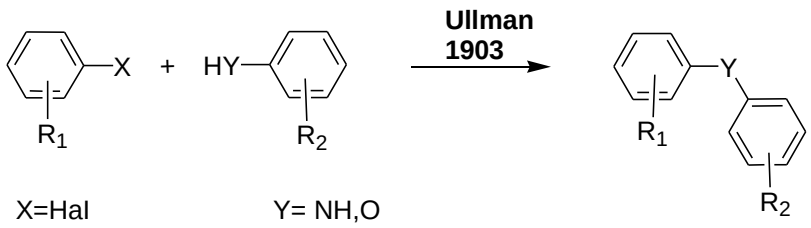

Then the Goldberg-Modified Ulmann Condensation Reaction was introduced (Goldberg, 1906). It's involves a copper-mediated (originally catalytic) formation of a C(aryl)-N bond after the reaction between an amide and aryl halide.

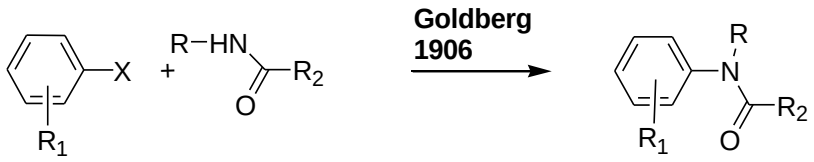

X=Hal

Numerous modification of the Ullmann couplings have been reported such as Chan-Evans-Lam-Modified Ulmann Condensation Reaction (1997-98), Batey-Modified Ullmann Condensation Reaction (2003) and many more (Ley et al., 2003).

The classic Ullmann and Goldberg reactions typically require harsh reaction conditions such as high temperatures, extended reaction time, and in some cases stoichiometric amounts of copper. The main reagent or catalyst use in Ullmann coupling reactions is copper. Many improvements have been made since the last century. Dimethylformamide has been used as the solvent to lower down the reaction temperatures and lower the proportion of copper. The use of an activated form of Cu powder, made by the reduction of copper(I) iodide with potassium, allows the reaction to carried out at even lower temperatures with improved yields.

Copper derivatives have numerous possibilities of intermediates due to different oxidation and coordination states of copper. Copper can be easily access from its four oxidation states from 0 to +3. A complete understanding of the reaction mechanism in currently elusive. However, there are four types of possible reaction that have been discussed by Hassan et al., (2002):

i. The first reaction implies the use of aromatic halides, generally iodides or bromides, as substrates and copper metal as the reagent. This kind of reaction involves the formation of a cuprate as an intermediate and copper halide as a byproduct and this known as “the Ullmann reaction”.

ii. The second reaction involves the formation of an aryl carbanion as the intermediate. As the oxidative addition to the copper is the limiting step in the “classical” Ullmann reaction, preparation of the carbanion provides milder conditions with a higher rate of reaction. With this methodology, a catalytic amount of copper, generally Cu (I), can be used, but conversely, a stoichiometric, or an even greater amount of base or organometallic is required. This reaction requires the reduction of the substrate (formation of the carbanion) and a transmetalation reaction followed by a reductive elimination of the copper intermediate complex.

iii. The third reaction is an oxidation of two C-H aromatic bonds to form a C-C bond. These reactions are performed because of the oxidative properties of copper (II), and the use of oxidation potential is required. Both catalytic and stoichiometric amounts of Cu (II) have been used.

iv. The last reaction is Pschorr reaction which involves the decomposition of diazonium in the presence of copper (generally Cu (I)) into radicals. This reaction was discovered before the Ullmann reaction and limited by the access to the required diazonium salt.

In term of reactivity of aryl halides with copper, as measured by the temperature required to initiate the reaction or by the yield of the biaryl obtained, it is prominently reliant on the structure of the halide. The order of reactivity of halogens have been found to be I > Br > Cl, and the activating effect is *o* > *p* > *m* (Davey et al., 1948). Strong

electronegative substituents such as nitro and carbomethoxyl groups predominantly at the *ortho* position provide an activating effect.

In modern organic synthesis, the aryl-aryl bond formation is the most important tool. This bond can be found in natural products such as alkaloids, numerous biological parts of pharmaceutical, agrochemical, and dyes. While in organic materials, the aryl-aryl bond formation is one of the most important aspects to acquire suitable materials for use in electronic organics such as materials for use in OLEDs and solar cells. Many organic materials have been reported before used the Ullmann reaction as the main synthetic pathway to get the desired product (Jiang et al., 2011; Kimoto et al., 2004; Levermore et al., 2012; Promarak et al., 2007; Thaengthong et al., 2011; Usluer et al., 2010; Zhang et al., 2004b).

3.2 Synthesis and Characterization

In this chapter, we will discuss the synthesis of organic materials that is suitable for OLEDs application. Our main target in this project is to synthesis dendrimers compounds based on carbazole derivatives that have molecular weight of more than 1000 g mol^{-1}. Our initial target molecules are 1,4-bis(3, 6-bis(carbazol-9-yl)carbazol-9-yl)benzene (**1**), 1,3-bis(3, 6-bis(carbazol-9-yl)carbazol-9-yl)benzene (**2**), 4,4'-bis(3, 6-bis(carbazol-9-yl)carbazol-9-yl)biphenyl (**3**) and 4,4'-bis(3, 6-bis(carbazol-9-yl)carbazol-9-yl)-2,2'-dimethylbiphenyl (**4**) as shown in Figure 3.1. We have chosen different core groups to give us a better idea of how our materials differ in their photochemical, thermal, and electrochemical properties in the next step of our study.

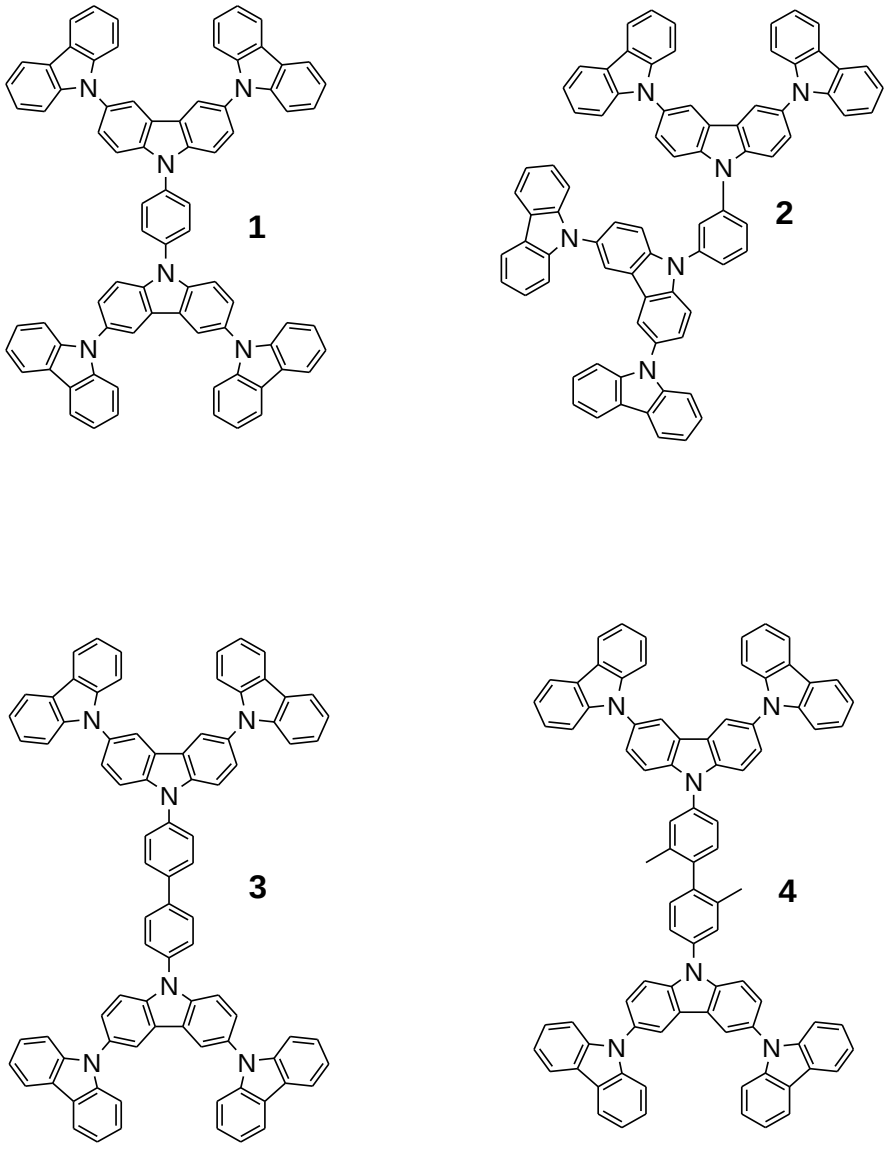

Figure 3.1: Molecular structure of **1**, **2**, **3** and **4**

3.2.1 Synthesis of known compounds

3.2.1.1 Preparation of 1,4-di(9H-carbazol-9-yl)benzene (5)

Before we synthesis the big molecules (**1-4**), we have synthesized known and low molecular weight compounds to find out the best reaction conditions. We have synthesized small molecules of 1,4-di(9H-carbazol-9-yl)benzene (**5**) or known as CCP (Koene et al., 1998). We have followed method from previous literature by Schroegel (Schroegel et al., 2011). In order to form the C-N bond, we have applied Ullmann condensation reaction as shown in Scheme 3.1. Finely copper powder was used as the

main catalyst of this reaction. The copper used was purified using an acidic solution to ensure its high purity level. Basic conditions were necessary for this reaction to occur and therefore potassium carbonate (K_2CO_3) was used as the base in this step. The reaction process use 18-crown-6 as phase transfer catalyst. 1,2-dichlorobenzene was selected as the solvent because of its ability to with stand the high temperatures applied in the Ullman reaction. The reaction mixture was refluxed for 24 hours under an inert atmosphere of nitrogen gas.

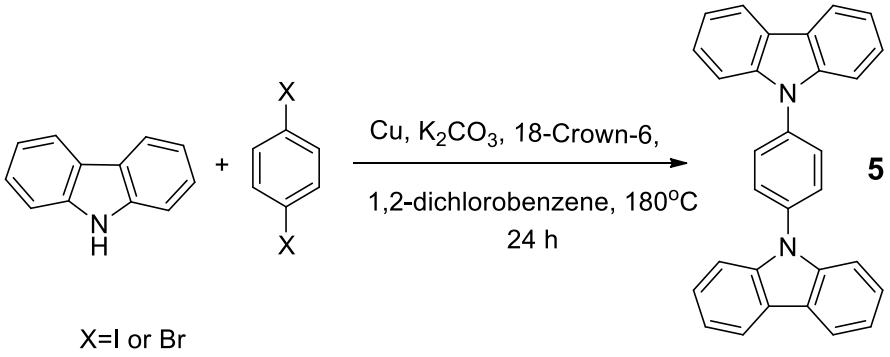

Scheme 3.1: Synthesis of compound **5**

After the reaction completion, a dark brown solution was observed and then filtered by vacuum suction to remove the inorganic materials. This solution then evaporated down under vacuum evaporator to yield a brownish solid, which was washed several times with acetone. Acetone was used because it was discovered that the excess of carbazole is easily removed by acetone washing and the products do not dissolve in acetone. The washed solid was then recrystallized from chloroform to yield a white solid material.

Synthesis work was started with small scale reaction and then was gradually scaled up in further reactions. All the experiments were heated under reflux using the same reaction conditions. The percentage of product isolated decreased as the amount of starting materials used (1,4-diodobenzene) increased from 59 % to 48 % as shown in

Table 3.1. The lower yield observed for the largest scale reaction (trial 4) was due to several factors. In the large-scale reaction, stirring of the reactions mixtures become less effective due to the high volume of chemicals used. Another factor was that the purification procedure for the larger scale reactions became harder to carry out, that led to the loss of final product and lower yield.

Table 3.1. Trials for compound **5**

Trial	Starting material		Product yield (g)	Product yield (%)	Reaction time (hour)
1	Carbazole	1,4-diiodobenzene	0.13	59	24
2	Carbazole	1,4-diiodobenzene	0.58	56	24
3	Carbazole	1,4-diiodobenzene	4.67	54	24
4	Carbazole	1,4-diiodobenzene	8.20	48	24
5	Carbazole	1,4-dibromobenzene	5.45	31	24

There was a noticeable difference when 1,4-diiodobenzene and 1,4-dibromobenzene was used as starting materials under the same reaction conditions. The use of 1,4-dibromobenzene as the starting material led to a low yield product of 31 %. This observation shows that using iodine-based starting materials for Ullmann reactions will produce a higher yield compared to the corresponding bromine-based starting

materials. This was due to the better leaving group effectiveness of aryl iodides compared to that of aryl bromides.

3.2.1.2 Preparation of 1,3-di(9H-carbazol-9-yl)benzene (6)

After the successful synthesis of compound **5**, we applied the same reaction conditions using a different core unit, namely 1,3-diiodobenzene, as shown in Scheme 3.2. Compound **6** otherwise known as mCP, was synthesized using carbazole and commercially available 1,3-diiodobenzene. Although the *meta*-linkages in mCP is more hindered compared to the *para*-linkage in CCP, the yield of the final product is still satisfactory at 77%. This result confines that the linkage position between carbazoles and the core are not a major problem in the synthesis of small molecules using Ullmann reaction.

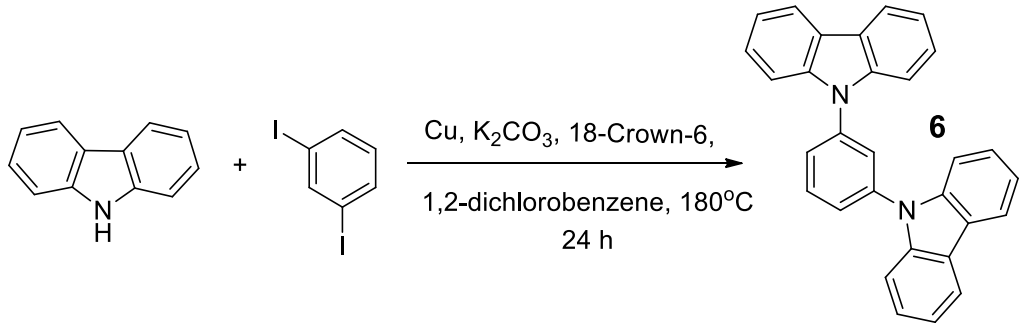

Scheme 3.2: Synthesis of compound **6**

3.2.1.3 Preparation of 1,4-di(9H-carbazol-9-yl)biphenyl (7)

The third compound that we have synthesized was compound **7** or known as CBP as shown in Scheme 3.3. The core unit, 4,4'-diiodobiphenyl (**23**) was prepared from commercially available biphenyl which was reacted with iodine under acidic conditions to produce the desired products, which was then recrystallized from ethanol to yield colorless crystals with a moderate yield of 63 % and 70 % as shown in Table 3.2.

Compound **23** was further reacted with carbazole to yield 4,4'-di(9H-carbazole-9-yl)biphenyl (**7**) under the same Ullman condensation reaction conditions as compound **5**. A brownish solid was formed before purification process. The mixture was then purified by recrystallization from chloroform to form a white solid material. Several trials for compound **7** are shown in Table 3.2. As expected, prolonging the reaction time from 24 hours to 48 hours produced a higher yield for larger scale reactions (trial 4) as compared to compound **5**.

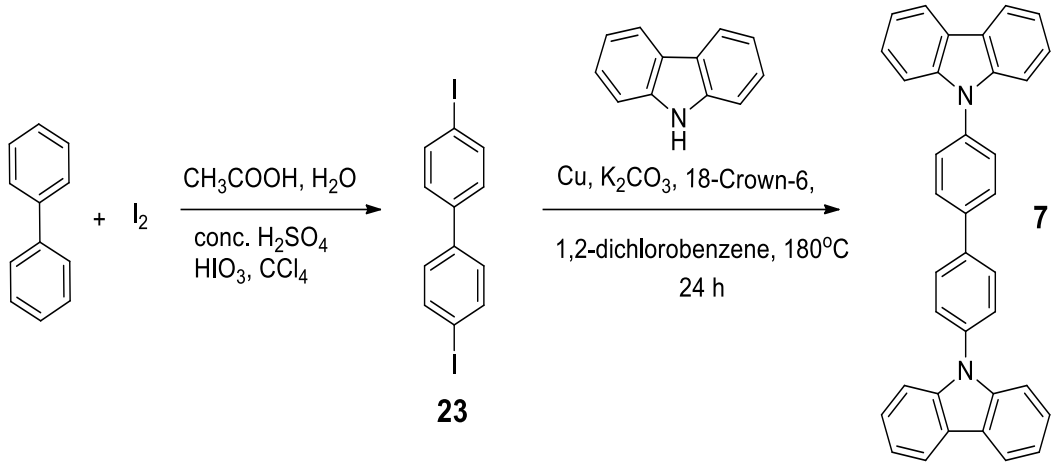

Scheme 3.3: Synthesis of compound **7**

Table 3.2: Trials for 4,4'-diiodobiphenyl (**23**)

Trial	Product yield (g)	Product yield (%)
1	2.5	63
2	5.67	70

Table 3.3: Trials for compound **7**

Trial	Product yield (g)	Product yield (%)	Reaction time (hours)
1	0.11	55	12
2	0.70	60	24
3	3.48	76	24
4	9.48	79	48

3.2.1.4 Preparation of 9,9'-(2,2'-dimethylbiphenyl-4,4'-diyl)bis(9H-carbazole) (8)

We also synthesized compound **8** or known as CDBP as shown in Scheme 3.5. Compound **8** was different compared to compound **7** with the addition of methyl moiety at the position of 2 and 2' of biphenyl core unit. This kind of compound will benefit in term of triplet energy as reported before (Schroegel et al., 2011). Even though the core unit used (4,4'-diiodo-2,2'-dimethylbiphenyl) more hinder or bulky compared to 4,4'-diiodobiphenyl, still the final product can reach to 61 %. Compared to compound **7**, the present of the methyl moiety can be seen clearly as singlet peak at 2.29 ppm from ^{1}H NMR spectra. There was also a peak at 20.15 ppm observed from ^{13}C NMR spectra indicating the presence of methyl group.

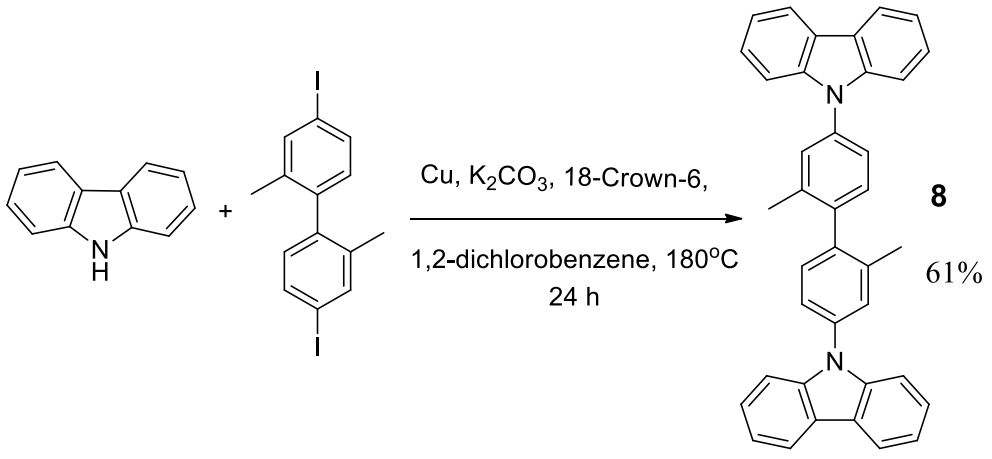

Scheme 3.4: Synthesis of compound **8**

3.2.2 Synthesis of dendrimers

After identifying the best reaction conditions for the Ullman reaction, we proceeded to synthesize the larger target compounds. In our initial plan, we tried to synthesis compound **1** using the method of Zhang et al. (2004b) with little modification. The synthesis pathway of compound **1** is shown in Scheme 3.5.

In this synthetic route, compound **5** was used as the starting material. Iodination at 3, 6 position of compound **5** using KI and KIO_3 lead to the formation of an intermediate (compound **17**). Compound **17** was then directly reacted with carbazole by using an Ullmann condensation reaction without a subsequent purification process. Although we managed to obtain the final product (compound **1**), the yield was very low at less than 5% (overall yield). This low yield is believed due to the difficulty of carbazole in reacting with compound **17** due to the bulky molecular structure, i.e., steric hindrance. Another reason is believed due to the unknown mixture of iodinated carbazoles in compound **17**, i.e., a mixture of *mono*, *di* and *tri*-substituted products. This mixture of isomers of iodinated compound **17**, make the last step produce a lot of undesired products, which renders the separation of the target compound by column chromatography difficult to achieve because the mixture compounds have a very similar polarity and molecular composition. We also tried to synthesize compounds **2**, **3** and **4**, but unfortunately neither of the product could be isolated or the yield of product was too low for further studies.

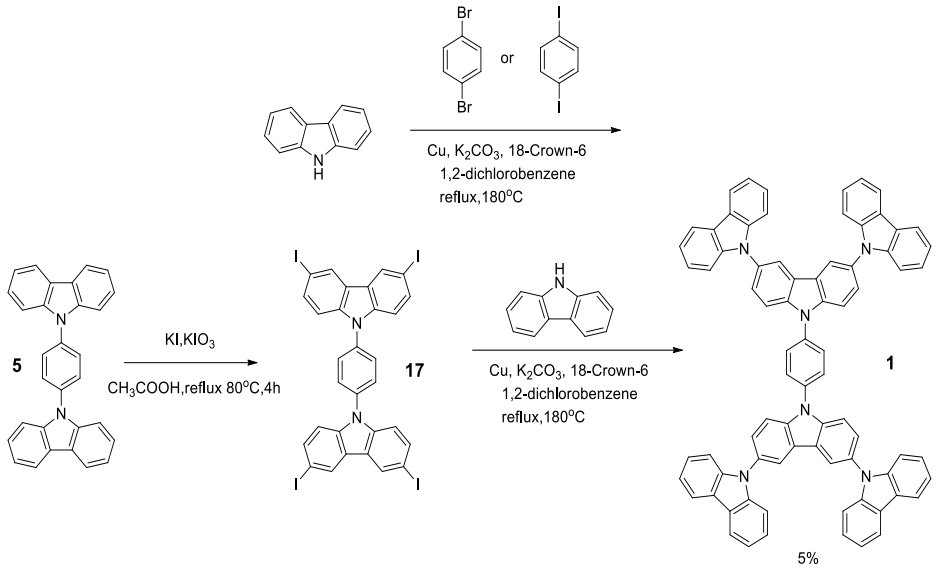

Scheme 3.5: Synthetic route for synthesis of compound **1**

After obtaining pure compound **1**, we have tested the solubility of compound **1** in 1 % w/v of chloroform and chlorobenzene in order to test its suitability as host for solution process OLED devices. We found out that compound **1** was not dissolved in the solvents that make it non-favorable candidate as host materials for OLEDs. Therefore, we have decided to stop synthesis of **1**, **2**, **3** and **4** because they have not met earlier expectation for use as solution processable host materials for OLEDs.

Because of the solubility problem, we had searched for another approach to increase the solubility of our compounds in commonly use solvent for OLEDs fabrication. We found out that from other works (Aizawa et al., 2012; Chen et al., 2012b) that solubility of the compound can be increased by adding alkyl group at the outer layer of the structure. So we decided to add a bulky alkyl group of *tert*-pentyl group at the outer layer of compound **1**,**2**,**3** and **4** to produce 1, 4-bis (3, 6-bis (3, 6-ditert-pentyl-carbazol-9-yl)carbazol-9-yl)benzene (**13**), 1, 3-bis (3, 6-bis (3, 6-ditert-pentyl-carbazol-9-yl)carbazol-9-yl)benzene (**14**), 4, 4'-bis (3, 6-bis (3, 6-ditert-pentyl-carbazol-9-yl)carbazol-9-yl)biphenyl (**15**) and 4, 4'-bis (3, 6-bis (3, 6-ditert-pentyl-carbazol-9-yl)carbazol-9-yl)-2,2'-dimethylbiphenyl (**16**) as shown in Figure 3.2.

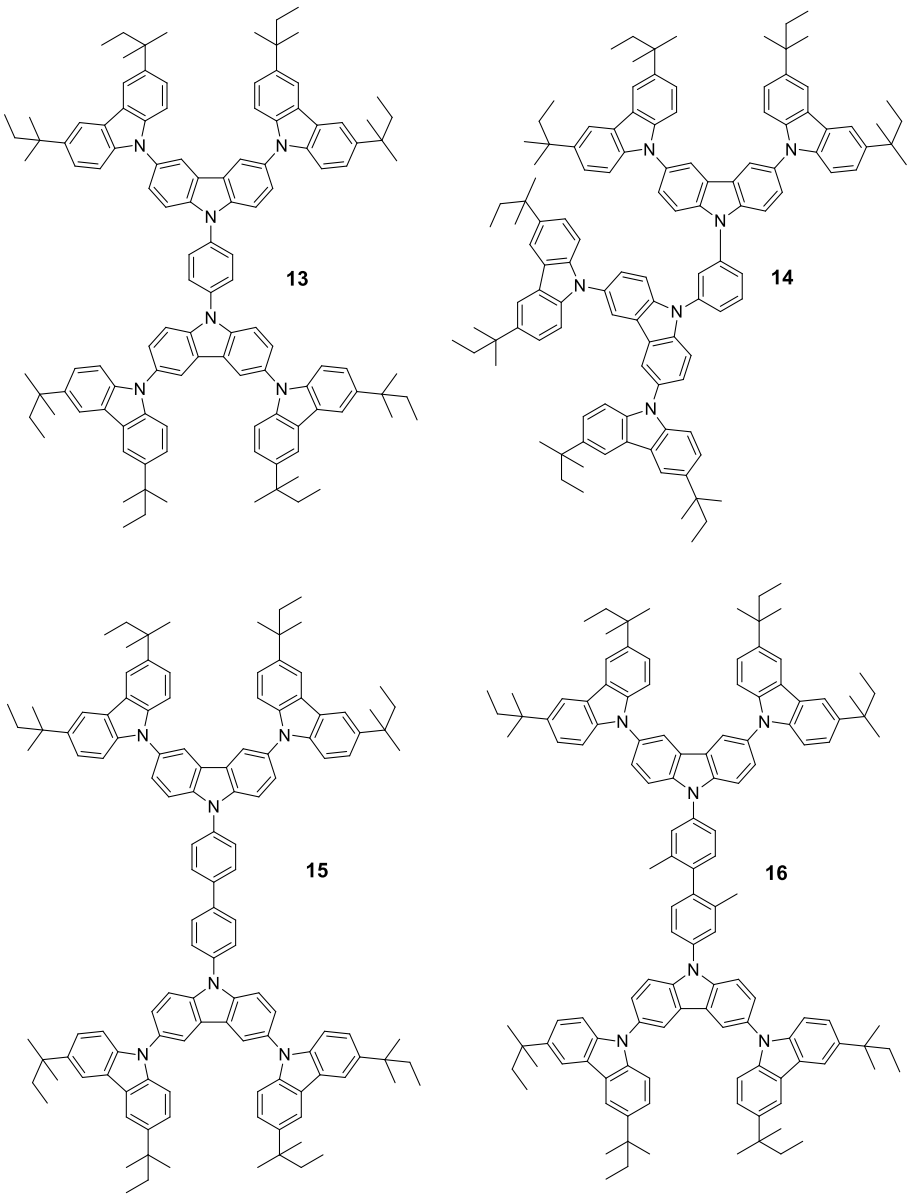

Figure 3.2: Molecular structure of **13**, **14**, **15** and **16**

In order to obtain big molecules with a high molecular weight, we have proposed a new synthetic pathway as shown in Scheme 3.6. We need to change our synthesis strategy because of the low yield produced and difficulty in purification by using previous synthetic pathway (Scheme 3.5). This pathway takes six steps to be completed with finalization by Ullmann reaction. We started with iodination of carbazole at 3 and 6 position to yielded iodinated carbazole (**18**). The second step was Friedel-craft alkylation reaction between carbazole and 2-chloro-2-methylbutane to produce compound **19**. As a result, a protected carbazole was obtained by the addition of *tert*-pentyl group at 3 and 6

positions. The third step was protection at N-H of 3,6-diiodocarbazole by using a protection group to produce **20a**/**20b**. Next step was coupling reaction between **20a/20b** with **19** to yield compound **21**. After that, we did deprotection of compound **21** to produce non-protected "wing" of compound **22**. The last step was Ullmann reaction between **22** with 1,4-diiodobenzene, 1,3-diiodobenzene, 4,4'-diiodobiphenyl and 4,4'-diiodo-2,2'-dimethylbiphenyl to yield compound **13**,**14**,**15** and **16** respectively.

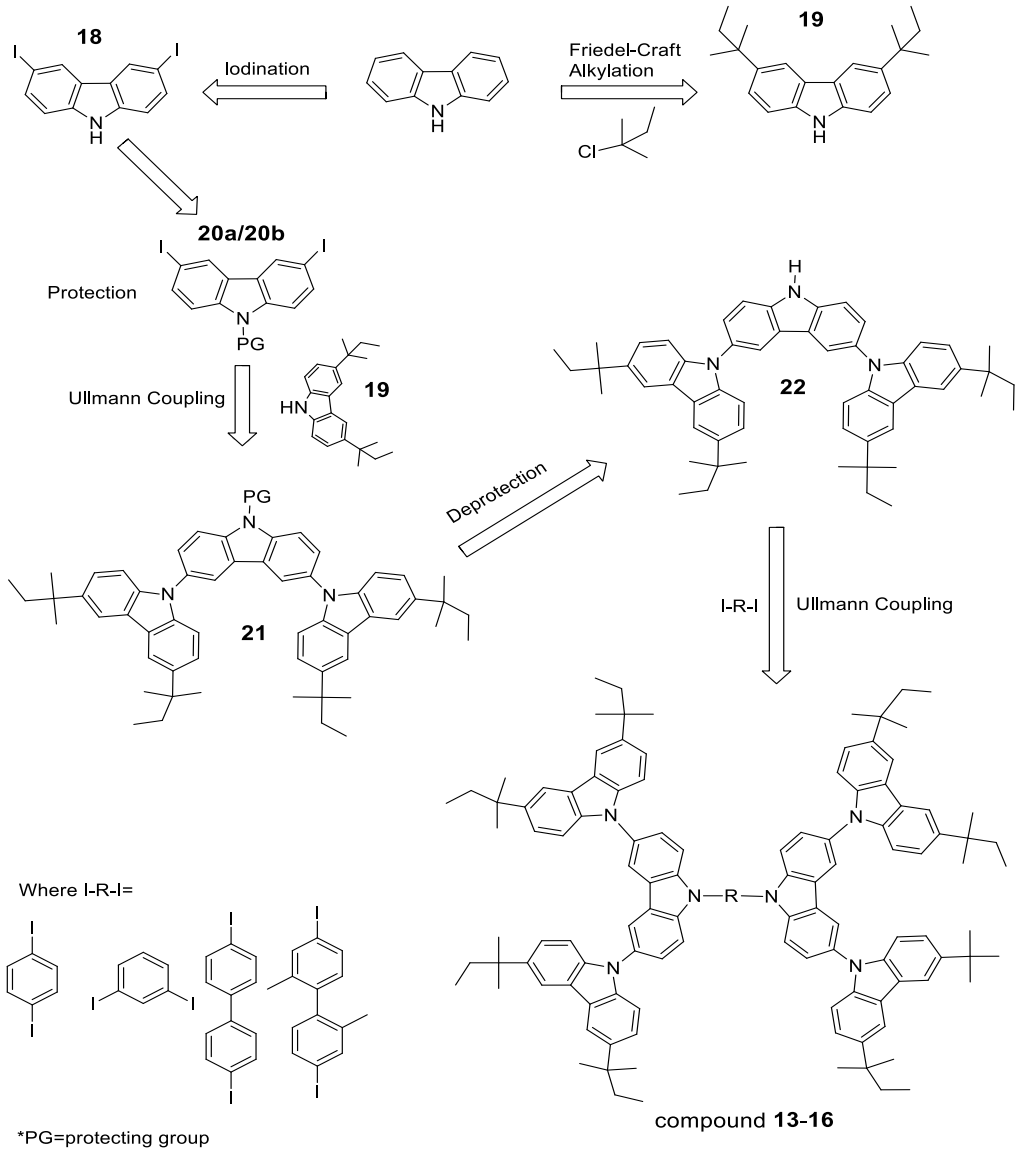

Scheme 3.6: General synthetic route to synthesis dendritic molecules

3.2.3 Iodination of carbazole

Carbazole was iodinated at 3 and 6 positions with KI and KIO_3 under acidic condition using acetic acid as the solvent to produced 3,6-diodocarbazole (**18**) as shown in Scheme 3.7.

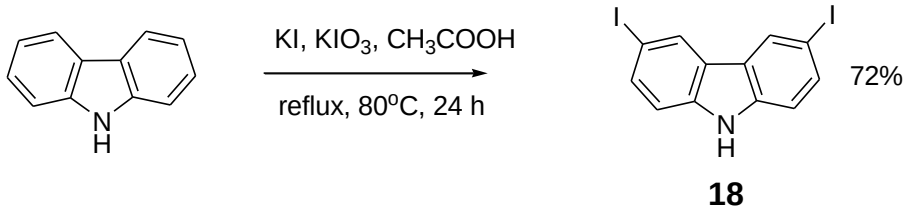

18

Scheme 3.7: Iodination of carbazole using KI and KIO_3

We also managed to get 3,6-diiodobenzene by method Michinobu et al. (2009) by using *N*-iodosuccinimide (NIS) as reagent as shown in Scheme 3.9. This reaction yielded almost same percentage of product around 70%.

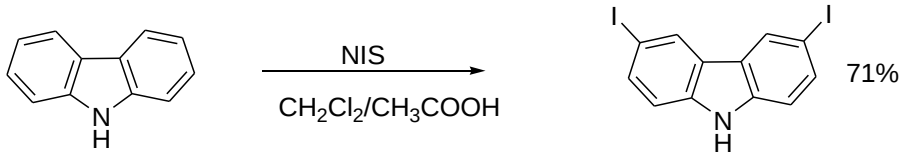

18

Scheme 3.8: Iodination of carbazole using NIS

KI and KIO_3 were mainly used in our experiment because there are cheap and non-toxic compared with other iodination reagent (such as NIS) that lead to low-cost production of a material. Other iodination reagents also have been reported to cause pollution problem to the environment (Adimurthy et al., 2003).

Because the need to use compound **18** in next step reaction we have synthesis compound **18** several times and the results are summarized in Table 3.4. Even the reaction

increases in volume, the percentage yield of product is still satisfactory at a moderate yield.

Table 3.4: Trials for compound **18**

Trial	Reagent		Product yield (g)	Product yield (%)
1	Carbazole	KI, KIO_3	4.2	72
2	Carbazole	KI, KIO3	16.5	66
3	Carbazole	KI, KIO3	37.5	74

3.2.4 Friedel-Craft Alkylation

In order to introduce alkyl group to 3 and 6 positions of carbazole, we have followed previous literature method (Neugebauer et al., 1972). Carbazole was reacted with two equilibriums of 2-chloro-2-methylbutane. $AlCl_3$ was served as the catalyst and dry dichloromethane as the solvent to obtain compound **10** as shown in Scheme 3.9. ^1H NMR spectra of compound **19** showed clear peaks at 1.76 ppm, 1.41 ppm and 0.71 ppm attributed to the alkyl group present. The trial for compound **19** was concluded in Table 3.5.

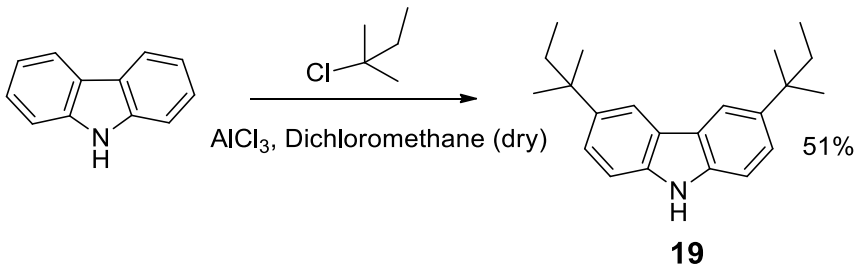

19

Scheme 3.9: Friedel-Craft alkylation of carbazole

Table 3.5: Trials for compound **19**

Trial	Product yield (g)	Product yield (%)
1	0.25	27
2	6.76	37
3	9.33	51

With compound **19** in our hand, we have decided to synthesis molecules almost similar with compound **5-8** but with the addition of alkyl group at the outer layer. Before proceeding to the synthesis of the dendrimers, we tried using compound **19** for the synthesis of low molecular weight compound by using the same Ullmann condensation reaction.

3.2.5 Synthesis of modified new compound with low molecular weight

After synthesized known materials (compound **5-8**), we decided to synthesized 1,4-bis(3,6-di-tert-pentyl-9H-carbazol-9-yl)benzene (**9**), 1,3-bis(3,6-di-tert-pentyl-9H-carbazol-9-yl)benzene (**10**), 4,4'-bis(3,6-di-tert-pentyl-9H-carbazol-9-yl)biphenyl (**11**) and 9,9'-(2,2'-dimethylbiphenyl-4,4'-diyl)bis(3,6-di-tert-pentyl-9H-carbazole) (**12**) with 3,6-di-tert-pentyl-9H-carbazole (**15**) as starting materials as shown in Scheme 3.10. Compounds **9-12** were prepared in a similar way as compound **5-8** with Ullmann condensation reactions to combine N-C bond.

There are slightly decrease in product yield of compound **10** compared to compound **9** for about 22 %. This observation is believed due to steric hindrance effect of *meta* position of compound **10** which result in difficulty of bulky compound **15** to react toward core group. On the other hand, compound **12** produce lower yield compared to compound **11**. The present of two methyl moieties in compound **11** played significant

role in reducing the product yield because of its bulkiness hindered compound **15** to react effectively toward Ullmann reaction.

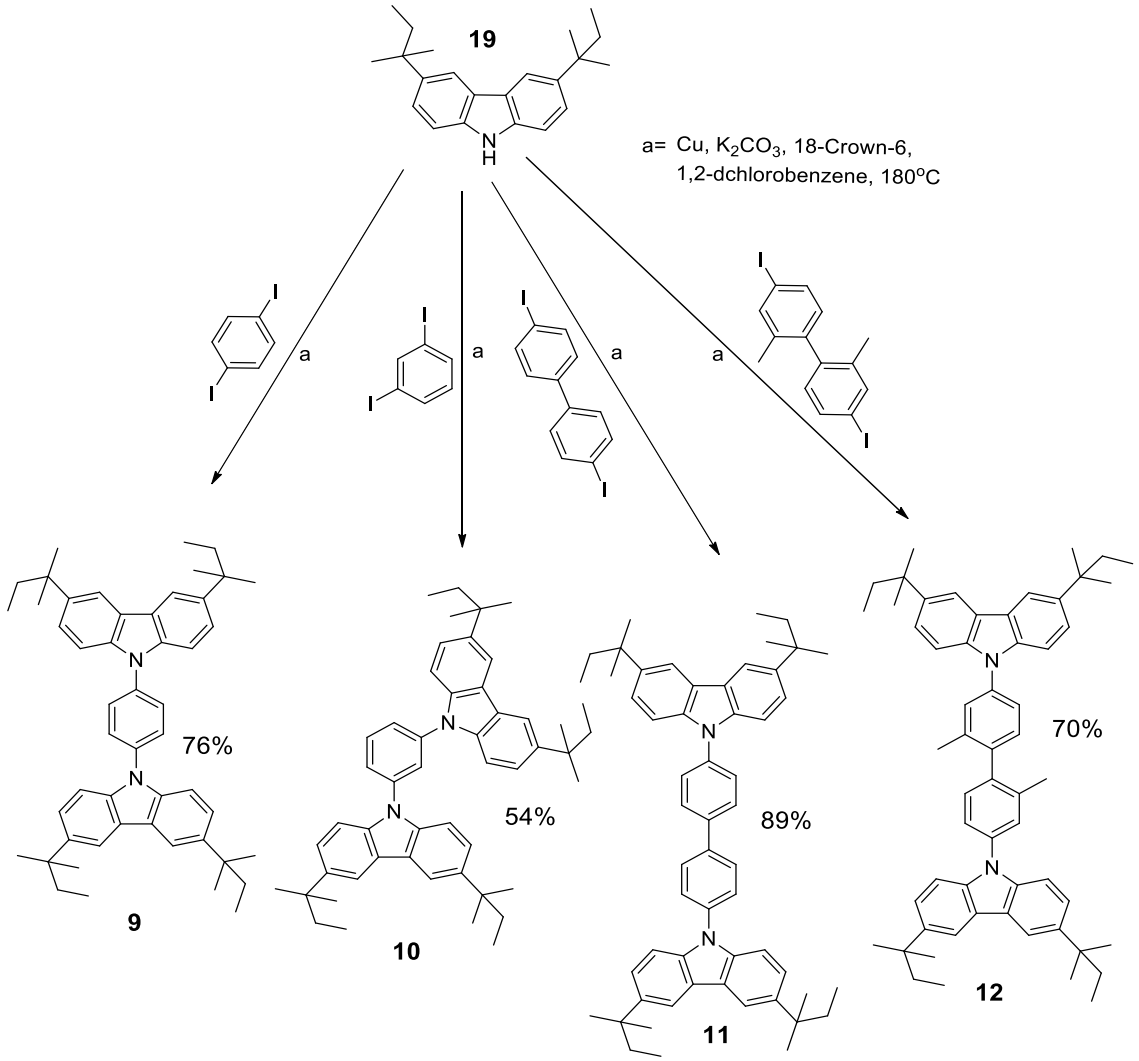

Scheme 3.10: Preparation of **9**, **10**, **11** and **12**

After successfully synthesized of compound **9-12** in satisfactory yield, we move on to synthesis our dendritic molecules. We have used compound **15** that we have prepared before to continue our main objective to synthesis compound **13-16**.

3.2.6 Protection of iodinated carbazole

Before proceed to the next step, we need to protect the iodinate carbazole (compound **18**) using a protecting group. Acetyl group was introduced at N atom replacing H atom as shown in Scheme 3.11. We use acetyl as it can be removed easily before our last step of this synthetic route. Acetic anhydride was used as the reagent. This reaction was refluxed for about 4 hours at 140 °C and a simple purification method was enough to get a pure product in 79 % yield.

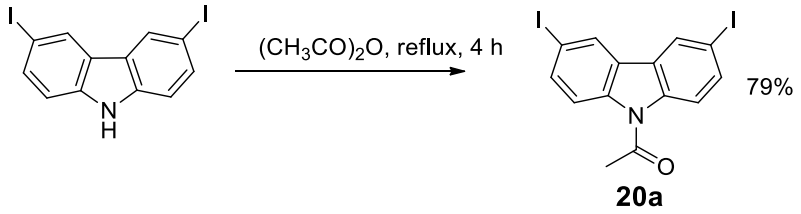

Scheme 3.11: Synthesis of compound **20a** using acetic anhydride

The ^{1}H NMR spectra clearly show a singlet sharp peak at the aliphatic region of 2.84 ppm indicating the present of -CH_3 group from the acetyl. While the ^{13}C NMR shows a peak at 27.68 nm to prove the present of the methyl group.

We also protect the iodinate carbazole with another protecting group which is *tert*-butyl carbamate or simply known as BOC. Anhydride $(BOC)_2O$ was used as the reagent, 4-dimethylaminopyridine (DMAP) as nucleophilic catalyst and acetone as the solvent. The reaction is shown in Scheme 3.12.

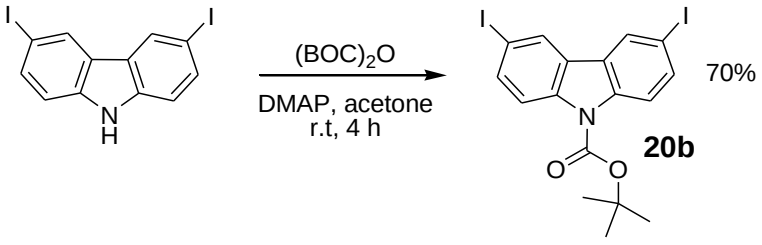

Scheme 3.12: Synthesis of compound **20b** using $(BOC)_2O$

This reaction also results in satisfactory yield which is 70 %, but less about 9% compared to the reaction with acetic anhydride. As a result, we decided to use the first method because of higher yield produced, simple purification process and much cheaper in term of cost. Table 3.6 summarized the trials result for **20a**.

Table 3.6: Trials for compound **20a**

Trial	Starting material		Product yield (g)	Product yield (%)
1	Compound 18	Acetic anhydride	1.64	74
2	Compound 18	Acetic anhydride	8.75	79
3	Compound 18	Acetic anhydride	16.94	77

3.2.7 Synthesis of "wing"

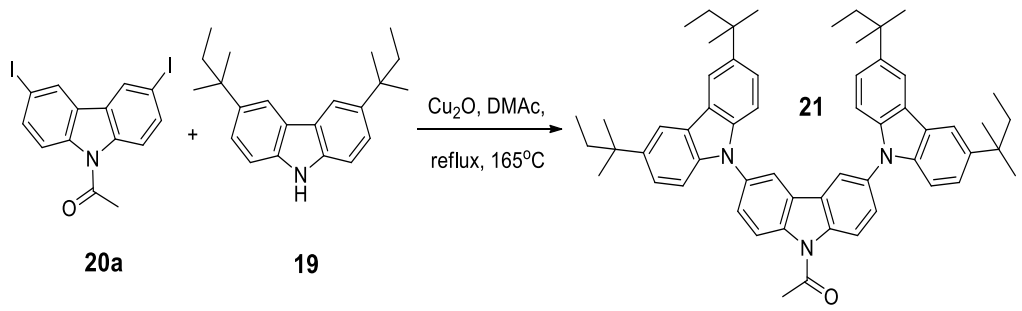

Scheme 3.13: Synthesis of compound **21**

This step involves Ullmann coupling reaction using copper (I) oxide as a catalyst and *N,N'*-dimethylacetamide (DMAc) as the solvent. This reaction produces a white powder after recrystallization from ethanol. Scheme 3.13 shows the synthesis of compound **21** and Table 3.7 summarized the trials we have done.

Table 3.7: Trials for compound **21**

Trial	Product yield (g)	Product yield (%)
1	0.71	67
2	2.65	74
3	6.93	78

We also tried several times to make our wing with similar condition and reagent as compound **5**, but unfortunately, we could not get target compound. There are no clear explanations of this phenomena from literature.

3.2.8 Deprotection of "wing"

It is necessary to removed protecting group before proceeding to the last step. The acetyl group was easily removed by using a base, potassium hydroxide (KOH) as a medium for the reaction as shown in Scheme 3.14. Table 3.8 summarized the trials for compound **22**.

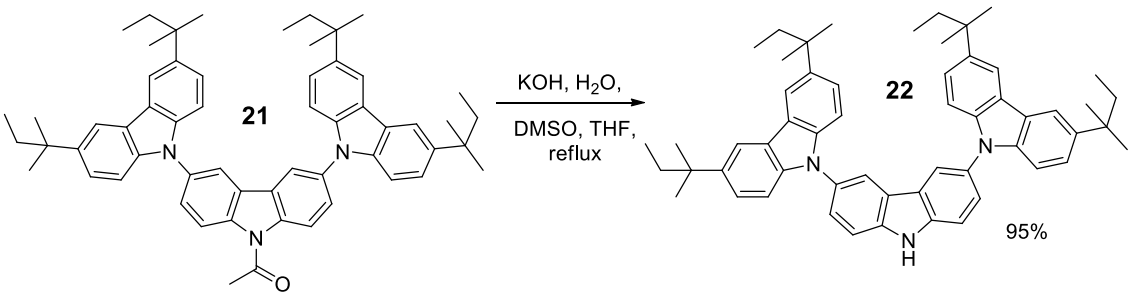

Scheme 3.14: Synthesis of compound **22**

Table 3.8: Trials for compound **22**

Trial	Product yield (g)	Product yield (%)
1	0.05	58
2	1.80	95
3	3.40	83

3.2.9 Final step: Synthesis of Novel Dendrimers

The synthesis of our target compound was finalized with Ullmann condensation reaction using the same reagent as compound **5** before. The wing was reacted with 1,4-diiodobenzene to produce compound **13**. After purification steps, it was tested for its solubility in chloroform and dichlorobenzene and it was discovered that compound **13** was easily dissolved in the solvents. This observation has proved that adding alkyl group to the dendrimers will increase their solubility in organic solvents. We continued our synthesis work with the reaction between the "wing" with 1,3-diiodobenzene, 4,4'-diiodobiphenyl and 4,4'-diiodo-2,2'-dimethylbiphenyl to yield compound **14**, **15** and **16** respectively. The purification process was conducted by flash column chromatography and recrystallization several times with chloroform to yield a pure white solid. As expected compound **14** has the lowest yield among others dendrimers because of steric hindrance effect of *meta* position.

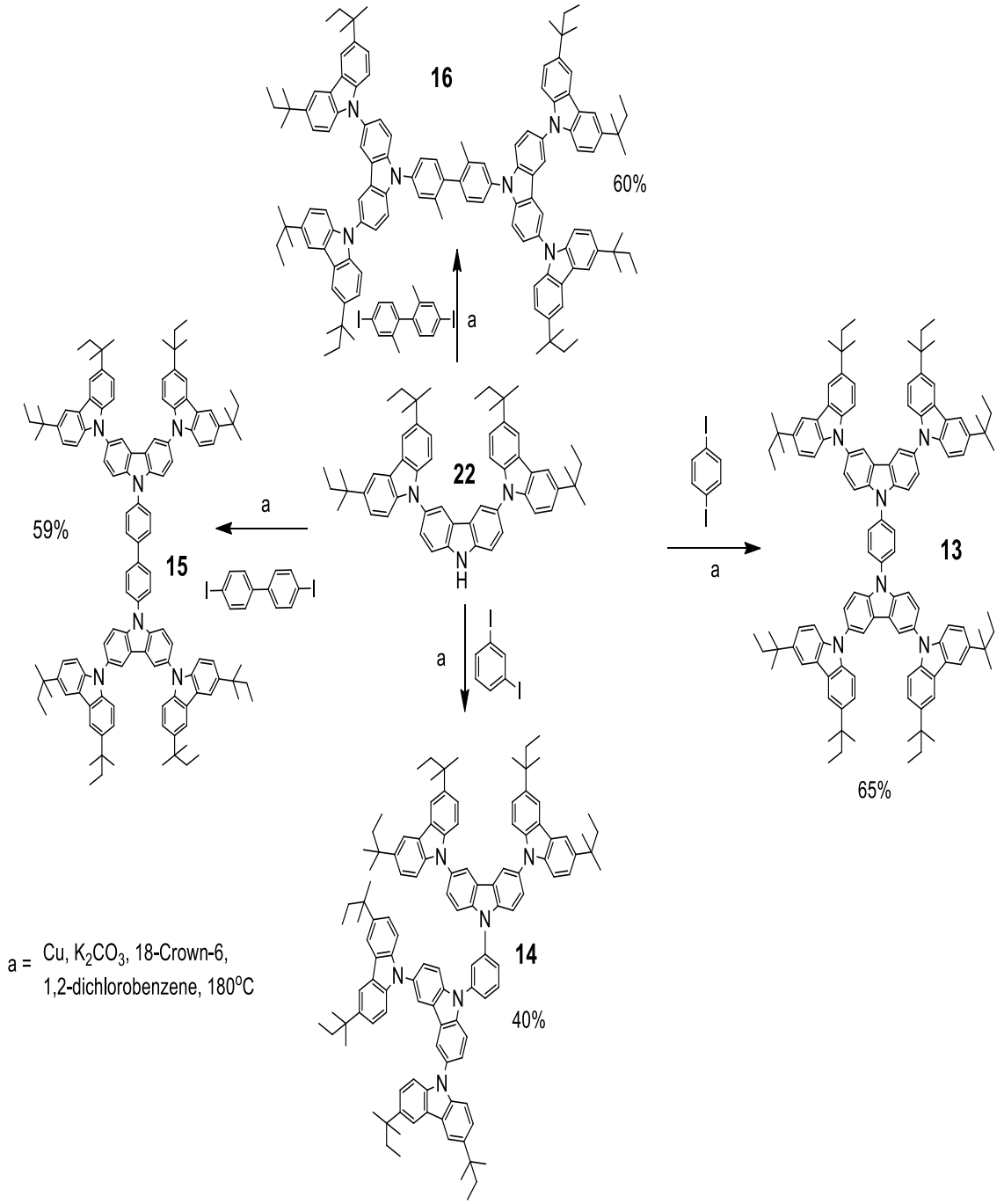

Scheme 3.15: Synthesis of **13**,**14**,**15** and **16**

The next step in this study is to conduct photophysical, thermal, and electrochemical analysis of our synthesized compounds in order to confirm its suitability as host materials for solution process OLEDs.

3.3 Photophysical Properties

Photophysical properties of all compounds were investigated by UV-Visible, photoluminescence (PL) and low-temperature phophorescence. Figure 3.4 and 3.5 show the UV-Visible absorption and photoluminescence emission spectra of the compounds in a solution of dichloromethane (CH_2Cl_2) at room temperature and their detailed photophysical data are summarized in Table 3.9.

3.3.1 UV-Visible

The UV-Visible experiment was conducted to determine the band gap of all molecules synthesized. The band gap or also known as energy gap of materials is important in solar cells, nanomaterials and as well as in semiconductors. Band gap is the energy difference between the top of the valance band and the bottom of the conduction band in semiconductors and insulators as illustrated in Figure 3.3. Band gap is the major factor in determining the electrical conductivity of a solid. In a semiconductor, the band gap is the minimum amount of energy required for an electron to be excited at the first LUMO level. In the same time, a hole is created in the conduction band and this electrons-holes cycle allows the semiconductor to conduct electrons.

In this project, the optical band gaps of all compounds were calculated from electronic absorption spectra by using the following equation as in the literature.

$$E_g = \frac{1240}{\lambda onset} \quad (3.1)$$

Where λ_{onset} is the onset of wavelength which can be determined by the intersection of two tangents on the absorption edges. λ_{onset} also indicates the electronic transition start wavelength.

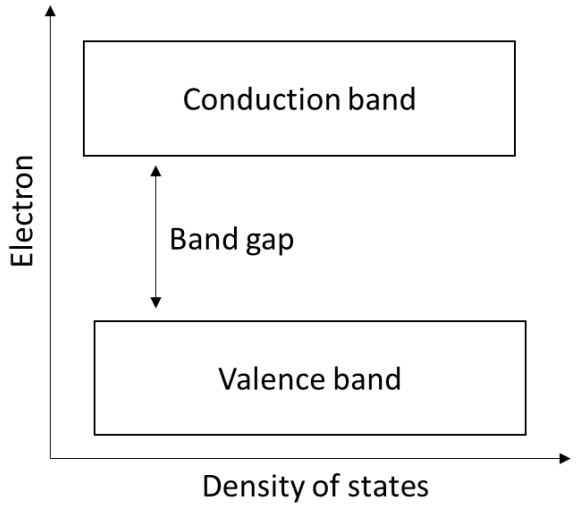

Figure 3.3: Band gap in semiconductor

Compound **5** showed two strong peaks at the wavelength of 241 nm and 296 nm that can be attributed to the π-π* transition in carbazole units as can be seen in Figure 3.4. Almost similar peaks were observed for compound **9** where strong peaks observed at 242 nm and 298 nm. While compound **13** showed the addition of peaks at 270 nm and 289 nm attributed to the π-π* transition of the outer layer of carbazole dendrons.Compound **5**, **9** and **13** have onset absorption at (λ_{onset}) at 351 nm, 359 nm, and 367 nm respectively based on the edge of the Uv-vis absorption peak. The optical bandgap of compound **5**, **9** and **13** was calculated to be 3.54 eV, 3.59 eV, and 3.38 eV respectively. This result shows a decrease trend of band gap from compound **5** to **9** for 0.04 eV and from compound **9** to **13** for 0.16 eV. A similar trend can be observed for other series of the compound with same core group where dendrimers of compound **14**, **15** and **16** show smaller band gap of 3.41 eV, 3.43 eV, and 3.45 eV respectively in comparison of the small molecules. Data for optical properties for all compounds were shown in Table 3.9.

3.3.2 Photoluminescence (PL)

For further understanding of optical properties of our molecules, we used PL experiment to investigate their excited state behavior. As shown in Figure 3.5, the PL spectra of compound **1** showed a maximum emission peak at 351 nm. There was a little shift toward the higher wavelength for compound **5** at 359 nm compared to compound **1**. This little red-shift observed was believed to be due to the effect of the *tert*-pentyl group. Meanwhile in compound **13**, maximum emission peak was observed to be red shifted to 403 nm. Compound **5** and **9** are red shifted to 52 nm and 44 nm respectively, compared to compound **13**. The deep-blue fluorescence observed for compound **13**, proved that it is suitable as blue host materials for OLEDs. The same phenomenon was observed for compound **14**, **15**, and **16** where the newly synthesized dendrimers showed a peak at deep-blue region of 400 nm, 409 nm, and 403 nm respectively. This observation clearly showed that compound **13, 14, 15** and **16** can be used as host materials for blue OLEDs.

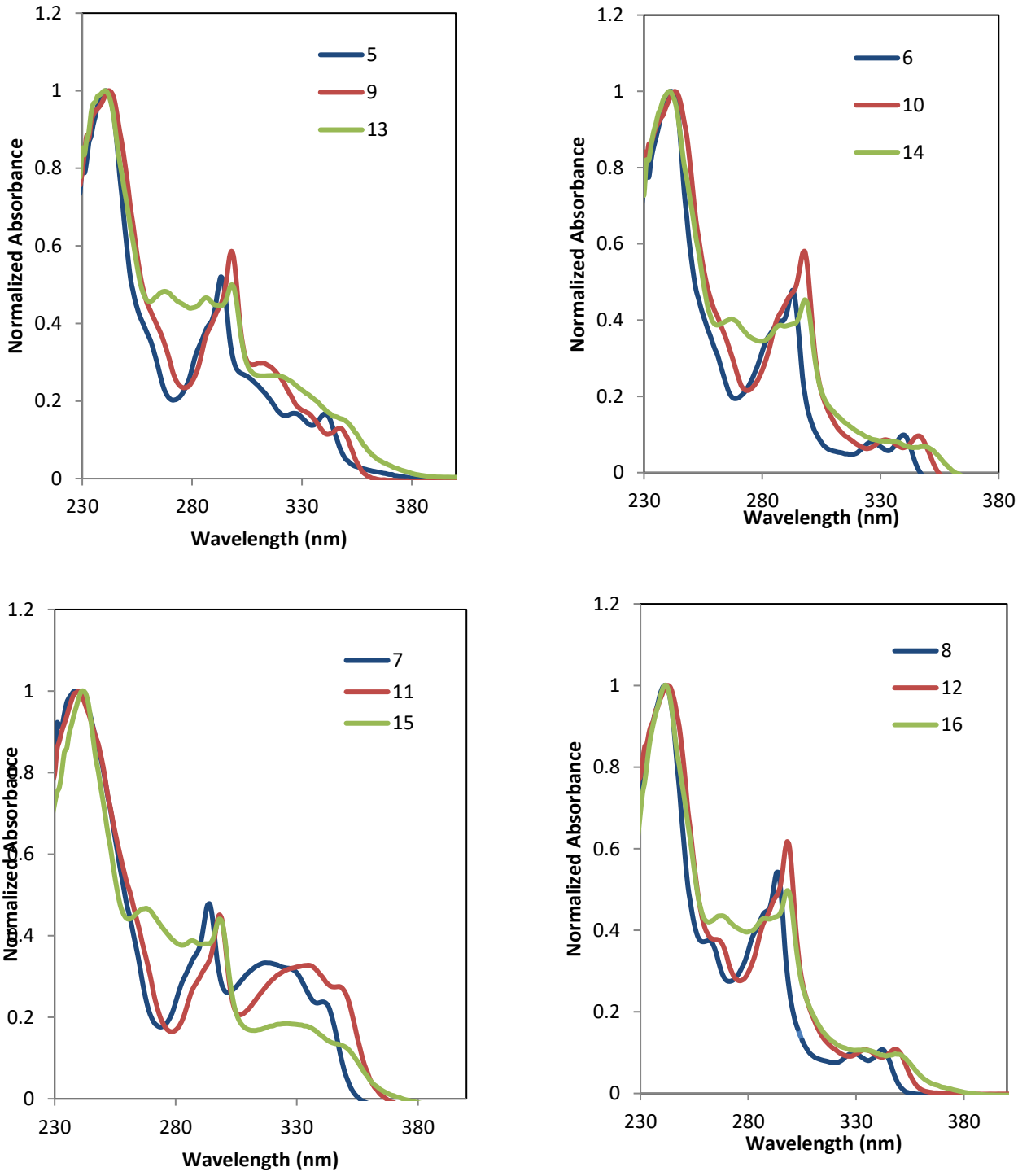

Figure 3.4: Normalized UV-Vis spectra of compounds **5-16** in dichloromethane

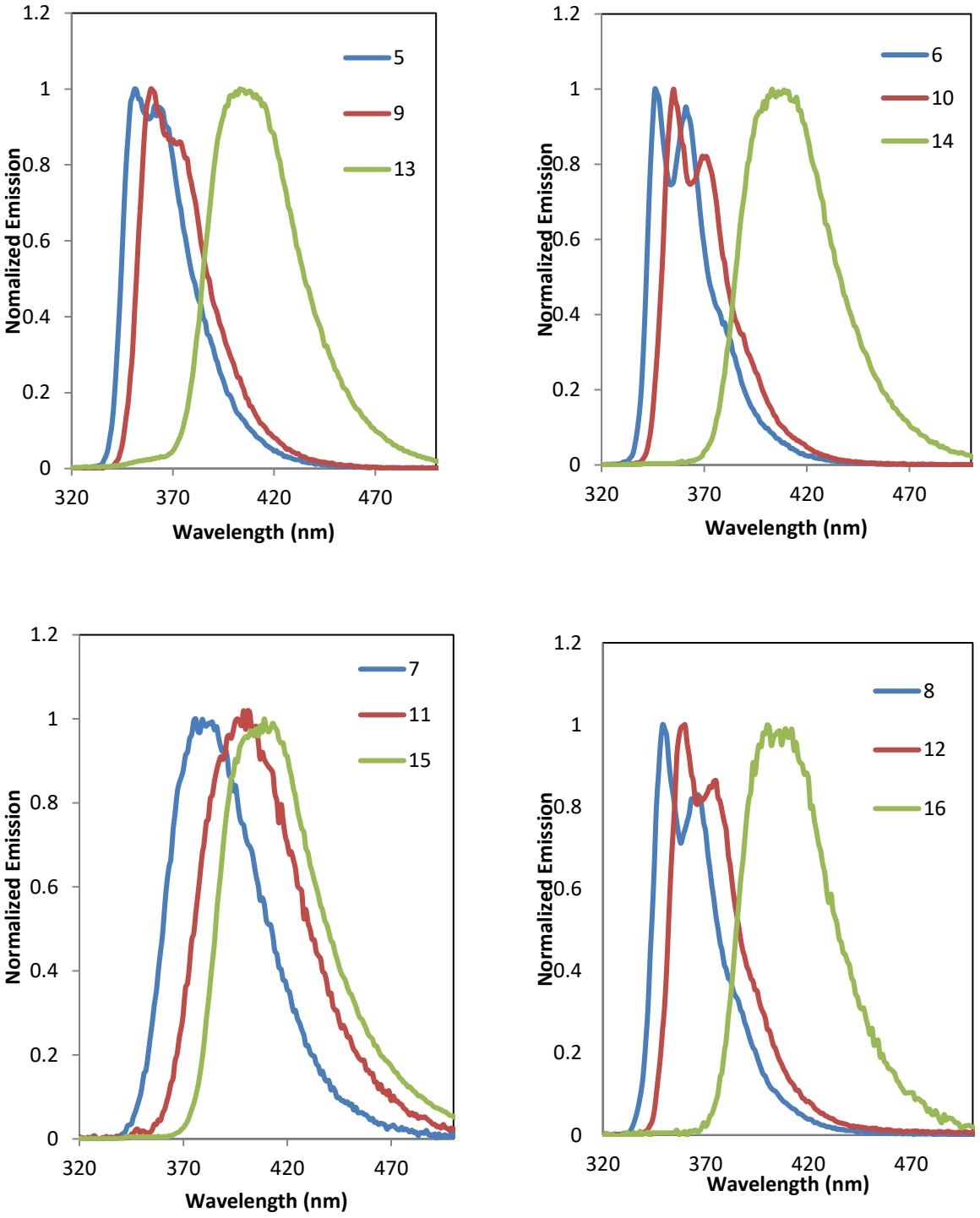

Figure 3.5: Normalized PL spectra of compounds **5-16** in dichloromethane

Table 3.9: Summary of optical properties for compounds **5-16**

Compound	λ abs, max (nm)	λonset (nm)	Eg (eV)[a]	PL λ emission, max
5	241	351	3.53	351
6	241	346	3.58	346
7	238	351	3.53	376
8	242	352	3.52	349
9	242	359	3.45	359
10	243	354	3.50	355
11	240	358	3.46	396
12	243	358	3.46	360
13	240	367	3.37	403
14	241	360	3.44	403
15	242	362	3.43	409
16	241	364	3.41	400

[a]optical band gap.

3.3.3 Phosphorescence

One of the important parameter of a host material is the triplet energy (E_T). E_T of materials determine the suitability of a given host for red, green or blue emitter. In our project, we focused on synthesized host materials that are suitable for blue emitter especially iridium (III) bis(4,6-(difluorophenyl)pyridine-*N*,$C^{2'}$) picolinate (FIrpic). So, we need to study their triplet energy before deciding on the best material to be used in the device fabrication step. The reason is that the materials must have E_T higher than E_T of

FIrpic (2.65 eV) (Holmes et al., 2003) to avoid energy back transfer from emitter guest to the host.

Triplet energy (E_T) of the dendrimers compound **13-16** was measured by low-temperature phosphorescene in dilution and solid forms as shown in Figure 3.6. The E_T was estimated from the highest energy 0-0 vibration peaks of the phosphorescence spectra at 77 K. Compound **16** shows the highest E_T compared to other dendrimers whether in dilute or solid with 2.82 eV and 2.92 eV respectively. This high E_T is the result of conjugation breaking by the core unit of this dendrimer, which is 2,2'-dimethylbiphenyl. If compared to compound **15**, the presence of biphenyl at the core of this structure will decrease E_T of this dendrimer to about 0.39 eV in solid and 0.17 eV in dilution. While the benzene ring at the core of the compound **13** and **14** which have different position (*para* and *meta*) do not give much different in term of E_T whether in solid (2.73 eV) or dilution (2.78 eV) for compound **13** and 2.71 eV (solid) and 2.79 eV (dilution) for compound **14**. Triplet energy of the compound **13-16** is summarized in Table 3.10. All dendrimers have enough triplet energy to serve as blue host materials for FIrpic except for compound **15** that have the same E_T with FIrpic.

Table 3.10: Triplet energy of **13-16** in dilute and solid form

Compound	Triplet Energy, E_T (eV)	
	Dilute	Solid
13	2.78	2.73
14	2.79	2.71
15	2.65	2.53
16	2.82	2.92

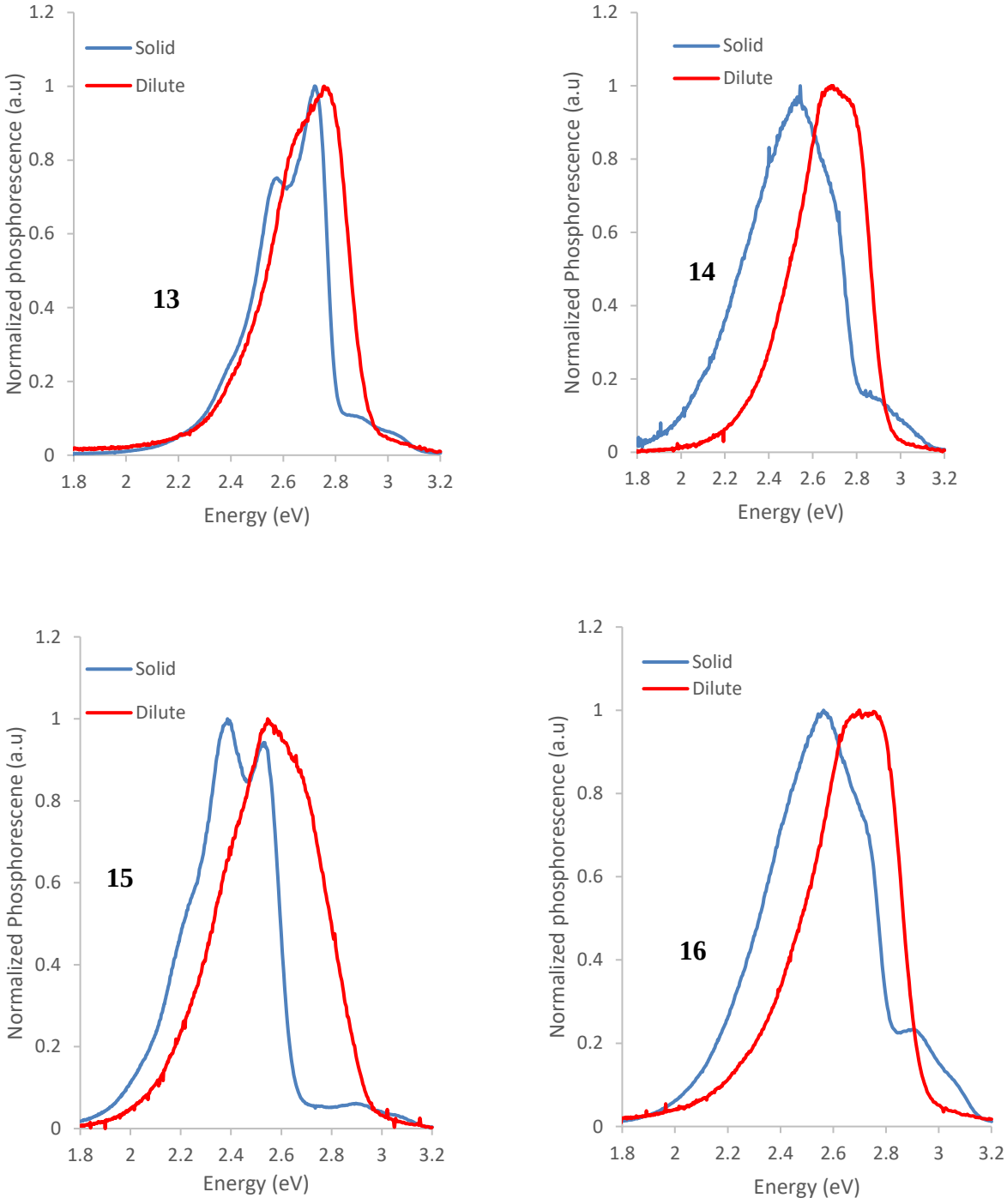

Figure 3.6: Triplet energy (E_T) of compound **13**, **14**, **15** and **16** in dilute and solid state

3.4 Thermal Properties

Thermogravimetric analysis (TGA) can be used to evaluate the thermal stability of a material including small organic molecules and dendrimers for OLEDs. No change in mass will be observed in certain temperature range indicating that the materials are thermally stable. Change of mass indicates the beginning of materials decomposition. At this point, materials are beginning to change in properties and can no longer serve as host for OLEDs.

For the purpose of measuring the number of characteristic properties of a material including glass transition temperatures (Tg), differential scanning calorimetry (DSC) is used. All amorphous materials will yield T_g during heating and it is the main characteristic transformation temperature of amorphous material. The glass transition event occurs when a hard, solid, amorphous material undergoes its transformation to a soft, rubbery, liquid phase. T_g is a valuable characterization parameter associated with a material and can provide very useful information regarding the thermal stability of a material. To be a suitable host material for OLEDs, the compounds need to be thermally stable at high temperature and have glass transition temperature for at least 100 ^oC.

3.4.1 TGA and DSC analysis

The thermal properties of dendrimers were investigated by using thermogravimetric analysis (TGA) and differential scanning calorimetry (DSC) at a scanning rate of 10 °C min^{-1} under a nitrogen atmosphere. Figure 3.7 represents the curves of compound **5-8**, **9-12**, and **13-16**. The decomposition temperature (T_d) corresponding to a 5% weight loss is 305 °C for compound **5**, while **9** and **13** possess T_d values as high as 404 °C and 502 °C, respectively.

The addition of *tert*-pentyl group at the outer layer of compound **9**, make it more thermally stable compared to compound **5**. There are about 99 °C different in T_d between compound **5** and **9**. This observation might be attributed to increasing in molecular weight from compound **5** (408.16 g mol^{-1}) to **9** (688.48 g mol^{-1}). Compared with compound **5** and **9**, an enhancement of T_d for about 198 °C and 98 °C were obtained in the dendrimer of compound **13**, which arises from its high molecular weight (1630.02 g mol^{-1}) and bulky carbazole dendrons at its outer layer. Other compounds with same core group series also showed the same trend where increasing in molecular weight will result in increased of the T_d value. Summary data of thermal properties for all compounds are listed in Table 3.11.

The morphological stability of all dendrimer is clearly seen in Figure 3.8. Distinct endothermic peaks related to the glass transition (T_g) appeared at 224 °C, 274 °C, 198 °C and 270 °C for compound **13**, **14**, **15** and **16** respectively. For use as host materials for OLEDs, the T_g value of a material needs to be higher than 100 ºC to avoid crystallization of the amorphous film during operation. By using organic glasses materials as the host, emitter can be uniformly diluted into the host and the effect of concentration quenching is minimized.

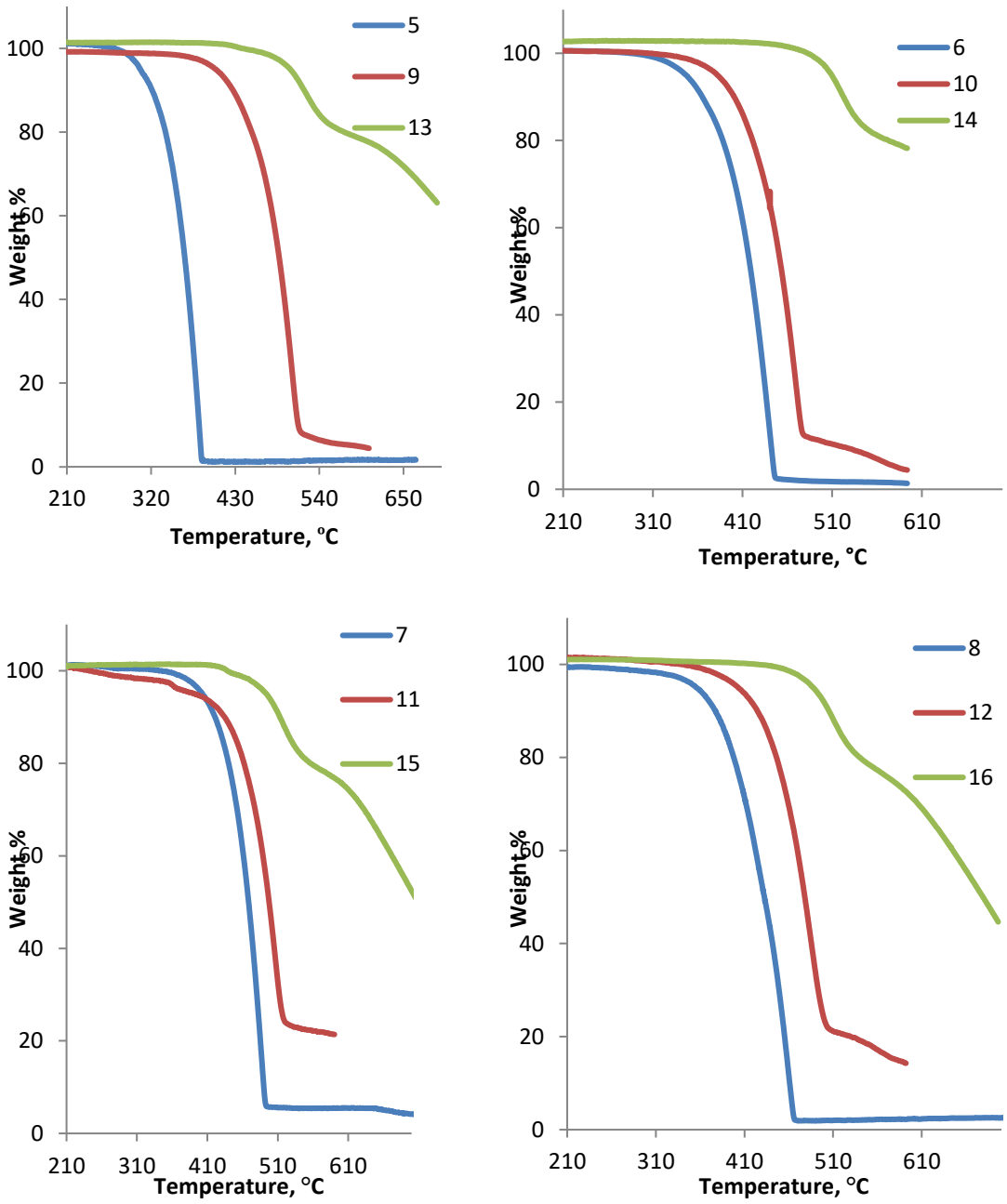

Figure 3.7: TGA traces of compound **5-16** tested at scan rate of 10 °C min^{-1} under a nitrogen atmosphere

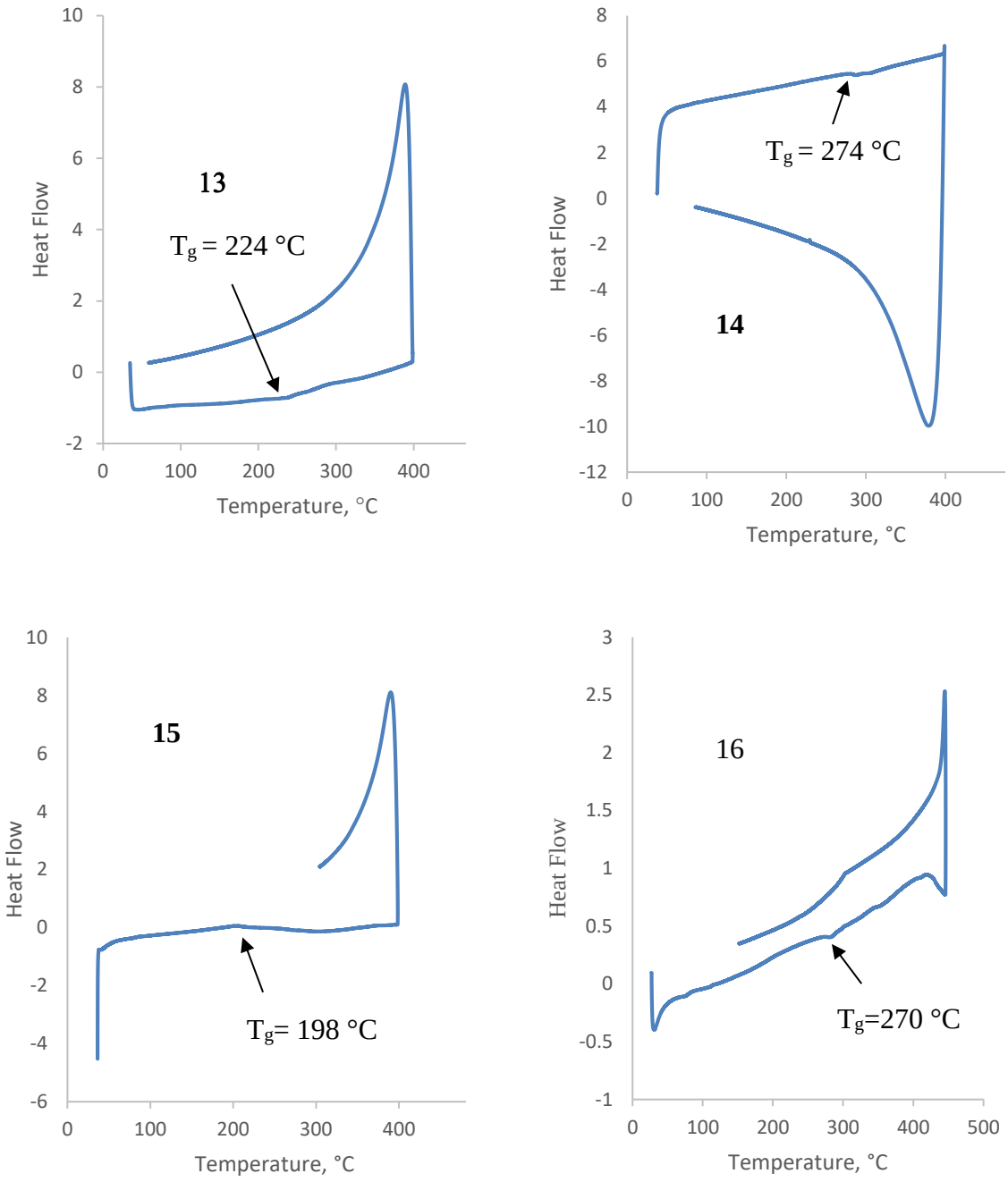

Figure 3.8: DSC traces of compound **13-16** tested at scan rate of 10 °C min^{-1} under a nitrogen atmosphere

Amorphous materials are an advantage to OLEDS due to the absence of grain boundaries that act as trap states (Shirota, 2000). The high T_g values for these dendrimers as a result from high molecular weight due to the presence of bulky carbazole dendrons (Jiang et al., 2012a; Zhang et al., 2004a). This result implies that dendrimers **13-16** would have excellent morphological stability, a favorable feature for the realization of long-term OLEDs.

Based on results from TGA and DSC, dendrimers **13-16** shows excellent thermal and amorphous stability that make them highly promising candidates to prepare stable amorphous thin films by solution casting for applications in OLEDs.

Table 3.11: Summary of T_d and T_g for compound **5-16**

Compound	T_d (°C)	T_g (°C)
5	305	-
6	346	-
7	383	-
8	355	-
9	404	-
10	381	-
11	394	-
12	403	-
13	502	224
14	508	274
15	494	198
16	487	270

3.5 Electrochemical Properties

In an organic semiconductor such as OLED devices, the energies of frontal orbital which are HOMO (highest occupied molecular orbital) and LUMO (lowest unoccupied molecular orbital) play an important role in determining the effectiveness of charge carrier (electron and holes) injection to the devices. The energy alignment between the organic materials and the emitters is crucial in the fabrication of a working device (Agarwal et al., 2011; Seo et al., 2011). Optimization of OLED devices can be achieved through efficient charge injection from electrode to semiconducting material, effective charge transport and charge confinement. The electrochemical data gave sufficient information which allows the estimation of relative position of HOMO and LUMO levels of the host materials used for device fabrication.

To investigate the electrochemical properties of our compounds, we have conducted cyclic voltammetry experiments for all compounds synthesized to estimate the HOMO and LUMO energy levels. Figure 3.9 shows cyclic voltammogram of dendrimer **13-16**.

The onset oxidation started at 0.52, 0.52, 0.52 and 0.53 V for compounds **13-16** respectively (Table 3.12). The highest occupied molecular orbital (HOMO) can be determined using the oxidation onset (E_{onset}) according to the following equations: HOMO=- E_{ox}-4.71eV, where E_{ox} are the onset potentials for oxidation relative to the Ag/Ag+ reference electrode.

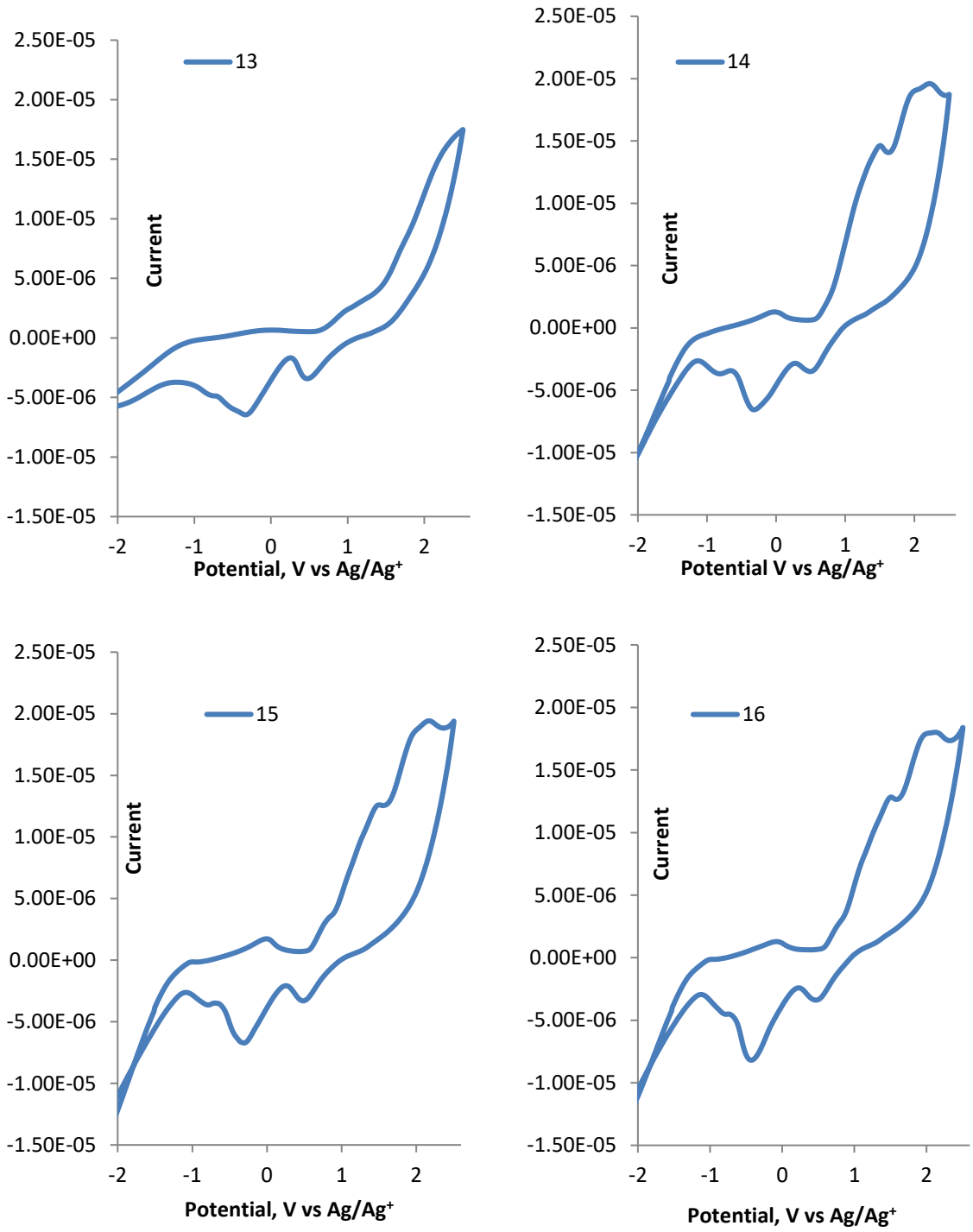

Figure 3.9: Cyclic voltammograms of compound **13-16** at scan rate 50 mV s^{-1} in dichloromethane

HOMO for compound **13**,**14**,**15** and **16** were determined to be -5.23 eV, -5.23 eV, -5.23 eV and -5.24 eV respectively (Table 3.12). The LUMO value was determined from the optical band gap and determined to be -1.85 eV, 1.78 eV, -1.80 eV, -1.83 eV for compound **13**, **14**, **15** and **16** respectively. All of the dendrimers have HOMO level that

are quite close to the work function of widely used hole injecting material PEDOT:PSS (5.1 eV) (Nardes et al., 2008) indicating that efficient hole injection into the emitting layer could be achieved by using compound **13**-**16** as host materials in the emitting layer of OLEDs.

Table 3.12: Cyclic voltammetry data of compounds **5**-**16**

Compounds	E_{ox}[a] (V)	E_{LUMO}[b](eV)	E_{HOMO}[c](eV)
5	0.55	-1.72	-5.26
6	0.56	-1.68	-5.27
7	0.58	-1.78	-5.29
8	0.56	-1.74	-5.27
9	0.54	-1.79	-5.25
10	0.59	-1.79	-5.30
11	0.58	-1.82	-5.29
12	0.55	-1.79	-5.26
13	0.52	-1.85	-5.23
14	0.52	-1.78	-5.23
15	0.52	-1.80	-5.23
16	0.53	-1.83	-5.24

[a] Onset oxidation and reduction potentials versus Ag/Ag^{+}.

[b] Calculate from optical bandgap $E_{LUMO}= E_g-E_{HOMO}$

[c] Estimated from the onset oxidation potential by using $E_{HOMO}= -E_{ox}-4.71eV$

3.6 Conclusion

In summary, this study has managed to synthesize four new dendrimers of compound **13**,**14**, **15** and **16** by using Ullmann reaction in six steps reaction pathway. These compounds have been tested in term of thermal, optical, and electrochemical properties. All of the dendrimers showed good thermal stability, high triplet energy and

appropriate HOMO and LUMO energy levels to serve as host materials for PhOLEDs. Compound **16** was found to be the best choice for the application as host material for blue, green and red OLED because of its high triplet energy (E_T = 2.82 eV) along with high glass transition temperature (T_g = 270 °C), high thermal decomposition stability (T_d = 470 °C) and suitable HOMO level (E_{HOMO}= -5.24 eV).

CHAPTER 4: DEVICE FABRICATION

4.1 Introduction

There are two different fabrication methods for OLED. The first one is vacuum deposition (Kang et al., 2009; Long et al., 2011; Yun et al., 2012) and the second one is wet/solution process such as spin coating method (Kim et al., 2014; Tsai et al., 2015; Xue et al., 2015; Yu et al., 2015b) and ink-jet printing (Gorter et al., 2013; Jung et al., 2012; Liu et al., 2013b; Nakata et al., 2011; Yoon et al., 2012). Vacuum deposition method is commonly used because of its simplicity in creating the multi-functional layer that can improve device performance (Reineke et al., 2009; Sun et al., 2006). However, vacuum deposition process is expensive and can waste OLED materials up to 80% (Kim et al., 2007).Therefore, the fabrication of large panel display and lighting are unfavorable by this method.

On the other hand, solution process method is gaining popularity because of its minimal cost compared to vacuum deposition system. Furthermore, the fabrication process can be done in an ambient environment. This method allows large area, low cost and roll-to-roll manufacturing process (So et al., 2007). To apply this method, OLED materials must have good solubility in the solvent used and also have high glass transition temperature, desirably T_g above 100 °C (Schroegel et al., 2011) . Crystallization can happen during the spin coating process and thermal annealing of solvent if low T_g material is used that can possibly lead to reliability issues. Crystallization of OLED thin film can cause electric field inhomogeneity leading to thermal breakdown and catastrophic failure (Han et al., 1996).

In this chapter, we will discuss the fabrication of single, double, and multi-layer phosphorescence organic light emitting diode (PhOLED) by solution process method.

The devices were fabricated based on compound **16** as the host for blue, green and red emitter PhOLED. We chose compound **16** as our host materials because of its suitable physical properties as well as its high triplet energy (2.82 eV) as discussed in Chapter 3. FIrpic, Ir(mppy)3 and Hex-Ir(phq)3 were used as the emitter for blue, green and red devices respectively. Figure 4.1 and Figure 4.2 shows the chemical structures of the materials used in this work and their energy levels respectively.

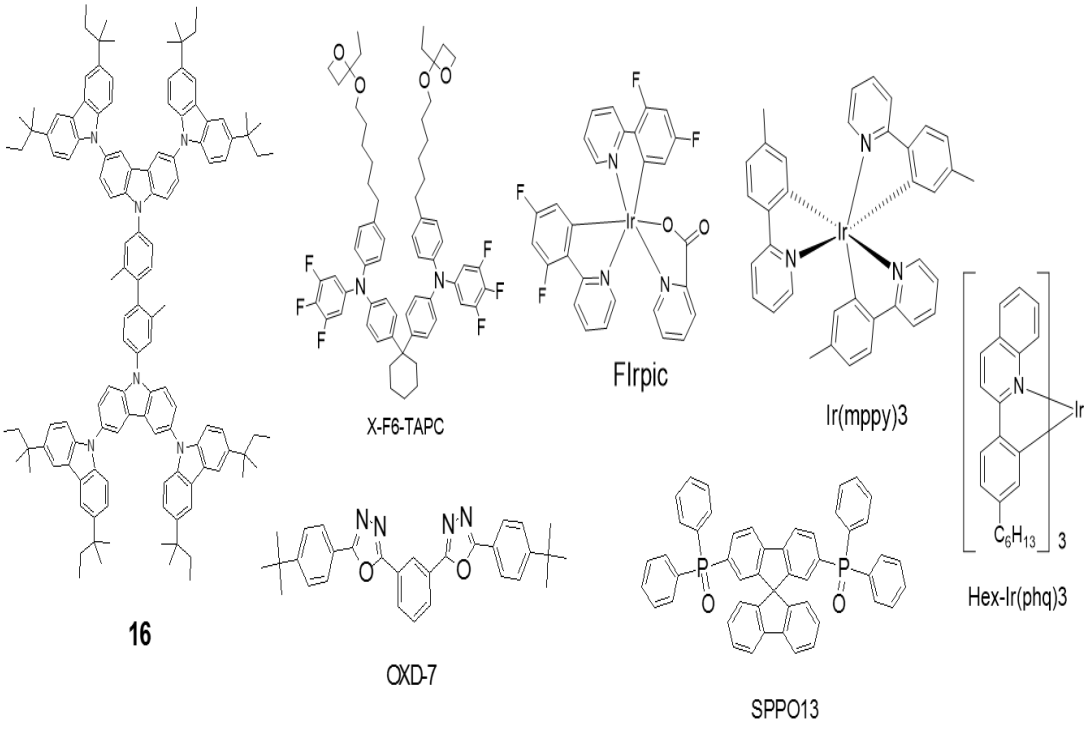

Figure 4.1: Chemical structure of chemicals used for device fabrication

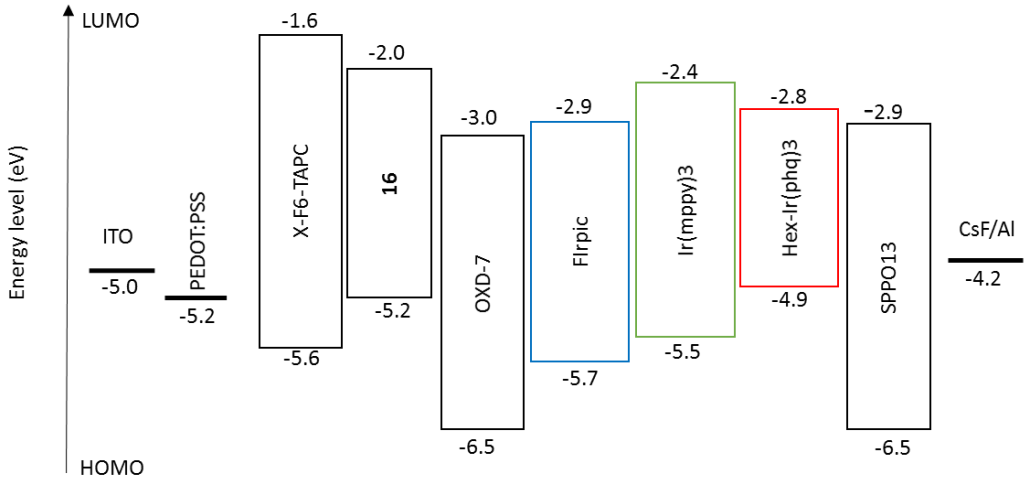

Figure 4.2: Energy levels of the materials

4.2 Single-layer PhOLEDs

Single layer device with the configuration of ITO (100 nm) / PEDOT:PSS (Al 4083) (40nm) / EML (60 nm)/ CsF (1 nm) / Al (100 nm) was fabricated by solution processing methods. PEDOT:PSS was used as the hole-injection layer. Electron-transporting material OXD-7 was mixed into the host materials to facilitate the electron transport in the emitting layer. FIrpic, Ir(mppy)3 and Hex-Ir(phq)3 with an optimize concentration of 10 wt. % was used as dopant emitters and CsF was used as the electron-injection layer. Figure 4.3 shows the luminance, current density, current efficiency, power efficiency characteristic of blue, green and red devices. All the devices data are summarized in Table 4.1. Maximum luminescence efficiency was found to be 6.2, 10.8 and 4.5 cd A^{-1} for blue, green and red OLEDs respectively. Meanwhile LE_{1000} was determined to be 1.3, 4.3 and 2.6 cd A^{-1} for blue, green and red respectively. The efficiency of the blue device showed about 3 times higher than the reported value of mCP with the maximum current efficiency of 1.8 cd A^{-1} with almost similar configuration (Jiang et al., 2010). This performance is achieved due to the excellent thermal stability of the dendritic host, which significantly enhances the capability of forming a stable amorphous thin film. As shown in Table 4.1, the electroluminescence (EL) spectra of

blue devices are identical with the CIE coordinates of (0.16,0.32), corresponding to the emission of FIrpic, and indicate the efficient energy transfer from hosts to FIrpic.

Table 4.1: Device performances of the solution-processed blue, green and red single layer PhOLEDs. The V_{on} is defined as voltage at a brightness of 1 cdm^{-2}. LE_{max} and PE_{max} are the maximum luminescence and power efficiencies respectively. LE_{1000} and PE_{1000} are the luminescence and power efficiency at 1000 cdm^{-2}

Device	V_{on} (V)	LE_{max} (cd/A)	PE_{max} (lm/W)	LE_{1000} (cd/A)	PE_{1000} (lm/W)	CIE_{1000}
Blue	6.5	6.2	1.85	1.3	0.5	(0.16,0.33)
Green	5.0	10.8	3.0	4.3	1.4	(0.31,0.63)
Red	5.0	4.5	1.04	2.6	0.8	(0.58,0.42)

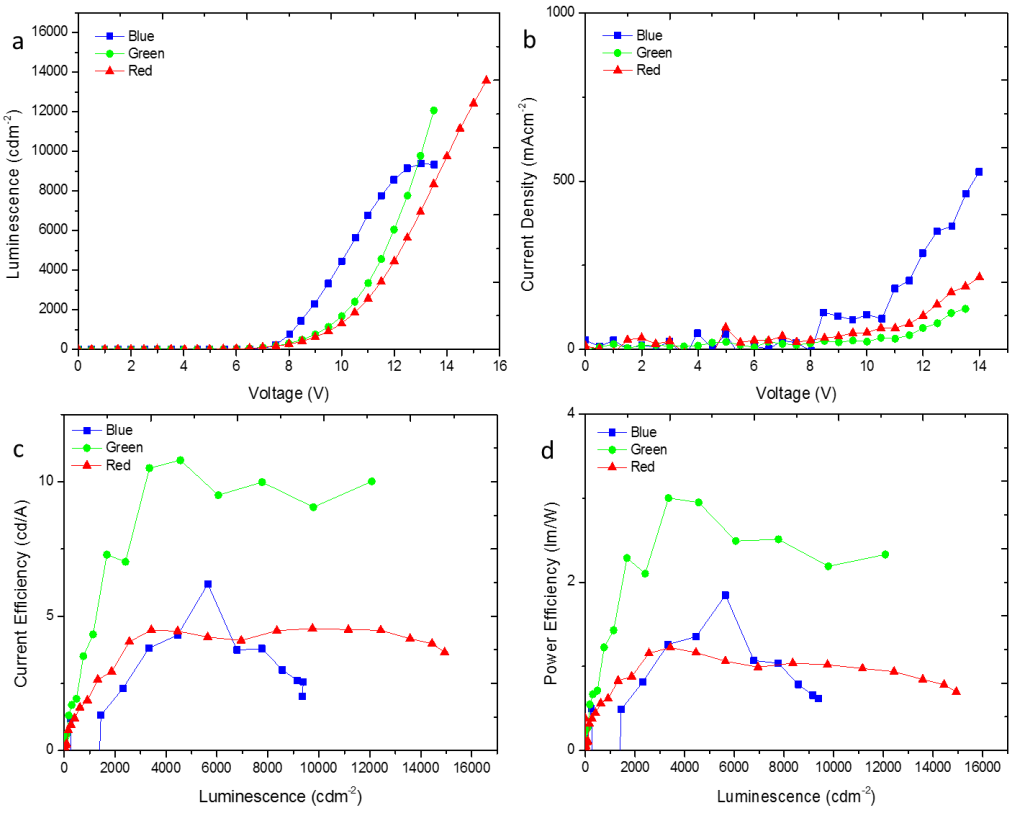

Figure 4.3: (a) Luminescence-voltage, (b) current density-voltage, (c) current efficiency-luminescence, (d) power efficiency-luminescence of blue, green and red of single layer devices

4.3 Double-layer PhOLEDs

Double layer PhOLEDs with the configuration of ITO (100 nm) / PEDOT:PSS (Al 4083) (40nm) / EML (40 nm)/ SPPO13 (30 nm) / CsF (1 nm) / Al (100 nm) was fabricated by solution processing methods. SPPO13 was acted as electron-transporting and hole-blocking layer (Tian et al., 2015; Yook et al., 2010). Blue, green and red devices showed luminous efficiency of 6.7, cd A^{-1}, 17.9 cd A^{-1} and 8.8 cd A^{-1} respectively as shown in Table 4.2. Compared to single layer device, double layer device shows an increase in efficiency for all devices. This increase in efficiency was almost double for green and red devices while for the blue device increase is just 0.2 cd A^{-1} from 6.5 cd A^{-1} to 6.7 cd A^{-1}. The turn-on voltage (V_{on}) also shows lower for all devices compared to single layer devices from 6.5 V, 5.0 V, and 5.0 V to 4.5 V, 4.5 V and 4.0 V for blue, green and red device respectively. This result indicated the effectiveness of SPPO13 as electron injection layer to confine excitons in the emissive layer in order to minimize excitons quenching and then enhance the efficiency of the devices. Figure 4.4 shows the luminance, current density, current efficiency and power efficiency of the double layer devices.

Table 4.2: Device performances of the solution-processed blue, green and red double layer PhOLEDs. The V_{on} is defined as voltage at a brightness of 1 cdm^{-2}. LE_{max} and PE_{max} are the maximum luminescence and power efficiencies respectively. LE_{1000} and PE_{1000} are the luminescence and power efficiency at 1000 cdm^{-2}

Device	V_{on} (V)	LE_{max} (cd/A)	PE_{max} (lm/W)	LE_{1000} (cd/A)	PE_{1000} (lm/W)	CIE_{1000}
Blue	4.5	6.7	2.3	6.3	2.3	(0.16, 0.36)
Green	4.5	17.9	6.2	6.3	2.6	(0.29, 0.63)
Red	4.0	8.8	3.7	3.5	1.6	(0.57, 0.43)

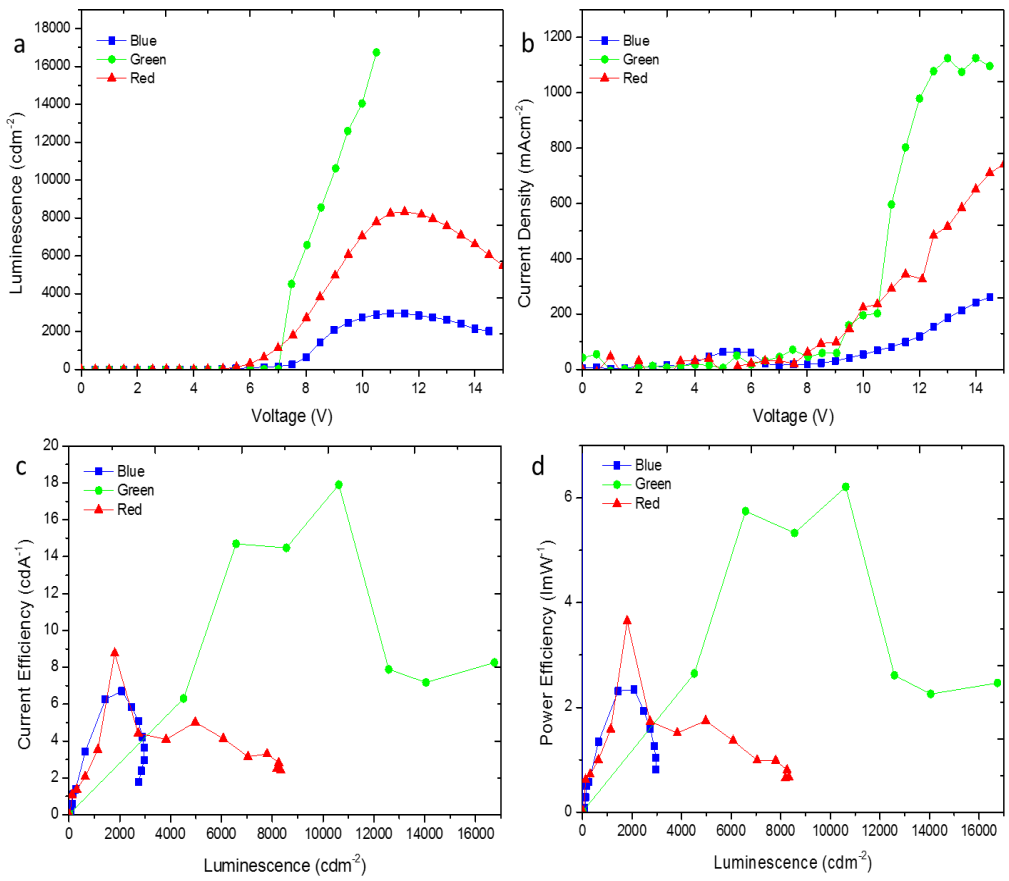

Figure 4.4: (a) Luminescence-voltage, (b) current density-voltage, (c) current efficiency-luminescence, (d) power efficiency-luminescence of blue, green and red of double layer devices

4.4 Multi-layer PhOLEDs

Multi-layer PhOLEDs with the configuration of ITO (100 nm) / PEDOT: PSS (40nm) / X-F6-TAPC (10 nm)/ EML (40 nm)/ SPPO13 (30 nm) / CsF (1 nm) / Al (100 nm) was fabricated. In order to confine both carriers and excitons, X-F6-TAPC and SPPO13 are used. X-F6-TAPC and SPPO13 have triplet energy of 2.87 eV (Liaptsis et al., 2013) and 2.73 eV (Chen et al., 2012a) respectively. This would be sufficient to confine the triplet excitons within the emissive layer. X-F6-TAPC also serves as an electron blocker (having LUMO of -1.6 eV) and modulate the charge balance while SPPO13 serves as a hole blocker (having HOMO of -6.5 eV) while assisting electron

injection and avoid cathode quenching. The ability of X-F6-TAPC to photo-crosslink and the insolubility of the host in 2,2,3,3-tetrafluoro-1-propanol allows the forming of multilayer solution processable phosphorescent light emitting diodes.

As shown in Table 4.3, blue, green and red devices achieved maximum efficiency of 9.3 cd A^{-1}, 24.4 cd A^{-1} and 9.9 cd A^{-1} respectively. These correspond to the power efficiency of 2.8 lm W^{-1}, 8.1 lm W^{-1} and 3.3 lm W^{-1} of the devices respectively. For the blue device, comparing to single and double layer device the enhancement of 2.8 cd A^{-1} and 2.6 cd A^{-1} were achieved, respectively. While for the green device, an increment by 13.6 cd A^{-1} and 6.5 cd A^{-1} were achieved from single and double layer device, respectively. On the other hand, the red device also shows enhancement in efficiency from single and double layer counterpart by 5.4 cd A^{-1} and 1.1 cd A^{-1} respectively. These results indicated that addition of X-F6-TAPC as the hole-transport layer in addition of SPPO13 as electron-transporting layer help hole mobility and electron injection that resulted in the increment of device efficiency.

All the devices can achieve brightness of 3000 cdm^{-2} and beyond as shown in Figure 4.5 (a). The efficiencies tend to peak near the 1000cdm^{-2}. This will be very useful for high brightness outdoor display with the electroluminescence spectra as shown in Figure 4.5 (c).

Table 4.3: Device performances of the solution-processed blue, green and red multilayer PhOLEDs. The V_{on} is defined as voltage at a brightness of 1 cdm^{-2}. LE_{max} and PE_{max} are the maximum luminescence and power efficiencies respectively. LE_{1000} and PE_{1000} are the luminescence and power efficiency at 1000 cdm^{-2}

Device	V_{on} (V)	LE_{max} (cd/A)	PE_{max} (lm/W)	LE_{1000} (cd/A)	PE_{1000} (lm/W)	CIE_{1000}
Blue	5.8	9.3	2.8	9.1	2.8	(0.16, 0.34)
Green	5.2	24.4	8.1	23.3	8.0	(0.30, 0.62)
Red	5.3	9.9	3.3	9.4	3.2	(0.57, 0.43)

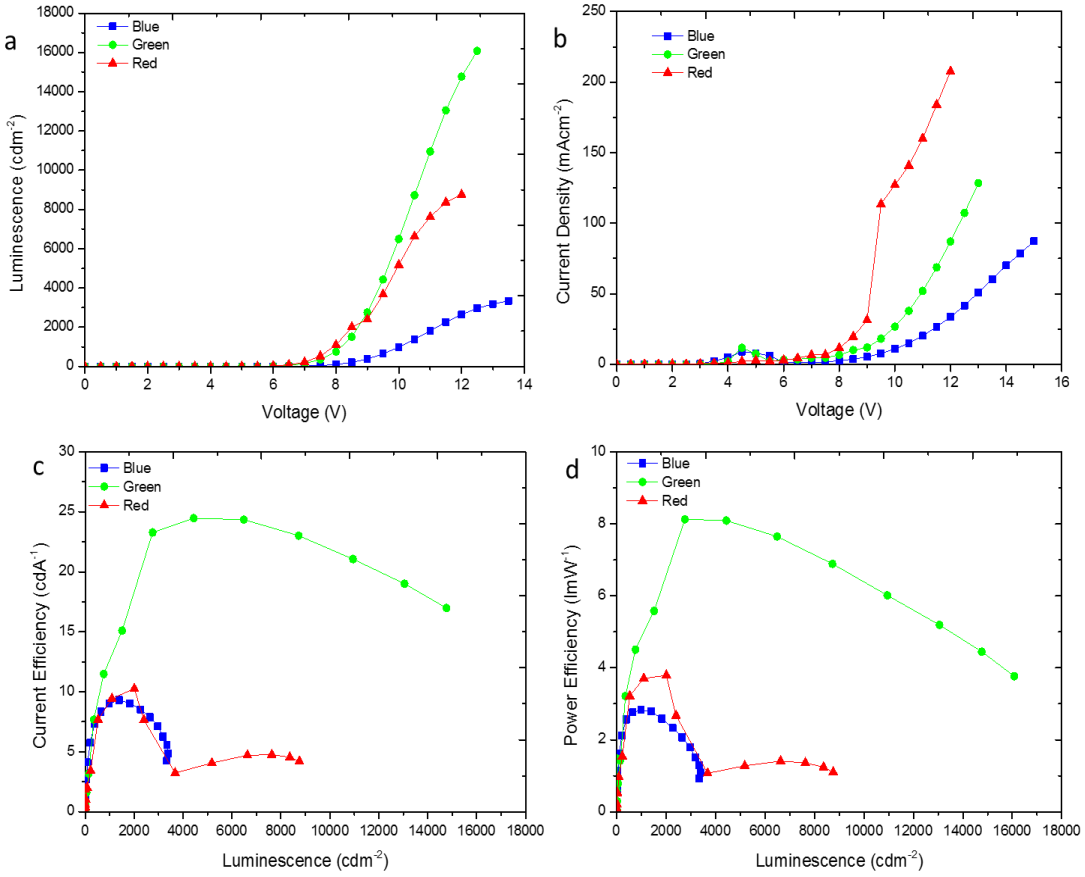

Figure 4.5: (a) Luminescence-voltage, (b) current density-voltage, (c) current efficiency-luminescence, (d) power efficiency-luminescence of blue, green and red of multi-layer devices

4.5 Thin Film Morphology

Solution process of small molecules tends to suffer from aggregation. One of the reasons of attaching *tert*-pentyl at the 3,6 positions is to prevent aggregation and to increase the solubility of compound **16** in organic solvents. In order to verify whether it can form a good uniform thin film, the morphologies of the neat and doped films of compound **16** are characterized by AFM. The root means square roughness, R_{RMS} of compound **16** on top of PEDOT: PSS is 0.292 nm while the doped compound **16** with OXD-7 and FIrpic with a ratio of 100:30:10 has an even smaller roughness of 0.233 nm as shown in Figure 4.6(a) and Figure 4.6(b) respectively. This indicates that compound **16** and the doped **16** have good film forming property.

To form the double layer and multilayer organic light emitting diode through solution processing, electron transporting SPPO13 will be used. SPPO13 is often vacuum deposited (Aizawa et al., 2012; Mostafa et al., 2013; Ye et al., 2015; Zhang et al., 2012a); however, it can be solution processed using isopropyl alcohol (IPA). We found that IPA processed SPPO13 on top of compound **16** has a poor film homogeneity resulting in the roughness of 0.591 nm as depicted in Figure 4.6(c). After testing with a range of solvents, it was found out that 2,2,3,3-tetrafluoro-1-propanol a type of fluorinated alcohol to be able to form a uniform thin film with roughness of 0.195 nm which is a significant improvement as seen in Figure 4.6(d). Fluorinated alcohol has been used to increase the electron injection property of the organic light emitting diodes and this could help to improve the electron injection of the device (Calvin Yi Bin et al., 2014).

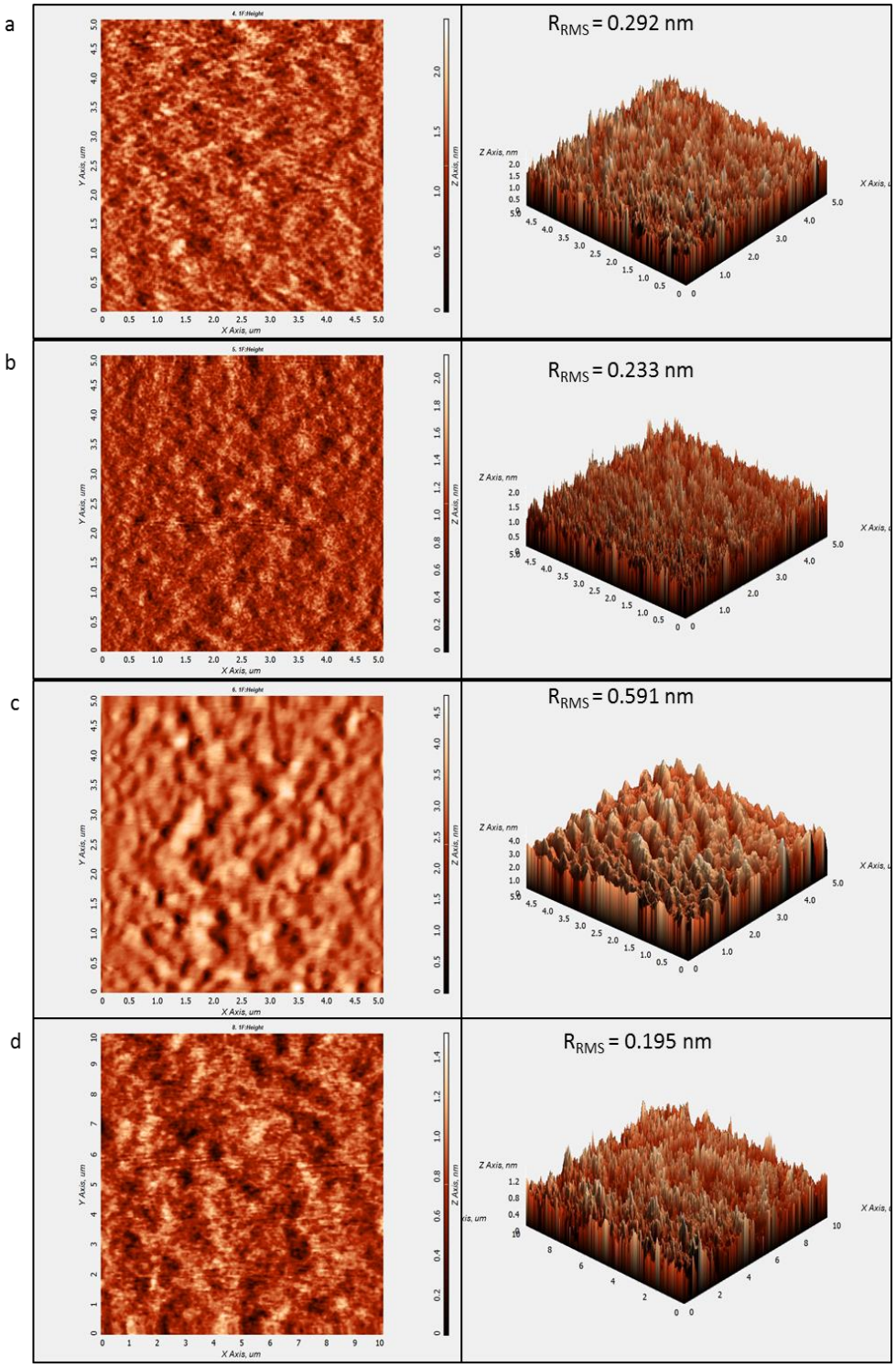

Figure 4.6: Surface morphology of (a) **16** on PEDOT: PSS, (b) doped **16** on PEDOT: PSS (c) SPPO13 processed using IPA solvent on top of **16** (d) SPPO13 processed using 2,2,3,3-tetrafluoro-1-propanol solvent on top of **16**

4.6 Conclusion

An increase in device efficiency has been observed from single layer devices to double layer devices in addition of SPPO13 as electron injection layer. Further increase in device efficiency can be observed in multilayer devices in conjunction with the addition of X-F6-TAPC as a hole transporting layer. Compound **16** has showed its ability to serve as universal host materials to triplet emitter of blue, green, and red. The AFM results showed that the surface roughness of SPPO13 can be improved by using fluorinated alcohol as the solvent to allow better electron injection to the emission layer.

CHAPTER 5: EXPERIMENTAL

5.1.1 Instrumentation for Chapter 3

Melting points were measured in glass capillaries recorded on Mel-Temp ii, Laboratory Devices and were not corrected. ^{1}H NMR and ^{13}C NMR spectra were recorded using either a JEOL Lambda FT-400 spectrometer, Bruker Avance III FT-400 spectrometer or Bruker Avance III FT-600 MHz and an internal standard of tetramethylsilane (TMS). Chemical shifts are reported in ppm on δ scale, and the coupling constant is given in Hz. Multiplicity of the signals is given as follows:s = singlet, d = doublet, t = triplet, q = quartet and m = multiplet.

For compounds with RMM <700 g mol^{-1} mass spectra were recorded using a Shimadzu QP5050A gas chromatography/mass spectrometer with electron impact (EI) at a source temperature of 200 °C. For compounds with RMM >700 g mol^{-1}, mass spectra were analyzed using a Bruker reflex IV matrix-assisted laser desorption/ionization (MALDI) time-of-flight (TOF) MS. A 384-well microliter plate format was used with a scout target. Sample were dissolved in dichloromethane directly used for measurement. CHN elemental analysis was obtained from CHNS/O 2400 Series II, Perkin Elmer analyzer and Thermo Finnigan Flash-1112EA.

Uv-Visible measurements were recorded using Cary 60 UV-Vis, Agilent Technologies. Fluorescence spectra were recorded by Cary Eclipse Fluorescence Spectrophotometer, Agilent Technologies. The samples were diluted in dichloromethane and the measurements were recorded at room temperature at the same setting and using quartz cells.

For triplet energy measurement, thin film samples were drop-casted onto a glass substrate heated at 60 °C from chloroform solution containing hosts at a concentration of

40 mg mL^{-1}. For dilute system, the samples were prepared at a concentration of 1 mg/mL dissolved in chlorobenzene. The samples were attached to the sample holder in a nitrogen cryostat (Janis). The samples were excited at 350 nm by a 150 fs pulsed Ti:sapphire laser (Spectra-Physics Hurricane) at 1 kHz repetition rate in conjunction with an ultrafast optical parametric amplifier (Quantronix TOPAS). A monochromator (Princeton Instruments Acton SP 2150) and then to a gated intensified CCD camera (Andor ICCD 334T) are used to capture the phosphorescence.

TGA and DSC analysis were performed on TGA 4000, Perkin Elmer and DSCQ20, TA instruments respectively. The cyclic voltammetry (CV) spectra were recorded using Potentiostat Galvanostat, Autolab. 0.1 M tetrabutylammonium perchlorate (TBAP) was used as a supporting electrolyte in dichloromethane solution and platinum as working electrode. The CV curves were referenced to an AgCl/Ag reference electrode and the scan rate was 50 mV s^{-1} in a potential range of -2.0 V to +2.5 V.

5.1.2. Working Procedures and Conditions for Chapter 3

Flash Column chromatography was performed using silica gel (0.063-0.2 mm) from the MERCK Company as the stationary phase. The used solvents are mentioned in the experimental section. Analytical Thin Layer Chromatography (TLC) was performed using MERCK 25 TLC plates 20 x 20 cm silica gel 60 F_{254} precoated aluminum plate. Spot was viewed under ultraviolet light and ethyl acetate:hexane as the solvent or eluent.

1,2-dichlorobenzene were dried using 3A˚ molecular sieves prior used. Others solvents purchased from commercial sources were used directly. Commercially available starting materials, reagents, and solvents were purchased from ALDRICH, ACROS, or MERCK Company. Carbazole from MERCK was undergoing recrystallization process several times using ethanol before used.

5.3 Experimental for Chapter 3

5.3.1 1,4-Di(9H-carbazol-9-yl)benzene (5) (Jeon et al., 2012; Jiang et al., 2012a; Schrogel et al., 2011; Zhang et al., 2004b)

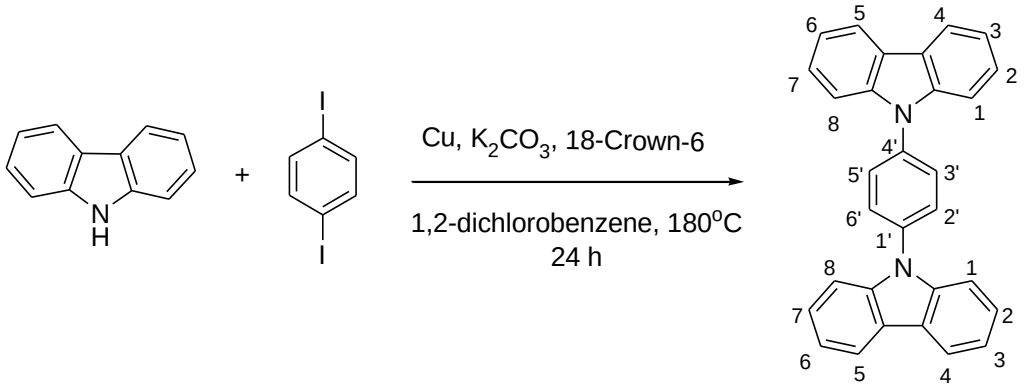

In a 50 cm^3 two neck round bottom flask equipped with a magnetic stirrer and a condenser topped with a nitrogen inlet, *o*-dichlorobenzene (5.00 cm^3), carbazole (0.22 g, 1.33 mmol), 1,4-diiodobenzene (0.20 g, 0.61 mmol), K_2CO_3 (0.67 g, 4.85 mmol), Cu powder (0.08 g, 1.21 mmol) and 18-Crown-6 (0.032 g, 0.12 mmol) were added. The mixture was heated at 180 °C using an oil bath and maintained at that temperature for 24 hours. After cooling to room temperature, the crude mixture was filtered to remove inorganic solid. The filtrate was concentrated under reduce pressure. The compound was purified by recrystallization from chloroform to afford a white powder (0.13 g, 59%). **Mp** 305-310°C; **^{1}H NMR** (ppm, 400 MHz, $CDCl_3$) δ_H : 8.18 (4H, d, *J* = 7.6 Hz, H-4,H-5), 7.81(s, 4H, H-2', H-3', H-5', H-6'), 7.56 (4H, d, *J* = 8.4 Hz, H-1, H-8), 7.46 (4H, t, *J* = 7.6, 7.2 Hz, H-3, H-6), 7.32 (4H, t, *J* = 7.6 Hz, 7.2 Hz, H-2, H-7); **^{13}C NMR** (ppm, 100 MHz, $CDCl_3$) δ_c : 140.77, 136.69, 128.39, 126.13, 123.58, 120.46, 120.28, 109.76; **MS (MALDI-TOF) [m/z]:** calcd for $C_{30}H_{20}N_2$, 408.16; found, 408.20.

5.3.2 1,3-Di(9H-carbazol-9-yl)benzene (6)(Jeon & Lee, 2012; Jiang et al., 2012a; Schrogel et al., 2011)

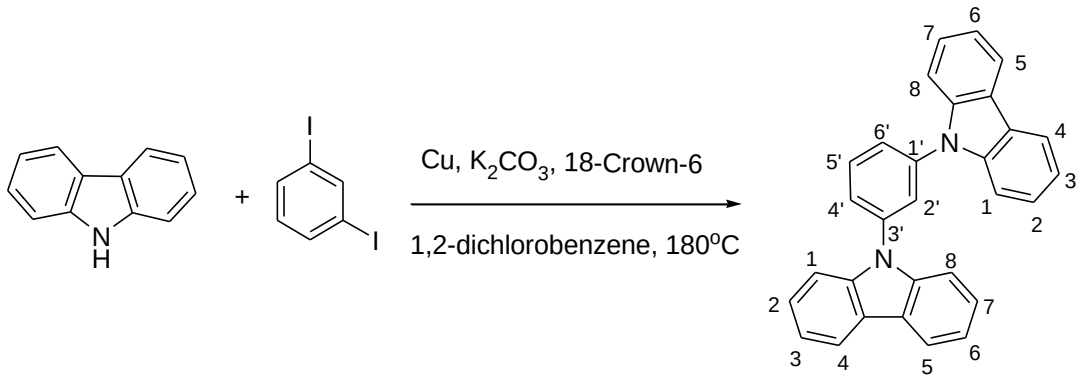

In a 100 cm^3 two neck round bottom flask equipped with a magnetic stirrer and a condenser topped with a nitrogen inlet, *o*-dichlorobenzene (50.00 cm^3), carbazole (5.32 g, 31.83 mmol), 1, 3-diiodobenzene (5.00 g, 15.16 mmol), K_2CO_3 (16.76 g, 121.28 mmol), Cu powder (1.93 g, 30.32 mmol) and 18-Crown-6 (0.80 g, 3.03 mmol) were added. The mixture was heated at 180 °C using an oil bath and maintained at that temperature for 48 hours. After cooling to room temperature, the crude mixture was filtered to remove inorganic solid. The filtrate was concentrated under reduce pressure. The compound was purified by recrystallization from chloroform to afford a white powder (4.75 g, 77 %). **Mp** 150-155 °C; **^{1}H NMR** (ppm, 400 MHz, $CDCl_3$) δ_H : 8.16 (4H, d, *J* = 7.76 Hz H-4, H-5), 7.86 (2H, m, ArH), 7.71 (2H, d, *J* = 8.00 Hz, ArH), 7.54 (4H, d, *J* = 8.20 Hz, H-1, H-8), 7.44 (4H, t, *J* = 7.76, 15.32 Hz, H-3, H-6), 7.32 (4H, t, *J* = 7.60, 14.88 Hz, H-2, H-7);**^{13}C NMR** (ppm, 100 MHz, $CDCl_3$) δ_c : 140.61, 139.38, 131.20, 126.16, 125.86, 125.35, 123.60, 120.45, 120.33, 109.69; **MS (MALDI-TOF) [m/z]:** calcd for $C_{30}H_{20}N_2$, 408.16; found, 408.16.

5.3.3 4,4'-Di (9H-carbazole-9-yl)-biphenyl (7) (Jeon & Lee, 2012; Jiang et al., 2012a; Schrogel et al., 2011)

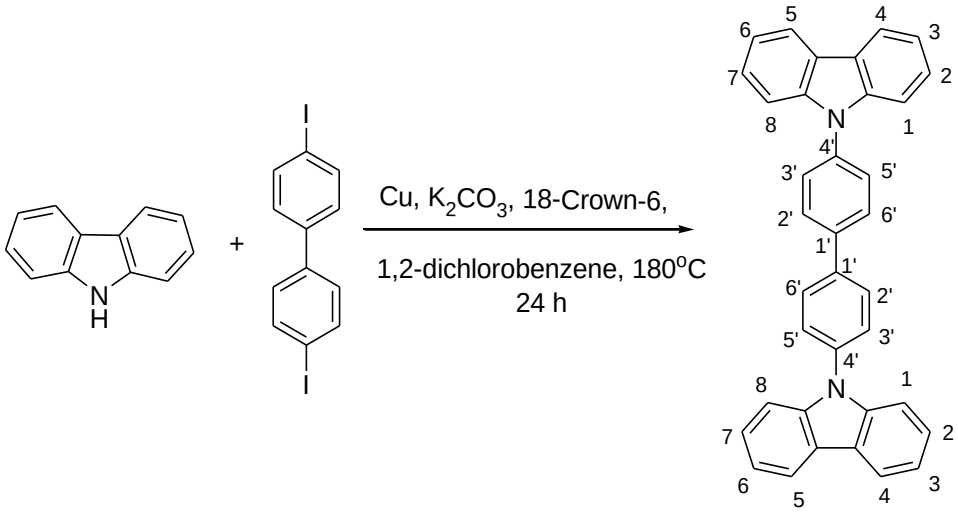

In a 50 cm^3 two neck round bottom flask equipped with a magnetic stirrer and a condenser topped with a nitrogen inlet, *o*-dichlorobenzene (10.00 cm^3), carbazole (0.18 g, 1.08 mmol), 4,4'-diiodobiphenyl (0.20 g, 0.49 mmol), K_2CO_3 (0.55 g, 3.94 mmol), Cu powder (0.06 g, 0.97 mmol) and 18-Crown-6 (0.03 g, 0.098 mmol) were added. The mixture was heated at 180 °C using an oil bath and maintained at that temperature for 24 hours. The slurry was then cooled and filtered using silica gel to remove inorganic mixture. Filtrate was reduced under high vacuum pump and then washed several times with acetone to yield a white powder (0.11 g, 55 %). **Mp** 260-265 °C; **^{1}H NMR** (ppm, 400 MHz, $CDCl_3$) δ_H : 8.17 (4H, d, *J* = 7.8 Hz, H-4, H-5), 7.92 (4H, d, *J* = 8.56 Hz , H-2', H-6'), 7.71 (4H, d, *J* = 8.32 Hz, H-3', H-5'), 7.51 (4H, d, *J* = 8.08 Hz, H-1, H-8), 7.43 (4H, td, *J* = 5.88 Hz, *J* = 1.2 Hz, H-3, H-6), 7.30 (4H, td, *J* = 6.84 Hz, H-2, H-7); **^{13}C NMR** (ppm, 100 MHz, $CDCl_3$) δ_c : 140.84, 139.31, 137.27, 128.53, 127.50, 126.03, 123.51, 120.38, 120.09, 109.83; **MS (MALDI-TOF) [m/z]:** calcd for $C_{36}H_{24}N_2$, 484.19; found, 484.59.

5.3.4 9,9'-(2,2'-Dimethylbiphenyl-4,4'-diyl)bis(9H-carbazole) (8) (Jeon & Lee, 2012; Jiang et al., 2012a; Schrogel et al., 2011)

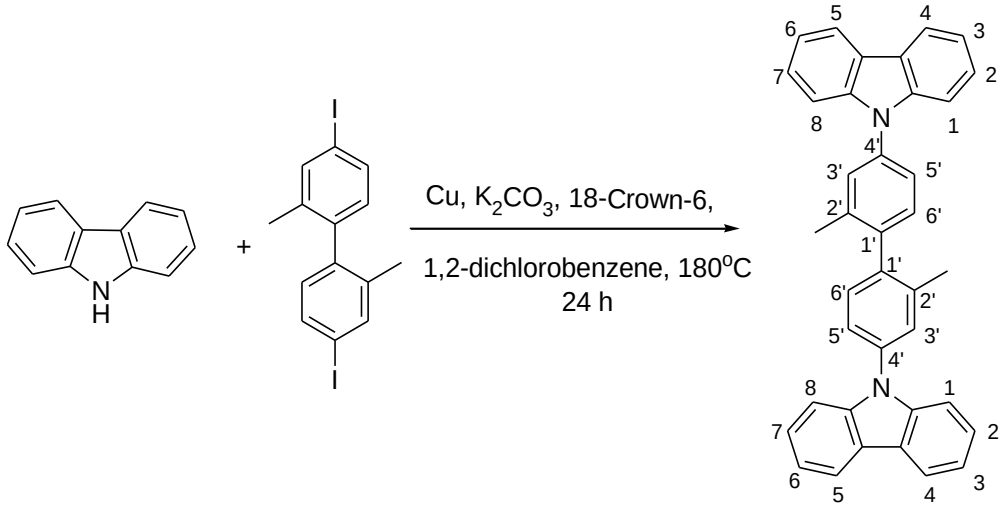

In a 50 cm^3 two neck round bottom flask equipped with a magnetic stirrer and a condenser topped with a nitrogen inlet, *o*-dichlorobenzene (5.00 cm^3), carbazole (0.17 g, 1.01 mmol), 4,4'-diiodo-2,2'-dimethylbiphenyl (0.20 g, 0.46 mmol), K_2CO_3 (0.25 g, 1.84 mmol), Cu powder (0.06 g, 0.92 mmol) and 18-Crown-6 (0.02 g, 0.09 mmol) were added. The mixture was heated at 180 °C using an oil bath and maintained at that temperature for 24 hours. After cooling to room temperature, the crude mixture was filtered to remove inorganic solid. The filtrate was concentrated under reduce pressure and then purified by column chromatography to yield a white powder. (Hexane: Ethyl acetate; 20:1) (0.14 g, 61 %). **Mp** °C: 110-115; **^{1}H NMR** (ppm, 400 MHz, $CDCl_3$) δ_H : 8.18 (4H, d, *J* = 7.72 Hz, H-4, H-5), 7.54-7.44 (14H, m, H-1, H-3, ,H-6, H-8, H-3', H-5', H-6'), 7.31 (4H, t, *J* = 7.40, 14.8 Hz, H-2, H-7), 2.29 (6H, s, -CH_3); **^{13}C NMR** (ppm, 100 MHz, $CDCl_3$) δ_c : 140.94, 140.00, 137.93, 136.90, 130.79, 128.34, 125.92, 124.32, 123.40, 129.34, 119.91, 109.92, 20.15; **MS (MALDI-TOF) [m/z]:** calcd for $C_{38}H_{28}N_2$, 512.23; found, 512.25.

5.3.5 1,4-Bis(3,6-di-*tert*-pentyl-9H-carbazol-9-yl)benzene (9) (Jeon & Lee, 2012; Jiang et al., 2012a; Schrogel et al., 2011)

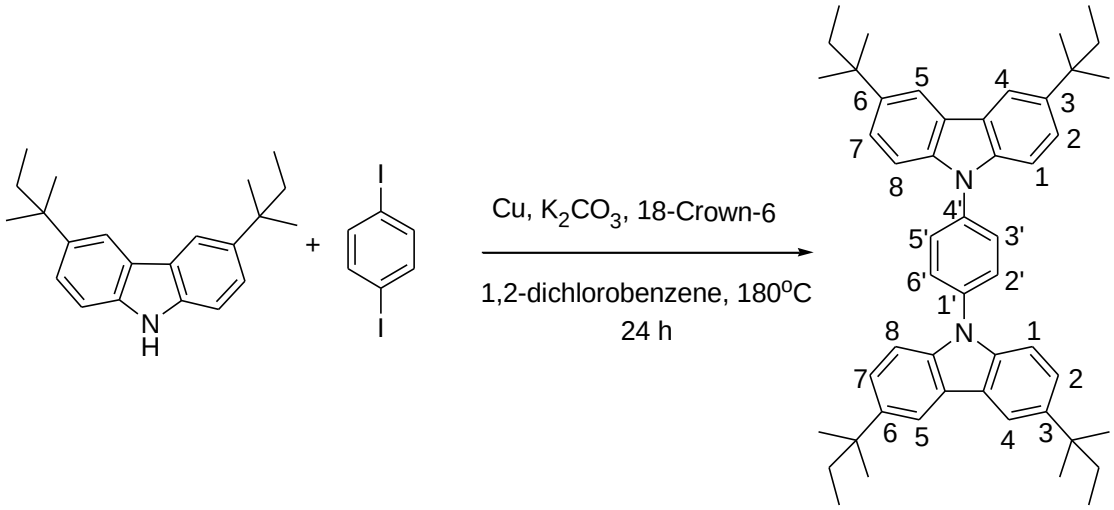

In a 50 cm^3 two neck round bottom flask equipped with a magnetic stirrer and a condenser topped with a nitrogen inlet, *o*-dichlorobenzene (10.00 cm^3), 3, 6-di-tert-pentyl-9H-carbazole (0.48 g, 1.56 mmol), 1,4-diiodobenzene (0.25 g, 0.76 mmol), K_2CO_3 (0.84 g, 6.08 mmol), Cu powder (0.10 g, 1.52 mmol) and 18-Crown-6 (0.04 g, 0.15 mmol) were added. The mixture was heated at 180 °C using an oil bath and maintained at that temperature for 24 hours. After cooling to room temperature, the crude mixture was filtered to remove inorganic solid. The filtrate was concentrated under reduce pressure and then purified by recrystallization from chloroform to get a white powder (0.39 g, 76%). **Mp** 270-275 °C; **^{1}H NMR** (ppm, 400 MHz, $CDCl_3$) δ_H : 8.10 (4H, d, *J* = 1.20 Hz, H-4, H-5), 7.78 (4H, s, H-2', H-3', H-5', H-6'), 7.50 (4H, d, *J* = 8.60 Hz, H-1, H-8), 7.45 (4H, dd, *J* = 1.56, 7.48 Hz, H-2, H-7), 1.80 (8H, q, *J* = 7.40, 7.44Hz, -CH_2-), 1.45 (24H, s, -$(CH_3)_2$), 0.75 (12H, *J* = 7.32 Hz, -CH_3); **^{13}C NMR** (ppm, 100 MHz, $CDCl_3$) δ_c : 141.33, 139.07, 136.70, 127.79, 124.25, 123.49, 117.19, 109.16, 37.98, 37.38, 29.14, 9.33; **MS (MALDI-TOF) [m/z]:** calcd for $C_{50}H_{60}N_2$, 688.48; found, 688.60.

5.3.6 1,3-Bis(3,6-di-tert-pentyl-9H-carbazol-9-yl)benzene (10) (Jeon & Lee, 2012; Jiang et al., 2012a; Schrogel et al., 2011)

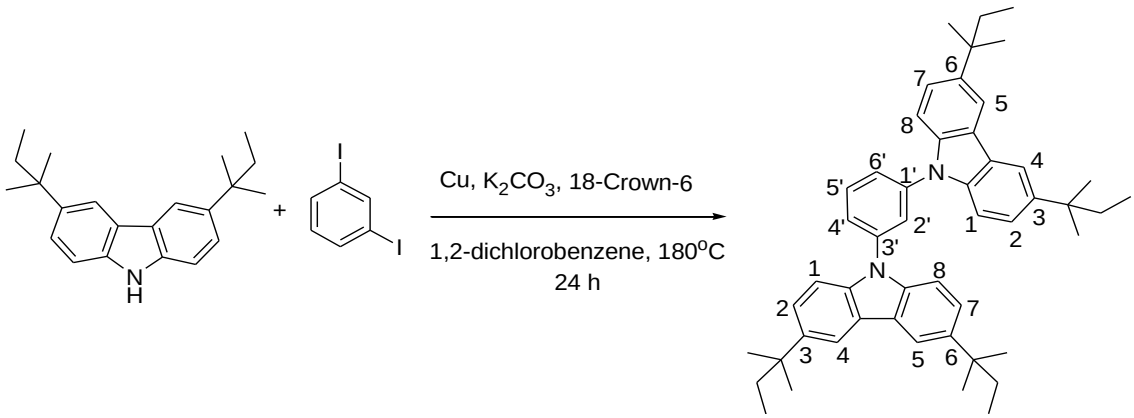

In a 50 cm^3 two neck round bottom flask equipped with a magnetic stirrer and a condenser topped with a nitrogen inlet, *o*-dichlorobenzene (10.00 cm^3), 3, 6-di-tert-pentyl-9H-carbazole (0.48 g, 1.56 mmol), 1,3-diiodobenzene (0.25 g, 0.76 mmol), K_2CO_3 (0.84 g, 6.08 mmol), Cu powder (0.10 g, 1.52 mmol) and 18-Crown-6 (0.04 g, 0.15 mmol) were added. The mixture was heated at 180 °C using an oil bath and maintained at that temperature for 24 hours. After cooling to room temperature, the crude mixture was filtered to remove inorganic solid. The filtrate was concentrated under reduce pressure and then purified by recrystallization from chloroform (0.28 g, 54%). **Mp** 205-210 °C; **^{1}H NMR** (ppm, 400 MHz, $CDCl_3$) δ_H : 8.07 (4H, s, H-4,H-5), 7.82 (1H,s, H-2'), 7.77 (1H, t, *J* = 7.92 Hz, H-5'), 7.65 (2H, d, *J* = 7.92 Hz, H-4', H-6'), 7.47 (4H, d, *J* = 8.64 Hz, H-2, H-7), 7.41 (4H, d, *J* = 8.68 Hz, H-1, H-8), 1.77 (8H, q, *J* = 7.36, 7.40 Hz, -CH_2-), 1.42 (24H, s, -$C(CH_3)_2$), 0.74 (12H, *J* = 7.28 Hz, -CH_3); **^{13}C NMR** (ppm, 100 MHz, $CDCl_3$) δ_c : 141.39, 139.73, 138.88, 130.84, 124.88, 124.45, 124.26, 123.53, 117.18, 109.15, 37.96, 37.35, 29.11, 9.30; **MS (MALDI-TOF) [m/z]:** calcd for $C_{50}H_{60}N_2$, 688.48; found, 688.61.

5.3.7 4,4'-Bis(3,6-di-tert-pentyl-9H-carbazol-9-yl)biphenyl (11) (Jeon & Lee, 2012; Jiang et al., 2012a; Schrogel et al., 2011)

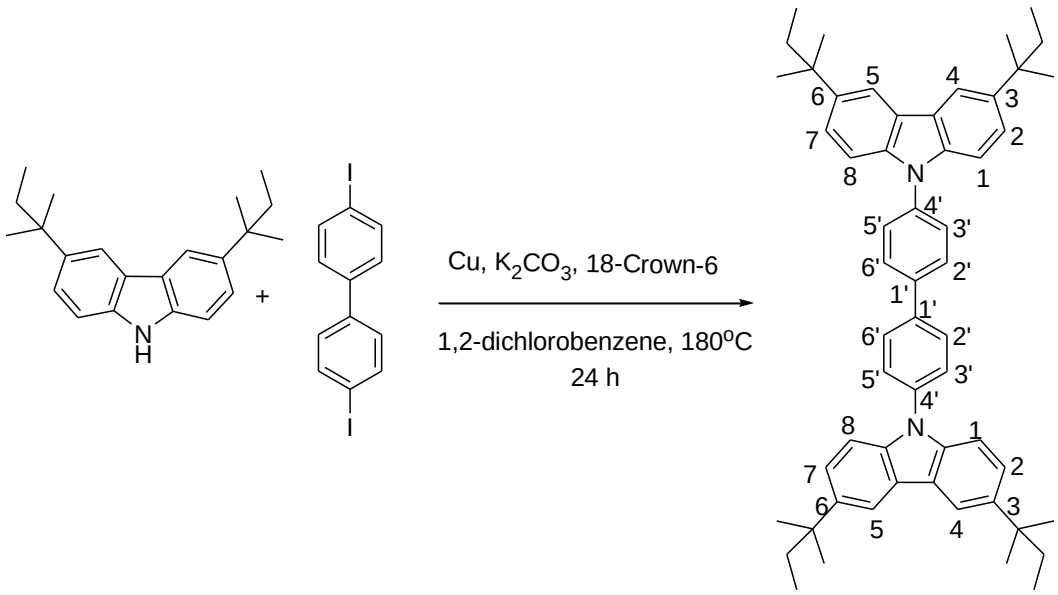

In a 50 cm^3 two neck round bottom flask equipped with a magnetic stirrer and a condenser topped with nitrogen inlet, *o*-dichlorobenzene (10.00 cm^3), 3, 6-di-tert-pentyl-9H-carbazole (0.39 g, 1.27 mmol), 4,4'-diiodobiphenyl (0.25 g, 0.62 mmol), K_2CO_3 (0.69 g, 4.96 mmol), Cu powder (0.08 g, 1.24 mmol) and 18-Crown-6 (0.03 g, 0.12 mmol) were added. The mixture was heated at 180 °C using an oil bath and maintained at that temperature for 24 hours. After cooling to room temperature, the crude mixture was filtered to remove inorganic solid. The filtrate was concentrated under reduce pressure and then purified by recrystallization from chloroform (0.42 g, 89%). **^{1}H NMR** (ppm, 400 MHz, $CDCl_3$) δ_H : 8.10 (4H, s, 4H, H-4,H-5), 7.90 (4H, d, *J* = 8.00 Hz, H-2', H-6'), 7.71 (4H, d, *J* = 7.40 Hz, H-3', H-5'), 7.43 (8H,m, H-1, H-2, H-7, H-8), 1.80 (8H, q, *J* = 6.84, 7.24Hz, $-CH_2-$), 1.45 (24H, s, $-C(CH_3)_2$), 0.75 (12H, *J* = 6.92 Hz, $-CH_3$); **^{13}C NMR** (ppm, 100 Mhz, $CDCl_3$) δ_c : 141.19, 139.08, 138.79, 128.31, 127.01, 124.17, 123.45, 117.14, 109.22, 37.97, 37.38, 29.14, 9.33; **MS (MALDI-TOF) [m/z]:** calcd for $C_{56}H_{64}N_2$, 764.51; found, 764.68.

5.3.8 9,9'-(2,2'-Dimethylbiphenyl-4,4'-diyl)bis(3,6-di-tert-pentyl-9H-carbazole) (12)

(Jeon & Lee, 2012; Jiang et al., 2012a; Schrogel et al., 2011)

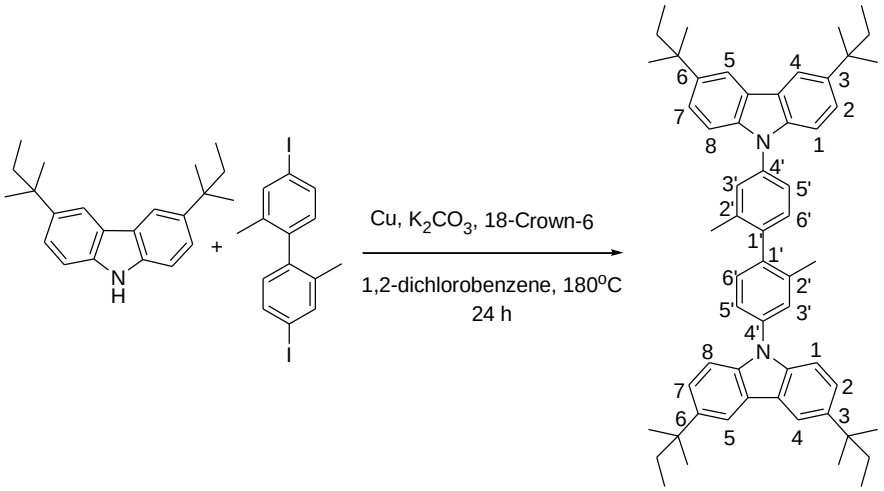

In a 50 cm^3 two neck round bottom flask equipped with a magnetic stirrer and a condenser topped with nitrogen inlet, *o*-dichlorobenzene (10.00 cm^3), 3, 6-di-tert-pentyl-9H-carbazole (0.36 g, 1.18 mmol), 4,4'-diiodo-2,2'-dimethylbiphenyl (0.25 g, 0.58 mmol), K_2CO_3 (0.64 g, 4.64 mmol), Cu powder (0.07g, 1.16 mmol) and 18-Crown-6 (0.03 g, 0.12 mmol) were added. The mixture was heated at 180 °C using an oil bath and maintained at that temperature for 24 hours. After cooling to room temperature, the crude mixture was filtered to remove inorganic solid. The filtrate was concentrated under reduce pressure and then purified by recrystallization from chloroform to yield an orange powder (0.32 g, 70%). **Mp** 290-295 °C; **^{1}H NMR** (ppm, 400 MHz, $CDCl_3$) δ_H : 8.09 (4H,s, H-4,H-5), 7.53 (2H, s, H-3'), 7.49 (6H, m, H-2, H-7, H-6'), 7.42 (m, 6H, H-1, H-8, H-5'), 2.26 (s, 6H, -CH_3 at C-2'), 1.80 (q, 8H, *J*=7.28, 7.36 Hz, -CH_2-), 1.45 (s, 24H, -$C(CH_3)_2$), 0.75 (t, 12H, *J* = 7.24 Hz, -CH_3); **^{13}C NMR** (ppm, 100 MHz, $CDCl_3$) δ_c :140.99, 139.54, 139.19, 137.75, 137.34, 130.68, 127.84, 124.07, 123.83, 123.34, 117.10, 109.30, 37.96, 37.40, 29.15, 20.11, 9.34; **MS (MALDI-TOF) [m/z]:** calcd for $C_{58}H_{68}N_2$, 792.54; found, 792.67.

5.3.9 3,6-Diiodo-9H-carbazole (18) (El-Khouly et al., 2013; Wang et al., 2012; Wu et al., 2011; Yu et al., 2015a; Zhang et al., 2010)

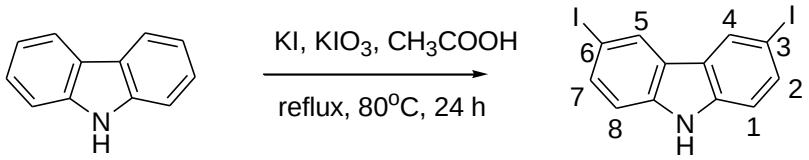

Carbazole (5.00 g, 29.94 mmol) was dissolved in acetic acid (50.00 cm^3) and then warmed to 80 °C. Potassium iodide (6.51 g, 39.22 mmol) and potassium iodate (4.99 g, 23.35 mmol) were added to this solution and the mixture was refluxed for 24 hours. The crude product was diluted with water and filtered with vacuum. The brown precipitates were stirred in the solution of sodium sulfite for 1 hour and filtered with vacuum. The product was recrystallized from dichloromethane to give a brownish solid (9.08 g, 72 %). **Mp** 145-150 °C; **^{1}H NMR** (ppm, 400 MHz, $CDCl_3$) δ_H : 8.32 (2H, s, H-4, H-5), 8.10 (1H, s, N-H), 7.69 (2H, dd, *J* = 1.08, 7.40 Hz, H-2, H-7), 7.22 (2H, d, *J* = 8.48 Hz, H-1, H-8); **^{13}C NMR** (ppm, 100 MHz, $CDCl_3$) δ_c : 138.51, 134.82, 129.39, 124.58, 112.69, 82.45; **MS (GC) [m/z]:** calcd for $C_{12}H_7I_2N$, 418.87; found, 419.00; **Anal. calcd** for $C_{12}H_7I_2N$**:** C, 34.40; H, 1.68; N, 3.34. Found: C, 34.42; H, 1.60; N, 3.31.

5.3.10 3,6-Di-*tert*-pentyl-9H-carbazole (19) (McClenaghan et al., 2003; Michinobu et al., 2009; Woon et al., 2015)

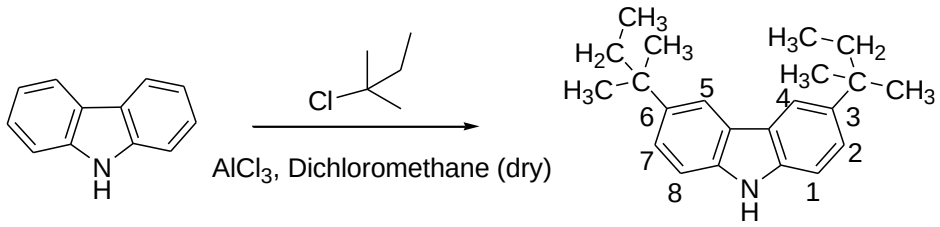

The mixture of carbazole (10.00 g, 59.88 mmol), anhydrous $AlCl_3$ (7.98g, 58.88mmol) and dry dichloromethane (200.00 cm^3) in a three-necked flask cooled to 0 ^oC was added dropwise a solution of 2-chloro-2-methylbutane (14.75 cm^3, 119.76 mmol) in dry dichloromethane (40.00 cm^3). After addition, the mixture was stirred for 10 min at the same temperature. Then the ice bath was removed and the reaction was continued for 24 hours. The mixture poured into ice-water (500.00 cm^3) and extracted with dichloromethane. The combined organic phase was dried over $MgSO_4$. After filtered, the filtration was evaporated to give a grey crude which was recrystallized from ethanol to afford a white powder (9.33 g, 51%). **Mp** 215-220 °C; **^{1}H NMR** (ppm, 400 MHz, $CDCl_3$) δ_H : 8.01 (2H, s, H-4, H-5), 7.83 (1H, s, N-H), 7.39 (2H, d, *J* = 8.48 Hz, H-2, H-7), 7.33 (2H, d, *J* = 8.52 Hz, H-1, H-8), 1.76 (4H, q, *J* = 7.40, 7.44 Hz, -CH_2-), 1.41(12H, s,-$C(CH_3)_2$), 0.71 (6H, t, *J* = 7.40 Hz, -CH_3); **^{13}C NMR** (ppm, 100 MHz, $CDCl_3$) δ_c :140.41, 137.96, 124.03, 123.31, 117.06, 109.96, 37.90, 37.42, 29.15, 9.31; **MS (GC) [m/z]:** calcd for $C_{22}H_{29}N$, 307.23; found, 307.00; **Anal. calcd** for $C_{22}H_{29}N$**:** C, 85.94; H, 9.51; N, 4.56. Found: C, 86.20; H, 9.00; N, 5.52.

5.3.11 *N*-(3,6-diiodo-9H-carbazol-9-yl)ethanone (20a) **modified method of** (Albrecht et al., 2008; Yu et al., 2015a)

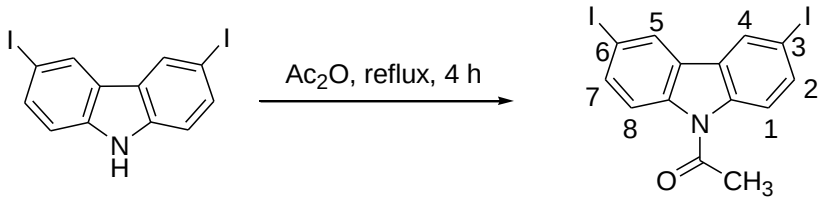

3,6-Diiodo-9H-carbazole (10.00 g, 23.87 mmol) was dissolved in acetic anhydride (50.00 cm^3). The mixture was refluxed at 140 ^oC for about 4 hours. The precipitates were filtered under vacuum and wash with water several times to afford white powder (8.76 g, 79 %). **Mp** 215-220 °C; **^{1}H NMR** (ppm, 400 MHz, $CDCl_3$) δ_H : 8.25 (2H, s, H-4,H-5), 7.96 (2H, d, *J* = 8.80 Hz,H-2,H-7), 7.78 (2H, d, *J* = 8.80 Hz, H-1,H-8), 2.84 (3H, s, -CH_3); **^{13}C NMR** (ppm, 100 MHz, $CDCl_3$) δ_c : 169.67, 137.95, 136.47, 128.99, 127.19, 118.01, 87.60, 27.68; **MS (GC) [m/z]:** calcd for $C_{14}H_9I_2NO$, 460.88; found, 461.00; **Anal. calcd** for $C_{14}H_9I_2NO$**:** C, 36.47; H, 1.97; N, 3.04. Found: C, 36.47; H, 1.71; N, 3.02.

5.3.12 *N*-(3,6-bis(3,6-ditert-pentyl-carbazol-9-yl)carbazole)ethanone (21) (El-Khouly et al., 2013; Wang et al., 2012; Yu et al., 2015a)

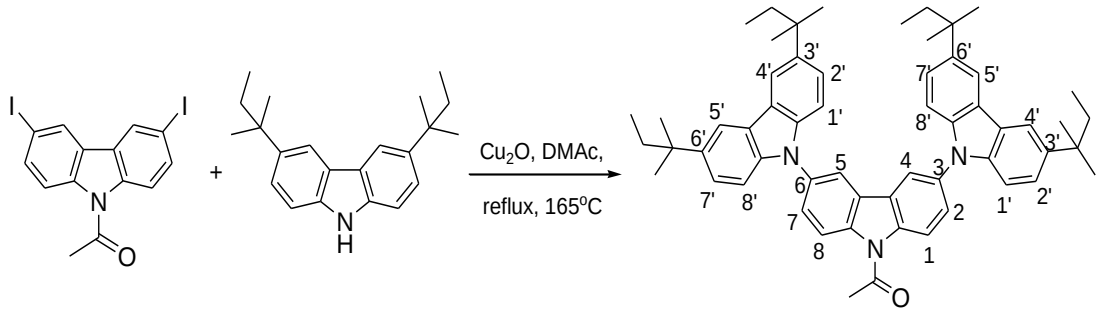

To a solution of 1-(3, 6-diiodo-9H-carbazol-9-yl)ethanone (2.00 g, 4.33 mmol) and 3, 6-Di-tert-pentyl-9H-carbazole (2.67 g, 8.68 mmol) in *N*,*N*-dimethylacetamide (30.00 cm^3) was added copper oxide (1.24 g, 8.68 mmol). The mixture was refluxed at 165 °C for 48 hours and cooled to room temperature and then diluted with water. The precipitates were filtered and recrystallized from ethanol to afford white powder (2.65 g, 74 %). **^{1}H NMR** (ppm, 400 MHz, $CDCl_3$) δ_H : 8.49 (2H, d, *J* = 8.88 Hz, H-4, H-5), 8.16 (2H, d, *J* = 2.04 Hz, H-2, H-7), 8.08 (4H, s, H-4', H-5'), 7.75 (2H, dd, *J* = 2.08 Hz, 6.76 Hz, H-1, H-8), 7.37 (8H, m, H-1', H-2', H-7', H-8'), 3.05 (3H, s, O=C-CH_3), 1.77 (8H, q, -CH_2-), 1.42 (24H, s, -$(CH_3)_2$), 0.72 (12H, t, -CH_3); **^{13}C NMR** (ppm, 100 MHz, $CDCl_3$) δ_c : 169.88, 141.17,139.46, 137.74, 134.38, 127.37, 126.71, 124.22, 123.35, 118.39, 117.56, 117.18, 108.92, 37.95, 37.36, 29.12, 27.79, 9.32; **MS (MALDI-TOF) [m/z]:** calcd for $C_{58}H_{65}N_3O$, 819.51; found, 820.11; **Anal. calcd** for $C_{58}H_{65}N_3O$**:** C, 84.94; H, 7.99; N, 5.12. Found: C, 84.56; H, 8.09; N, 5.18.

5.3.13 3,6-Bis(3,6-ditert-pentyl-carbazol-9-yl)carbazole (22) (El-Khouly et al., 2013; Yu et al., 2015a)

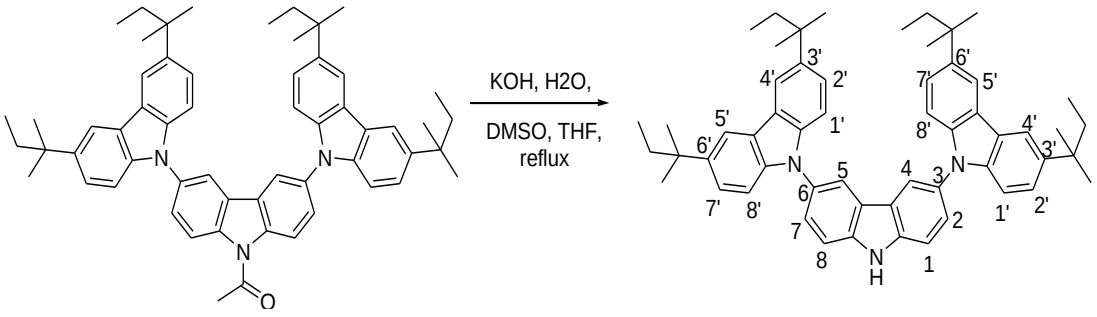

To a solution of *N*-(3,6-bis(3,6-ditert-pentyl-carbazol-9-yl)carbazole)ethanone (2.00 g, 2.44 mmol) in THF (6.00 cm^3), DMSO (3.00 cm^3) and water (1.00 cm^3) were added. The mixture was stirred for 10 min. KOH (1.20 g, 21.4 mmol) was added subsequently to the mixture and then refluxed for 4 hours. The crude was diluted with water and neutralize with HCl solution (6 N). The crude was filtered and recrystallised from mixture of hexane: ethyl acetate (1:1) to give white solid. (1.80 g, 95 %). **Mp** 285-290 °C; **^{1}H NMR** (ppm, 400 MHz, $CDCl_3$) δ_H : 8.41 (1H, s, N-H), 8.19 (2H, s, H-4, H-5), 8.08 (4H, s, H-4', H-5'), 7.67 (4H, m, H-1, H-2, H-7, H-8), 7.36 (8H, m,H-1',H-2', H-7', H-8'), 1.77 (8H, q, *J* = 7.32, 7.44 Hz, -CH_2-), 1.42 (24H, s, -$(CH_3)_2$), 0.72 (12H, t, *J* = 7.28 Hz, -CH_3); **^{13}C NMR** (ppm, 100 MHz, $CDCl_3$) δ_c : 140.66, 140.08, 139.01, 130.49, 125.95, 124.11, 124.02, 123.07, 119.42, 117.03, 111.81, 109.04, 37.92, 37.39, 29.15, 9.33; **MS (MALDI-TOF) [m/z]:** calcd for $C_{56}H_{63}N_3$, 777.50; found, 777.64; **Anal. calcd** for $C_{56}H_{63}N_3$**:** C, 86.44; H, 8.16; N, 5.40. Found: C, 85.87; H, 8.41; N, 5.38.

5.3.14 1,4-Bis(3,6-bis(3,6-ditert-pentyl-carbazol-9-yl)carbazol-9-yl)benzene (13)

(Jeon & Lee, 2012; Jiang et al., 2012a; Schrogel et al., 2011; Woon et al., 2015)

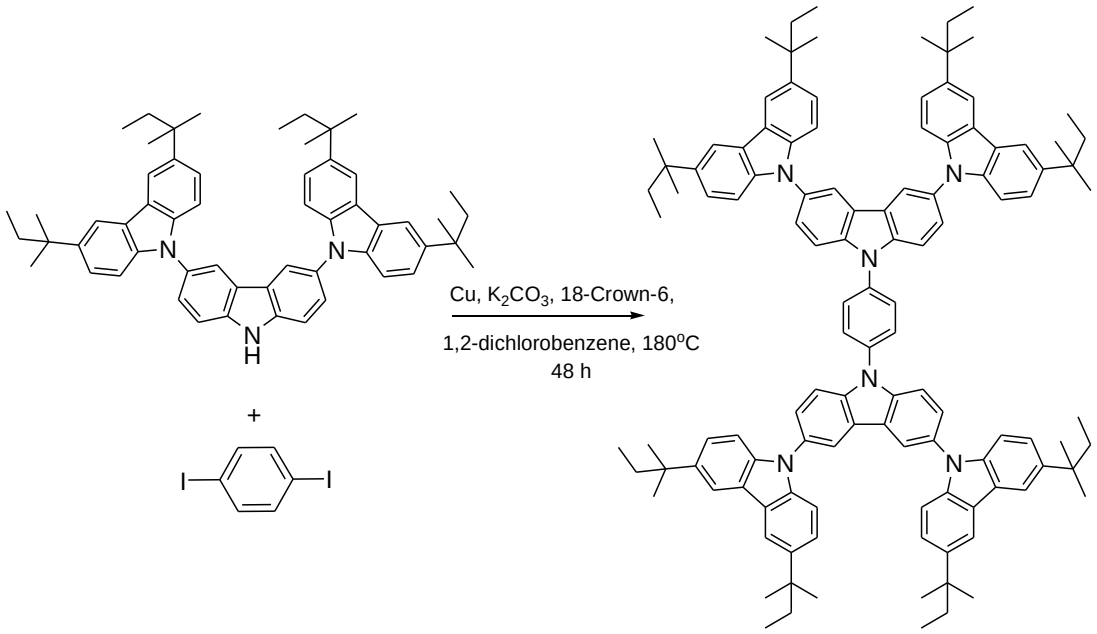

In a 50 cm^3 two neck round bottom flask equipped with a magnetic stirrer and a condenser topped with a nitrogen inlet, *o*-dichlorobenzene (10.00 cm^3), 3,6-bis(3,6-ditert-pentyl-carbazol-9-yl)carbazole (0.51 g, 0.66 mmol), 1,4-diiodobenzene (0.10 g, 0.30 mmol), K_2CO_3 (0.33 g, 2.40 mmol), Cu powder (0.04 g, 0.60 mmol) and 18-Crown-6 (0.02 g, 0.06 mmol) were added. The mixture was heated at 180 °C using an oil bath and maintained at that temperature for 48 hours. After cooling to room temperature, the crude mixture was filtered to remove inorganic solid. The filtrate was concentrated under reduced pressure and purify using column chromatography (hexane: ethyl acetate; 30:1) to give a white powder. The compound was further purified by recrystallization from chloroform (0.45 g, 90 %). **^{1}H NMR** (ppm, 400 MHz, $CDCl_3$) δ_H : 8.32 (4H, d, J = 1.28 Hz), 8.12 (8H,s), 8.10(4H,s), 7.86 (4H, d, J = 8.68 Hz), 7.73 (4H, dd, J = 1.52, 7.12 Hz),

7.41 (8H, d, *J* = 9.28 Hz), 7.38 (8H, d, *J* = 8.56 Hz), 1.80 (16H, q, *J* = 7.28, 7.40 Hz), 1.43 (48H, s), 0.75 (24H, t, *J* = 7.28 Hz); **^{13}C NMR** (ppm, 100 MHz, $CDCl_3$) δ_c : 140.85, 140.20, 140.00, 136.88, 131.39, 128.80, 126.19, 124.32, 124.10, 123.16, 119.50, 117.14, 111.09, 109.01, 37.96, 37.40, 29.16, 9.35; **MS (MALDI-TOF) [m/z]:** calcd for $C_{118}H_{128}N_6$, 1630.02; found, 1630.58; **Anal. calcd** for $C_{118}H_{128}N_6$**:** C, 86.93; H, 7.91; N, 5.15. Found: C, 86.44; H, 8.22; N, 5.14.

5.3.15 1,3-Bis(3,6-bis(3,6-ditert-pentyl-carbazol-9-yl)carbazol-9-yl)benzene (14)

(Jeon & Lee, 2012; Jiang et al., 2012a; Schrogel et al., 2011)

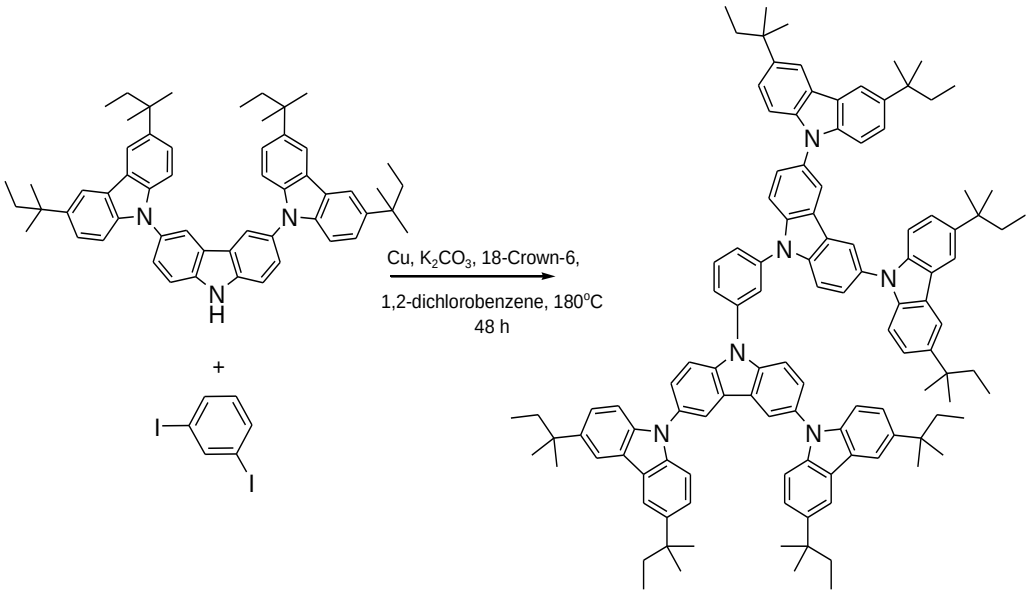

In a 50 cm^3 two neck round bottom flask equipped with a magnetic stirrer and a condenser topped with a nitrogen inlet, *o*-dichlorobenzene (10.00 cm^3), 3,6-bis(3,6-ditert-pentyl-carbazol-9-yl)carbazole (0.52 g, 0.67 mmol), 1,3-diiodobenzene (0.10 g, 0.30 mmol), K_2CO_3 (0.33 g, 2.40 mmol), Cu powder (0.04 g, 0.60 mmol) and 18-Crown-6 (0.03 g, 0.12 mmol) were added. The mixture was heated at 180 °C using an oil bath and maintained at that temperature for 48 hours. After cooling to room temperature, the crude mixture was filtered to remove inorganic solid. The filtrate was concentrated under reduced pressure and purify using column chromatography (hexane: ethyl acetate; 30:1) to give a white powder. The compound was further purified by recrystallization from chloroform (0.19 g, 40 %). **^{1}H NMR** (ppm, 400 MHz, $CDCl_3$) δ_H : 8.30 (4H,d, *J* = 1.88 Hz), 8.18 (1H,t, *J* = 1.76Hz), 8.08 (8H, d, *J* = 1.08 Hz), 8.05 (1H, s), 7.98 (2H, dd, *J* = 1.76, 6.56 Hz), 7.83 (4H, d, *J* = 8.72Hz), 7.71 (4H, dd, *J* = 2.00, 6.72 Hz), 7.39 (8H, dd, *J* = 1.64, 7.08 Hz), 7.36 (8H, d, *J* = 8.60 Hz), 1.79 (16H, q, *J* = 7.32, 7.44 Hz), 1.42 (48H,

s), 0.73 (24H, t, *J* = 7.32 Hz); **^{13}C NMR** (ppm, 100 MHz, $CDCl_3$) δ_c : 140.85, 140.08, 139.97, 139.33, 131.46, 126.58, 125.50, 124.36, 124.11, 123.16, 119.51, 117.12, 111.00, 109.00, 37.95, 37.39, 29.16, 9.34; **MS (MALDI-TOF) [m/z]:** calcd for $C_{118}H_{128}N_6$, 1630.02; found, 1630.01.

5.3.16 4,4'-Bis(3,6-bis(3,6-ditert-pentyl-carbazol-9-yl)carbazol-9-yl)biphenyl (15)

(Jeon & Lee, 2012; Jiang et al., 2012a; Schrogel et al., 2011)

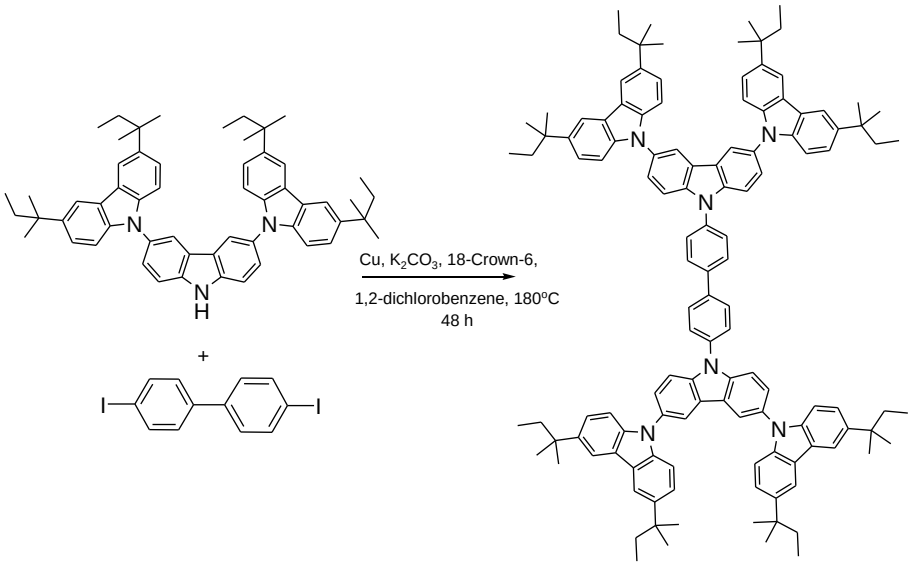

In a 50 cm^3 two neck round bottom flask equipped with a magnetic stirrer and a condenser topped with a nitrogen inlet, *o*-dichlorobenzene (10.00 cm^3), 3,6-bis(3,6-ditert-pentyl-carbazol-9-yl)carbazole (0.48 g,0.62 mmol), 4,4'-diiodobiphenyl (0.10 g, 0.25 mmol), K_2CO_3 (0.56 g, 4.0 mmol), Cu powder (0.03g,0.50 mmol) and 18-Crown-6 (0.02g, 0.05 mmol) were added. The mixture was heated at 180 °C using an oil bath and maintained at that temperature for 96 hours. After cooling to room temperature, the crude mixture was filtered to remove inorganic solid. The filtrate was concentrated under reduced pressure and purify using column chromatography (hexane: ethyl acetate; 50:1) to give a white powder. The compound was further purified by recrystallization from chloroform (0.25 g, 59 %). **^{1}H NMR** (ppm, 400 MHz, $CDCl_3$) δ_H : 8.30 (4H, d, *J* = 1.88 Hz), 8.10 (8H, d, *J* = 1.24 Hz), 8.08 (4H, d, *J* = 8.48 Hz), 7.93 (4H, d, *J* = 8.44 Hz), 7.76 (4H, d, *J*= 8.64 Hz), 7.68 (4H, dd, *J* = 1.96, 6.72 Hz), 7.41 (8H, dd, *J* = 1.72, 7.00 Hz), 7.37 (8H, d, *J*= 8.56 Hz), 1.80 (16H,q, *J* = 7.32, 7.44 Hz), 1.43 (48H, s), 0.75 (24H, t, *J* = 7.32 Hz); **^{13}C NMR** (ppm, 100 MHz, $CDCl_3$) δ_c: 140.80, 140.32, 140.06, 139.81, 136.99, 131.11, 128.93, 127.66, 126.07, 124.16, 124.09, 123.14, 119.41, 117.12, 111.17,

109.05, 37.96, 37.42, 29.18, 9.36; **MS (MALDI-TOF) [m/z]:** calcd for $C_{124}H_{132}N_6$, 1706.05; found, 1706.71.

5.3.17 4,4'-Bis(3,6-bis(3,6-ditert-pentyl-carbazol-9-yl)carbazol-9-yl)-2,2'-dimethylbiphenyl (16) (Jeon & Lee, 2012; Jiang et al., 2012a; Schrogel et al., 2011)

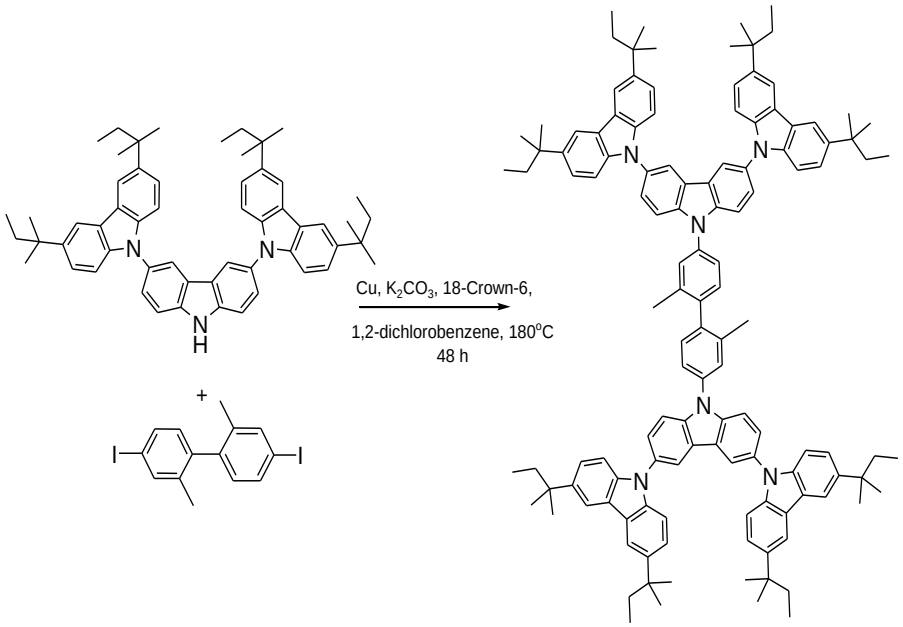

In a 50 cm^3 two neck round bottom flask equipped with a magnetic stirrer and a condenser topped with a nitrogen inlet, *o*-dichlorobenzene (10.00 cm^3), 3,6-bis(3,6-ditert-pentyl-carbazol-9-yl)carbazole (0.50 g, 0.64 mmol), 4,4'-diiodo-2,2'-dimethylbiphenyl (0.13 g, 0.29 mmol), K_2CO_3 (0.64 g, 4.64 mmol), Cu powder (0.04 g, 0.58 mmol) and 18-Crown-6 (0.03 g, 0.12 mmol) were added. The mixture was heated at 180 °C using an oil bath and maintained at that temperature for 96 hours. After cooling to room temperature, the crude mixture was filtered to remove inorganic solid. The filtrate was concentrated under reduced pressure and purify using column chromatography (hexane: ethyl acetate; 50:1) to give a white powder. The compound was further purified by recrystallization from chloroform (0.30 g, 60 %). **^{1}H NMR** (ppm, 400 MHz, $CDCl_3$) δ_H: 8.29 (4H, s), 8.10 (8H, s), 7.78-7-59 (14H, m), 7.41 (8H, d, *J* = 8.80 Hz), 7.37 (8H, d, *J* = 8.56 Hz), 2.42 (6H, s), 1.80 (16H, q, *J* = 7.32, 7.40 Hz), 1.43 (48H, s), 0.75 (24H, t, *J* = 7.24 Hz); **^{13}C NMR** (ppm, 100 MHz, $CDCl_3$) δ_c : 140.76, 140.49, 140.44, 140.08, 138.39, 136.64, 130.94, 128.50, 125.99, 124.49, 124.07, 124.03, 123.11, 119.38, 117.10,

111.24, 109.05, 37.95, 37.41, 29.17, 20.32, 9.35; **MS (MALDI-TOF) [m/z]:** calcd for $C_{126}H_{136}N_6$, 1734.09; found, 1734.64. **Anal. calcd** for $C_{126}H_{136}N_6$**:** C, 87.25; H, 7.84; N, 4.84. Found: C, 87.00; H, 7.62; N, 4.83.

5.3.18 4,4'-Diiodobiphenyl (23) (Xiong et al., 2007)

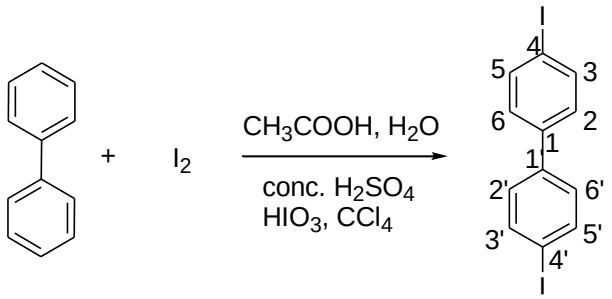

A mixture of biphenyl (1.54 g, 10.00 mmol), acetic acid (10.00 cm^3), water (1.00 cm^3), conc. Sulfuric acid (1.00 cm^3), iodine (2.79 g, 11.00 mmol), periodic acid (1.25 g, 5.50 mmol) and carbon tetrachloride (2.00 cm^3) was maintained at 80 ^oC for about 4 hours with a magnetic stirrer. The slurry product was cooled to room temperature and poured into water. The solution was extracted with dichloromethane (3 x 50 cm^3). After the combined dark purple organic layer was decolorized with sodium sulfite, it was washed with water, dried over anhydrous Na_2SO_4, filtered and evaporated to dryness to get a slightly yellow solid and recrystallized from ethanol to afford a colorless crystal. (2.8 g, 65%). **Mp** 186-188 °C; **^{1}H NMR** (ppm, 400 MHz, $CDCl_3$) δ_H : 7.72 (4H, d, *J* = 8.52 Hz, H-3, H-5, H-3', H-5'), 7.22 (4H, d, *J* = 11 Hz, H-2, H-6, H-2', H-6'); **^{13}C NMR** (ppm, 100 MHz, $CDCl_3$) δ_c : 139.57, 138.01, 128.69, 93.51; **MS (GC) [m/z]:** calcd for $C_{12}H_8I_2$, ; 405.87 found, 406.00.

5.4 Experimental for Chapter 4

5.4.1 General information

All materials were purchased and used as received without further purification. OXD-7, SPPO13, X-F6-TAPC, FIrpic, Ir(mppy)3, Hex-Ir(phq)3 were purchased form Luminescence Technology Corp. Single layer device structure consists of ITO (100 nm) / PEDOT: PSS (Al 4083) (40nm) / EML (60 nm)/ CsF (1 nm) / Al (100 nm), double layer device structure consists of ITO (100 nm) / PEDOT:PSS (Al 4083) (40nm) / EML (50 nm)/ SPPO13 (30 nm) / CsF (1 nm) / Al (100 nm) and multi-layer device structure consists of ITO (100 nm) / PEDOT:PSS (Al 4083) (40nm) / X-F6-TAPC (10 nm)/ EML (40 nm)/ SPPO13 (30 nm) / CsF (1 nm) / Al (100 nm) have been fabricated as shown in Figure 5.1.

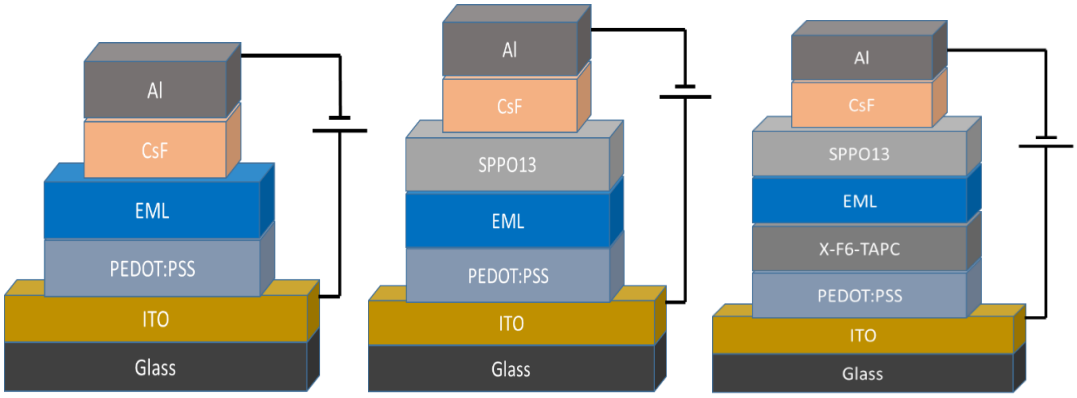

Figure 5.1: Structure of single, double and multi-layer devices

The EML layer for the device is **16**: FIrpic or Ir(mppy)3 or Hex-Ir(phq)3:OXD-7 with a blending ratio of 100:30:10. Electroluminescence intensities were measured using SM442 Spectrometer. AFM was measured using AFM (NT-MDT Solver Next) with non-contact mode.

5.4.2 Device fabrication process

Bare ITO deposited on polished soda lime glass was used as substrate. The ITO/glass substrates were purchased from Luminescence Technology Corporation, Taiwan. The thickness of the ITO and glass was 120 nm and 1.1 mm respectively. The size of the substrate was 15 mm × 20 mm. The substrates were cleaned sequentially using deionized water (DI), acetone, isopropyl alcohol, and DI water again for 15 minutes. Figure 5.2 shows the ITO pattern dimensions.

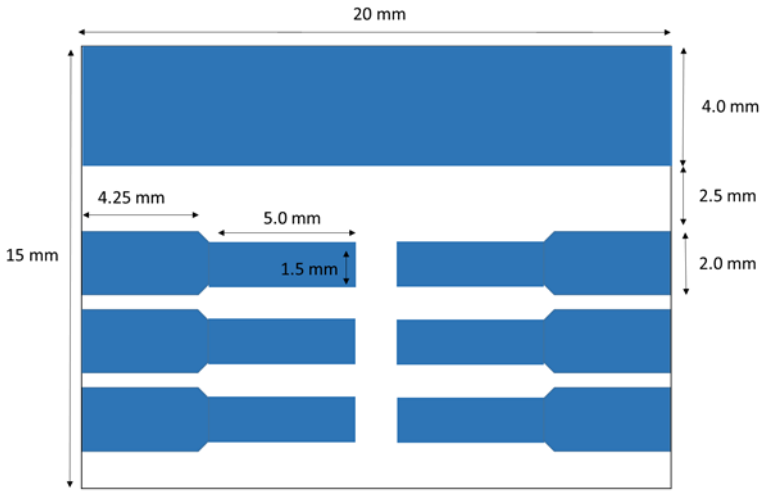

Figure 5.2: Patterned ITO dimensions

The patterned ITO substrates were treated using oxygen plasma at 35 W for 5 minutes. This process is important to remove organic contaminants through the chemical reaction of highly reactive oxygen radicals. Furthermore, this treatment will increase the ITO work function and generate surface hydroxylation which improves the surface wettability.

Immediately after the oxygen plasma treatment, an aqueous dispersion of PEDOT: PSS was spin-coated onto the substrates to form a 40 nm film. Then, the samples were baked in N_2 glove box environment for 10 minutes at 150 °C. X-F6-TAPC and 4-octyloxydiphenyliodonium (OPPI) as photoinitiator is mixed at 12.5% in toluene to be

spin-coated to form 10 nm thin film and then irradiated with UV light (310 nm, 185 mW/cm^2, 3 minutes) before baking at 80 °C for 20 minutes (for multi-layer device only). The EML dissolved in chlorobenzene was spin coated on top of PEDOT: PSS (for single and double layer device only) or X-F6-TAPC (for multilayer device only) and then baked at 80 °C for 20 minutes. Following that, 30 nm SPPO13 dissolved in 2,2,3,3-tetrafluoro-1-propanol (a type of fluorinated alcohol) was spin coated on top of EML and then baked at 80 °C for 20 minutes (for double and multi-layer device only). Next, 1 nm of CsF and 100 nm of Al was vacuum deposited at a base pressure of 2.5×10^{-4} mbar without breaking the vacuum. All the devices were encapsulated using UV curable epoxy and glass lid.

All the fabrication process except the PEDOT: PSS film deposition was carried out in a glovebox with oxygen less than 100 ppm and moisture below 40 ppm. The OLED device consists of six areas defined by overlapping of the cathode and anode. The active area of the device was 4.5 mm^2.

5.4.3 Current-voltage-luminance (I-V-L) measurement

I-V-L measurement is the most basic and important measurement for OLED. The I-V-L measurements were carried out using Konica Minolta CS-200 integrated with a Keithley 236 source-measuring-unit (SMU). The measurement was carried out in a dark enclosure to avoid stray light. Voltage from the SMU was applied across the OLED and simultaneously the current, luminance of the devices was captured by the chroma meter. OLED efficiency is characterized by current efficiency and power efficiency. These efficiencies can be calculated from I-V-L data. Current efficiency (cd/A) is the luminance (L) generated by the device per unit current (I). Current efficiency from luminance in forward direction can be calculated using:

$$\eta_{CE} = {}^{L}/_{I} \tag{5.1}$$

with L and I is the measured brightness and operating current respectively.

While power efficiency or luminous efficiency (lm/W) of the device in forward direction can be calculated using (Reineke et al., 2013):

$$\eta_{CE} = \eta_{CE}.\pi.\int_{D/V} \tag{5.2}$$

where

$$\int_D = \frac{1}{\pi I_0}\int_0^{\pi/2}\int_{-\pi}^{+\pi} I\,(\theta,\phi) sin\theta\; d\phi d\theta \tag{5.3}$$

The f_D factor takes into the consideration of the light intensity distribution in forward hemisphere. I_0 is measured light intensity in forward direction and V is the operating voltage. The I-V-L measurement setup is shown in Figure 5.3.

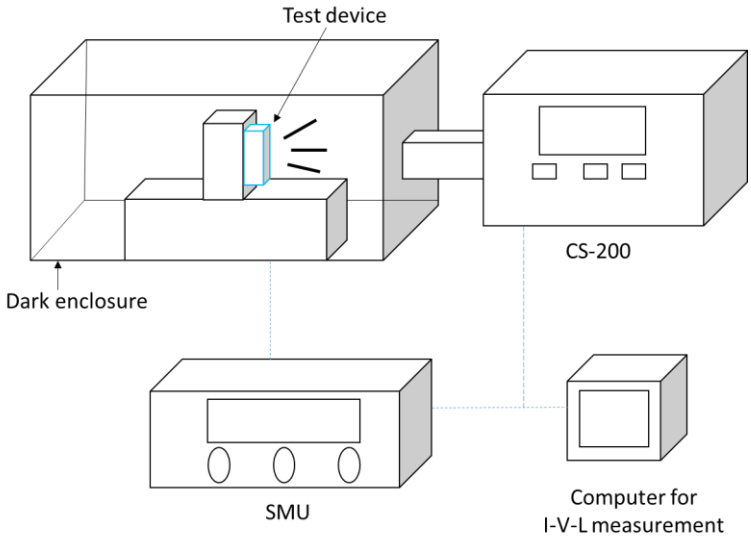

Figure 5.3: I-V-L measurement setup

5.4.4 Surface profiler

Surface thickness of a thin film is usually measured by using surface profilometer. The profilometer will give data of the difference between the high and low point of a surface in nanometers scale. There are two types of profilometers which are contact and non-contact profilometer. Contact profilometer not suitable for very soft and easily damageable surface. Hard and damage surface also can damage the stylus used. Meanwhile, non-contact profilometer uses a beam of light to get surface information. Since there is no contact with the sample surface, this profilometer can be safely used to measure any surface. Basically, profilometers consist of two parts; a detector to collect surface information and a sample stage to hold the sample tested. During the scanning, the stylus is moved across the sample surface at a constantly velocity while maintaining a constant applied stylus force. As the stylus is moved, the contact force between the stylus and the surface is sensed by a displacement capacitance sensor. This information is feedbacked to the computer and the surface profile can be modelled. It is crucial to applied suitable stylus force during scanning. Too low force will result in lost contact with the sample surface and too high force may damage the sample during the scanning process. Generally, the recommended stylus load is in between 1 mg-2 mg. In this work, the film thickness was measured using P-6 profilometer (KLA-Tencor). The stylus load was set at 1 mg with the tip radius of 2 μm. Figure 5.4 shows the simplified schematic diagram of a surface profiler.

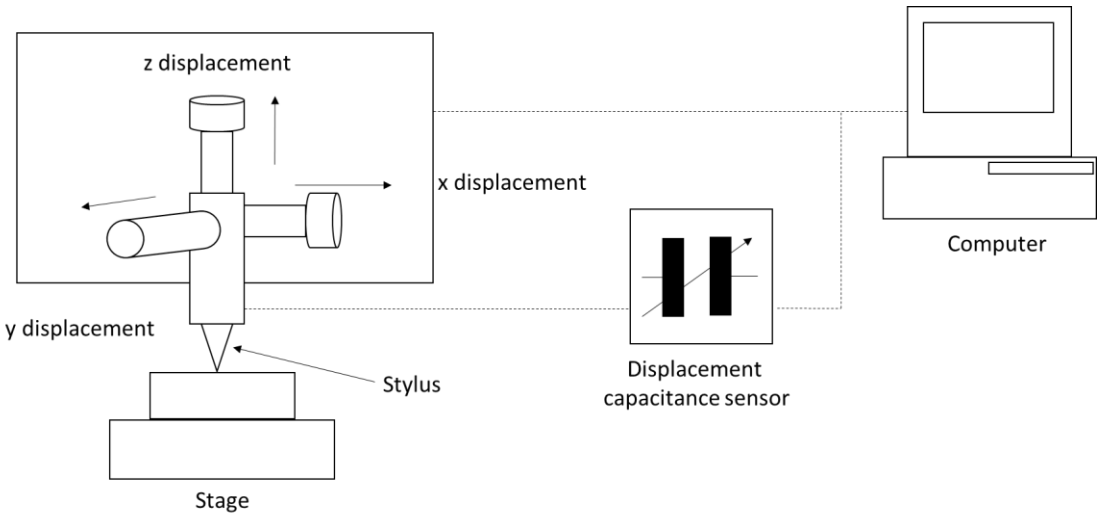

Figure 5.4: Simplified schematic diagram of a surface profiler

CHAPTER 6: SUMMARY AND FUTURE WORKS

6.1 Summary

We have succeeded in the synthesis of four new compounds based on carbazole dendrimers using an Ullmann reaction. The dendrimers **13-16** incorporated *tert*-pentyl groups at the outer layer to ensure their solubility in organic solvents used for device fabrication processes, such as drop casting, spin coating, etc. All carbazole dendrimers show suitable thermal properties with high T_d and T_g values that lead to the formation of a good thin film in solution-processed PhOLEDs. A limited number of known small OLED materials **5-8**, were also synthesized. New small OLED materials, modified from **5-8** have also been synthesized (compound **9-12**). All of these compounds have been fully characterised by common analytical spectroscopic methods.

The bandgap energy, E_g of the dendrimers was determined from UV-Vis spectra to be in the range of 3.37 eV – 3.44 eV. The emission spectra of **13-16** show peaks between 400 nm – 409 nm that indicate that the materials can be use as host materials for blue OLEDs. These dendrimers show triplet energy in the range of 2.65 eV to 2.82 eV that is suitable for use with blue, green and red emitters as the dopants. Compound **16** were found to have the highest triplet energy because of the non-planar core structure that enables it to maintain high triplet energy.

The HOMO level of the dendrimers was determined from evaluation of the oxidation peak of cyclic voltammetry and the LUMO level was obtained from the bandgap value obtained from UV-Vis spectra. The HOMO level for **13**, **14**, **15** and **16** were determined to be -5.23 eV, -5.23 eV, -5.23 eV and -5.24 eV, respectively. All of the dendrimers exhibit a HOMO level quite close to the work function of PEDOT: PSS, indicating that efficient hole injection into the emitting layer could be achieved by using **13-16** as host materials in the emitting layer of OLEDs.

Compound **16** was chosen to be used as host materials for single, double and multilayer PhOLEDs for blue, red and green through solution process method. Single layer devices show low current and power efficiency compared to those of similar double layer devices. An increment in efficiency for double layer device was achieved due to addition of electron transport layer, SPPO13. The presence of the hole transport layer, X-F6-TAPC in multilayer devices further increase the efficiency of all devices.

The morphological nature of the thin film surface was studied using AFM. The AFM results show that the surface roughness of SPPO13 can be improved by using fluorinated alcohol as the deposition solvent to allow better electron injection to the emission layer. We found that IPA-processed SPPO13 on top of **16** has a poor film homogeneity resulting in roughness of 0.591 nm, while we found out that 2,2,3,3-tetrafluoro-1-propanol to be able to form uniform thin film with roughness of 0.195 nm which is a significant improvement.

6.2 Future works

For synthesis of OLED materials, several suggestions can be made as follow:

1. Computational methods could be used to design more interesting molecules. This part is important before the start of synthesis work to avoid time wasting and reduce the cost of synthesis of a new material. Computational method can predict the E_T, HOMO and LUMO of a novel material (Milián-Medina et al., 2012; Nguyen et al., 2010; Yang et al., 2008).
2. Careful and organise comparison needs to be done by using different Ullmann methods or other methods to maximise the yield of product. This study could reduce the cost of the production of a material for OLEDs and PhOLEDs.

3. Increase the molecular weight of the dendrimers in increasing dendron generations to enhance their physical properties. It is important to improve the thermal properties of OLED material to ensure long lifetime of OLED devices.
4. Bipolar host materials based on carbazole dendrimers can be further developed. Bipolar host materials have advantages of high triplet energy and balanced charge transport properties (Byeon et al., 2015; Feng et al., 2015; Lin et al., 2015; Lu et al., 2015). Carbazole unit can be combined with electron transport type materials such as triazine, phosphine oxide and pyridine.
5. Recently, thermally activated delayed-fluorescence materials (TADF) have been reported (Albrecht et al., 2015; Chen et al., 2016; Higuchi et al., 2015; Tao et al., 2014). TADF materials have the advantages in term of their high internal quantum efficiency and inexpensive (rare-metal-free) materials. There still lot to explore in TADF area because the reported external quantum efficiency (EQE) still very low.

REFERENCES

Adachi, C., Kwong, R. C., Djurovich, P., Adamovich, V., Baldo, M. A., Thompson, M. E., & Forrest, S. R. (2001). Endothermic energy transfer: A mechanism for generating very efficient high-energy phosphorescent emission in organic materials. *Applied Physics Letters, 79*(13), 2082-2084.

Adachi, C., Tokito, S., Tsutsui, T., & Saito, S. (1988). Electroluminescence in organic films with three-layer structure. *Japanese Journal of Applied Physics, 27*(2A), L269.

Adimurthy, S., Ramachandraiah, G., Ghosh, P. K., & Bedekar, A. V. (2003). A new, environment friendly protocol for iodination of electron-rich aromatic compounds. *Tetrahedron Letters, 44*(27), 5099-5101.

Agarwal, N., Nayak, P. K., Ali, F., Patankar, M. P., Narasimhan, K. L., & Periasamy, N. (2011). Tuning of HOMO levels of carbazole derivatives: New molecules for blue OLED. *Synthetic Metals, 161*(5–6), 466-473.

Aizawa, N., Pu, Y.-J., Sasabe, H., & Kido, J. (2012). Solution-processable carbazole-based host materials for phosphorescent organic light-emitting devices. *Organic Electronics, 13*(11), 2235-2242.

Alayrac, C., Schollmeyer, D., & Witulski, B. (2009). First total synthesis of antiostatin A1, a potent carbazole-based naturally occurring antioxidant. *Chemical Communications*(12), 1464-1466.

Albrecht, K., Kasai, Y., Kimoto, A., & Yamamoto, K. (2008). The Synthesis and Properties of Carbazole−Phenylazomethine Double Layer-Type Dendrimers. *Macromolecules, 41*(11), 3793-3800.

Albrecht, K., Matsuoka, K., Fujita, K., & Yamamoto, K. (2015). Carbazole Dendrimers as Solution-Processable Thermally Activated Delayed-Fluorescence Materials. *Angewandte Chemie International Edition, 54*(19), 5677-5682.

Albrecht, K., & Yamamoto, K. (2009). Dendritic Structure Having a Potential Gradient: New Synthesis and Properties of Carbazole Dendrimers. *J. Am. Chem. Soc., 131*(6), 2244-2251.

Ameen, S., Lee, S. B., Yoon, S. C., Lee, J., & Lee, C. (2016). Diphenylaminocarbazoles by 1,8-functionalization of carbazole: Materials and application to phosphorescent organic light-emitting diodes. *Dyes and Pigments, 124*, 35-44.

Ananthakrishnan, S. J., Varathan, E., Subramanian, V., Somanathan, N., & Mandal, A. B. (2014). White Light Emitting Polymers from a Luminogen with Local Polarity Induced Enhanced Emission. *The Journal of Physical Chemistry C, 118*(48), 28084-28094.

Baldo, M. A., O'Brien, D. F., You, Y., Shoustikov, A., Sibley, S., Thompson, M. E., & Forrest, S. R. (1998). Highly efficient phosphorescent emission from organic electroluminescent devices. *Nature, 395*(6698), 151-154.

Ban, X., Jiang, W., Zheng, Z., Wang, J., Xia, L., Zhou, J., & Sun, Y. (2015). Tuning the energy gap and charge balance property of bipolar host by molecular modification: Efficient blue electrophosphorescence devices based on solution-process. *Organic Electronics, 24*, 65-72.

Bashir, M., Bano, A., Ijaz, S. A., & Chaudhary, A. B. (2015). Recent Developments and Biological Activities of N-Substituted Carbazole Derivatives: A Review. *Molecules, 20*(8)

Bi, Y.-G., Feng, J., Li, Y.-F., Zhang, Y.-L., Liu, Y.-S., Chen, L., . . . Sun, H.-B. (2014). Arbitrary Shape Designable Microscale Organic Light-Emitting Devices by Using Femtosecond Laser Reduced Graphene Oxide as a Patterned Electrode. *ACS Photonics, 1*(8), 690-695.

Birks, J. B. (1970). *Photophysics of aromatic molecules*. London: Wiley.

Borsche, W. (1908). Ueber Tetra- und Hexahydrocarbazolverbindungen und eine neue Carbazolsynthese. (Mitbearbeitet von. A. Witte und W. Bothe.). *Justus Liebigs Annalen der Chemie, 359*(1-2), 49-80.

Bouaziz, Z., Issa, S., Gentili, J., Gratz, A., Bollacke, A., Kassack, M., . . . Le Borgne, M. (2015). Biologically active carbazole derivatives: focus on oxazinocarbazoles and related compounds. *Journal of Enzyme Inhibition and Medicinal Chemistry, 30*(2), 180-188.

Burroughes, J. H., Bradley, D. D. C., Brown, A. R., Marks, R. N., Mackay, K., Friend, R. H., . . . Holmes, A. B. (1990). Light-emitting diodes based on conjugated polymers. *Nature, 347*(6293), 539-541.

Byeon, S. Y., Hwang, S. H., Kim, O. Y., & Lee, J. Y. (2015). 22.4: Synthesis of Host Materials for Blue Phosphorescent Organic Light Emitting Diodes (OLEDs) with High Efficiency and Low Driving Voltage. *SID Symposium Digest of Technical Papers, 46*(1), 323-325.

Calvin Yi Bin, N., Keat Hoe, Y., Thomas, J. W., Noor Azrina, T., Kai Lin, W., Thanit, S., . . . Prayoon, S. (2014). High efficiency solution processed fluorescent yellow organic light-emitting diode through fluorinated alcohol treatment at the emissive layer/cathode interface. *Journal of Physics D: Applied Physics, 47*(1), 015106.

Chen, D., Liu, K., Gan, L., Liu, M., Gao, K., Xie, G., . . . Su, S.-J. (2016). Modulation of Exciton Generation in Organic Active Planar pn Heterojunction: Toward Low Driving Voltage and High-Efficiency OLEDs Employing Conventional and Thermally Activated Delayed Fluorescent Emitters. *Advanced Materials, 28*(31), 6758-6765.

Chen, J., Shi, C., Fu, Q., Zhao, F., Hu, Y., Feng, Y., & Ma, D. (2012a). Solution-processable small molecules as efficient universal bipolar host for blue, green and red phosphorescent inverted OLEDs. *Journal of Materials Chemistry, 22*(11), 5164-5170.

Chen, L., Ma, Z., Ding, J., Wang, L., Jing, X., & Wang, F. (2012b). Effect of dendron generation on properties of self-host heteroleptic green light-emitting iridium dendrimers. *Organic Electronics, 13*(10), 2160-2166.

Chen, Y., Liang, W., Choi, W. H., Huang, J., Dong, Q., Zhu, F., & Su, J. (2015). High thermal-stability benzocarbazole derivatives as bipolar host materials for phosphorescent organic light-emitting diodes. *Dyes and Pigments, 123*, 196-203.

Cheng, G., Chan, K. T., To, W.-P., & Che, C.-M. (2014). Color tunable organic light-emitting devices with external quantum efficiency over 20% based on strongly luminescent gold(III) complexes having long-lived emissive excited states. *Advanced Materials (Deerfield Beach, Fla.), 26*(16), 2540-2546.

Cho, J.-S., Kimoto, A., Higuchi, M., & Yamamoto, K. (2005). Synthesis of Diphenylamine-Substituted Phenylazomethine Dendrimers and the Performance of Organic Light-Emitting Diodes. *Macromolecular Chemistry and Physics, 206*(6), 635-641.

Cho, S. H., Yoon, J., & Chang, S. (2011). Intramolecular Oxidative C−N Bond Formation for the Synthesis of Carbazoles: Comparison of Reactivity between the Copper-Catalyzed and Metal-Free Conditions. *Journal of the American Chemical Society, 133*(15), 5996-6005.

Choi, J. W., Kulshreshtha, C., Kennedy, G. P., Kwon, J. H., Jung, S.-H., & Chae, M. (2011). Solution-processed bulk heterojunction organic solar cells with high polarity small molecule sensitizer. *Solar Energy Materials and Solar Cells, 95*(8), 2069-2076.

Davey, W., & Latter, R. W. (1948). 63. The preparation of symmetrical dinitrodiphenyls by the Ullmann reaction. *Journal of the Chemical Society (Resumed)*(0), 264-265.

Drechsel, E. (1888). Ueber Elektrolyse des Phenols mit Wechselströmen. *Journal für Praktische Chemie, 38*(1), 65-74.

Drolet, N., Morin, J. F., Leclerc, N., Wakim, S., Tao, Y., & Leclerc, M. (2005). 2,7-Carbazolenevinylene-Based Oligomer Thin-Film Transistors: High Mobility Through Structural Ordering. *Advanced Functional Materials, 15*(10), 1671-1682.

Duan, L., Hou, L., Lee, T.-W., Qiao, J., Zhang, D., Dong, G., . . . Qiu, Y. (2010). Solution processable small molecules for organic light-emitting diodes. *Journal of Materials Chemistry, 20*(31), 6392-6407.

Duan, L., Qiao, J., Sun, Y., & Qiu, Y. (2011). Strategies to Design Bipolar Small Molecules for OLEDs: Donor-Acceptor Structure and Non-Donor-Acceptor Structure. *Advanced Materials, 23*(9), 1137-1144.

Dumur, F. (2015). Carbazole-based polymers as hosts for solution-processed organic light-emitting diodes: Simplicity, efficacy. *Organic Electronics, 25*, 345-361.

El-Khouly, M. E., Lee, S.-H., Kay, K.-Y., & Fukuzumi, S. (2013). Synthesis and fast electron-transfer reactions of fullerene-carbazole dendrimers with short linkages. *New Journal of Chemistry, 37*(10), 3252-3260.

Fan, Y., Chen, J., & Ma, D. (2013). Enhancement of light extraction of green top-emitting organic light-emitting diodes with refractive index gradually changed coupling layers. *Organic Electronics, 14*(12), 3234-3239.

Feng, Y., Li, P., Zhuang, X., Ye, K., Peng, T., Liu, Y., & Wang, Y. (2015). A novel bipolar phosphorescent host for highly efficient deep-red OLEDs at a wide luminance range of 1000-10 000 cd m-2. *Chemical Communications, 51*(63), 12544-12547.

Forrest, S. R. (2004). The path to ubiquitous and low-cost organic electronic appliances on plastic. *Nature, 428*(6986), 911-918.

Fyfe, D. (2009). LED Technology: Organic displays come of age. *Nat Photon, 3*(8), 453-455.

Ghosh, A. P., Gerenser, L. J., Jarman, C. M., & Fornalik, J. E. (2005). Thin-film encapsulation of organic light-emitting devices. *Applied Physics Letters, 86*(22), 223503.

Głuszyńska, A. (2015). Biological potential of carbazole derivatives. *European Journal of Medicinal Chemistry, 94*, 405-426.

Goldberg, I. (1906). Ueber Phenylirungen bei Gegenwart von Kupfer als Katalysator. *Berichte der deutschen chemischen Gesellschaft, 39*(2), 1691-1692.

Gorter, H., Coenen, M. J. J., Slaats, M. W. L., Ren, M., Lu, W., Kuijpers, C. J., & Groen, W. A. (2013). Toward inkjet printing of small molecule organic light emitting diodes. *Thin Solid Films, 532*, 11-15.

Graebe, C., & Ullmann, F. (1896). Ueber eine neue Carbazolsynthese. *Justus Liebigs Annalen der Chemie, 291*(1-2), 16-17.

Graebe, C. G. (1872). *Ber. Dtsch. Chem. Ges., 5*(12)

Grigalevicius, S., Simokaitiene, J., Grazulevicius, J. V., Ma, L., & Xie, Z. (2008). Hole-transporting polymers containing carbazol-3,9-diyl and 1,4-phenylene fragments in the main chain. *Synthetic Metals, 158*(19–20), 739-743.

Gu, W., Qiao, C., Wang, S.-F., Hao, Y., & Miao, T.-T. (2014). Synthesis and biological evaluation of novel N-substituted 1H-dibenzo[a,c]carbazole derivatives of dehydroabietic acid as potential antimicrobial agents. *Bioorganic & Medicinal Chemistry Letters, 24*(1), 328-331.

Gustafsson, G., Cao, Y., Treacy, G. M., Klavetter, F., Colaneri, N., & Heeger, A. J. (1992). Flexible light-emitting diodes made from soluble conducting polymers. *Nature, 357*(6378), 477-479.

Han, E.-M., Do, L.-M., Yamamoto, N., & Fujihira, M. (1996). International Symposium on Ultra Materials for PicotransferCrystallization of organic thin films for electroluminescent devices. *Thin Solid Films, 273*(1), 202-208.

Hassan, J., Sévignon, M., Gozzi, C., Schulz, E., & Lemaire, M. (2002). Aryl−Aryl Bond Formation One Century after the Discovery of the Ullmann Reaction. *Chemical Reviews, 102*(5), 1359-1470.

Hauser, F. M., & Rhee, R. P. (1978). New synthetic methods for the regioselective annelation of aromatic rings: 1-hydroxy-2,3-disubstituted naphthalenes and 1,4-dihydroxy-2,3-disubstituted naphthalenes. *The Journal of Organic Chemistry, 43*(1), 178-180.

Helfrich, W., & Schneider, W. G. (1965). Recombination Radiation in Anthracene Crystals. *Physical Review Letters, 14*(7), 229-231.

Hieda, Y., Anraku, M., Choshi, T., Tomida, H., Fujioka, H., Hatae, N., . . . Hibino, S. (2014). Antioxidant effects of the highly-substituted carbazole alkaloids and their related carbazoles. *Bioorganic & Medicinal Chemistry Letters, 24*(15), 3530-3533.

Higuchi, T., Nakanotani, H., & Adachi, C. (2015). High-Efficiency White Organic Light-Emitting Diodes Based on a Blue Thermally Activated Delayed Fluorescent Emitter Combined with Green and Red Fluorescent Emitters. *Advanced Materials, 27*(12), 2019-2023.

Holmes, R. J., Forrest, S. R., Tung, Y.-J., Kwong, R. C., Brown, J. J., Garon, S., & Thompson, M. E. (2003). Blue organic electrophosphorescence using exothermic host–guest energy transfer. *Applied Physics Letters, 82*(15), 2422-2424.

Hwang, S.-H., Moorefield, C. N., & Newkome, G. R. (2008). Dendritic macromolecules for organic light-emitting diodes. *Chemical Society Reviews, 37*(11), 2543-2557.

. Introduction to Fluorescence. (2006). In J. R. Lakowicz (Ed.), *Principles of Fluorescence Spectroscopy* (pp. 1-26). Boston, MA: Springer US.

Ito, C., Itoigawa, M., Nakao, K., Murata, T., Kaneda, N., & Furukawa, H. (2012). Apoptosis of HL-60 leukemia cells induced by carbazole alkaloids isolated from Murraya euchrestifolia. *Journal of Natural Medicines, 66*(2), 357-361.

Jeon, S. O., & Lee, J. Y. (2012). Comparison of symmetric and asymmetric bipolar type high triplet energy host materials for deep blue phosphorescent organic light-emitting diodes. *Journal of Materials Chemistry, 22*(15), 7239-7244.

Jiang, W., Duan, L., Qiao, J., Dong, G., Zhang, D., Wang, L., & Qiu, Y. (2011). High-triplet-energy tri-carbazole derivatives as host materials for efficient solution-processed blue phosphorescent devices. *J. Mater. Chem., 21*(13), 4918-4926.

Jiang, W., Duan, L., Qiao, J., Zhang, D., Dong, G., Wang, L., & Qiu, Y. (2010). Novel star-shaped host materials for highly efficient solution-processed phosphorescent organic light-emitting diodes. *Journal of Materials Chemistry, 20*(29), 6131-6137.

Jiang, W., Ge, Z., Cai, P., Huang, B., Dai, Y., Sun, Y., . . . Qiu, Y. (2012a). Star-shaped dendritic hosts based on carbazole moieties for highly efficient blue phosphorescent OLEDs. *Journal of Materials Chemistry, 22*(24), 12016-12022.

Jiang, W., Tang, J., Yang, W., Ban, X., Huang, B., Dai, Y., . . . Qiu, Y. (2012b). Synthesis of carbazole-based dendrimer: host material for highly efficient solution-processed blue organic electrophosphorescent diodes. *Tetrahedron, 68*(29), 5800-5805.

Jung, S.-H., Kim, J.-J., & Kim, H.-J. (2012). High performance inkjet printed phosphorescent organic light emitting diodes based on small molecules commonly used in vacuum processes. *Thin Solid Films, 520*(23), 6954-6958.

Kamaladin, G., & Mozhgan, H. (2015). Effect of substituents moiety in organic sensitiser based on carbazole on the performance of nanostructure dye-sensitised solar cells. *Pigment & Resin Technology, 44*(5), 292-299.

Kang, H.-S., Park, K.-N., Cho, Y.-R., Park, D.-W., & Choe, Y. (2009). Enhanced performance of organic electroluminescence diodes with a 2-TNATA:C60 hole injection layer. *Journal of Industrial and Engineering Chemistry, 15*(5), 752-757.

Kim, B. S., Jang, W. B., Jung, H. G., & Jang, J. (2014). Solution Processed PLED on Transparent Plastic Substrate for Flexible Display. *Molecular Crystals and Liquid Crystals, 601*(1), 237-244.

Kim, D.-H., Choi, D. H., Park, J. J., Lee, S. T., & Kwon, J. H. (2008). Novel Green Small-molecule Host Materials for Solution-processed Organic Light-emitting Diodes. *Chemistry Letters, 37*(11), 1150-1151.

Kim, E., Han, Y., Kim, W., Choi, K. C., Im, H.-G., & Bae, B.-S. (2013). Thin film encapsulation for organic light emitting diodes using a multi-barrier composed of MgO prepared by atomic layer deposition and hybrid materials. *Organic Electronics, 14*(7), 1737-1743.

Kim, H., Byun, Y., Das, R. R., Choi, B.-K., & Ahn, P.-S. (2007). Small molecule based and solution processed highly efficient red electrophosphorescent organic light emitting devices. *Applied Physics Letters, 91*(9), 093512.

Kim, S., Kwon, H.-J., Lee, S., Shim, H., Chun, Y., Choi, W., . . . Lee, S. Y. (2011). Low-Power Flexible Organic Light-Emitting Diode Display Device. *Advanced Materials, 23*(31), 3511-3516.

Kimoto, A., Cho, J.-S., Higuchi, M., & Yamamoto, K. (2004). Synthesis of Asymmetrically Arranged Dendrimers with a Carbazole Dendron and a Phenylazomethine Dendron. *Macromolecules, 37*(15), 5531-5537.

Koene, B. E., Loy, D. E., & Thompson, M. E. (1998). Asymmetric Triaryldiamines as Thermally Stable Hole Transporting Layers for Organic Light-Emitting Devices. *Chemistry of Materials, 10*(8), 2235-2250.

Kulkarni, A. P., Tonzola, C. J., Babel, A., & Jenekhe, S. A. (2004). Electron Transport Materials for Organic Light-Emitting Diodes. *Chemistry of Materials, 16*(23), 4556-4573.

Lee, C. W., & Lee, J. Y. (2014a). A hole transport material with ortho- linked terphenyl core structure for high power efficiency in blue phosphorescent organic light-emitting diodes. *Organic Electronics, 15*(2), 399-404.

Lee, J., Koh, T.-W., Cho, H., Schwab, T., Lee, J.-H., Hofmann, S., . . . Gather, M. C. (2015). Transparent organic light-emitting diodes with different bi-directional emission colors using color-conversion capping layers. *Journal of Luminescence, 162*, 180-184.

Lee, N.-J., Lee, D.-H., Kim, D.-W., Lee, J.-H., Cho, S. H., Jeon, W. S., . . . Suh, M. C. (2012). Highly efficient soluble materials for blue phosphorescent organic light–emitting diode. *Dyes and Pigments, 95*(2), 221-228.

Lee, Y.-T., Chang, Y.-T., Lee, M.-T., Chiang, P.-H., Chen, C.-T., & Chen, C.-T. (2014b). Solution-processed bipolar small molecular host materials for single-layer blue phosphorescent organic light-emitting diodes. *Journal of Materials Chemistry C, 2*(2), 382-391.

Lengvinaite, S., Grazulevicius, J. V., Grigalevicius, S., Lai, Y. M., Wang, W. B., & Jou, J. H. (2010). Polyethers containing 2-phenylindol-1-yl moieties as host materials for light emitting diodes. *Synthetic Metals, 160*(15–16), 1793-1796.

Levermore, P. A., Dyatkin, A. B., Elshenawy, Z., Pang, H., Silvernail, J., Krall, E., . . . Forrest, S. R. (2012). Phosphorescent organic light-emitting diodes for high-efficacy long-lifetime solid-state lighting. *Journal of Photonics for Energy, 2*(1), 021205-021201-021205-021208.

Ley, S. V., & Thomas, A. W. (2003). Modern Synthetic Methods for Copper-Mediated C(aryl)□O, C(aryl)□N, and C(aryl)□S Bond Formation. *Angewandte Chemie International Edition, 42*(44), 5400-5449.

Li, J., & Liu, D. (2009). Dendrimers for organic light-emitting diodes. *Journal of Materials Chemistry, 19*(41), 7584-7591.

Li, J., Zhang, T., Liang, Y., & Yang, R. (2013). Solution-Processible Carbazole Dendrimers as Host Materials for Highly Efficient Phosphorescent Organic Light-Emitting Diodes. *Adv. Funct. Mater., 23*(5), 619-628.

Liaptsis, G., & Meerholz, K. (2013). Crosslinkable TAPC-Based Hole-Transport Materials for Solution-Processed Organic Light-Emitting Diodes with Reduced Efficiency Roll-Off. *Advanced Functional Materials, 23*(3), 359-365.

Lifka, H., Verschuren, C. A., Bruls, D. M., & Tanase, C. (2011). P-169: Single Side Emitting Transparent OLED Lamp. *SID Symposium Digest of Technical Papers, 42*(1), 1737-1739.

Lin, W.-C., Lin, H.-W., Mondal, E., & Wong, K.-T. (2015). Efficient solution-processed green and white phosphorescence organic light-emitting diodes based on bipolar host materials. *Organic Electronics, 17*, 1-8.

Liu, S., Wu, R., Huang, J., & Yu, J. (2013a). Color-tunable and high-efficiency organic light-emitting diode by adjusting exciton bilateral migration zone. *Applied Physics Letters, 103*(13), 133307-133307-133305.

Liu, Z., Wang, G., Xie, H., Wu, Z., Li, Y., Jiang, C., . . . Wang, H. (2013b). 46.1: Invited Paper: Ink-jet Printed 17-inch AMOLED Display with Amorphous IGZO TFTs Backplane. *SID Symposium Digest of Technical Papers, 44*(1), 634-636.

Lo, S.-C., & Burn, P. L. (2007). Development of Dendrimers: Macromolecules for Use in Organic Light-Emitting Diodes and Solar Cells. *Chemical Reviews, 107*(4), 1097-1116.

Long, M., Koppe, B. E., Redden, N. P., Boroson, M. L., Hatwar, T. K., & Hamer, J. W. (2011). Enabling High-Throughput, Low-Cost Manufacturing of OLED Display and Lighting Panels. *MRS Proceedings, 1212*

Lu, T., You, J., Zhao, D., Wang, H., Miao, Y., Liu, X., . . . Wang, S. (2015). Synthesis of novel s-triazine/carbazole based bipolar molecules and their application in phosphorescent OLEDs. *Journal of Materials Science: Materials in Electronics, 26*(9), 6563-6571.

Maneerat, W., Phakhodee, W., Cheenpracha, S., Ritthiwigrom, T., Deachathai, S., & Laphookhieo, S. (2013). Clausenawallines G–K, carbazole alkaloids from Clausena wallichii twigs. *Phytochemistry, 88*, 74-78.

Maria Stefania, S., Rosamaria, L., Anna, C., Maria Francesca, S., Assunta, P., Camillo, R., . . . Marcello, M. (2015). (6-Bromo-1,4-dimethyl-9H-carbazol-3-yl-methylene)-hydrazine (Carbhydraz) Acts as a GPER Agonist in Breast Cancer Cells. *Current Topics in Medicinal Chemistry, 15*(11), 1035-1042.

Masuyama, S., Seki, T., Toriyama, S., & Nishimura, S. (2015). P-127: Highly Efficient Light Extraction Technologies Applicable for Transparent OLED Lighting using a Corrugated Substrate. *SID Symposium Digest of Technical Papers, 46*(1), 1643-1646.

McClenaghan, N. D., Passalacqua, R., Loiseau, F., Campagna, S., Verheyde, B., Hameurlaine, A., & Dehaen, W. (2003). Ruthenium(II) Dendrimers Containing Carbazole-Based Chromophores as Branches. *Journal of the American Chemical Society, 125*(18), 5356-5365.

Michinobu, T., Osako, H., & Shigehara, K. (2009). Synthesis and Properties of Conjugated Poly(1,8-carbazole)s. *Macromolecules, 42*(21), 8172-8180.

Milián-Medina, B., & Gierschner, J. (2012). Computational design of low singlet–triplet gap all-organic molecules for OLED application. *Organic Electronics, 13*(6), 985-991.

Mingxiao, Z., Zhijian, C., Lixin, X., Bo, Q., & Qihuang, G. (2013). High-Color-Quality Blue Top-Emitting Organic Light-Emitting Diodes with Enhanced Contrast Ratio. *Japanese Journal of Applied Physics, 52*(5S1), 05DC17.

Moonsin, P., Prachumrak, N., Namuangruk, S., Jungsuttiwong, S., Keawin, T., Sudyoadsuk, T., & Promarak, V. (2013). Novel bis(fluorenyl)benzothiadiazole-cored carbazole dendrimers as highly efficient solution-processed non-doped green emitters for organic light-emitting diodes. *Chemical Communications, 49*(57), 6388-6390.

Morgan, N. T., Zhang, Y., Molitor, E. J., Bell, B. M., Holmes, R. J., & Cussler, E. L. (2014). Understanding rate-limiting processes for the sublimation of small molecule organic semiconductors. *AIChE Journal, 60*(4), 1347-1354.

Mostafa, M., Afshin, S., Sohrab Ahmadi, K., & Mohammad Sadegh, Z. (2013). The effects of polymer molecular weight on the performance of single-layer polymer light emitting diodes. *Physica Scripta, 2013*(T157), 014028.

Nakajima, Y., Nakata, M., Takei, T., Fukagawa, H., Motomura, G., Tsuji, H., . . . Yamamoto, T. (2014). Development of 8-in. oxide-TFT-driven flexible AMOLED display using high-performance red phosphorescent OLED. *Journal of the Society for Information Display, 22*(3), 137-143.

Nakata, M., Sato, H., Nakajima, Y., Fujisaki, Y., Takei, T., Shimizu, T., . . . Fujikake, H. (2011). 16.4: Low-Temperature Fabrication of Flexible AMOLED Displays Using Oxide TFTs with Polymer Gate Insulators. *SID Symposium Digest of Technical Papers, 42*(1), 202-205.

Nardes, A. M., Kemerink, M., de Kok, M. M., Vinken, E., Maturova, K., & Janssen, R. A. J. (2008). Conductivity, work function, and environmental stability of PEDOT:PSS thin films treated with sorbitol. *Organic Electronics, 9*(5), 727-734.

Neugebauer, F. A., & Fischer, H. (1972). tert.-Butyl-substituierte Carbazole. *Chemische Berichte, 105*(8), 2686-2693.

Nguyen, H. T., & Truong, T. N. (2010). A virtual screening approach for electronic properties of conjugated organic materials using semi-empirical molecular orbital theory. *Chemical Physics Letters, 499*(4–6), 263-267.

Noda, M., Kobayashi, N., Katsuhara, M., Yumoto, A., Ushikura, S., Yasuda, R., . . . Urabe, T. (2011). An OTFT-driven rollable OLED display. *Journal of the Society for Information Display, 19*(4), 316-322.

Ochung', A. A., Manguro, L. A. O., Owuor, P. O., Jondiko, I. O., Nyunja, R. A., Akala, H., . . . Opiyo, S. A. (2015). Bioactive carbazole alkaloids from Alysicarpus ovalifolius (Schumach). *Journal of the Korean Society for Applied Biological Chemistry, 58*(6), 839-846.

Oda, N., Kajii, H., & Ohmori, Y. (2013). Characteristics of Solution-Processed Phosphorescent Organic Light-Emitting Diodes Utilizing Low Molecular Carbazole Derivative as a Host Material. *Molecular Crystals and Liquid Crystals, 581*(1), 70-75.

Park, I.-K., Suh, S.-E., Lim, B.-Y., & Cho, C.-G. (2009). Aryl Hydrazide beyond as Surrogate of Aryl Hydrazine in the Fischer Indolization: The Synthesis of N-Cbz-indoles, N-Cbz-carbazoles, and N,N′-Bis-Cbz-pyrrolo[2,3-f]indoles. *Organic Letters, 11*(23), 5454-5456.

Park, J., Noh, Y.-Y., Huh, J. W., Lee, J., & Chu, H. (2012a). Optical and barrier properties of thin-film encapsulations for transparent OLEDs. *Organic Electronics, 13*(10), 1956-1961.

Park, J. W., & Lee, J. H. (2014). Heat dissipation property of cover glasses with heat sink films for transparent organic light-emitting diodes. *Semiconductor Science and Technology, 29*(9), 095023.

Park, M. S., Choi, D. H., Lee, B. S., & Lee, J. Y. (2012b). Fused indole derivatives as high triplet energy hole transport materials for deep blue phosphorescent organic light-emitting diodes. *Journal of Materials Chemistry, 22*(7), 3099-3104.

Park, S. K., Ryu, M., Yang, S., Byun, C., Hwang, C., Cho, K. I., . . . Kim, K.-B. (2010). 18.1: Invited Paper: Oxide TFT Driving Transparent AMOLED. *SID Symposium Digest of Technical Papers, 41*(1), 245-248.

Promarak, V., Ichikawa, M., Sudyoadsuk, T., Saengsuwan, S., Jungsuttiwong, S., & Keawin, T. (2007). Synthesis of electrochemically and thermally stable amorphous hole-transporting carbazole dendronized fluorene. *Synthetic Metals, 157*(1), 17-22.

Ramesh, N., Rajeshwaran, G. G., & Mohanakrishnan, A. K. (2009). Synthesis of di-, tri-, and tetra-substituted carbazole analogs involving annulation methodology. *Tetrahedron, 65*(18), 3592-3602.

Reineke, S., Lindner, F., Schwartz, G., Seidler, N., Walzer, K., Lussem, B., & Leo, K. (2009). White organic light-emitting diodes with fluorescent tube efficiency. *Nature, 459*(7244), 234-238.

Reineke, S., Thomschke, M., Lüssem, B., & Leo, K. (2013). White organic light-emitting diodes: Status and perspective. *Reviews of Modern Physics, 85*(3), 1245-1293.

Romero, D. B., Schaer, M., Leclerc, M., Adès, D., Siove, A., & Zuppiroli, L. (1996). The role of carbazole in organic light-emitting devices. *Synthetic Metals, 80*(3), 271-277.

Roy, J., Jana, A. K., & Mal, D. (2012). Recent trends in the synthesis of carbazoles: an update. *Tetrahedron, 68*(31), 6099-6121.

Sasabe, H., & Kido, J. (2013). Development of high performance OLEDs for general lighting. *Journal of Materials Chemistry C, 1*(9), 1699-1707.

Sathiyan, G., Sivakumar, E. K. T., Ganesamoorthy, R., Thangamuthu, R., & Sakthivel, P. (2016). Review of carbazole based conjugated molecules for highly efficient organic solar cell application. *Tetrahedron Letters, 57*(3), 243-252.

Scholz, S., Kondakov, D., Lüssem, B., & Leo, K. (2015). Degradation Mechanisms and Reactions in Organic Light-Emitting Devices. *Chemical Reviews, 115*(16), 8449-8503.

Schroegel, P., Tomkeviciene, A., Strohriegl, P., Hoffmann, S. T., Koehler, A., & Lennartz, C. (2011). A series of CBP-derivatives as host materials for blue phosphorescent organic light-emitting diodes. *J. Mater. Chem., 21*(7), 2266-2273.

Schrogel, P., Tomkeviciene, A., Strohriegl, P., Hoffmann, S. T., Kohler, A., & Lennartz, C. (2011). A series of CBP-derivatives as host materials for blue phosphorescent organic light-emitting diodes. *Journal of Materials Chemistry, 21*(7), 2266-2273.

Seo, J. H., Seo, B. M., Koo, J. R., Lee, K. H., You, J. N., Yoon, S. S., & Kim, Y. K. (2011). Blue organic light-emitting diodes with efficient host-dopant energy level alignment. *Current Applied Physics, 11*(3, Supplement), S356-S358.

Service, R. F. (2005). Organic LEDs Look Forward to a Bright, White Future. *Science, 310*(5755), 1762-1763.

Shimizu, M., Mochida, K., Asai, Y., Yamatani, A., Kaki, R., Hiyama, T., . . . Furutani, H. (2012). Efficient blue electroluminescence of silylene-bridged 2-(2-naphthyl)indole. *Journal of Materials Chemistry, 22*(10), 4337-4342.

Shin, H.-J., Takasugi, S., Park, K.-M., Choi, S.-H., Jeong, Y.-S., Song, B.-C., . . . Ahn, B.-C. (2015). 7.1: Invited Paper: Novel OLED Display Technologies for Large-Size UHD OLED TVs. *SID Symposium Digest of Technical Papers, 46*(1), 53-56.

Shirota, Y. (2000). Organic materials for electronic and optoelectronic devices. *Journal of Materials Chemistry, 10*(1), 1-25.

So, F., Krummacher, B., Mathai, M. K., Poplavskyy, D., Choulis, S. A., & Choong, V.-E. (2007). Recent progress in solution processable organic light emitting devices. *Journal of Applied Physics, 102*(9), 091101.

Sudyoadsuk, T., Moonsin, P., Prachumrak, N., Namuangruk, S., Jungsuttiwong, S., Keawin, T., & Promarak, V. (2014). Carbazole dendrimers containing oligoarylfluorene cores as solution-processed hole-transporting non-doped emitters for efficient pure red, green, blue and white organic light-emitting diodes. *Polymer Chemistry, 5*(13), 3982-3993.

Sun, Y., Giebink, N. C., Kanno, H., Ma, B., Thompson, M. E., & Forrest, S. R. (2006). Management of singlet and triplet excitons for efficient white organic light-emitting devices. *Nature, 440*(7086), 908-912.

Takayuki, U., Masaaki, S., Tatsuya, M., & Yujiro, N. (2013). Glare-Tunable Transparent Electrochemical Smart Window Coupled with Transparent Organic Light-Emitting Diode. *Applied Physics Express, 6*(4), 041604.

Tang, C. W., & VanSlyke, S. A. (1987). Organic electroluminescent diodes. *Applied Physics Letters, 51*(12), 913-915.

Tao, Y., Yang, C., & Qin, J. (2011). Organic host materials for phosphorescent organic light-emitting diodes. *Chemical Society Reviews, 40*(5), 2943-2970.

Tao, Y., Yuan, K., Chen, T., Xu, P., Li, H., Chen, R., . . . Huang, W. (2014). Thermally activated delayed fluorescence materials towards the breakthrough of organoelectronics. *Advanced Materials (Deerfield Beach, Fla.), 26*(47), 7931-7958.

Thaengthong, A. M., Saengsuwan, S., Jungsuttiwong, S., Keawin, T., Sudyoadsuk, T., & Promarak, V. (2011). Synthesis and characterization of high Tg carbazole-based amorphous hole-transporting materials for organic light-emitting devices. *Tetrahedron Letters, 52*(37), 4749-4752.

Thejo Kalyani, N., & Dhoble, S. J. (2012). Organic light emitting diodes: Energy saving lighting technology—A review. *Renewable and Sustainable Energy Reviews, 16*(5), 2696-2723.

Tian, Y., Peng, J., Xu, X., & Li, L. (2015). Solution-processed organic light-emitting diodes with enhanced efficiency by using a non-conjugated polymer doped small-molecule hole-blocking layer. *RSC Advances, 5*(119), 98075-98079.

Tokito, S. (2004). Recent Progress in Phosphorescent Materials for Organic Light-Emitting Devices. *Journal of Photopolymer Science and Technology, 17*(2), 307-313.

Tokito, S., Iijima, T., Suzuri, Y., Kita, H., Tsuzuki, T., & Sato, F. (2003). Confinement of triplet energy on phosphorescent molecules for highly-efficient organic blue-light-emitting devices. *Applied Physics Letters, 83*(3), 569.

Trattnig, R., Figueira-Duarte, T. M., Lorbach, D., Wiedemair, W., Sax, S., Winkler, S., . . . Müllen, K. (2011). Deep blue polymer light emitting diodes based on easy to synthesize, non-aggregating polypyrene. *Optics Express, 19*(S6), A1281-A1293.

Tsai, M. H., Lin, H. W., Su, H. C., Ke, T. H., Wu, C. c., Fang, F. C., . . . Wu, C. I. (2006). Highly Efficient Organic Blue Electrophosphorescent Devices Based on 3,6-Bis(triphenylsilyl)carbazole as the Host Material. *Advanced Materials, 18*(9), 1216-1220.

Tsai, Y.-S., Chittawanij, A., Hong, L.-A., Ou, C.-Y., Juang, F.-S., Wang, C.-C., & Lai, S.-H. (2015). Adjusting dopant concentrations in solution process to optimize the white phosphorescent organic light-emitting diodes. *Microelectronic Engineering, 138*, 31-35.

Ueno, S., Yomogida, M., Suzuki, M., Konishi, Y., & Azuma, K. (2013). Highly Reliable Encapsulation Films for OLEDs Composed of SiNx and SiOxCy Prepared Using SWP-CVD. *ECS Transactions, 50*(41), 57-64.

Ullmann, F. (1903). Ueber eine neue Bildungsweise von Diphenylaminderivaten. *Berichte der deutschen chemischen Gesellschaft, 36*(2), 2382-2384.

Ullmann, F., & Bielecki, J. (1901). Ueber Synthesen in der Biphenylreihe. *Berichte der deutschen chemischen Gesellschaft, 34*(2), 2174-2185.

Usluer, O., Demic, S., Egbe, D. A. M., Birckner, E., Tozlu, C., Pivrikas, A., . . . Sariciftci, N. S. (2010). Fluorene-Carbazole Dendrimers: Synthesis, Thermal, Photophysical and Electroluminescent Device Properties. *Advanced Functional Materials, 20*(23), 4152-4161.

van Dijken, A., Bastiaansen, J. J. A. M., Kiggen, N. M. M., Langeveld, B. M. W., Rothe, C., Monkman, A., . . . Brunner, K. (2004). Carbazole Compounds as Host Materials for Triplet Emitters in Organic Light-Emitting Diodes: Polymer Hosts for High-Efficiency Light-Emitting Diodes. *Journal of the American Chemical Society, 126*(24), 7718-7727.

Vincett, P. S., Barlow, W. A., Hann, R. A., & Roberts, G. G. (1982). Electrical conduction and low voltage blue electroluminescence in vacuum-deposited organic films. *Thin Solid Films, 94*(2), 171-183.

Wang, C., Chen, S., Wang, K., Zhao, S., Zhang, J., & Wang, Y. (2012). Luminescent Dendrimers Composed of Quinacridone Core and Carbazole Dendrons: Structure, Electrochemical, and Photophysical Properties. *The Journal of Physical Chemistry C, 116*(33), 17796-17806.

Wang, X., Wang, S., Ma, Z., Ding, J., Wang, L., Jing, X., & Wang, F. (2014). Solution-Processible 2,2'-Dimethyl-biphenyl Cored Carbazole Dendrimers as Universal Hosts for Efficient Blue, Green, and Red Phosphorescent OLEDs. *Adv. Funct. Mater., 24*(22), 3413-3421.

Wang, Z. B., Helander, M. G., QiuJ, Puzzo, D. P., Greiner, M. T., Hudson, Z. M., . . . Lu, Z. H. (2011). Unlocking the full potential of organic light-emitting diodes on flexible plastic. *Nat Photon, 5*(12), 753-757.

White, M. S., Kaltenbrunner, M., Glowacki, E. D., Gutnichenko, K., Kettlgruber, G., Graz, I., . . . Sariciftci, N. S. (2013). Ultrathin, highly flexible and stretchable PLEDs. *Nat Photon, 7*(10), 811-816.

Woon, K. L., Hasan, Z. A., Ong, B. K., Ariffin, A., Griniene, R., Grigalevicius, S., & Chen, S.-A. (2015). Triplet states and energy back transfer of carbazole derivatives. *RSC Advances, 5*(74), 59960-59969.

Wu, Y., Guo, H., James, T. D., & Zhao, J. (2011). Enantioselective Recognition of Mandelic Acid by a 3,6-Dithiophen-2-yl-9H-carbazole-Based Chiral Fluorescent Bisboronic Acid Sensor. *The Journal of Organic Chemistry, 76*(14), 5685-5695.

Xie, H., Zhang, K., Duan, C., Liu, S., Huang, F., & Cao, Y. (2012). New acceptor-pended conjugated polymers based on 3,6- and 2,7-carbazole for polymer solar cells. *Polymer, 53*(25), 5675-5683.

Xie, Y.-M., Cui, L.-S., Zu, F.-S., Igbari, F., Xue, M.-M., Jiang, Z.-Q., & Liao, L.-S. (2015). High efficiency and low driving voltage blue/white electrophosphorescence enabled by the synergistic combination of singlet and triplet energy of bicarbazole derivatives. *Organic Electronics, 26*, 25-29.

Xiong, M. J., Li, Z. H., & Wong, M. S. (2007). Synthesis and Functional Properties of Star-Burst Dendrimers that Contain Carbazole as Peripheral Edges and Triazine as a Central Core. *Australian Journal of Chemistry, 60*(8), 603-607.

Xue, S., Qiu, X., Yao, L., Wang, L., Yao, M., Gu, C., . . . Wu, H. (2015). Fully solution-processed and multilayer blue organic light-emitting diodes based on efficient small molecule emissive layer and intergrated interlayer optimization. *Organic Electronics, 27*, 35-40.

Yamae, K., Tsuji, H., Kittichungchit, V., Ide, N., & Komoda, T. (2013). Highly efficient white organic light-emitting diodes with over 100 lm/W for next-generation solid-state lighting. *Journal of the Society for Information Display, 21*(12), 529-540.

Yamashita, M., Horiguchi, H., Hirano, K., Satoh, T., & Miura, M. (2009). Fused Ring Construction around Pyrrole, Indole, and Related Compounds via Palladium-Catalyzed Oxidative Coupling with Alkynes. *The Journal of Organic Chemistry, 74*(19), 7481-7488.

Yang, B., Kim, S.-K., Xu, H., Park, Y.-I., Zhang, H., Gu, C., . . . Ma, Y. (2008). The Origin of the Improved Efficiency and Stability of Triphenylamine-Substituted Anthracene Derivatives for OLEDs: A Theoretical Investigation. *ChemPhysChem, 9*(17), 2601-2609.

Yang, G.-Z., Wu, Y., & Chen, Y. (2012). Alkaloids from the Stems of Glycosmis pentaphylla. *Helvetica Chimica Acta, 95*(8), 1449-1454.

Yang, W., Chen, Y., Jiang, W., Ban, X., Huang, B., Dai, Y., & Sun, Y. (2013). A carbazole-based dendritic host material for efficient solution-processed blue phosphorescent OLEDs. *Dyes Pigm., 97*(2), 286-290.

Ye, J., Fu, L., Liu, H., Chang, C., & Zhang, C. (2015). New fluorescent emitter for efficient deep-blue electroluminescence with unusual roll-up character. *Materials Letters, 158*, 392-394.

Yeh, S. J., Wu, M. F., Chen, C. T., Song, Y. H., Chi, Y., Ho, M. H., . . . Chen, C. H. (2005). New Dopant and Host Materials for Blue-Light-Emitting Phosphorescent Organic Electroluminescent Devices. *Advanced Materials, 17*(3), 285-289.

Yong-Qiang, Y., & Yu, D. (2014). Optimization of Al2O3 Films Deposited by ALD at Low Temperatures for OLED Encapsulation. *The Journal of Physical Chemistry C, 118*(32), 18783-18787.

Yoo, S. G., Jeon, S. K., Hwang, S.-H., & Lee, J. Y. (2015). A strong hole transport type host material for high quantum efficiency blue phosphorescent organic light-emitting diodes. *Journal of Industrial and Engineering Chemistry, 32*, 72-76.

Yook, K. S., Jang, S. E., Jeon, S. O., & Lee, J. Y. (2010). Fabrication and Efficiency Improvement of Soluble Blue Phosphorescent Organic Light-Emitting Diodes Using a Multilayer Structure Based on an Alcohol-Soluble Blue Phosphorescent Emitting Layer. *Advanced Materials, 22*(40), 4479-4483.

Yook, K. S., & Lee, J. Y. (2012). Organic Materials for Deep Blue Phosphorescent Organic Light-Emitting Diodes. *Advanced Materials, 24*(24), 3169-3190.

Yook, K. S., & Lee, J. Y. (2014). Small Molecule Host Materials for Solution Processed Phosphorescent Organic Light-Emitting Diodes. *Advanced Materials, 26*(25), 4218-4233.

Yoon, D. G., Jo, S. M., & Chin, B. D. (2012). P-120: Inkjet-Printable Composite Electrode and Device Architectures for the Inverted Phosphorescent OLED. *SID Symposium Digest of Technical Papers, 43*(1), 1511-1513.

You, J., Li, G., Wang, R., Nie, Q., Wang, Z., & Li, J. (2011). Pyrene-cored dendrimer with carbazole derivatives as dendrons: synthesis, properties and application in white light-emitting diode. *Physical Chemistry Chemical Physics, 13*(39), 17825-17830.

Youn, S. W., Bihn, J. H., & Kim, B. S. (2011). Pd-Catalyzed Intramolecular Oxidative C–H Amination: Synthesis of Carbazoles. *Organic Letters, 13*(14), 3738-3741.

Yu, J., Lin, H., Wang, F., Lin, Y., Zhang, J., Zhang, H., . . . Wei, B. (2012). Sunlight-like, color-temperature tunable white organic light-emitting diode with high color rendering index for solid-state lighting application. *Journal of Materials Chemistry, 22*(41), 22097-22101.

Yu, L.-F., Ge, C.-W., Wang, J.-T., Xiang, X., & Li, W.-S. (2015a). Modification of a donor-acceptor photovoltaic polymer by integration of optoelectronic moieties into its side chains. *Polymer, 59*, 57-66.

Yu, Y., Wu, Z., He, L., Jiao, B., & Hou, X. (2015b). A solvent/non-solvent system for achieving solution-processed multilayer organic light-emitting devices. *Thin Solid Films, 589*, 852-856.

Yuan, Z.-G., Wang, Q., Zheng, A., Zhang, K., Lu, L.-Q., Tang, Z., & Xiao, W.-J. (2016). Visible light-photocatalysed carbazole synthesis via a formal (4+2) cycloaddition of indole-derived bromides and alkynes. *Chemical Communications, 52*(29), 5128-5131.

Yun, W. M., Jang, J., Nam, S., Kim, L. H., Seo, S. J., & Park, C. E. (2012). Thermally Evaporated SiO Thin Films As a Versatile Interlayer for Plasma-Based OLED Passivation. *ACS Applied Materials & Interfaces, 4*(6), 3247-3253.

Zhang, B., Tan, G., Lam, C.-S., Yao, B., Ho, C.-L., Liu, L., . . . Wang, L. (2012a). High-Efficiency Single Emissive Layer White Organic Light-Emitting Diodes Based on Solution-Processed Dendritic Host and New Orange-Emitting Iridium Complex. *Advanced Materials, 24*(14), 1873-1877.

Zhang, J.-L., Nan, Y.-X., Li, H.-G., Qiu, W.-M., Yang, X., Wu, G., . . . Wang, M. (2012b). A new wide bandgap organic semiconductor and its application in organic UV sensors with tunable response wavelength. *Sensors and Actuators B: Chemical, 162*(1), 321-326.

Zhang, Q., Chen, J., Cheng, Y., Wang, L., Ma, D., Jing, X., & Wang, F. (2004a). Novel hole-transporting materials based on 1,4-bis(carbazolyl)benzene for organic light-emitting devices. *Journal of Materials Chemistry, 14*(5), 895-900.

Zhang, Q., Chen, J., Cheng, Y., Wang, L., Ma, D., Jing, X., & Wang, F. (2004b). Novel hole-transporting materials based on 1,4-bis(carbazolyl)benzene for organic light-emitting devices. *J. Mater. Chem., 14*(5), 895-900.

Zhang, T., Liu, D., Wang, Y., Bao, S., & Zhang, S. (2015). Novel carbazole dendronized oligofluorenes for solution-processed organic light-emitting diodes. *Dyes and Pigments, 122*, 295-301.

Zhang, X., Wu, Y., Ji, S., Guo, H., Song, P., Han, K., . . . Zhao, J. (2010). Effect of the Electron Donor/Acceptor Orientation on the Fluorescence Transduction Efficiency of the d-PET Effect of Carbazole-Based Fluorescent Boronic Acid Sensors. *The Journal of Organic Chemistry, 75*(8), 2578-2588.

Zhang, Z., Yan, P., Yue, S., Chen, Y., Wu, Q., Qu, D., . . . Liu, S. (2013). Low driving voltage white organic light-emitting diodes with high efficiency and low efficiency roll-off. *Organic Electronics, 14*(9), 2172-2176.

Zhao, Z.-H., Jin, H., Zhang, Y.-X., Shen, Z., Zou, D.-C., & Fan, X.-H. (2011). Synthesis and Properties of Dendritic Emitters with a Fluorinated Starburst Oxadiazole Core and Twisted Carbazole Dendrons. *Macromolecules, 44*(6), 1405-1413.

Zhou, L., Xiang, H.-Y., Shen, S., Li, Y.-Q., Chen, J.-D., Xie, H.-J., . . . Tang, J.-X. (2014). High-Performance Flexible Organic Light-Emitting Diodes Using Embedded Silver Network Transparent Electrodes. *ACS Nano, 8*(12), 12796-12805.

LIST OF PUBLICATIONS AND PAPERS PRESENTED

Publications

1. Woon, Kai Lin, **Hasan, Zainal A.**, Ong, Bee Kian, Ariffin, Azhar Griniene, Raimonda Grigalevicius, Saulius, Chen, Show-An, Triplet states and energy back transfer of carbazole derivatives. *RSC Advances*, **2015**. 5(74): p. 59960-59969
2. **Zainal Abidin Hasan**, Kai Lin Woon, Wah Seng Wong, Azhar Ariffin , Show-An Chen, Solution processed multilayer red, green and blue phosphorescent organic light emitting diodes using carbazole dendrimer as a host, *Journal of Luminescence*, **2017**,183: p. 150–158

Paper Presented

1. High Triplet, High Glass Transition, Thermally Stable Carbazole Dendrimers as Blue Host Materials for Organic Light-Emitting Diodes, **Zainal Abidin Hasan**, Azhar Ariffin, Woon Kai Lin, Oral presentation at ICRIL International Conference of Innovation in Science and Technology 2015, UTM KL

APPENDIX

1. ^{1}H NMR spectra
2. ^{13}C NMR spectra

^{1}H NMR

^{1}H NMR:Compound **5**

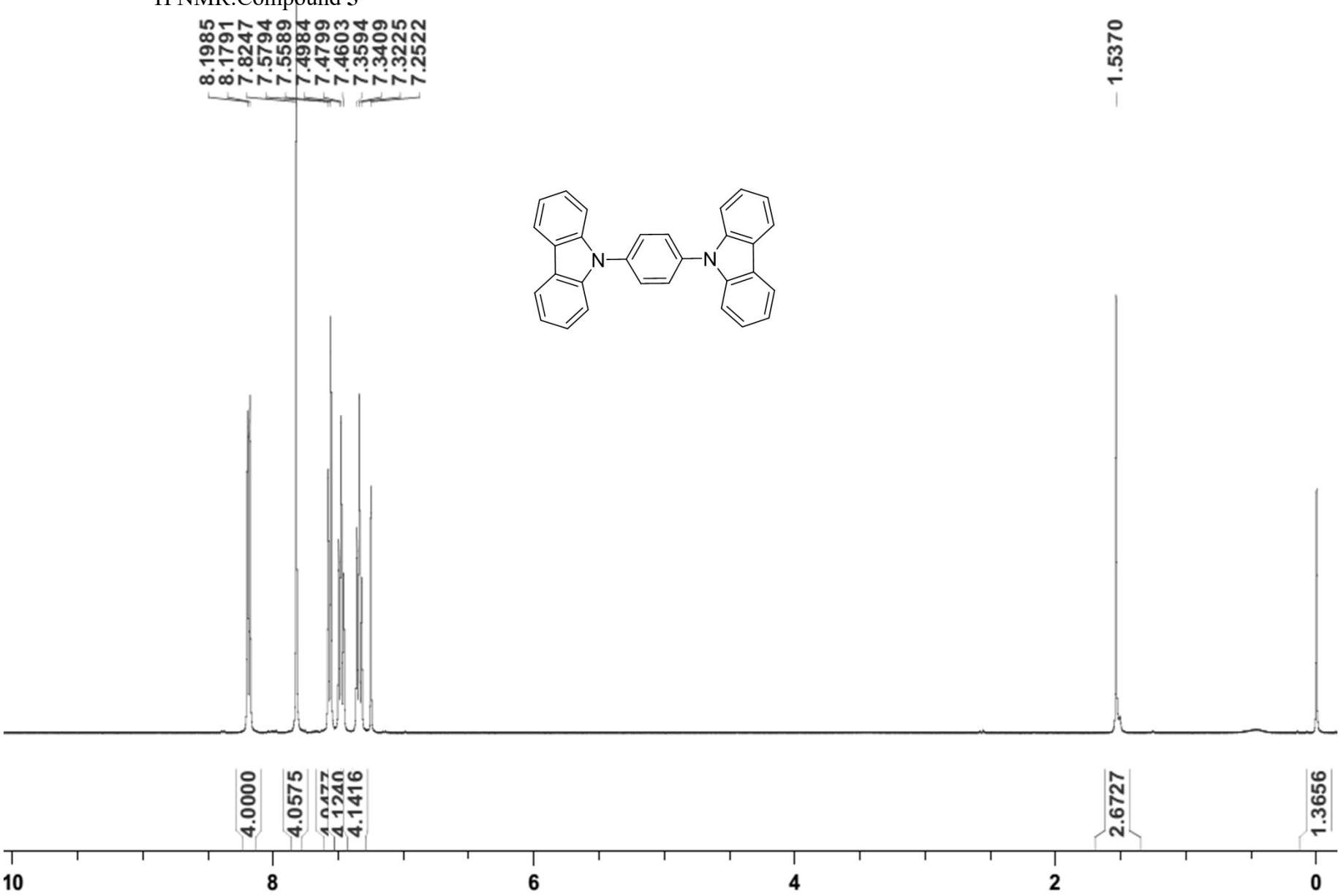

^{1}H NMR:Compound **6**

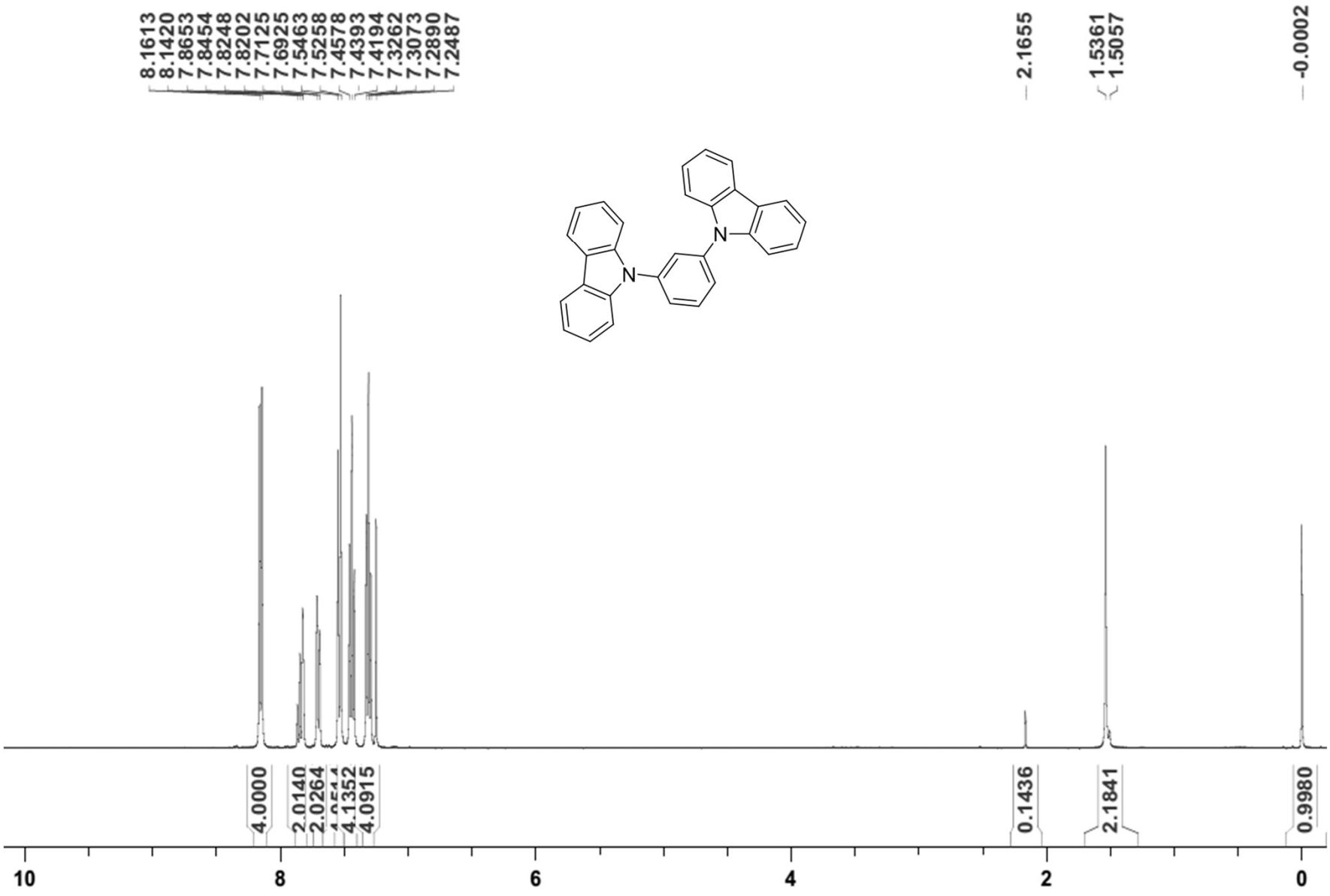

^{1}H NMR:Compound **7**

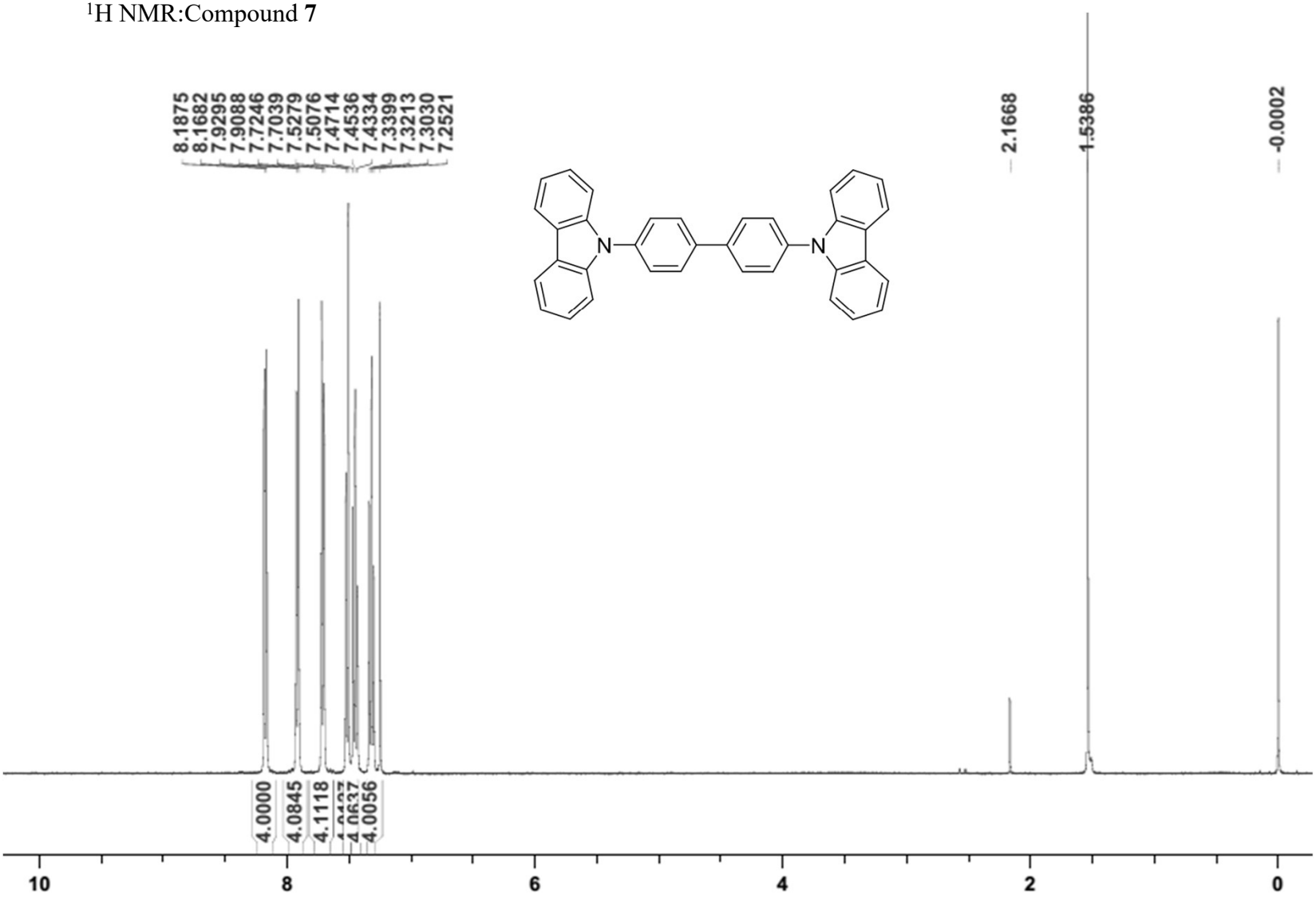

^{1}H NMR:Compound **8**

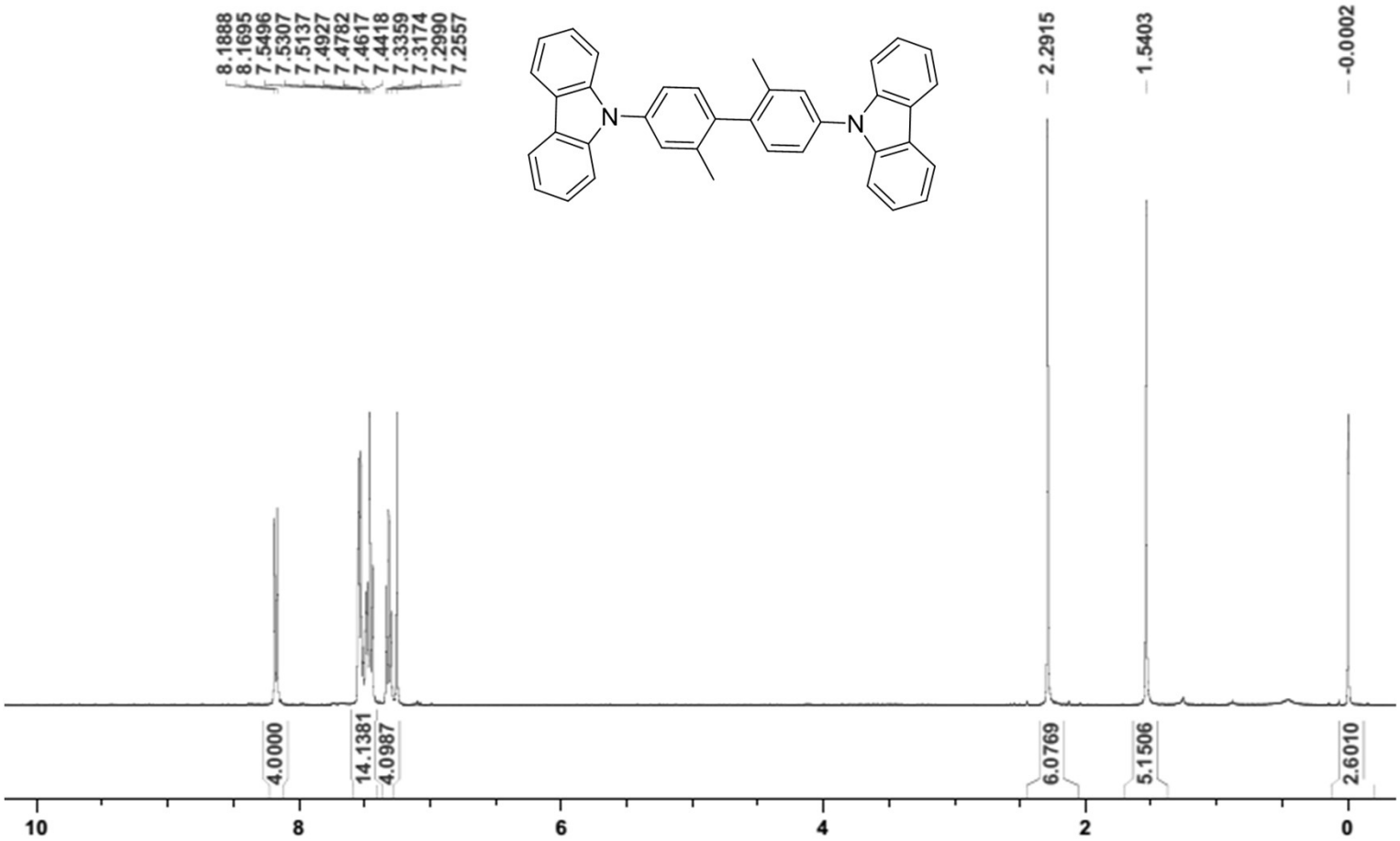

^{1}H NMR:Compound **9**

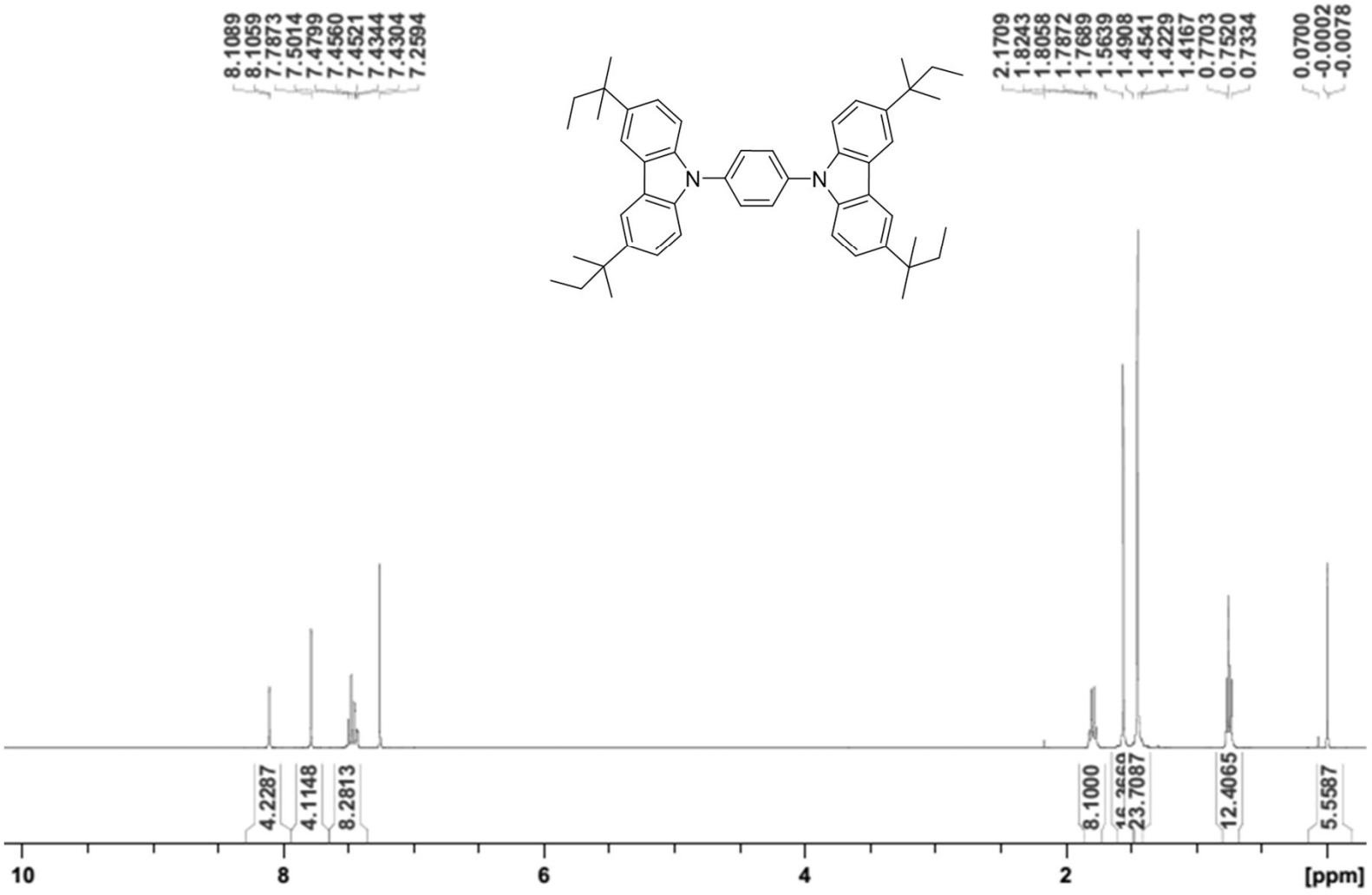

^{1}H NMR:Compound **10**

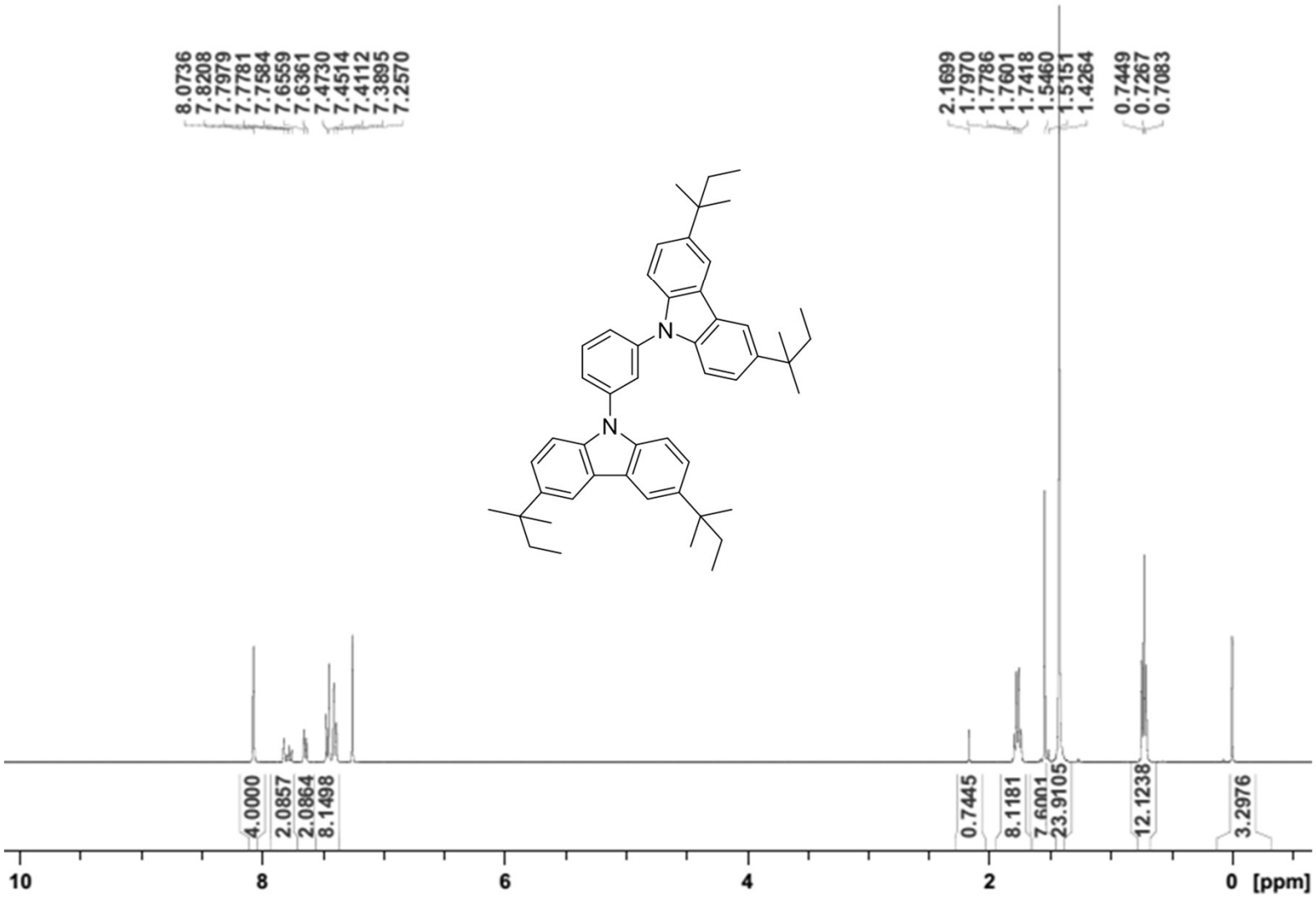

^{1}H NMR:Compound **10**

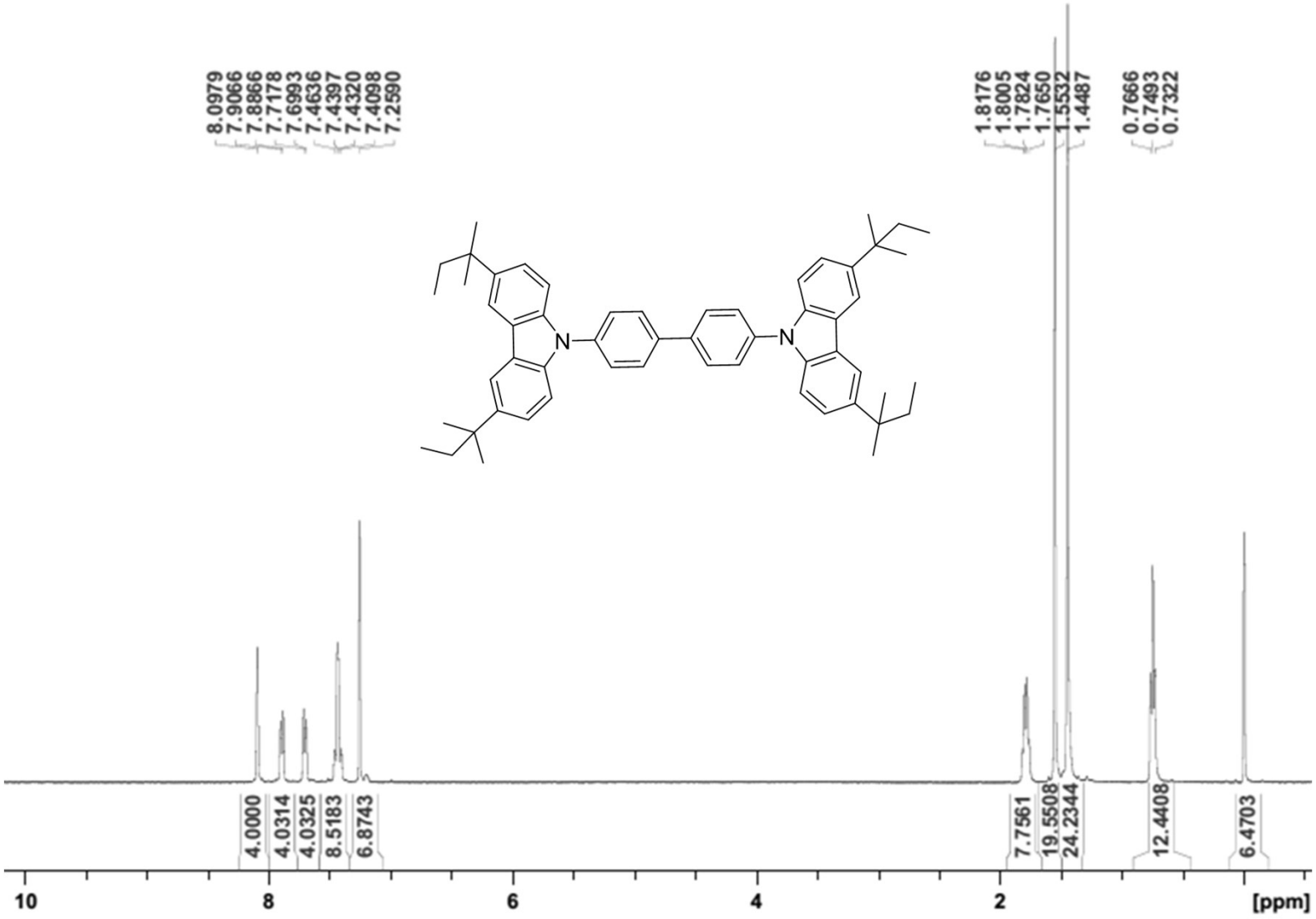

^{1}H NMR:Compound **11**

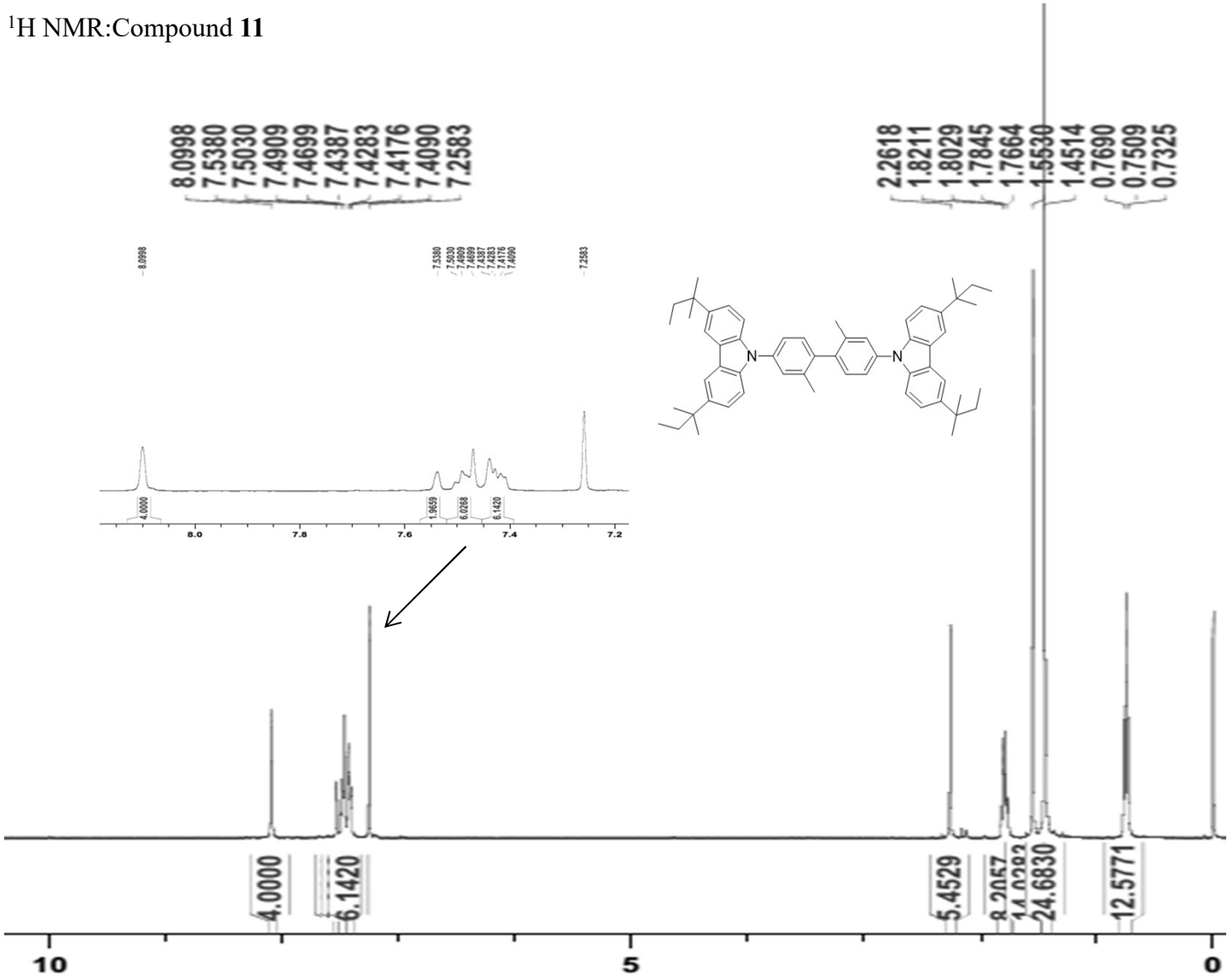

^{1}H NMR:Compound **13**

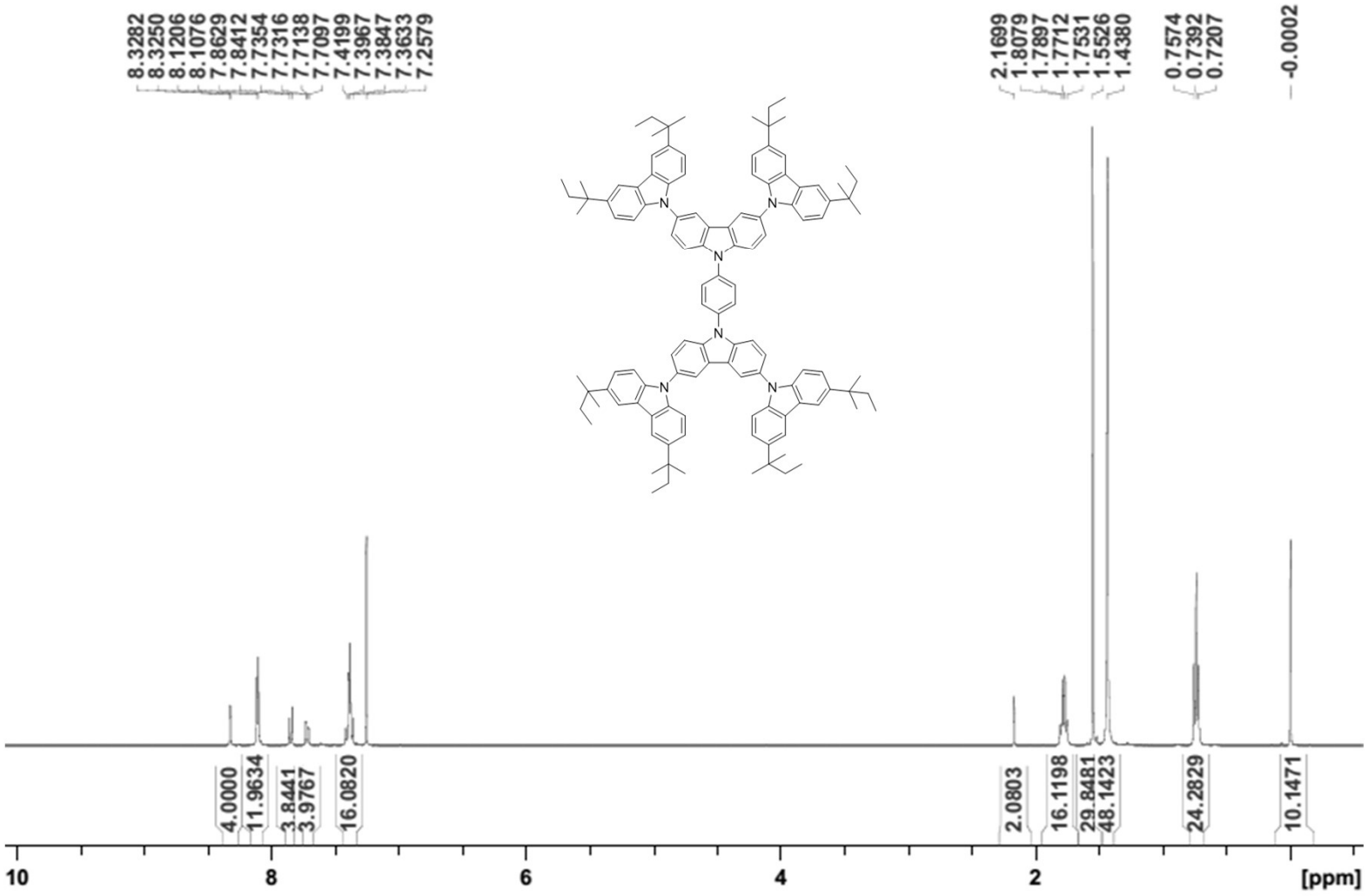

^{1}H NMR:Compound **14**

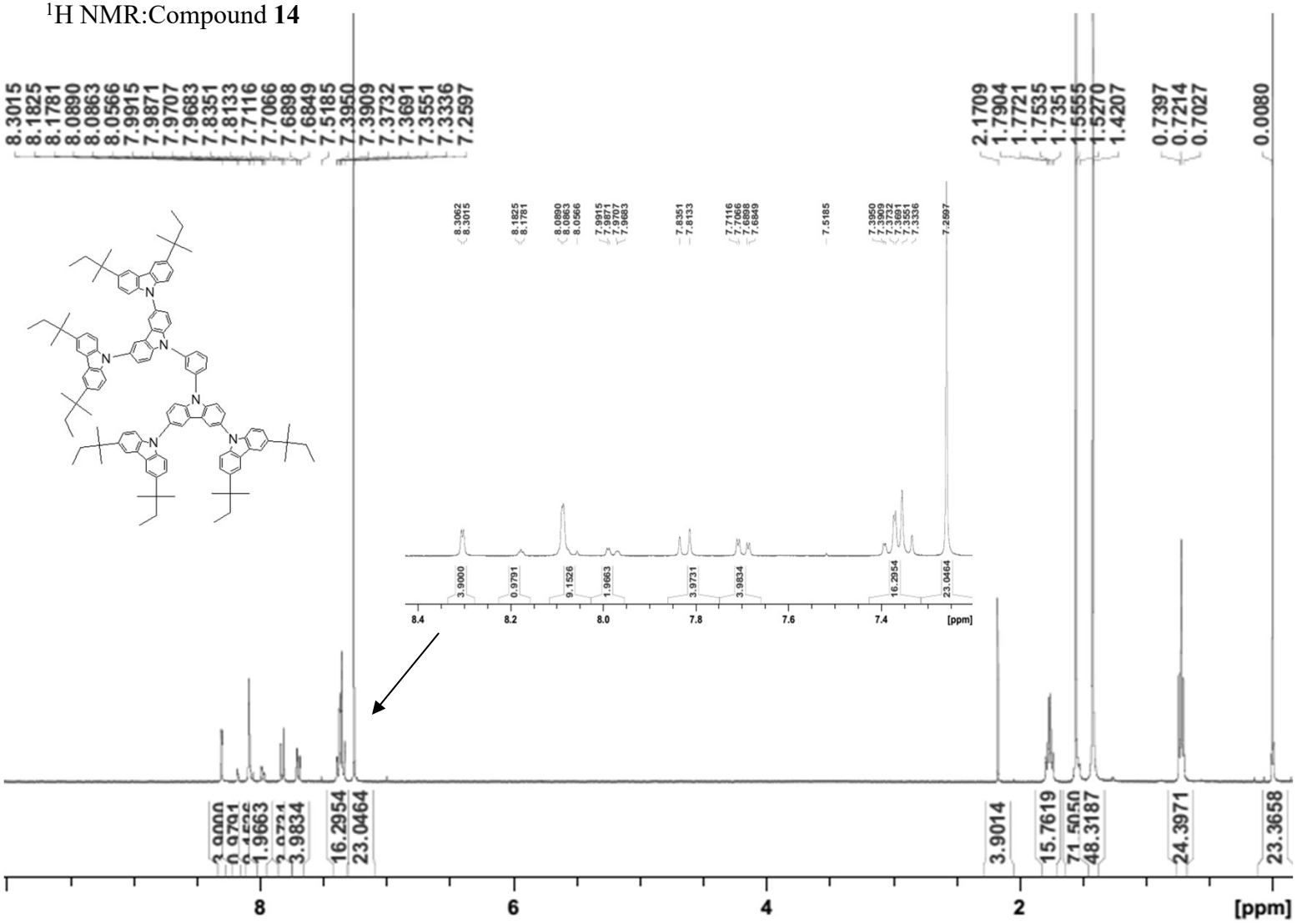

^{1}H NMR:Compound **15**

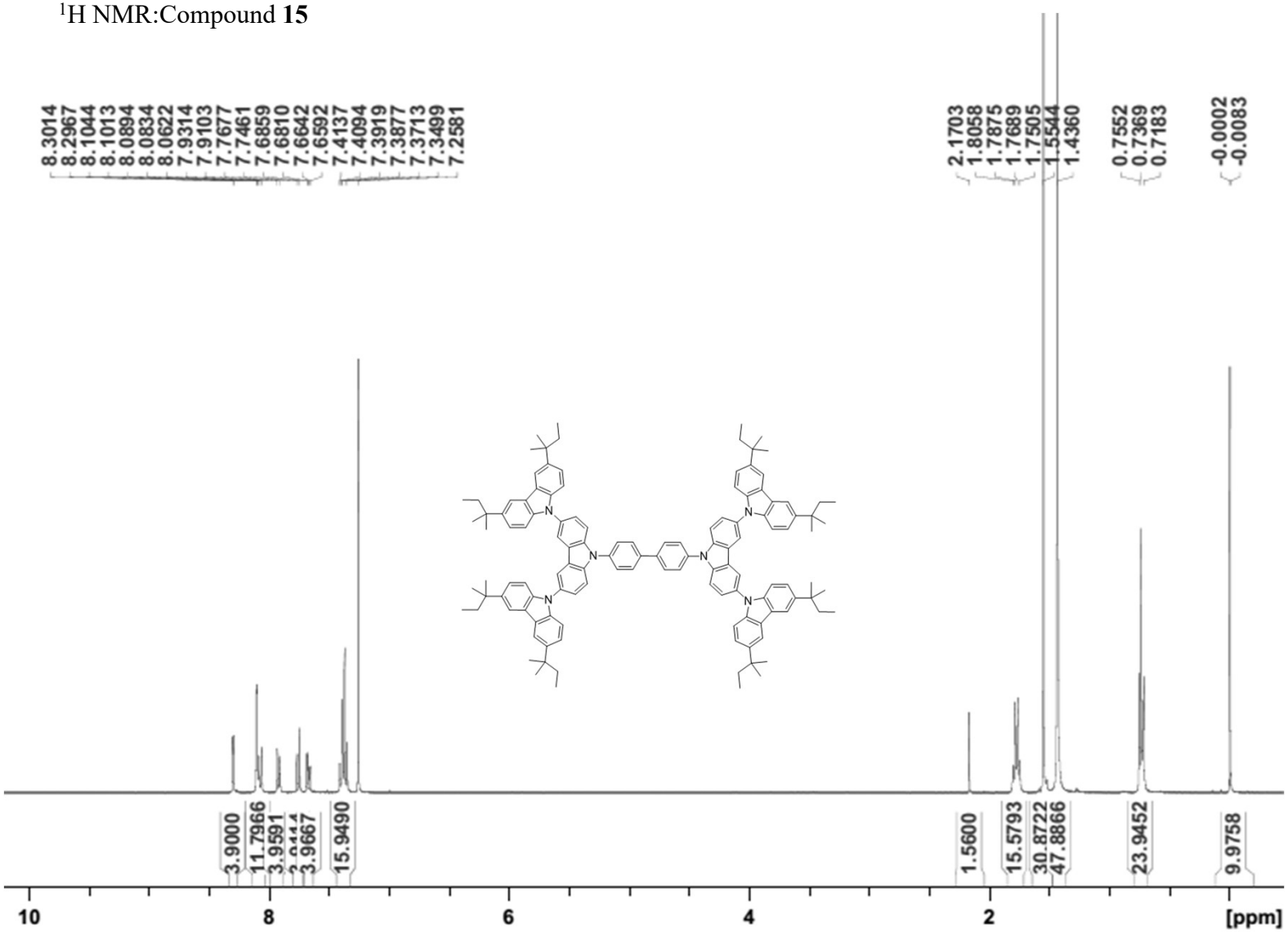

^{1}H NMR:Compound **16**

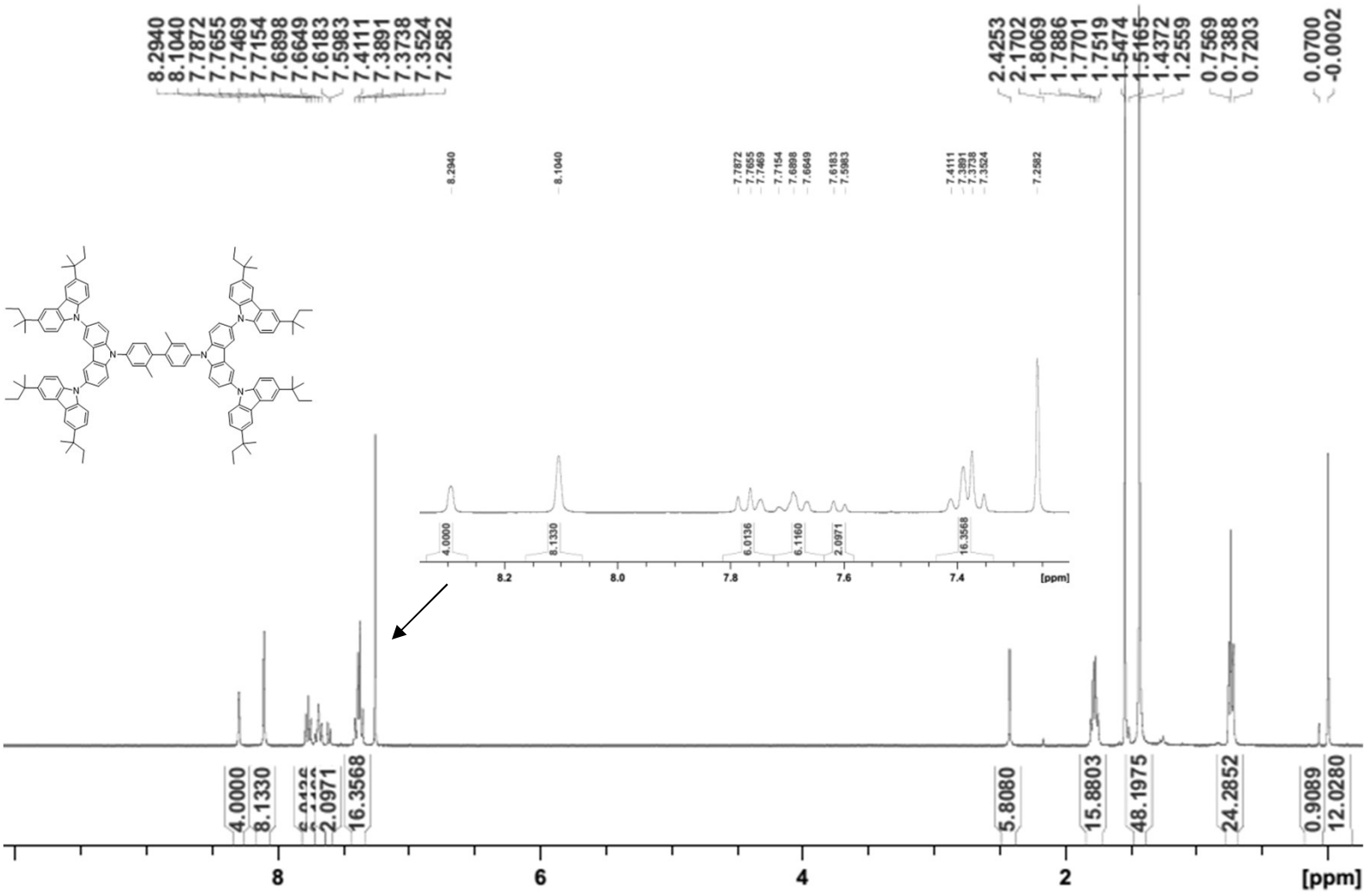

^{1}H NMR:Compound **18**

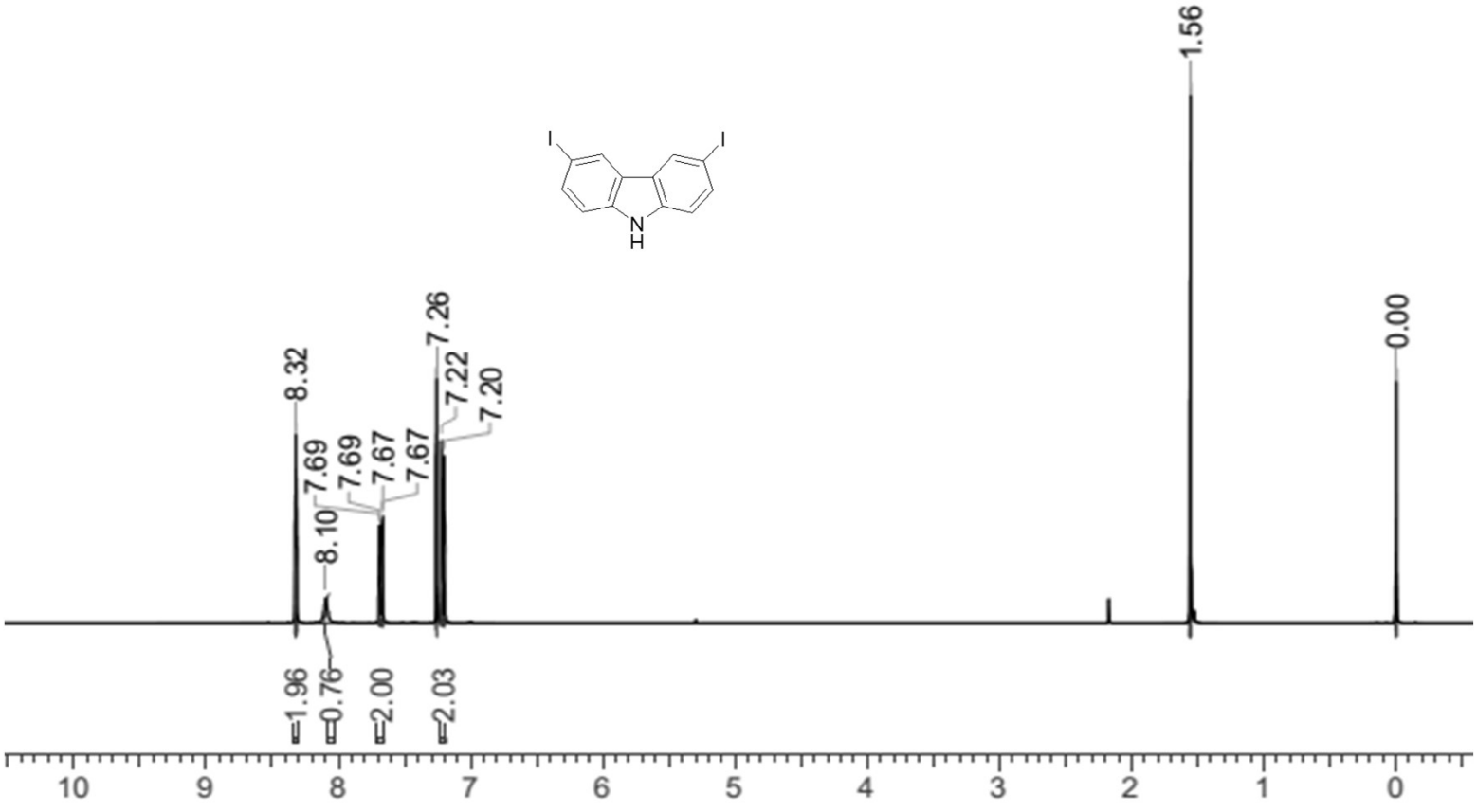

^{1}H NMR:Compound **19**

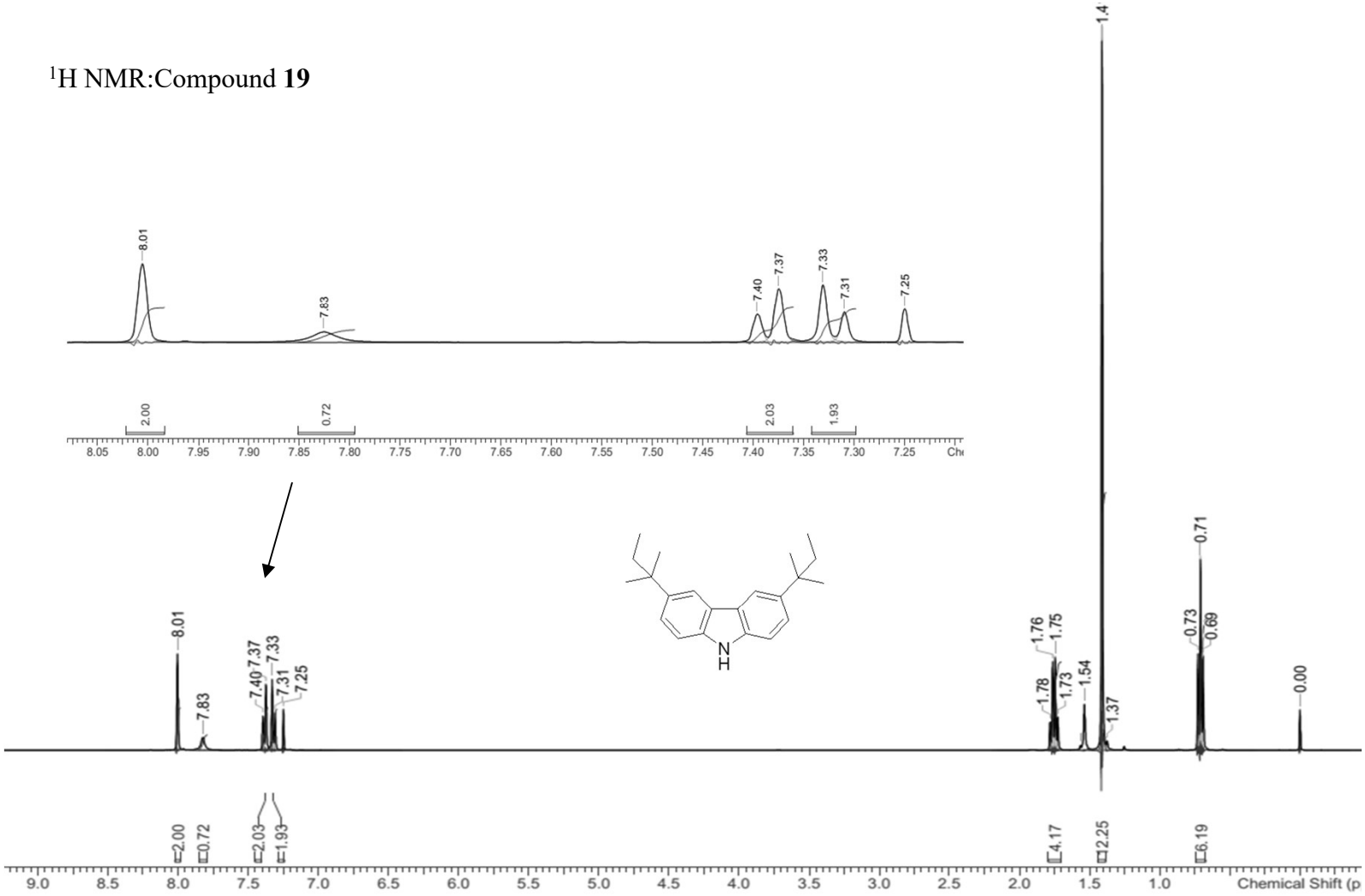

^{1}H NMR:Compound **20a**

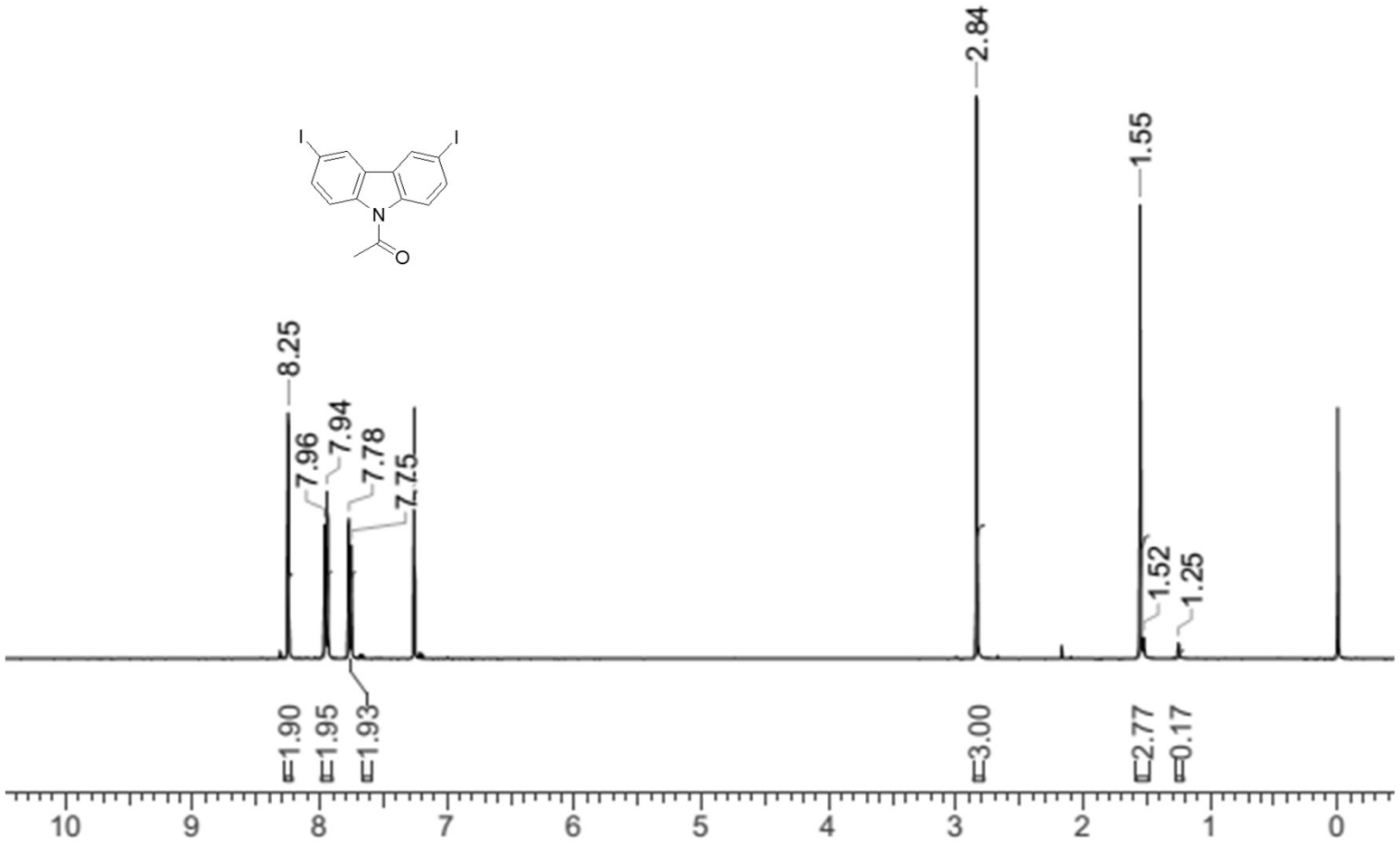

^{1}H NMR:Compound **21**

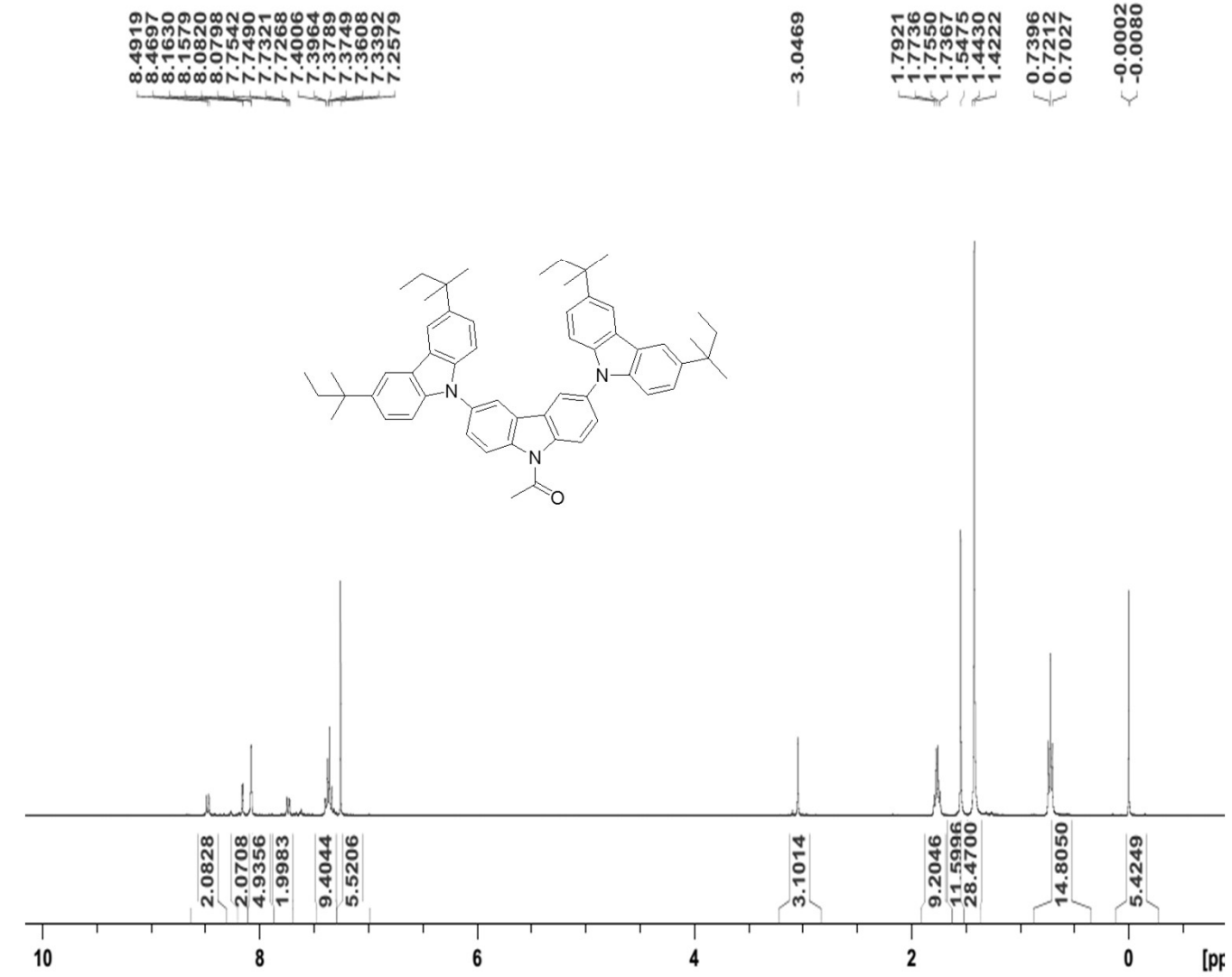

^{1}H NMR:Compound **22**

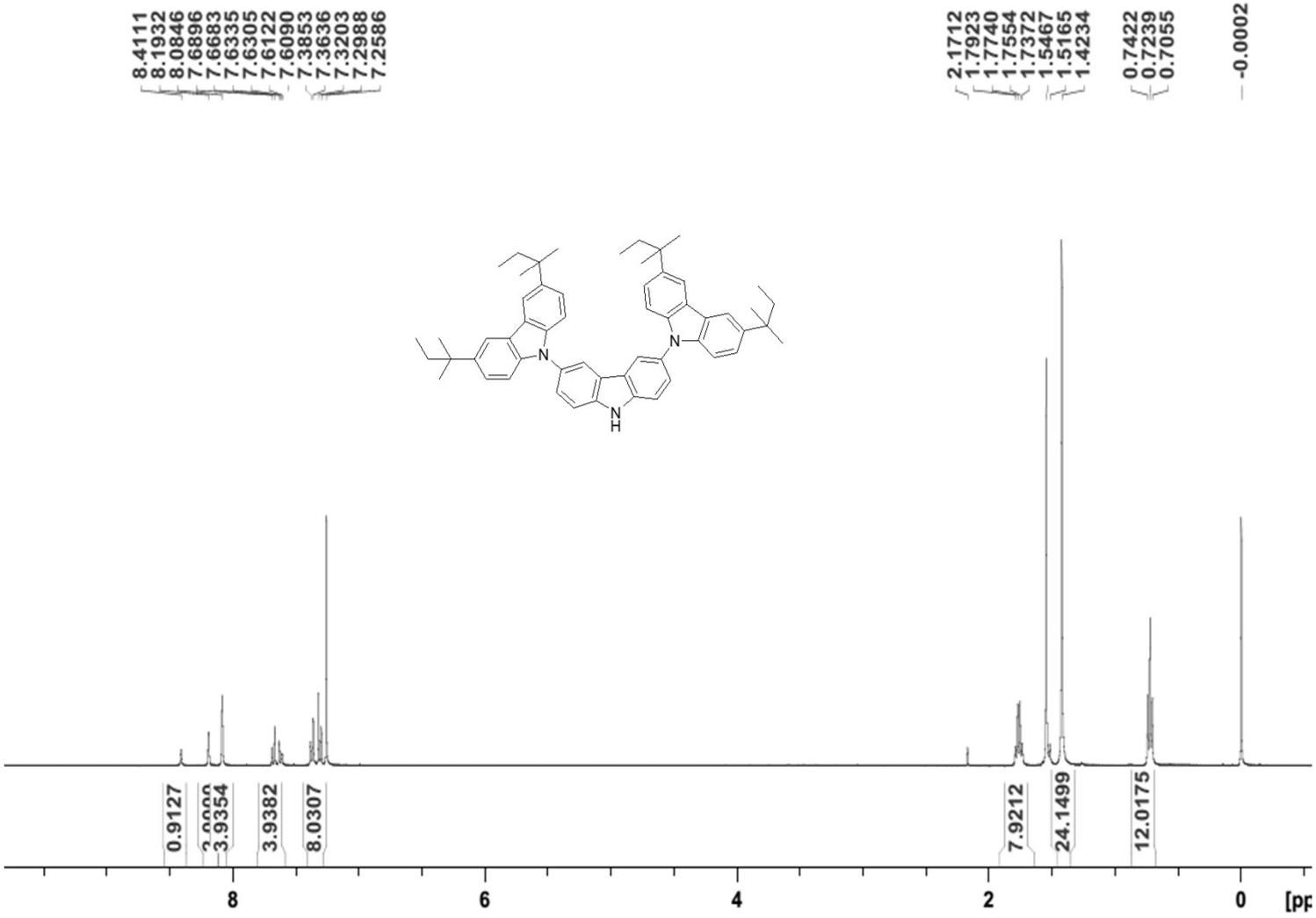

^{1}H NMR:Compound **23**

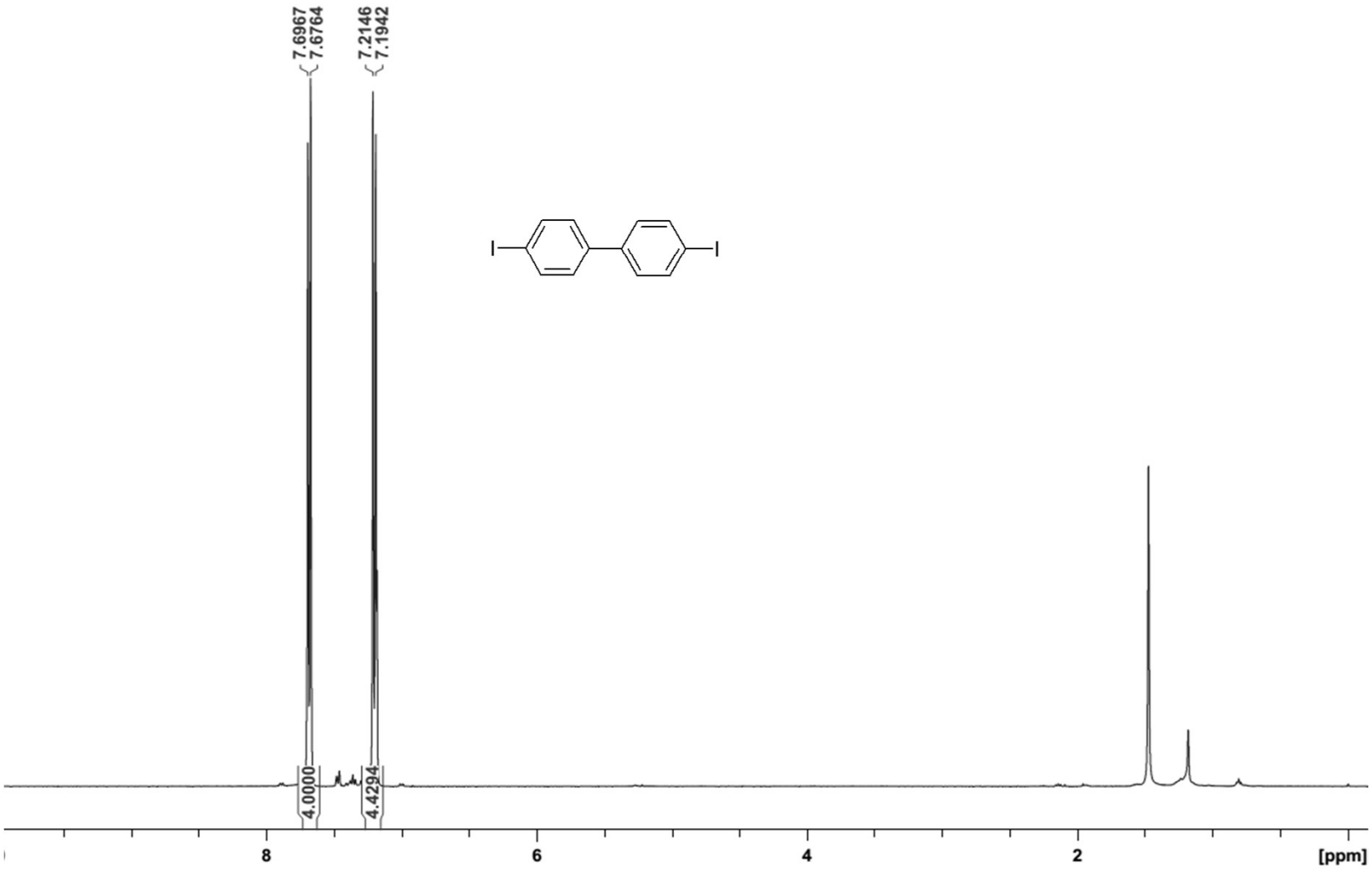

^{13}C NMR

^{13}C NMR:Compound **5**

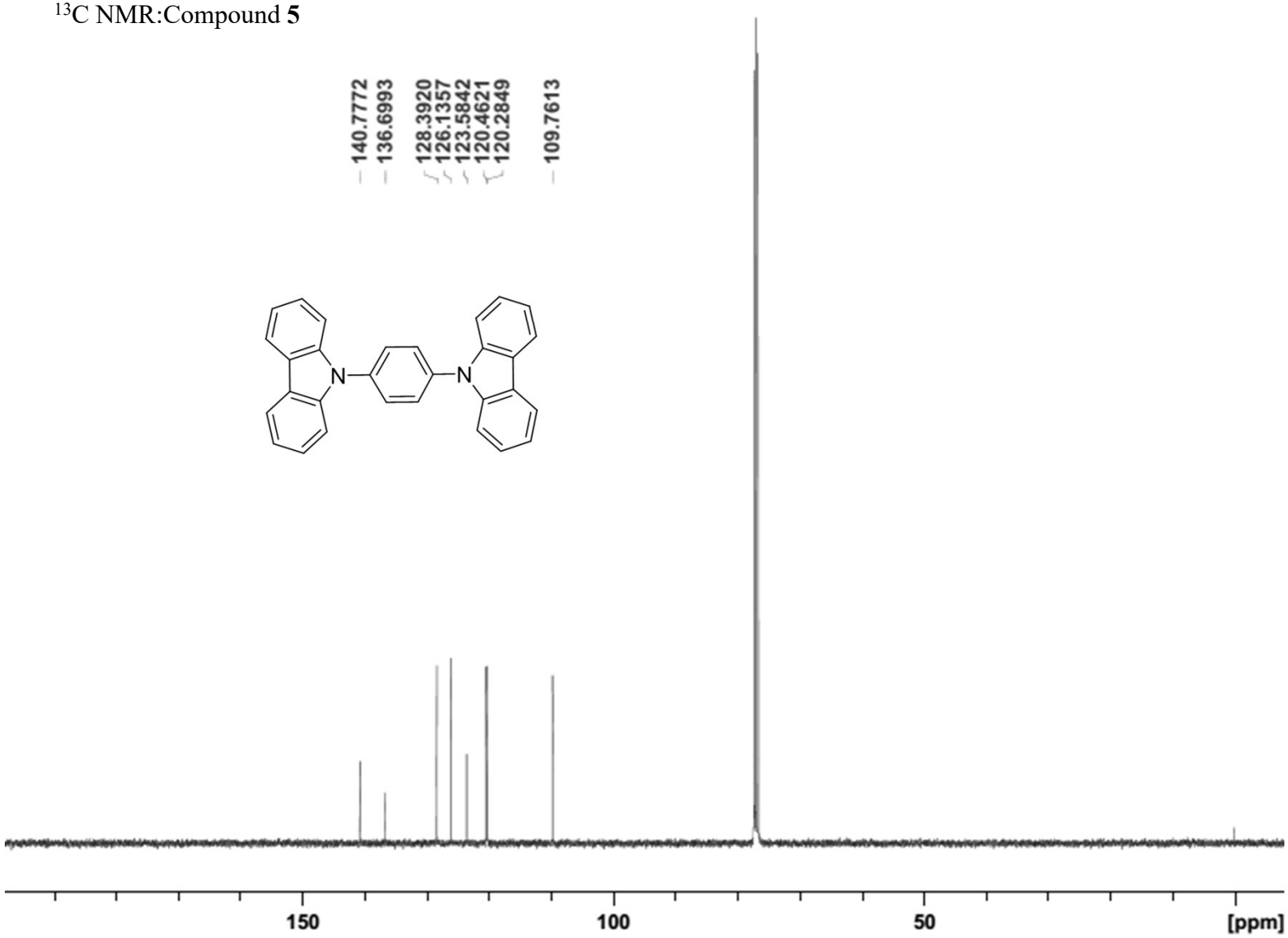

^{13}C NMR:Compound **6**

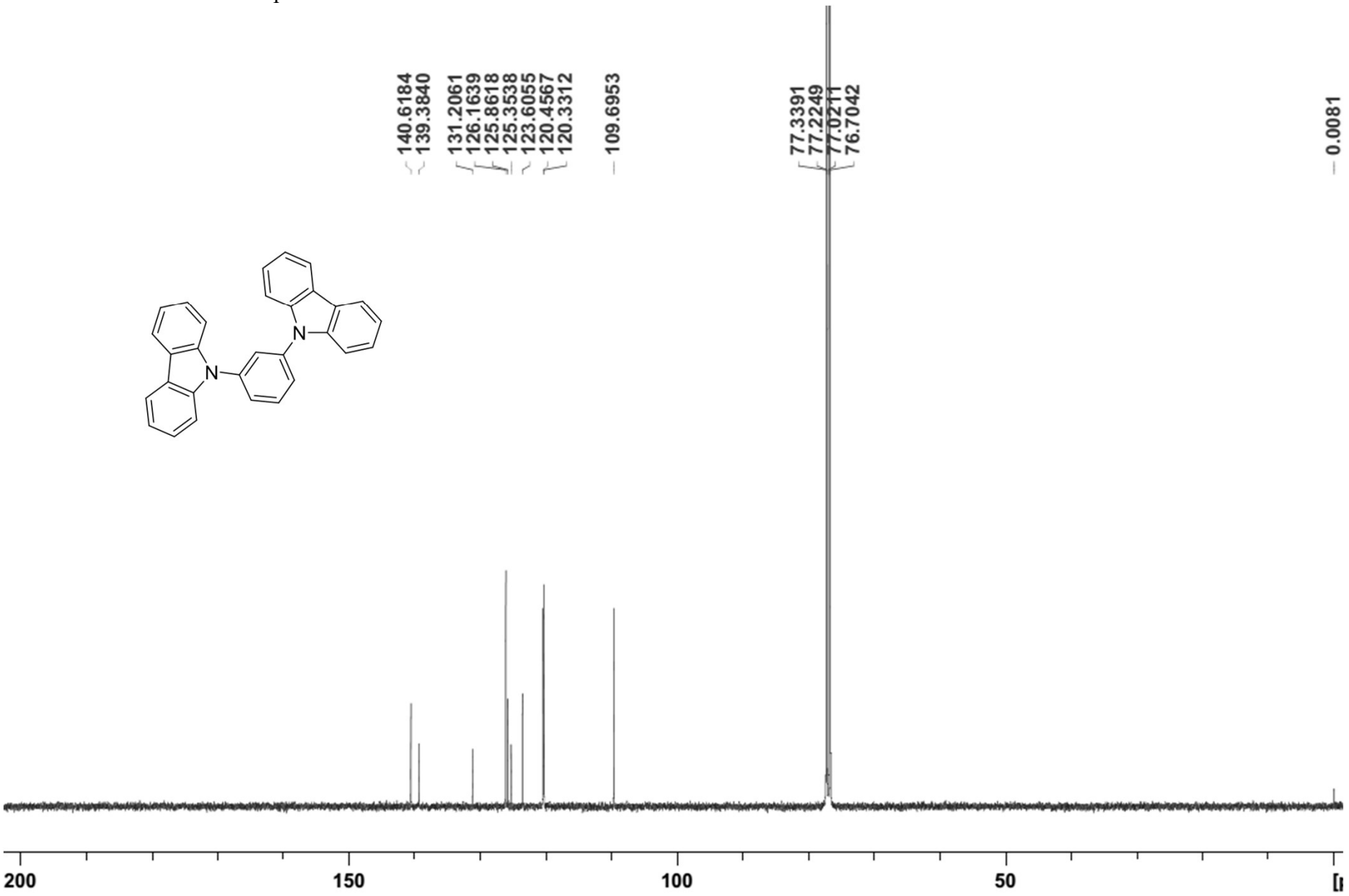

^{13}C NMR:Compound **7**

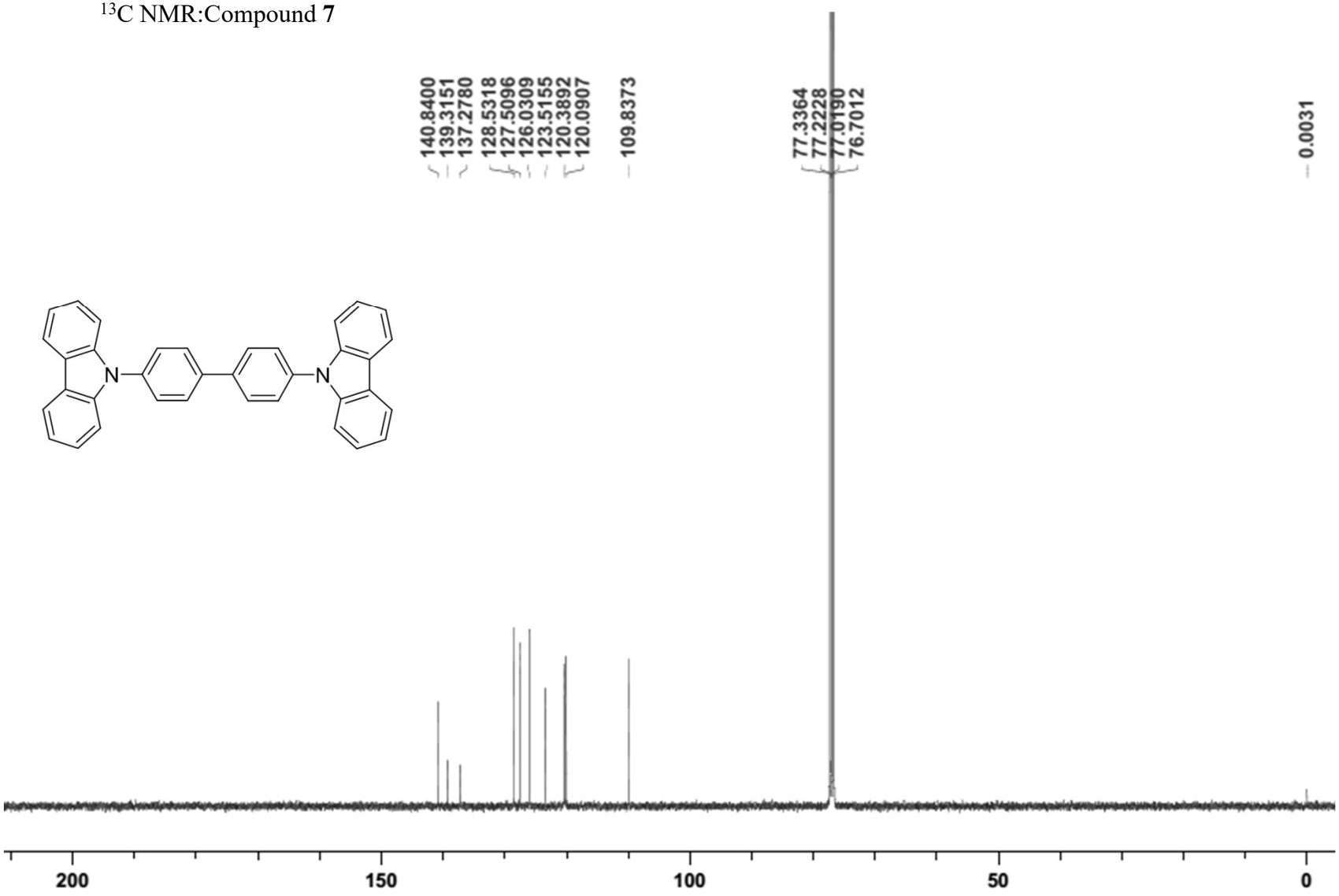

^{13}C NMR:Compound **8**

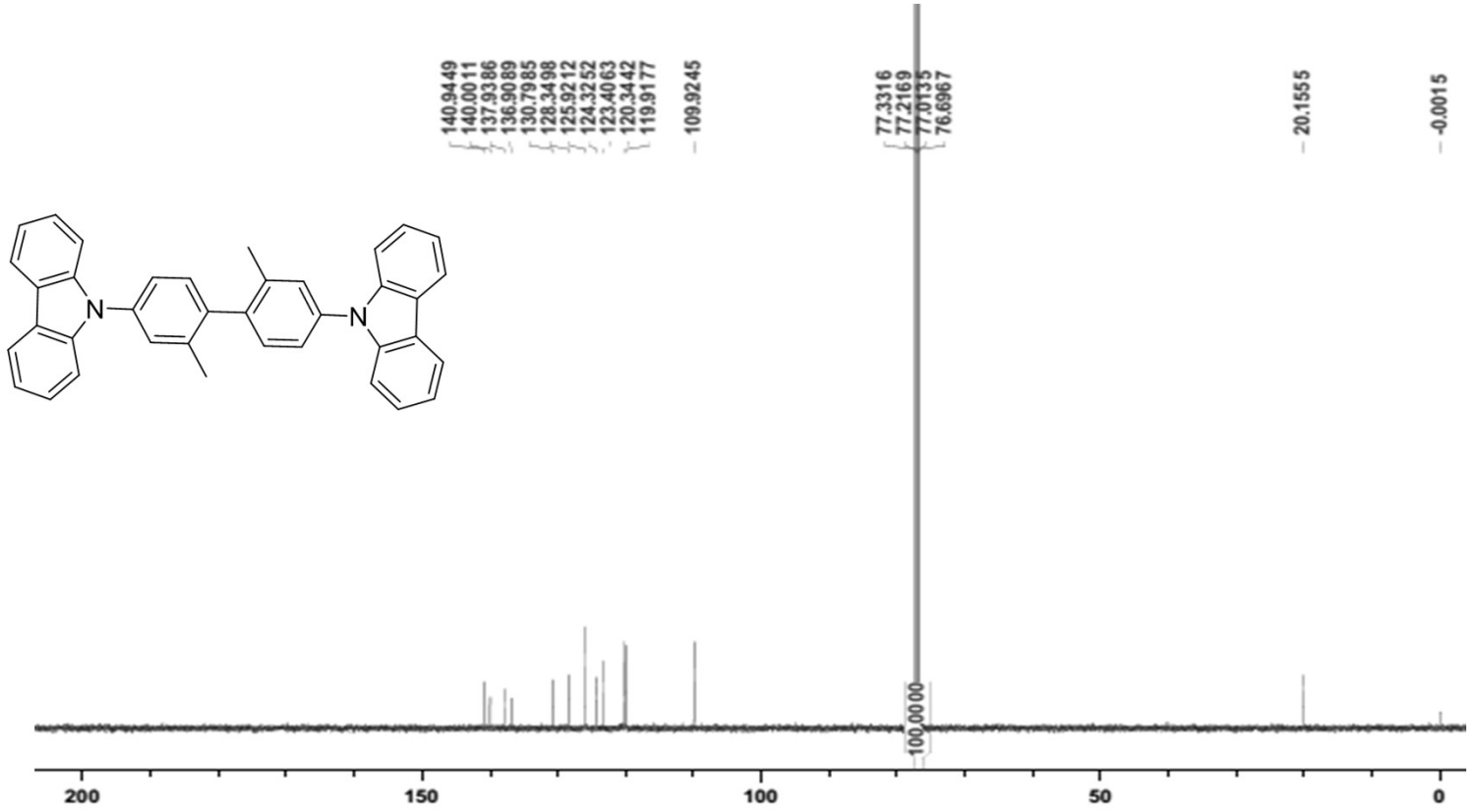

^{13}C NMR:Compound **9**

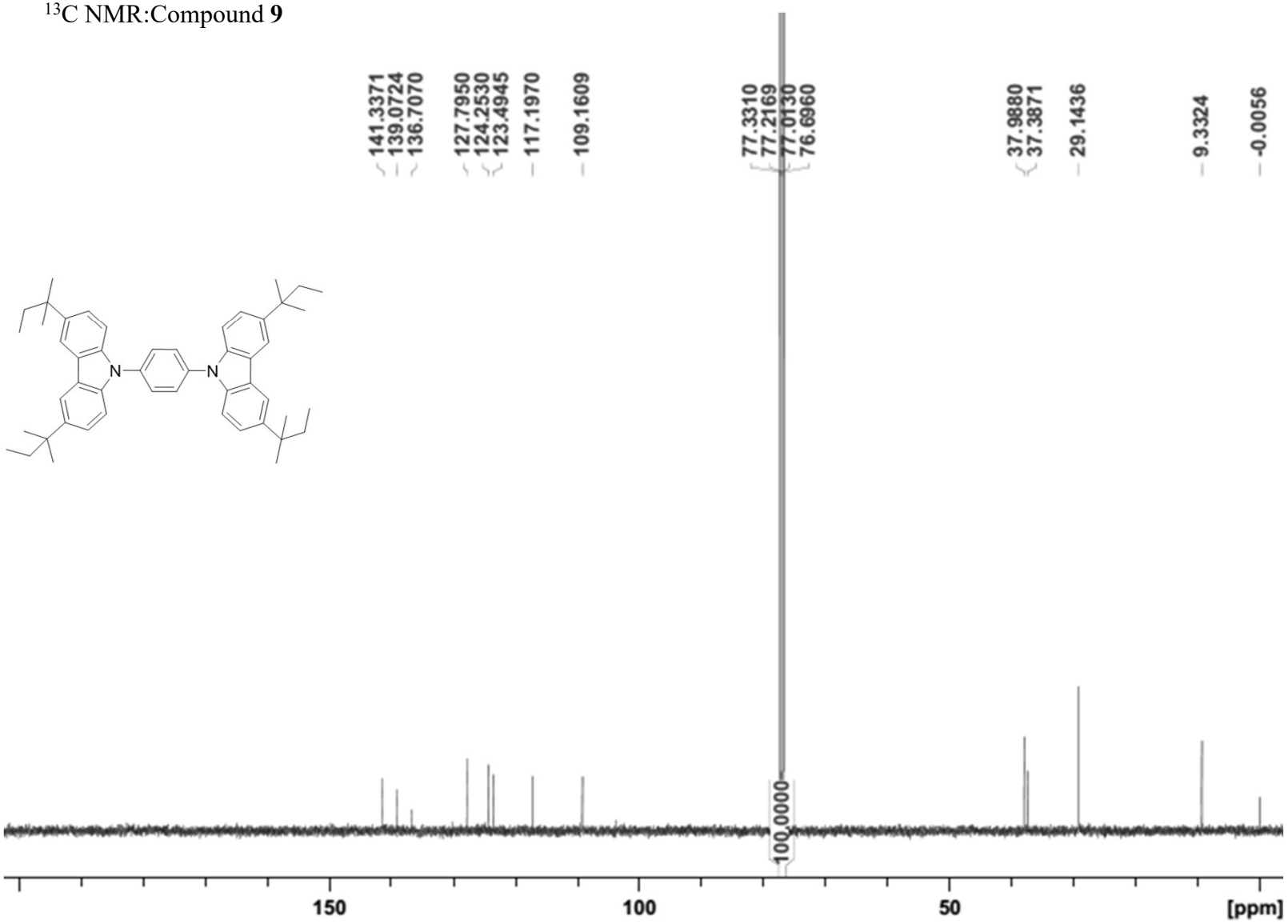

^{13}C NMR:Compound **10**

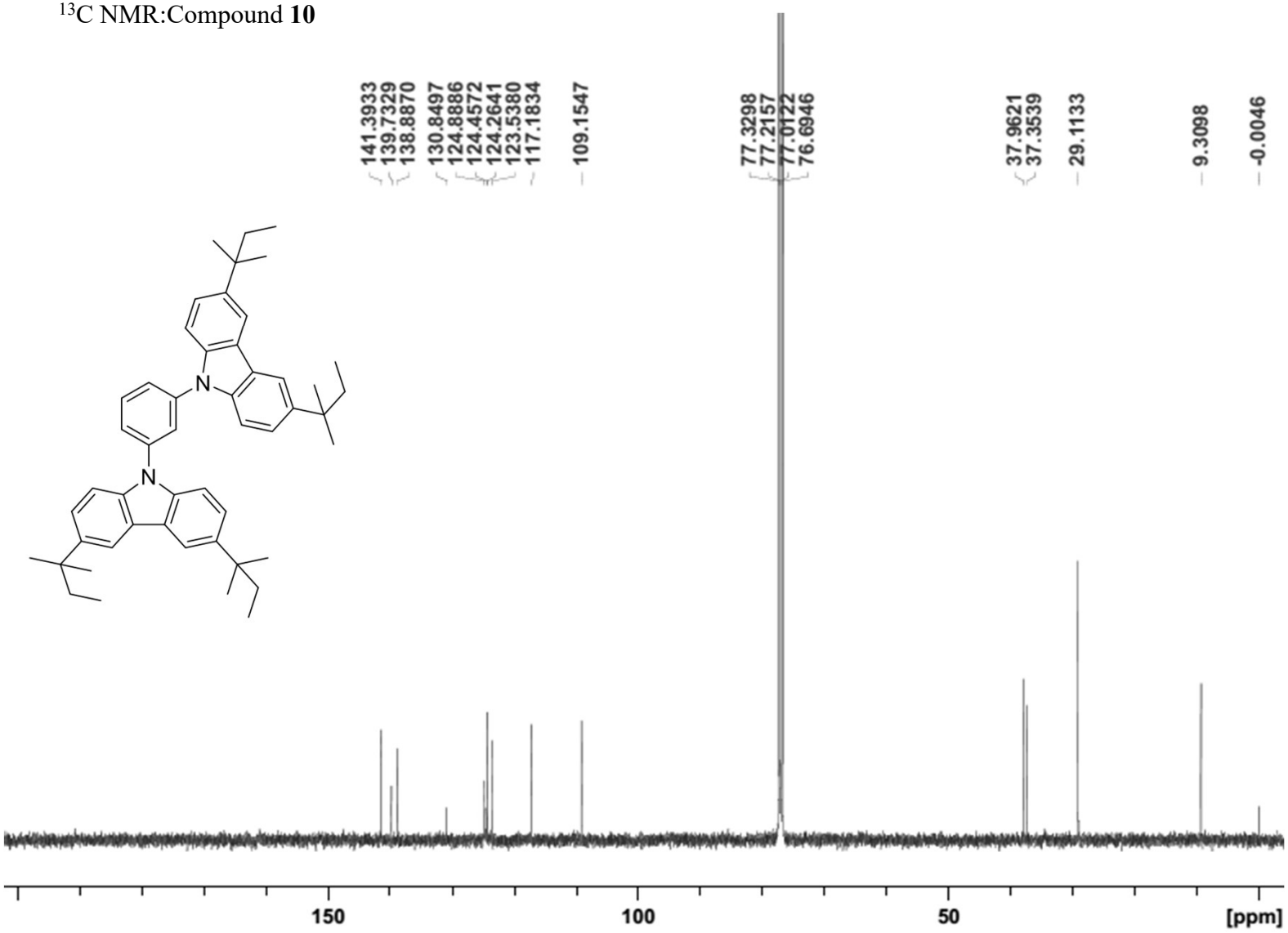

^{13}C NMR:Compound **11**

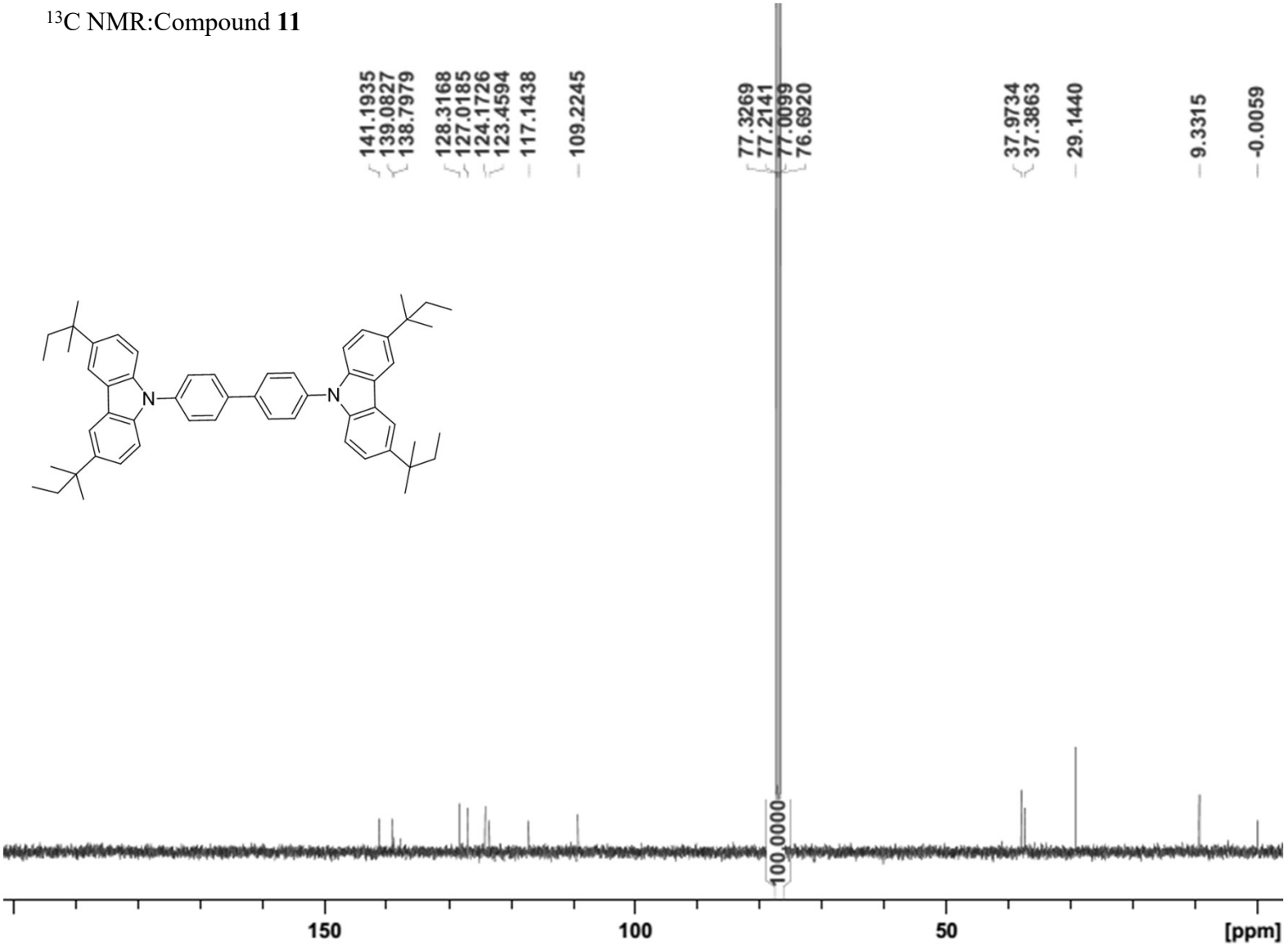

^{13}C NMR:Compound **12**

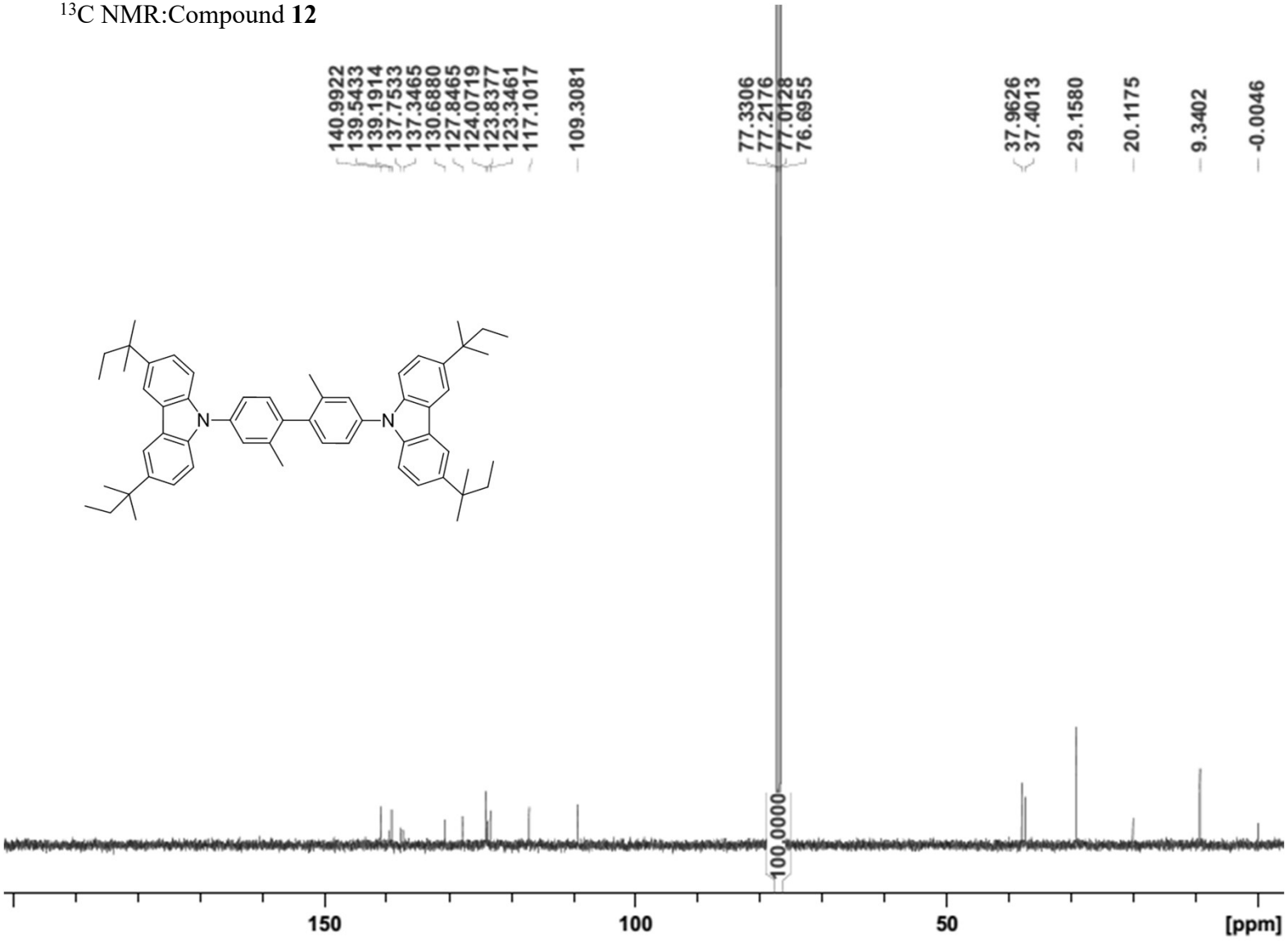

^{13}C NMR:Compound **13**

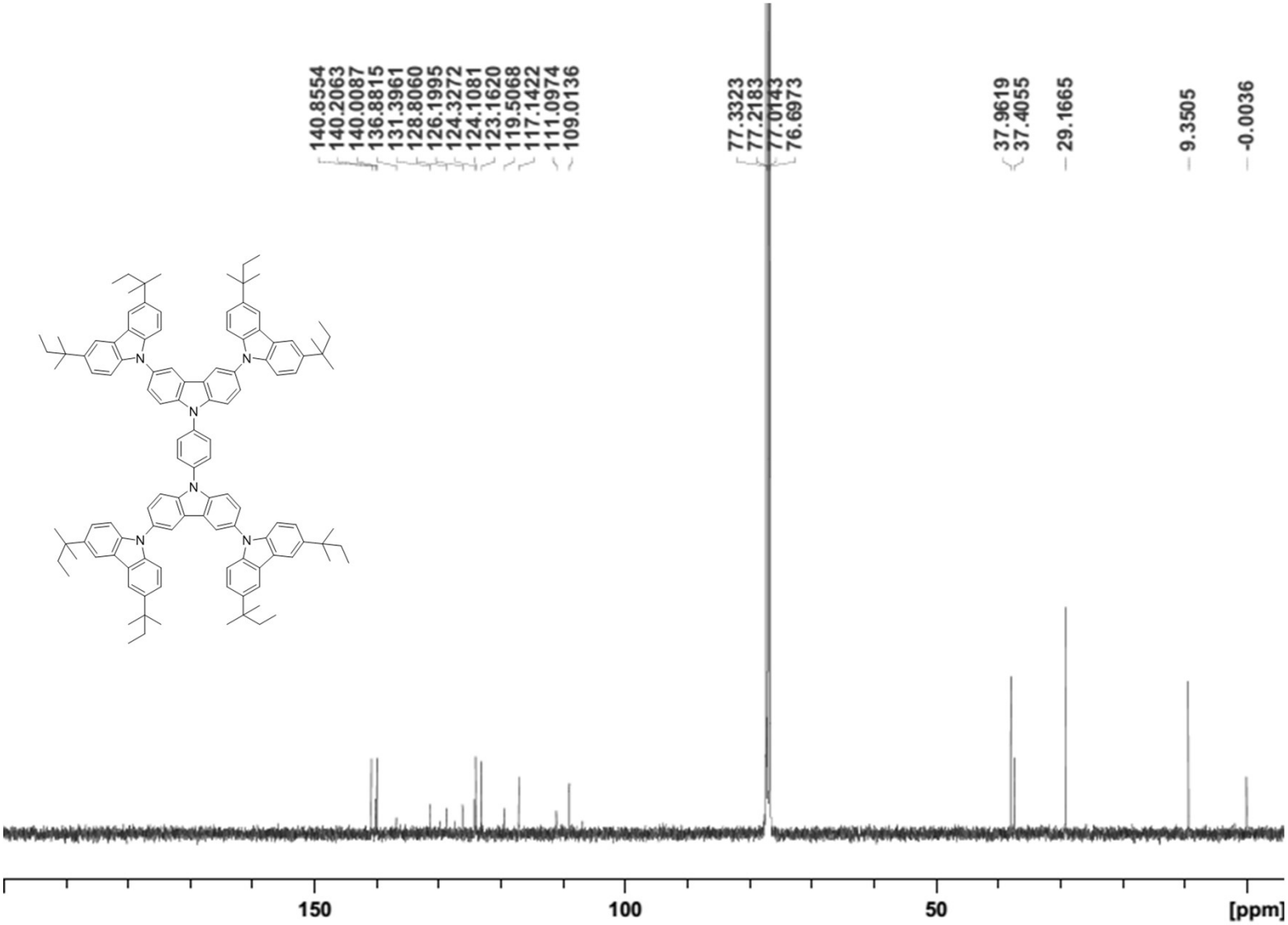

^{13}C NMR:Compound **14**

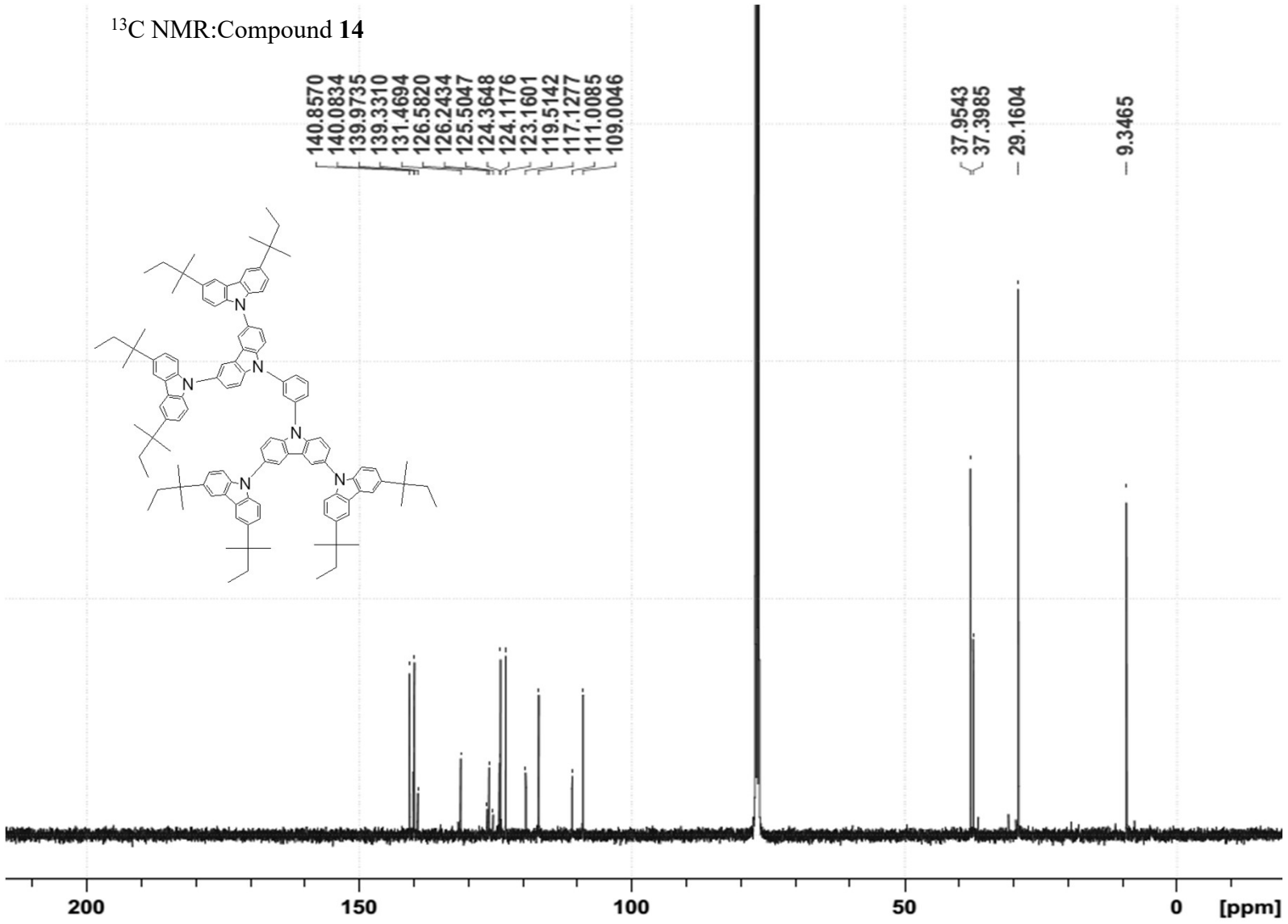

^{13}C NMR:Compound **15**

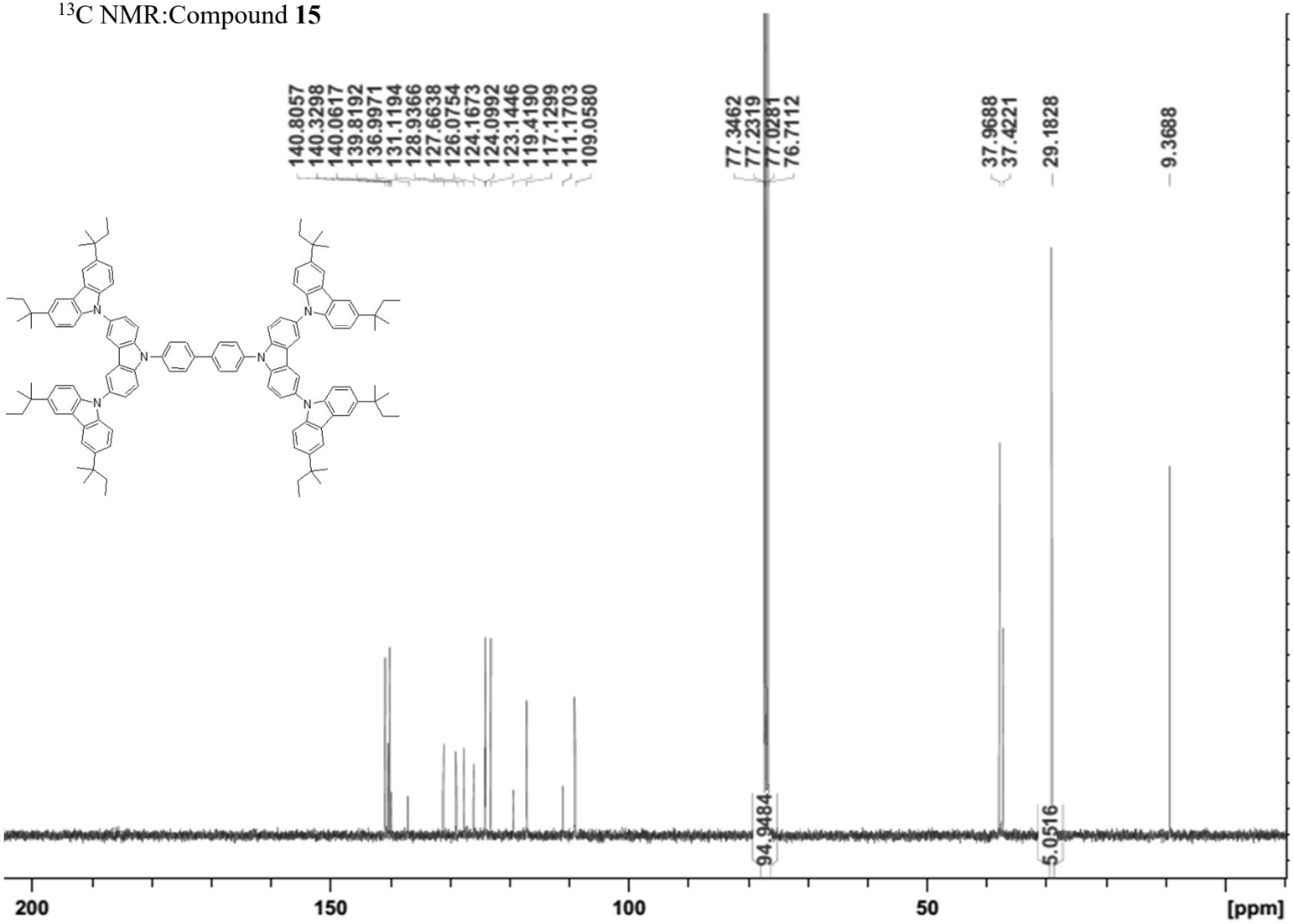

^{13}C NMR:Compound **16**

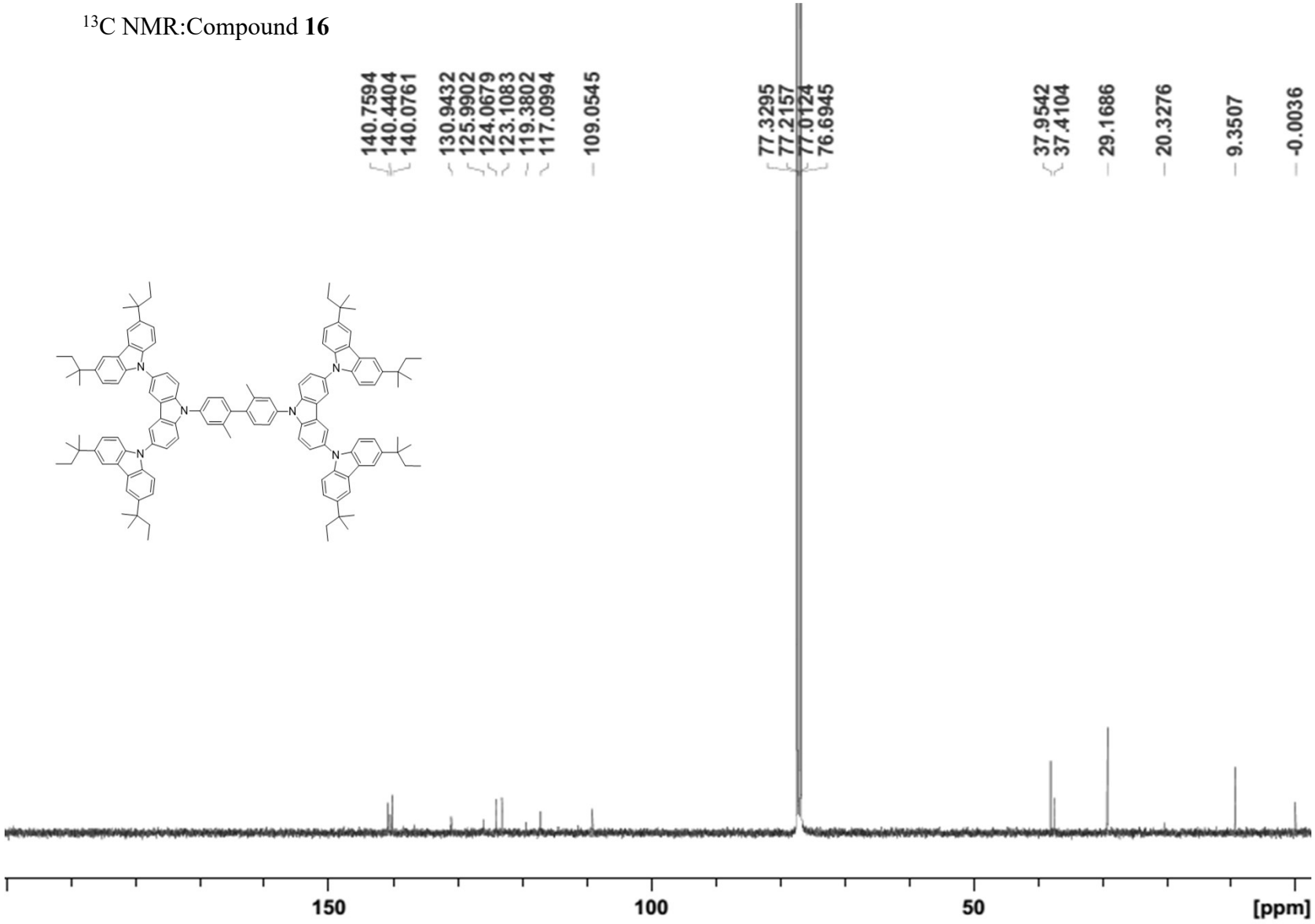

^{13}C NMR:Compound **18**

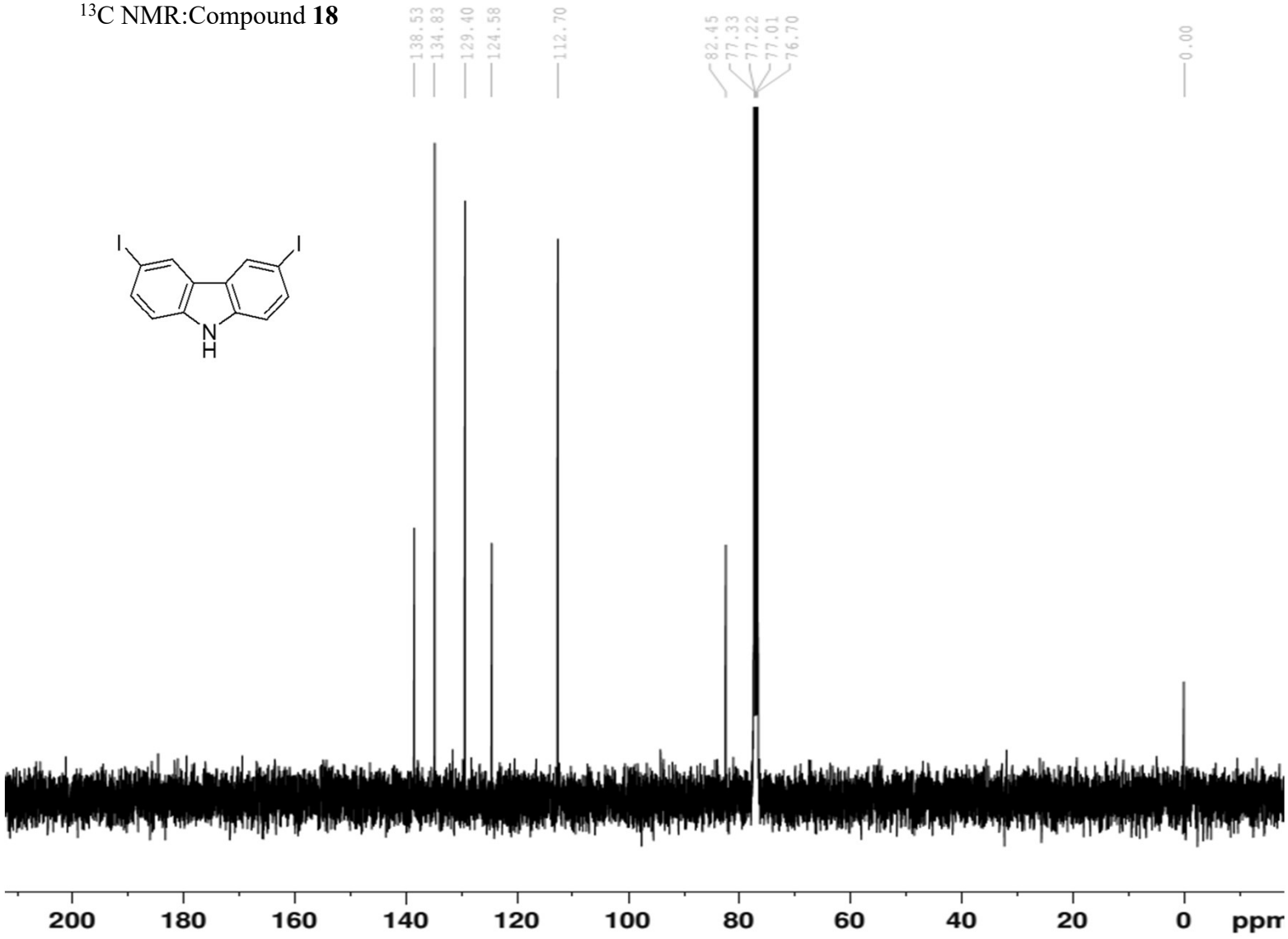

^{13}C NMR:Compound **19**

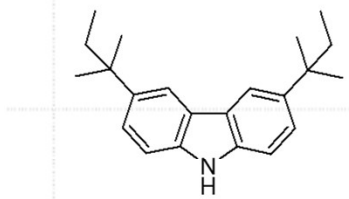

^{13}C NMR:Compound **20a**

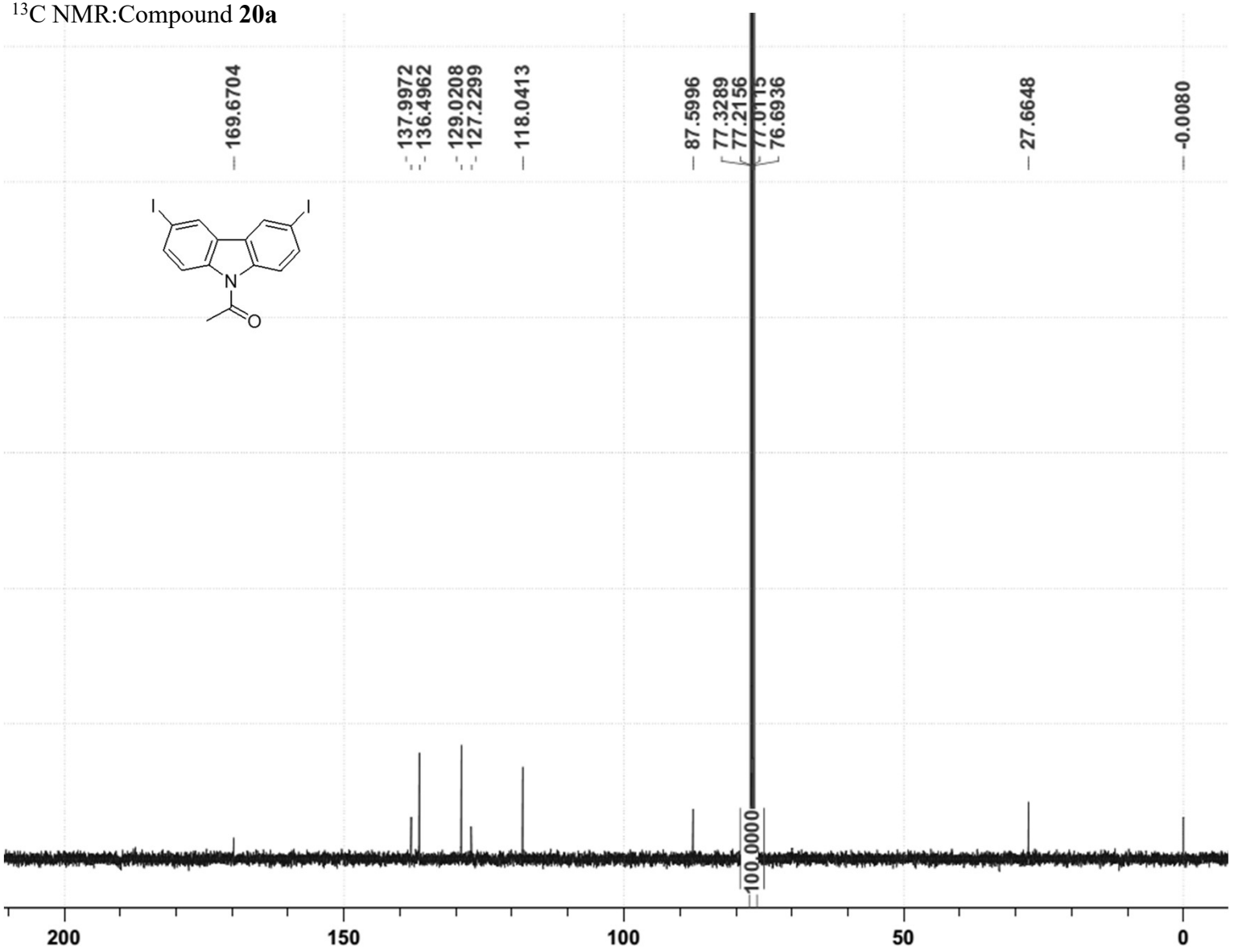

^{13}C NMR:Compound **21**

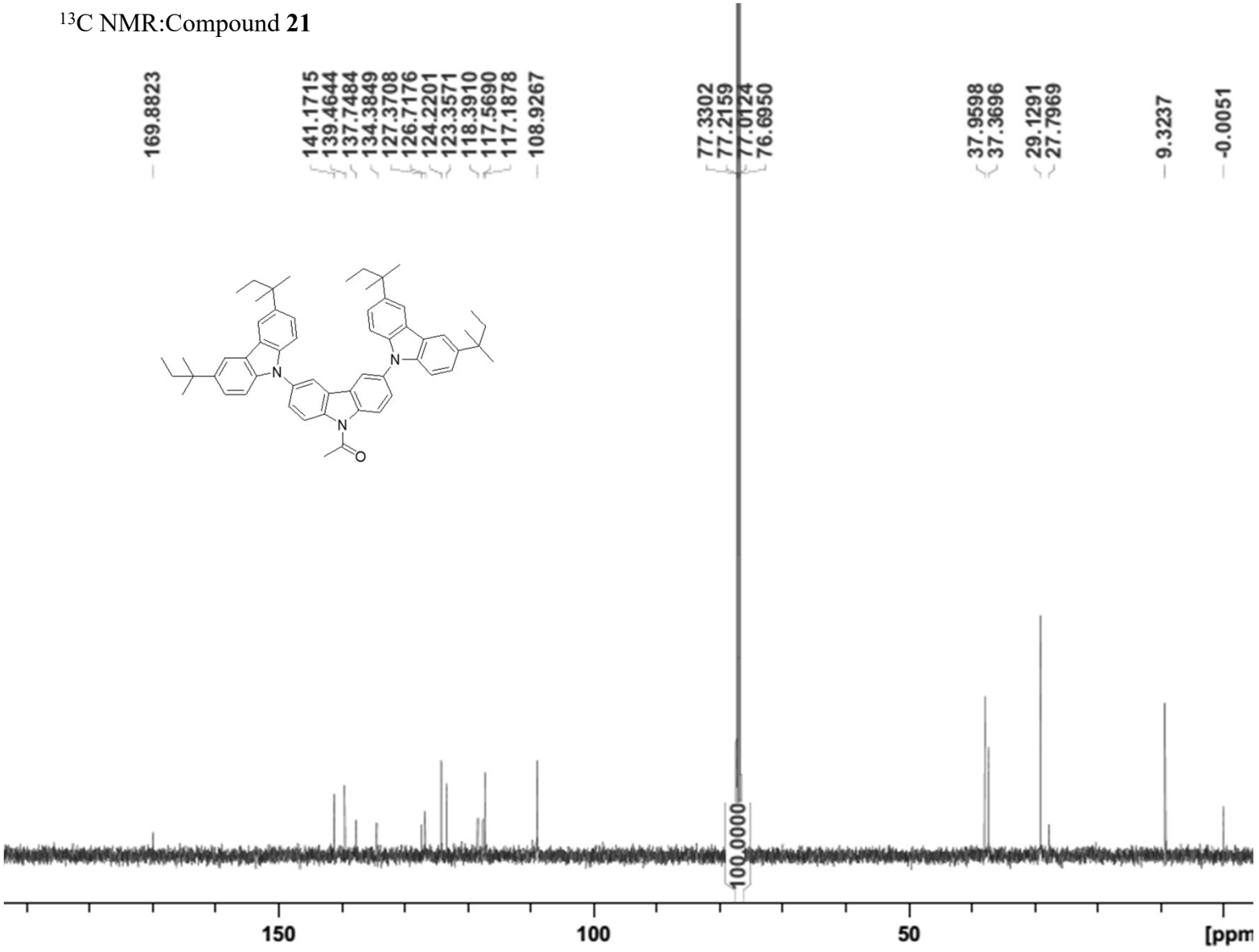

^{13}C NMR:Compound **22**

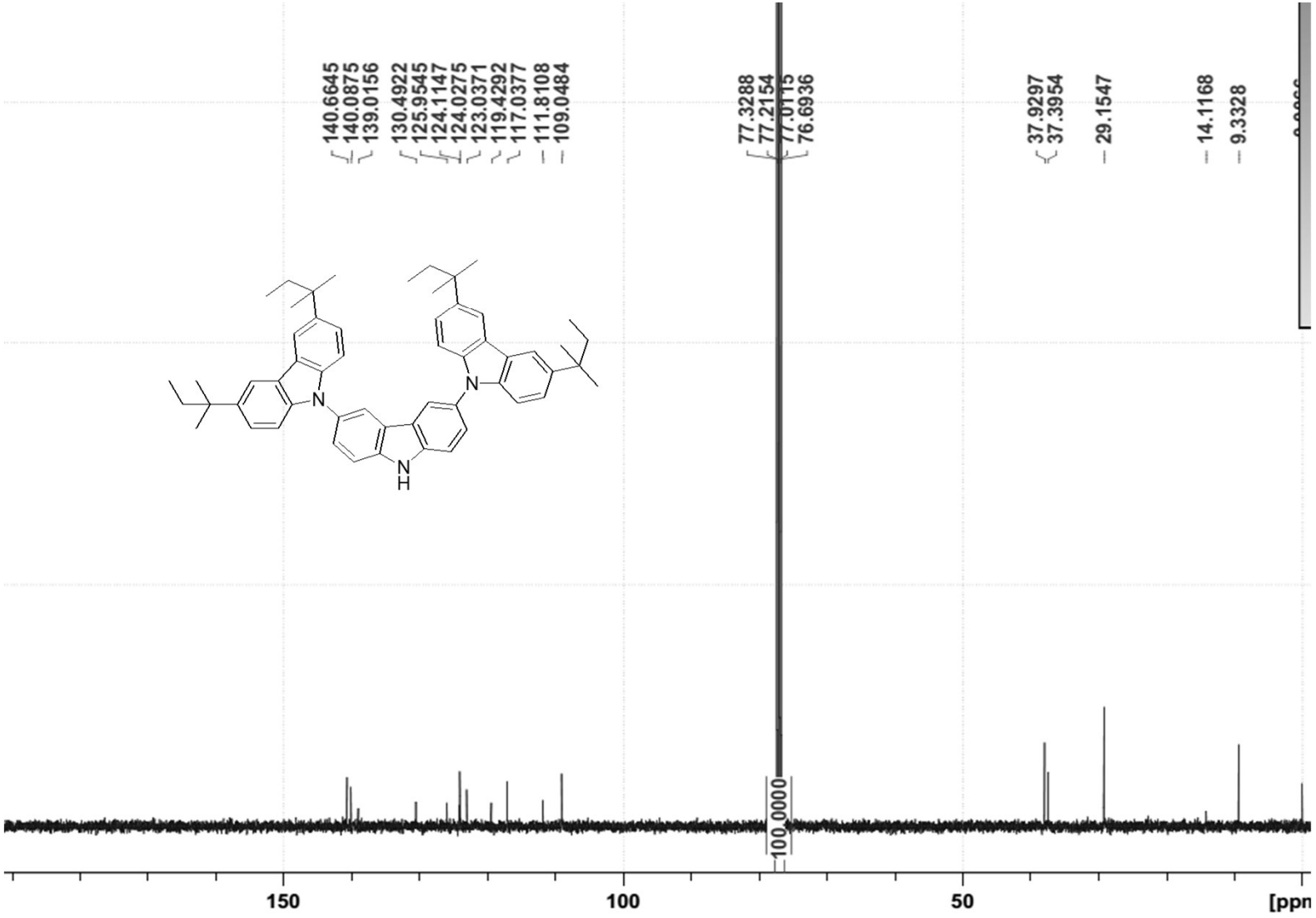

^{13}C NMR:Compound **23**